GENETIC CONTROL OF PROGRAMMED CELL DEATH

IN *CAENORHABDITIS ELEGANS*

DISSERTATION

ZUR

ERLANGUNG DER NATURWISSENSCHAFTLICHEN DOKTORWÜRDE
(DR. SC. NAT.)

VORGELEGT DER

MATHEMATISCH-NATURWISSENSCHAFTLICHEN FAKULTÄT

DER

UNIVERSITÄT ZÜRICH

VON

KIMON DOUKOUMETZIDIS - HADJADJ

AUS

GRIECHENLAND - FRANKREICH

PROMOTIONSKOMITEE

PROF. MICHAEL O. HENGARTNER (VORSITZ, LEITER DER DISSERTATION)

PROF. ERNST HAFEN

PROF. ALEX HAJNAL

PROF. NEKTARIOS TAVERNARAKIS

ZÜRICH 2008

GENETIC CONTROL OF PROGRAMMED CELL DEATH

IN *CAENORHABDITIS ELEGANS*

SUBMITTED IN ACCORDANCE WITH REQUIREMENTS OF

THE UNIVERSITY OF ZURICH

FOR THE DEGREE OF

DOCTOR OF PHILOSOPHY

KIMON DOUKOUMETZIDIS - HADJADJ

UNIVERSITY OF ZURICH

To my beloved family,

Μαρια, Χρυσα και Λιλλη

Nothing shocks me. I'm a scientist.

Indiana Jones

ACKNOWLEDGMENTS

First of all I would like to thank Michael Hengartner, my supervisor, for giving me the opportunity to do a Ph.D. in his lab. I would like to express my gratitude to the other members of my thesis committee, Prof. Alex Hajnal and Prof. Nektarios Tavernarakis for their precious feedback and, notably, their support during all these years. Finally, I would like to thank Prof. Ernst Hafen for taking time out of his busy schedule to serve as my senior committee member.

I would like to thank the many people who taught me molecular biology, and helped me learn how to ask the right questions and how to find the right answers: Dr. Fotis Kafatos and Dr. George Christophides (EMBL, currently at Imperial College), Dr. Jacques Ghysdael (Curie Institute) and especially Dr. Veronique Joliot (University Paris 7), who has been a very good advisor and friend for the past 9 years.

A special thanks goes to Lukas, Andi *et al.*, for making the lab a tolerable and even at times an enjoyable place to come to everyday. They occasionally made it an impossible place to work in as well but that's another story. I thank Sergio for his "heavy-weight" help with spotting and Marko for arguing about every possible subject on a 24/7 basis. Another special "thank you" goes to Johannes Bischoff and Gerlinde Reim for the many pleasant coffee breaks and entertaining discussions, as well as to Jim (Jimipedia) Phelan for his interesting ideas and for helping the whole lab all keep in touch with fascinating papers.

I also thank Dr. Jason Kinchen and Prof. Kodi Ravichandran from the University of Virginia, Charlottesville for the excellent collaboration regarding the role of *dyn-1* in phagosome maturation. Jason, with whom I closely interacted during many years, has been a great source of scientific advice, of motivation and of constructive (most of the time) criticism.

Another person who contributed significantly to the work presented in this thesis is Johann Almendinger. I thank Johann for his precious help during our RNAi screen, but also for his patience (especially during the good old times of his diploma work), his good will and his attitude towards work and life. Johann has been not only

a valuable and hard-working collaborator but also a good friend. I feel privileged I had the opportunity to interact with him during my stay in Switzerland.

I would like to deeply acknowledge my mother and my grandmother for their unconditional love and support, their endless patience and their encouragement through my entire life, especially when it was most needed. I also thank them for trying to understand why I spent 4 years of my life working with a worm.

Finally, I thank Lilli, my constant source of scientific inspiration, who taught me everything I know about DNA damage responses and who shepherded me during the first months of my Ph.D. Lilli was always there to celebrate the good results, but also to question them, and to elaborate new plans and hypotheses when things would go wrong (and from my experience I can say that things DO go wrong quite often in research). I would need hundreds of pages to enumerate all the reasons I thank Lilli for but since my thesis is anyway too long I will only write one more. I thank Lilli for making the bad days good ones.

ZUSAMMENFASSUNG

Programmierter Zelltod, ein Prozess auch bekannt als Apoptose, ist eine Form von Selbstmord. Dieser Begriff umfasst die Entscheidung einer Zelle zu sterben, das tatsächliche Absterben und schliesslich das Beseitigen der Zelle. Die Forschung der letzten 20 Jahre hat eine Menge von Komponenten und Regulatorgenen der Apoptose identifiziert. Auf diese Weise wurde die Apoptose als von grösster Bedeutung für die Entwicklung, Homöostase und Erkrankung von Organismen erkannt. In meiner Dissertation habe ich mit einem Projekt zur "Leben-Tod" - Entscheidung einer Zelle begonnen und später habe ich mich mit den Themen der Zell-Phagozytose und der Apoptose nach erfolgter DNA-Schädigung beschäftigt.

Wie in den Teilen 2 und 3 beschrieben ist, haben wir einen Screen für neue Gene, die im Prozess der Phagozytose von abgestorbenen Zellen wirken, gemacht. Durch "candidate gene" und "reverse genetic" Methoden haben wir mehr als ein Dutzend von involvierten Genen identifiziert. Die meisten von diesen waren bisher noch nicht im Zusammenhang mit Phagozytose charakterisiert worden. Mit weiteren genetischen und zellbiologischen Untersuchungen in *C. elegans* und in Säugetierzellen haben wir einen konservierten genetischen Signalweg, der die Reifung des Phagosoms vermittelt, entdeckt. Diese Funde haben unsere bisherige Erkenntnis über die Phagozytose abgestorbener Zellen verbessert. Zusätzlich haben sie demonstriert, dass der Fadenwurm *C. elegans* ein sehr gutes System ist, um die komplexen Ereignisse der Phagosomenreifung zu studieren.

In einem Grossteil meines Studiums habe ich die Signaltransduktionswege, die nach DNA-Schädigung in den Keimzellen von *C. elegans* aktiviert werden, erforscht. Genotoxischer Stress ist eine grosse Bedrohung für die Integrität des Genoms und die physiologischen Zellfunktionen. Um diese Integrität zu kontrollieren und um sicherzustellen, dass die genetische Information mit hoher Genauigkeit weitergegeben wird, haben eukaryotische Zellen eine robuste und komplexe Antwort auf die Schädigung der DNA entwickelt. Diese Antwort besteht aus Zellzyklus-Arretierung wie auch dem Einleiten von Reparaturprozessen, kann aber auch zum programmierten Zelltod führen, falls die Schäden an der DNA irreparabel ist. Zellen mit Defekten in diesen Signaltransduktionswegen können auf Schäden an der DNA

nicht angemessen reagieren, was wiederum eine erhöhte Wahrscheinlichkeit einer neoplastischen Veränderung mit sich bringt. In den Teilen 5 und 6 beschreibe ich zwei gemeinschaftliche Projekte, die darauf abzielen, die Apoptose - Mechanismen von Keimzellen nach UV-Strahlung (UV-C) zu entschlüsseln.

Dafür haben wir die Gene, die für die Apoptose nach UV-C Schäden notwendig sind, näher untersucht. Wir haben herausgefunden, dass die Komponenten der "nucleotide excision repair" (NER) - Maschinerie, die UV-C Schäden (Pyrimidindimere und 6-4 Photoprodukte) erkennt und repariert, eine aktive Rolle in der Zellzyklus-Arretierung und der Apoptose spielen. Weitere Experimente haben eine entscheidende Rolle für den "homologous recombination" (HR) Mechanismus, der DNA-Doppelstrangbrüche repariert, bei der Einleitung der Apoptose nach UV-C Strahlung gezeigt. Tatsächlich gibt es eine umfangreiche Beeinflussung zwischen den NER und HR Reparaturmechanismen nach erfolgter UV-C Bestrahlung. Diese Funde zeigen, wie komplex die Signalwege im Zusammenhang mit DNA-Schädigung auch im Nematoden *C. elegans* sind, und werden uns helfen, mehr Einsicht in die Signaltransduktionskaskaden von Säugetieren zu gewinnen.

In den zwei letzten Teilen meiner Dissertation beschäftige ich mich mit unerwarteten und faszinierenden Resultaten. In Teil 7 beschreibe ich die Isolierung und erste genetische Charakterisierung von einem neuen Allel von *nuc-1*. Dieses Gen ist das *C. elegans* DNase II - Homolog, ein Enzym, das DNA von abgestorbenen Zellen degradiert. Meine Daten zeigen, dass NUC-1 zwei neue Funktionen hat: die Modulation der Apoptose-Antwort auf Schädigung der DNA und die Regulierung der Lebensdauer von *C. elegans*. Wie eine DNase das Altern beeinflusst, bleibt noch eine sehr interessante, jedoch unbeantwortete Frage. Schliesslich berichte ich in Teil 8, dass Mutationen in gewissen Komponenten des DAF-2/Insulin Signalweges die Aktivierung der Apoptose nach DNA-Schädigung aufheben können. Diese pro-apoptotische Funktion hängt nicht von der Präsenz von DAF-16 ab, einem FOXO Transkriptionsfaktor, der die meisten biologischen Wirkungen des DAF-2/Insulin Signalweges in *C. elegans* übermittelt.

SUMMARY

Programmed cell death, a process also known as apoptosis, is an elaborate form of genetically controlled cell suicide. A very broad term, programmed cell death encompasses processes as different as the decision of a cell whether to live or to die, the execution of the death sentence and, once a cell dies, its subsequent clearance. Research over the last 20 years has identified numerous components and regulators of apoptosis and has underscored the important role of the apoptotic program in development, homeostasis and disease. During the last four years my research interests were two-fold: originally attracted by the field of germ line apoptosis, where very little is known regarding the life-versus-death decision, I found myself working in the fields of cell corpse engulfment and DNA damage-induced apoptosis.

In Chapters 2 and 3 we took advantage of the recently developed RNA-interference methodology to screen for novel genes involved in the process of cell corpse engulfment. Using both candidate-based and unbiased reverse genetic approaches we discovered over a dozen of genes, most of them with previously uncharacterized roles in engulfment. Our subsequent genetic and cell biology studies in *C. elegans* but also in a mammalian cell culture system led to the establishment of a conserved genetic pathway that mediates phagosome maturation. These studies have significantly improved our understanding of cell corpse clearance and they have further demonstrated that the nematode is an attractive system to study *in vivo* the complex series of events occurring after corpse internalization.

The second major part of my Ph.D. research focuses on the signaling pathways that are activated following DNA damage in the *C. elegans* germ line. Genotoxic stress is a major threat to genome integrity and to physiological cellular functions. Cells possess robust mechanisms that can sense and repair DNA lesions, or activate apoptosis if this damage is irreparable. Inability to mount these responses is directly associated with many human pathologies and notably tumorigenesis. In Chapters 5 and 6 I describe two collaborative projects aiming to dissect the mechanisms that trigger germ cell death following UV-C light treatment, a common and potent mutagen. Taking advantage of the *C. elegans* powerful genetics we investigated the genetic requirements for UV-C-induced apoptosis and we delineated

a UV-C-specific signaling pathway. Importantly, we found that components of the Nucleotide Excision Repair (NER) pathway, which is involved in the recognition and repair of UV-C induced lesions (pyrimidine dimers and 6-4 PPs), also play a crucial role in activating cell cycle arrest and apoptosis, via the recruitment of the 9-1-1 checkpoint complex and the activation of a kinase signaling cascade.

The next step we took was to dissect the mechanism by which NER triggers apoptosis. In a separate study, presented in Chapter 6, we found a crucial role for components of the Homologous recombination (HR) pathway, which is responsible for the restoration of DNA double strand breaks, in the induction of cell death following exposure to UV-C. Our genetic and protein localization experiments revealed the existence of an extensive crosstalk between the NER and the HR pathways after UV treatment. This is, to our knowledge, the first *in vivo* demonstration that NER and HR components can also possess signaling properties in addition to their role in DNA repair. This work revealed how surprisingly complex DNA damage signalling in *C. elegans* is, and will significantly improve our understanding of DNA damage responses not only in the nematode but also in other species.

The last two chapters of my thesis deal with quite unexpected and fascinating findings. In Chapter 7, I describe the isolation and the preliminary genetic characterization of a novel allele of *nuc-1*, the *C. elegans* DNase II homolog, an enzyme involved in apoptotic DNA degradation. My results suggest that NUC-1 has at least two novel functions in the worm, one in modulating the apoptotic response upon DNA damage and another in regulating the worm's lifespan. How does a DNase affect aging and DNA damage-induced apoptosis remains a very intriguing but largely unanswered question.

Finally, in Chapter 8 I report that loss of function mutations in certain components of the DAF-2/insulin signaling pathway abrogate the apoptotic response following DNA damage. Intriguingly, this pro-apoptotic function does not depend on the presence of DAF-16, a FOXO transcription factor that mediates most of the biological outputs of insulin signaling in *C. elegans*. This is, to my knowledge, the first report of an *in vivo* pro-apoptotic role for the DAF-2/AGE-1 module following genotoxic stress and could reveal novel mechanisms by which insulin signaling promotes tumour progression.

Despite the advances we have made in understanding DNA damage signaling the last 6 years, the work described in chapters 7 and 8 illustrates that there are plenty of questions remaining to be answered. It also reveals that even a simple model system, like *C. elegans,* is characterized by a surprising degree of complexity in its responses and interactions with the surrounding environment.

TABLE OF CONTENTS

LIST OF FIGURES

CHAPTER 8 - COMPONENTS OF THE DAF-2/INSULIN SIGNALING PATHWAY REGULATE DNA DAMAGE-INDUCED APOPTOSIS IN THE *C. ELEGANS* GERM LINE

LIST OF TABLES

CHAPTER 1

PROGRAMMED CELL DEATH IN *C. ELEGANS*

CHAPTER 1

PROGRAMMED CELL DEATH IN *C. ELEGANS*

1.1 INTRODUCTION

Programmed cell death or apoptosis is a genetically controlled physiological process that plays a fundamental role during animal development in both vertebrates (Glucksmann, 1950) and invertebrates (Truman, 1984). Apoptosis serves to remove superfluous, damaged or harmful cells in a wide variety of physiological contexts. These include morphogenesis and metamorphosis during development, where cell death is used to sculpt the structures of the future organism, to form the proper shapes of organs by removing cells and deleting unneeded structures, and to control the appropriate number of cells that are overproduced. Later in life, apoptosis is used to maintain tissue homeostasis by, for example, eliminating immature lymphocytes that have inappropriate receptor specificities during the establishment of the immune tolerance, or virus-infected and injured cells. Programmed cell death plays, therefore, an ubiquitous role throughout the life of an organism and makes use of several control circuits that regulate the delicate balance between the survival and the death of cells. As one can well imagine, deregulation of apoptosis may lead to the accumulation of harmful cells, and thus have severe consequences for the organism.

Indeed, the pathogenesis of many human diseases has been associated with several types of deregulation of programmed cell death that result in either excessive or insufficient apoptosis. Suppression of the apoptotic machinery and inappropriate survival of cells that should die may cause autoimmune diseases and are among the hallmarks of cancer (Hanahan and Weinberg, 2000; Thomson, 1995). Consistently, loss of the gene encoding one of the major players of programmed cell death in mammals, Apaf-1, has been shown to be involved in tumorigenicity (Yoshida, 2003). On the other hand, abnormal upregulation of programmed cell death leading to the death of cells that normally survive has been shown to contribute to neurodegenerative diseases (Yuan and Yankner, 2000).

1.2 APOPTOSIS DURING *C. ELEGANS* EARLY DEVELOPMENT

As with most metazoans, programmed cell death is a major feature of the *C. elegans* developmental program. Of the 1090 cells that are generated during the development of the hermaphrodite, 131 somatic cells die by apoptosis in a highly reproducible way (Sulston and Horvitz, 1977; Sulston et al., 1983). Namely, always the same cells die and each one of these cells dies at a well-defined and invariant point in development. The morphology of cells undergoing programmed cell death in *C. elegans* has been described at both the light and electron microscopy levels (Robertson and Thomson, 1982; Sulston and Horvitz, 1977) and was found to exhibit many similarities to the morphological changes that undergo dying mammalian cells. Over the last few years, genetic studies of *C. elegans* cell deaths led to the discovery of a variety of genes that play a role in apoptosis. Several of these genes have been shown to be conserved across a wide range of species including mammals (Liu and Hengartner, 1999; Metzstein et al., 1998) suggesting that the basic molecular mechanisms mediating life or death sentences are universal.

Extensive genetic screens for mutants that are defective for the execution of apoptosis led to the identification of a core apoptotic machinery responsible for all developmentally regulated programmed cell deaths that occur in the soma (Figure 1.1 and Table 1.1). All developmental cell deaths require three genes *ced-3, ced-4* (cell death abnormality) and *egl-1* (egg-laying defective), which are involved in the execution of cells destined to die. A fourth gene, *ced-9*, has a prosurvival activity and normally protects cells from an inappropriate activation of the apoptotic pathway. *ced-3, ced-4* and *ced-9* form the core apoptotic machinery while *egl-1* is a negative regulator of CED-9 and has a pro-apoptotic activity. Epistasis and double mutant analysis has allowed these genes to be ordered into a genetic pathway for programmed cell death that contains four distinct, genetically separable steps: the decision of individual cells whether to live, the execution of the apoptotic program in the cell that has decided to die, the engulfment of the dying cell by one of its neighbors, and finally the degradation of the dying cell within the engulfing cell (Figure 1.1). While the pro-apoptotic stimuli mediating the commitment of a cell to trigger the apoptotic program and die are often cell-type specific, the three last steps are common to all cell deaths. Recent studies, however, in both mammals and *C. elegans* suggested that these four steps are partially overlapping, changing the

traditional view of phagocytes as passive scavengers that remove the apoptotic corpses (Conradt, 2001). It has been known for a long time that, in certain instances, phagocytes are able to induce apoptosis in seemingly healthy target cells (Hedgecock et al., 1983; Sulston et al., 1980). Interestingly, it has also been shown that phagocytes can actively promote the execution of programmed cell death in doomed cells, by feeding back positively onto the execution machinery of apoptotic cells downstream of *ced-9* (Hoeppner et al., 2001; Reddien et al., 2001).

In the following sections I summarize the basics of programmed cell death in the nematode, while emphasizing the key genetic studies leading to the discovery of the conserved core apoptotic machinery. In parallel, I also briefly discuss the regulation of apoptosis in mammalian systems, where the pathways are extremely complex.

1.2.1 ced-3 and Caspases

Mutations in the *ced-3* gene were identified as such that suppress the presence of persistent cell corpses seen in mutant animals defective in cell corpse engulfment. *ced-3* is essential for programmed cell death in *C. elegans,* as loss of CED-3 function completely prevents almost all normally occurring programmed cell deaths, except of these taking place in the tail of males (Ellis and Horvitz, 1986). Weaker loss of function alleles of *ced-3,* result in a partial suppression of death and in these animals only a fraction of cells die in a stochastic way. Mosaic analysis and ectopic expression experiments suggested that *ced-3* functions cell autonomously to promote programmed cell death (Ellis and Horvitz, 1986; Shaham and Horvitz, 1996b; Yuan and Horvitz, 1990).

ced-3 encodes a member of the CED-3/ICE (Interleukin-1□ converting enzyme) family of cysteine proteases (Xue et al., 1996; Yuan et al., 1993), named caspases for cysteine aspases, because they have active-site cysteines and cleave their substrates on the carboxyl side of an aspartate residue (Alnemri et al., 1996). Overexpression of CED-3 or any of the other ICE family members induces apoptotic cell death in mammalian cells (Kumar et al., 1994; Miura et al., 1993; Wang et al., 1994). These deaths can be prevented by simultaneous overexpression of either *bcl-2*, the mammalian *ced-9* homolog, or in the case of CED-3 and ICE, of viral caspase

inhibitors, such as *crmA* or p35 (Martinou et al., 1995; Rabizadeh et al., 1993; Ray et al., 1992; Xue and Horvitz, 1995) that act by blocking the proteolytic activity of these enzymes. Although the first mammalian caspase, caspase-1 or ICE, was identified to be an important regulator of inflammatory response, many members of the caspase family, but not all, have been shown to play a central role in the execution of programmed cell death in metazoans. These act by triggering intracellular proteolytic cascades that ultimately lead to the degradation of vital components of the cellular machinery. At least 8 of the 14 different caspases identified in mammals (Alnemri et al., 1996; Nicholson and Thornberry, 1997) have been shown to play an important role during apoptosis (Budihardjo et al., 1999; Earnshaw et al., 1999; Fesik and Shi, 2001; Salvesen and Dixit, 1997; Salvesen and Dixit, 1999; Thornberry and Lazebnik, 1998). In contrast, while *C. elegans* genome codes for multiple caspases (Shaham, 1998), CED-3 is the only caspase whose role in programmed cell death is well-defined.

Caspases that are involved in programmed cell death are generally divided into two categories according to whether they act upstream or downstream in the intracellular proteolytic cascade. Initiator caspases, which include caspase-2, -8, -9 and –10 are upstream molecules, which upon activation by several types of pro-apoptotic stimuli will transduce the apoptotic signals to the effector caspases located downstream. Once activated, effector caspases, including caspase-3, -6 and –7, mediate the proteolytic cleavage of key substrate molecules thereby promoting dismantling of the cellular machinery. In mammals, the known cellular substrates comprise a broad spectrum of functionally different molecules including structural components (such as nuclear lamin and actin), regulatory proteins (such as DNA-dependent protein kinase and MDM2), inhibitors of deoxyribonuclease (such as DFF40 and ICAD) and other pro-apoptotic proteins and caspases (Shi, 2002). In contrast, very little is known about CED-3 targets, although it was one of the first caspases identified.

Individual caspases have different substrate specificities that are determined by the pattern of amino acids upstream of the cleavage site (Nicholson and Thornberry, 1997). A common feature to all members of the caspase family, though, is that they are synthesized as inactive zymogens, which have a very low intrinsic enzymatic activity and must undergo proteolytic activation during apoptosis. Once these killing

enzymes are unleashed, their activity is tightly controlled by several mechanisms, which have been well characterized at the structural level (Shi, 2002). One of the most important categories of regulators of caspase activity is the protein family of Inhibitors of Apoptosis (IAPs) (Deveraux and Reed, 1999). Additional levels of regulation are provided by SMAC (Second mitochondria-derived activator of caspases), and its murine homolog Diablo (Direct IAP-binding protein with low pI), which bind to IAPs and abrogates caspase inhibition.

1.2.2 ced-4 and Apaf-1

Similar to *ced-3*, mutations in the *ced-4* gene were identified as such that suppress the presence of persistent cell corpses seen in mutant animals defective in cell corpse engulfment. *ced-4* is also essential for programmed cell death in *C. elegans*; *ced-4(lf)* mutations completely prevent almost all developmental cell deaths, except of these occurring in the male's tail (Ellis and Horvitz, 1986). Genetic mosaic analysis has indicated that *ced-4* gene activity is needed within those cells that undergo programmed cell death (Yuan and Horvitz, 1990) and that *ced-4*, like *ced-3,* act cell autonomously to promote the death fate of these cells. Ectopic expression experiments using *ced-3, ced-4* and *ced-9* demonstrated that *ced-4* is negatively regulated by *ced-9* and positioned *ced-4* genetically upstream of *ced-3* (Shaham and Horvitz, 1996b).

Unlike *ced-3* though, the *ced-4* gene produces multiple, alternatively spliced transcripts that seem to perform different functions. A small transcript, the first to be identified, which is abundant and encodes a short isoform, CED-4_S, with a pro-apoptotic activity (Yuan and Horvitz, 1992) and a second slightly larger transcript but much less abundant, that encodes a large isoform, CED-4_L (Shaham and Horvitz, 1996a). Overexpression of CED-4_L inhibits apoptosis suggesting that this large isoform has an opposite effect on cell death from that of the major protein CED-4_S. The molecular mechanism by which CED-4_L exerts its anti-apoptotic effects as well as the physiological function of this isoform remain to be determined.

The most abundant isoform, CED-4_S, consists of 549 amino-acids (Yuan and Horvitz, 1992) and is similar to the mammalian apoptotic protease activating factor-1, Apaf-1, which was identified several years after *ced-4* was cloned (Zou et al., 1997).

Sequence analysis revealed that CED-4 possesses both an amino-terminal caspase recruitment domain (CARD) (Hofmann et al., 1997), which allows it to bind the CARD domain of CED-3, and a nucleotide binding domain (NBD or P-loop). Mutations in the phosphate-binding loop of CED-4 disrupt its ability to induce chromatin condensation in yeast (James et al., 1997) and to process CED-3 *in vitro* and *in vivo*, both in insect (Seshagiri and Miller, 1997) and mammalian cells (Chinnaiyan et al., 1997a), suggesting that the NBD is essential for CED-4 activity. CED-4 protein also contains two other regions that show some similarity to the EF-hand family of Ca^{++}-binding domains, but site directed mutagenesis experiments indicated that these regions are not essential for the ability of CED-4 to activate CED-3 (Horvitz et al., 1994). Finally, one region within CED-4 binds to CED-9 (see below) and this interaction has been shown to play an important role in sequestrating the CED-4 in an inactive complex on the mitochondrial membrane.

CED-4 is thought to exert its pro-apoptotic effects by acting as a catalyst for CED-3 self-processing (Chinnaiyan et al., 1997a), facilitating the formation of active CED-3 caspase. Biochemical studies demonstrated that CED-4 was able to oligomerize via homotypic interactions (Chinnaiyan et al., 1997b) in a nucleotide-dependent manner, and that CED-4 oligomerization is necessary for CED-3 activation to occur (Yang et al., 1998). The oligomerization domain of CED-4 is distinct from the NH2-terminal CARD domain that binds to CED-3 (Chinnaiyan et al., 1997b), smaller than the sequence required for CED-9 interaction (Ottilie et al., 1997) and is encompassed in a domain that is similar to mammalian Apaf-1 (Li et al., 1997; Zou et al., 1997). CED-4 can, therefore, simultaneously associate with itself and CED-3; Its oligomerization is thought to bring the associated CED-3 proteins into close proximity, and thus facilitating their subsequent proteolytic activation (Yang et al., 1998) in a similar way to the "induced proximity" model that explains mammalian caspase activation (Salvesen and Dixit, 1999).

The mammalian CED-4 homolog, Apaf-1, was originally discovered from HeLa cell extracts as a cytochrome *c*-dependent activator of caspase-3 (Zou et al., 1997). Cytochrome *c* is a major pro-apoptotic molecule and it is known to translocate from mitochondria into the cytoplasm, in response to a variety of apoptotic stimuli (Bossy-Wetzel et al., 1998; Kluck et al., 1997). Sequence analysis revealed that CED-4 and Apaf-1 contain similar protein domains sharing the same topology on the

primary structure. The NH2-terminal region of Apaf-1 exhibits a striking similarity to the NH2-terminal CARD domain of CED-3 and it has been shown that this region can directly interact with the initiator procaspase-9. The midportion of Apaf-1 has 22% identity and 48% homology to CED-4 and contains a nucleotide binding domain (NBD) that dATP/ATP binds to. In contrast to CED-4, however, Apaf-1 contains a long carboxy-terminal extension that contains multiple WD40 repeats that bind cytochrome *c*. This WD rich region seems to negatively regulate the activity of Apaf-1, since its deletion generates a constitutively active form (Hu et al., 1998; Srinivasula et al., 1998).

Structural studies of the Apaf-1/Procaspase-9 complex provided intriguing hits on its activation and function. In the presence of cytochrome *c* and dATP/ATP, Apaf-1 oligomerizes to form an heptameric wheel-like platform for procaspase-9 assembly (Acehan et al., 2002; Li et al., 1997) in a two step reaction. First, binding of cytochrome *c* to the WD-40 repeats induces a conformational change, an "open" Apaf-1 conformation (Hu et al., 1998; Srinivasula et al., 1998). Second, binding of dATP or ATP to the NBD triggers Apaf-1 oligomerization and association with procaspase-9, generating the cytochrome *c*/Apaf-1/Caspase-9 "apoptosome" (Cain et al., 2000; Jiang and Wang, 2000; Saleh et al., 1999; Zou et al., 1999). The CARD of Apaf-1 specifically interacts with that of the procaspase-9, through complementary charged surfaces (Qin et al., 1999) and it has been suggested that the CARDs of CED-4 and CED-3 probably interact in a similar way.

1.2.3 ced-9 and the Bcl-2-like family

The *ced-9* gene was originally defined by a gain-of-function allele that blocks programmed cell death (Hengartner et al., 1992). Loss-of-function alleles, which were isolated by identifying *cis* dominant suppressors, lead to an ectopic activation of programmed cell death in cells that normally live, resulting in sterility and maternal effect lethality (Hengartner et al., 1992). Genetic studies have also shown that *ced-9* exerts its anti-apoptotic effects by preventing the activation of the death genes *ced-3* and *ced-4* and suggested that *ced-9* acts upstream of these (Hengartner et al., 1992; Shaham and Horvitz, 1996b).

ced-9 encodes a 280 amino-acid protein exhibiting sequence and functional similarity to Bcl–2 (B cell lymphoma 2) (Hengartner and Horvitz, 1994), a mammalian proto-oncogene which was originally discovered by a dominant gain-of-function mutation commonly found in follicular lymphomas (Tsujimoto et al., 1984). The mammalian Bcl-2 gene can functionally substitute for *ced-9* in *C. elegans* (Hengartner and Horvitz, 1994) and overexpression of either Bcl-2 or *ced-9* prevents or slows down apoptosis in a large variety of cells under conditions that normally lead to cell death. Consequently, it has been proposed that the products of theses genes are involved in protecting cells that should survive from programmed cell death.

Biochemical studies shed some light on the molecular mechanism by which *ced-9* exerts its anti-apoptotic effect in *C. elegans*. CED-9 directly interacts with CED-4 (Chinnaiyan et al., 1997b; James et al., 1997; Spector et al., 1997) likely through the conserved BH1, BH2 and BH3 domains (Bcl-2 Homology domain), suggesting that CED-9 controls cell death by binding to and regulating CED-4 activity. Furthermore, cellular biology studies demonstrated that CED-9 mainly localizes on the outer mitochondrial membrane both in mammalian cells (Wu et al., 1997) and in *C. elegans* (Chen et al., 2000) where it sequesters CED-4 in an inactive complex, thereby restricting the pro-apoptotic activity of the latter. Because CED-4 has also been shown to physically interact with the prodomain of CED–3 (Chinnaiyan et al., 1997b), it has been suggested that all these three proteins form an inactive protein complex on the mitochondrial membrane (Chinnaiyan et al., 1997b; Irmler et al., 1997). Consistently, in cells committed to die, CED-4 is released from CED-9, oligomerizes and translocates from mitochondria to nuclear membranes prior to caspase activation (Chen et al., 2000). Because CED-9 binding to CED-4 is mutually exclusive with CED-4 oligomerization, sequestration of CED-4 by CED-9 to the outer mitochondrial membrane prevents triggering of programmed cell death in cells that should survive.

Over the last few years many proteins have been identified to be similar to Bcl-2 and CED-9, forming a large family of Bcl-2 like proteins. While *C. elegans* encodes only two members of the Bcl-2 family, CED-9 and EGL-1, higher eukaryotes posses up to 30 homologs (Adams and Cory, 2001; Gross et al., 1999; Puthalakath and Strasser, 2002). Members of the Bcl-2 family are in the heart of apoptotic signaling in higher eukaryotes as they integrate diverse survival and death signals that

are generated from inside or outside the cells (Adams and Cory, 2001; Strasser et al., 2000). Typically, members of the Bcl-2 family are categorized into two classes according to whether they promote or inhibit apoptosis.

Anti-apoptotic members comprise the prototypic Bcl-2, Bcl-x_L (Boise et al., 1993), Bcl-w (Boise et al., 1993), A1/Bfl-1 (Choi et al., 1995; Lin et al., 1996), Mcl–1(Kozopas et al., 1993), Boo/Diva (Inohara et al., 1998; Song et al., 1999) and the *C. elegans ced-9* (Hengartner et al., 1992). All these proteins have three or four regions with extensive amino acid sequence similarity with Bcl-2 (Bcl-2 Homology regions BH1-BH4). As with the *C. elegans* CED-9, Bcl-2 survival factors can interfere with the formation of the Apaf-1/Caspase-9 apoptosome in mammals, thereby preventing apoptosis. However, their mode of action seems different, as survival Bcl-2-like proteins do not directly bind to the *ced-4* homolog, Apaf-1 (Conus et al., 2000; Haraguchi et al., 2000; Hausmann et al., 2000; Moriishi et al., 1999). It is currently believed that one way by which these proteins can act is by preventing mitochondrial perforation so that none of the mitochondrial pro-apoptotic factors (cytochrome c, Smac/Diablo and Hrt2/Omi) is released to stimulate the formation of the apoptosome (Adrain et al., 2001; Kluck et al., 1997; van Loo et al., 2002).

The group of pro-apoptotic members, which contain two or three BH regions, includes the mammalian Bax (Oltvai et al., 1993), Bak (Chittenden et al., 1995; Kiefer et al., 1995), Bcl-x_S (a splice variant of the *bcl-x* gene (Boise et al., 1993) and Bok/Mtd (Hsu et al., 1997). However, the most potent inducers of apoptosis fall into a third group of proteins defined by the presence of a single BH3 domain which otherwise have no structural resemblance to the Bcl-2 family or any other known protein. The so-called BH3-only proteins comprise mammalian Bad (Yang et al., 1995), Bik/Nbk (Boyd et al., 1995; Han et al., 1996), Bid (Wang et al., 1996), Hrk/DP5 (Inohara et al., 1997), Bim/Bod (Hsu et al., 1998; O'Connor et al., 1998), Blk (Hegde et al., 1998) and the *C. elegans* EGL-1 (Conradt and Horvitz, 1998). Genetic studies begin to reveal that each of the ten so far identified BH3–only proteins in mammals may sense a different pro-apoptotic stimulus and then relay the signal to the multidomain Bcl-2 family members. In healthy cells, BH-3 proteins are kept inert by transcriptional and translational mechanisms thereby preventing inappropriate cell deaths (Huang and Strasser, 2000; Puthalakath and Strasser, 2002). In response to an apoptotic signal these proteins are activated by either one or several

mechanisms that include transcriptional induction, post-translational phosphorylation, proteolysis and cytoskeletal sequestration.

Pro-apoptotic and anti-apoptotic members of the Bcl-2 protein family can physically interact and it is believed that these interactions play a major role in determining whether a cell should live or die (Reed et al., 1998). Although it is not fully understood how exactly these proteins mediate life or death sentences at a molecular level, it is obvious that Bcl-2 family members act like checkpoints through which survival and death signals must pass before they determine the cell's fate.

1.2.4 egl-1

The *egl-1* gene was originally defined by gain-of-function mutations that provoke a dominant egg-laying defect due to the loss of the two functional Hermaphrodite Specific Neurons (HSNs). This defect was found to be caused by the ectopic programmed deaths of these neurons (Ellis and Horvitz, 1986) which normally innervate the vulval muscles and drive egg-laying (Trent et al., 1983). Further studies led to the isolation of a *cis* dominant suppressor of *egl-1(gf)* egg-laying defect and the identification of a loss-of-function mutation in the *egl-1* gene. Analysis of this mutation showed that the loss of *egl-1* function prevents not only the ectopic deaths of the HSNs but most if not all developmentally regulated programmed cell deaths of somatic cells (Conradt and Horvitz, 1998). This finding suggested that *egl-1* encodes a novel pro-apoptotic regulator of the *C. elegans* death machinery.

ced-3(lf), ced-4(lf) and ced-9(gf) are all epistatic to *egl-1(gf)* : they suppress the ectopic deaths of the HSNs in hermaphrodites caused by the *egl-1(gf)* mutation, and restore a non-Egl phenotype, suggesting that *egl-1* is specifically involved in the cell death pathway and that it acts genetically upstream of *ced-3*, *ced-4* and *ced-9*. By contrast, loss of *egl-1* function, while preventing somatic cell death just as loss of *ced-3* or *ced-4* function do, does not suppress the *ced-9(lf)* induced lethality. Moreover, it has been demonstrated that *egl-1* has no effect on programmed cell death in a *ced-9(0)* background suggesting that *ced-9* activity must be present and functional for *egl-1* to exert its effect. Together, these findings led to the placement of *egl-1* genetically upstream of *ced–9* and showed that it functions as a negative regulator of the latter (Conradt and Horvitz, 1998).

The *C. elegans egl-1* gene encodes a small protein of 91 amino-acids which presents molecular and functional similarity to the "BH3-only" subfamily of the Bcl-2-like proteins discussed previously. Biochemical studies demonstrated that EGL-1 exerts its effect on programmed cell death through a direct physical interaction with CED-9, which is mediated by a short region of 9 amino-acids in the center of the protein similar to the BH-3 domain. Binding of EGL-1 to CED–9 results in the displacement of CED-4 from the mitochondria associated complex, thereby allowing CED-4 to trigger cell death. *egl-1* expression is regulated at the transcriptional level. Depending on the cell type and the developmental stage, it can be either enhanced or suppressed and several transcription factors including CES-1, CES-2 (Ellis and Horvitz, 1991) and TRA-1A (Conradt and Horvitz, 1999) have been shown to be involved in this process.

Transcriptional upregulation of *egl-1* by cell type specific transcription factors was though to be the only mechanism regulating the onset of apoptotic deaths in *C. elegans*. A recent study by Maurer and coworkers shows, however, that although *egl–1* expression is, in many cases, a prerequisite for apoptotic cell death, it may not be the actual trigger for the process (Maurer et al., 2007). The authors took advantage of the *C. elegans* powerful genetics to demonstrate that in the tail-spike cells the rate-limiting step for cell death initiation is the transcriptional upregulation of the caspase gene, *ced-3*. These findings suggest that the transcriptional upregulation of caspases might play a key role controlling the timing of cell death during animal development. Inspired by this novel mode of regulation the authors extend their conclusions to most of the *C. elegans* embryonic deaths by speculating that the asymmetric segregation/activation of CED-3 protein (or mRNA) might be the key rate-limiting steps for death initiation.

1.2.5 icd-1 and apoptotic cell death independent of ced-3

The ubiquitously expressed apoptotic machinery needs to be activated in cells that are destined to die but also to be kept quiescent in cells that need to survive. Recently, a novel major regulator of apoptotic cell death in *C. elegans* was identified (Bloss et al., 2003). Bloss and coworkers discovered that RNAi-mediated inactivation of a gene they named *icd-1* (inhibitor of cell death-1) resulted in the accumulation of

large numbers of dying cells in worm embryos. The authors also showed that at least some of the cells that die in *icd-1*(RNAi) animals should have normally survived suggesting that *icd-1* acts as an anti-apoptotic factor. This hypothesis was further supported by the observation that overexpression of *icd-1* is able to inhibit apoptosis in cells that are normally destined to die.

Epistasis analysis of *icd-1* with known cell death regulators revealed that loss of CED-4 function suppressed the increased cell death in *icd-1(RNAi)* embryos but, interestingly, loss of the caspase CED-3 did not. While quite surprising this observation is in agreement with previous genetic studies reporting that in embryos lacking *ced-3* activity a small but consistent number of apoptotic deaths still occurred (Shaham et al., 1999) and which suggested the existence of another functional caspase or of caspase-independent cell death pathway.

icd-1 encodes for the *C. elegans* β subunit of the nascent polypeptide-associated complex (bNAC). The function of this complex is not well understood but there is evidence suggesting that it functions during translation to target proteins to subcellular locations, such as the mitochondria (Rospert et al., 2002). ICD-1 could therefore act by targeting proteins important for apoptosis, such as nascent CED-9 on ribosomes to mitochondria but this theory has to be tested. The recent discovery of *icd-1* and its unusual involvement in apoptosis suggest that despite extensive genetic investigations *C. elegans* has still a lot to teach us about programmed cell death.

1.2.6 Mitochondria and apoptosis in C. elegans

It has been known for quite a long time that mitochondria lie in the heart of apoptotic signaling in mammals, where most apoptotic cell deaths are mediated by a mitochondria-specific signaling pathway. Mitochondria are the cell's power plants but can also be viewed as docking platforms where several proteins important for apoptosis, such as members of the Bcl-2 family of proteins, the endonuclease G or the apoptosis-inducing factor (AIF), localize and interact with eachother. Upon a variety of pro-apoptotic stimuli (e.g. oxidative stress, DNA damage) mitochondria undergo a series of structural changes characterized by permeabilization of the outer membrane, uncoupling of the oxidative phosphorylation and swelling of the intermembranal space; this resuls in the release of several apoptogenic proteins in the cytoplasm,

including the notorious cytochrome *c* which will lead to the activation of caspases and ultimately to cellular demise.

Recent studies have uncovered an additional behaviour of mitochondria during the apoptotic process, by showing that they fragment into smaller pieces (Karbowski and Youle, 2003). The significance of this fragmentation in the apoptotic context is currently not well understood. It has been hypothesized that fragmentation could be important for the release of mitochondrial proteins since interfering with this process was found to delay release of cytochrome *c* during apoptosis (Frank et al., 2001). More experiments need to be performed in order to understand the exact role of mitochondrial fission during programmed cell death.

A recent study from Barbara Conradt's laboratory tried to address the significance of this phenomenon in *C. elegans* (Jagasia et al., 2005). Using a combination of elegant genetic and cell biology approaches the authors of this study showed that mitochondrial fragmentation also occurs in cells undergoing apoptosis in *C. elegans* embryos, in a *ced-3*-independent but *egl-1*-dependent way. This demonstrates that mitochondrial fission in the worm is a very early event during programmed cell death and relies on the initiation of the apoptotic program. Conradt and colleagues went one step further and examined the potential contribution of this process in cell killing. They performed overexpression experiments in order to artificially promote or inhibit fragmentation and examined the effect on programmed cell death in each case. Interestingly, there seemed to be a correlation between lack of fragmentation and increased cell survival while in conditions promoting fragmentation some cells that would have normally lived died.

This study is the first report of an active involvement of mitochondria in programmed cell death in the worm and it extends the, so far, many similarities between the mammalian and worm apoptotic pathways. But how does mitochondrial fission induces apoptosis? The authors speculate that fragmentation might lead to the release of a cytochrome *c*-like factor, which would then act to potentiate the CED-4-mediated activation of CED-3. Future studies of the involvement of mitochondrial division in programmed cell death will undoubtedly further our understanding of this process.

1.3 PROGRAMMED CELL DEATH IN THE *C. ELEGANS* GERM LINE

1.3.1 The C. elegans *adult hermaphrodite germ line*

The germ line is one of the best characterized and most extensively studied tissues in *C. elegans*, as it is amenable to both genetic and developmental analysis (Hubbard and Greenstein, 2000; Kimble and Ward, 1988; Schedl, 1997). The gonad of adult hermaphrodite worms consists of two symmetrical U-shaped tubes whose proximal ends are linked to a common uterus (Figure 1.2); these two so-called gonad arms are equivalent and have been well characterized at an ultrastructural level (Hall et al., 1999; Hirsh et al., 1976).

Inside each gonad arm, germ cells display a distal-to-proximal polarity in their pattern of proliferation, meiotic prophase progression, and gametogenesis. In the distal region, syncytial germ line nuclei are surrounded by incomplete membranes and are connected to a common cytoplasm, also called rachis, via cytoplasmic bridges. *C. elegans* germ cells, like those in many organisms, undergo a pre-meiotic period of proliferation followed by a period during which some enter meiosis while others remain mitotic. There is always a remaining pool of mitotic cells that can be regarded as a germ line stem cell population since it persists for the entire life of the organism, is self renewing and produces cells that will ultimately differentiate as gametes. Each gonad arm can be virtually subdivided into distinct specialized regions in which complex cell cycle regulation events take place progressively determining the fate of germ cells as they move through the gonad. The distal portion of the gonad is capped by a distal tip cell (DTC) which is responsible for maintaining the stem cell potential of neighboring germ cells by promoting their mitotic proliferation and/or inhibiting entry into meiosis. As germ line nuclei progress proximally out of the distal mitotic zone, they bypass the influence of the DTC, enter meiosis and progress into the pachytene stage of meiotic prophase I. The region where germ cells undergo the transition from the mitotic cell cycle to meiotic prophase is called the transition zone (Crittenden et al., 1994). Germ cell nuclei within the transition zone have a characteristic croissant-shaped morphology. Progression beyond the pachytene stage of meiosis I requires activation of the MAP kinase signaling pathway (Church et al., 1995) and occurs near the bend of the gonad arm. Gametogenesis takes place in the proximal arm of the gonad where germ cells differentiate into oocytes or sperm (sperm development occurs earlier during development and won't be discussed here).

It was recently shown that germ cells have a third fate available to them, that is, to undergo apoptosis (Gumienny et al., 1999). Previous work in the Hengartner lab has shown that in the *C. elegans* germ line apoptosis occurs in response to at least two different stimuli: a physiological signal that is used to eliminate germ cells during oogenesis (Gumienny et al., 1999) and a DNA damage signal that also triggers a checkpoint response (Gartner et al., 2000). These two types of death are discussed below.

1.3.2 Physiological programmed cell death

Apoptosis is a major fate of the *C. elegans* germ line. In wild type hermaphrodites over 50% of all potential oocytes die during meiotic maturation (Gumienny et al., 1999). Genetic studies have shown that germ cell death is mediated by the same execution machinery as somatic cell deaths: strong loss-of-function mutations in either *ced-3* or *ced-4* provoke a dramatic decrease in germ cell death (Gumienny et al., 1999). Furthermore, *ced-9(lf)* mutants have increased levels of germ cell corpses indicating that the pro-survival function of *ced-9* is conserved in the germ line (Gumienny et al., 1999). However several lines of evidence suggest that the molecular mechanism that regulates the core apoptotic complex differs significantly between the soma and the germ line.

First, the gain-of-function *ced-9(n1950)* mutation and the loss-of-function *egl-1* mutation, both of which prevent most somatic cell deaths (Conradt and Horvitz, 1998; Hengartner et al., 1992), do not affect germ line cell death (Gumienny et al., 1999). Intriguingly, while these findings strongly suggest that physiological apoptosis is triggered by a BH3-independent pathway, no such mechanism has been described so far in the worm. Indeed, both in mammalian systems and *C. elegans*, BH3-proteins, that comprise the Bax-like death factors and the large group of BH3-only proteins such as EGL-1 and Bad, lie in the heart of apoptotic signaling where all known pro-apoptotic signals converge. Thus, the study of physiological programmed cell death in *C. elegans* could potentially reveal additional regulatory mechanisms that trigger apoptosis via a BH3-independent circuit.

Second, programmed cell death in the germ line occurs in a syncytium where all germ cell nuclei have access to a common cytoplasm and, as a result, to a common

pool of cytoplasmic factors. Therefore, physiological programmed cell death should make use of special mechanisms to restrict activation of the apoptotic program only to the dying germ cell. Ultrastructural studies revealed that cells fated to die rapidly cellularize, thereby physically isolating the doomed cell from its neighbors (Gumienny et al., 1999). The mechanism by which this is achieved as well as the molecular nature of the factors involved in this process remain to be determined. An attractive hypothesis would be that cellularization is triggered upon proteolytic cleavage of a target protein by the active form of CED-3. If this is correct, then identification of CED-3 targets could shed some light on how cells isolate themselves from the common syncytium.

Third, while apoptosis in somatic tissues follows a highly reproducible pattern, apoptosis in the *C. elegans* germ line occurs in a stochastic way. In other words, it is impossible to predict in advance which cell is fated to die and which cells are fated to live. The only reproducible feature of physiological apoptosis is that death always occurs in the same anatomical region of the gonad, near the bend of each U-shaped tube.

Finally, apoptotic germ cell is death is functionally linked to meiotic progression as the RAS/MAP kinase pathway, which is required for exit from the pachytene stage (Church et al., 1995), is also required for programmed cell death in the germ line (Gumienny et al., 1999). In *C. elegans* several members of this signaling pathway are known including LET-60 Ras, LIN-45 Raf, MEK–2 MAPK/ERK kinase and MPK-1 MAP kinase (MAPK) (Kayne and Sternberg, 1995). Mutations in any of these four genes result in sterility by blocking the transition from pachytene to diakinesis during meiosis I prophase (Church et al., 1995). These mutations also block physiological apoptosis and epistasis analysis suggested that pachytene arrested cells are protected from undergoing programmed cell death through a *ced-9*-dependent mechanism (Gumienny et al., 1999).

1.3.3 Genes affecting physiological germ line apoptosis

How is germ cell death regulated? To date, very few genes have been discovered to regulate apoptosis in the *C. elegans* germ line by using both forward and reverse genetic screens or candidate-based approaches (Table 1.1). These factors

consist of a predicted E3 ubiquitin ligase (R05D3.4), a p38/MAP kinase (PMK-3) and four predicted RNA-binding proteins: CGH-1 (DEAD-box RNA helicase), CAR-1 (Boag et al., 2005), CPB-3 (CPEB polyA binding family), DAZ-1 (Karashima et al., 2000) and GLA-3 (TIS-11-like protein) (Boag et al., 2005; Kritikou et al., 2006; Lettre et al., 2004; Navarro et al., 2001).

While the roles of R05D3.3 and PMK-3 in regulating germ cell death remain completely unknown, the role of the RNA-binding proteins has been addressed to a certain extent. Previous studies have uncovered a network of extensive physical interactions among these proteins; CGH-1 and CAR-1 physically interact and are components of a conserved RNA-protein complex, while CBP-3 is functionally associated with CGH-1 orthologs in other species. Additionally, CBP-3 has been reported to physically interact with DAZ-1 in *C. elegans* both in *in vitro* and *in vivo* experiments (Hasegawa et al., 2006). All these physical interactions suggest that these proteins might act in a similar way to regulate germ line apoptosis and establish a link between RNA metabolism and germ cell death. The exact nature of this link as well as how these factors activate the core apoptotic machinery haven't been determined.

The discovery that RNA-binding proteins play a role in germ line apoptosis is not very surprising. In many animals germ line specification and development are known to involve characteristic RNA-protein structures, such as the P granules in *C. elegans* or the polar granules in Drosophila (Saffman and Lasko, 1999). Because loss of CGH-1 or of any of the aforementioned RNA-binding factors also result in severe germ line defects and sterility it is hard to say if these genes regulate the expression of pro-survival factors that normally protect cells from undergoing programmed cell death or of factors that are essential for cellular homeostasis and whose loss triggers programmed cell death. Identification of the target mRNAs bound by these various proteins might help distinguish between these two possibilities.

1.3.4 DNA damage-induced apoptosis

The maintenance of genomic stability is critical for the well being of all organisms, from bacteria to higher eukaryotes. To preserve the integrity of their genomes, cells possess several DNA repair systems as well as efficient proofreading mechanisms, which ensure the perpetuation of an intact genomic material. In addition,

higher organisms have developed various checkpoint control systems that, in case of damage, can arrest progression through the cell cycle. Mutations affecting the components of the repair or the checkpoint control machinery are closely linked to cancer initiation and progression (Hanahan and Weinberg, 2000).

Recent studies from the Hengartner lab led to the discovery of a conserved checkpoint pathway in the *C. elegans* germ line that, in response to DNA damage, mediates the induction of two spatially separated events. In the distal region of the gonad the proliferation of mitotic germ cells is blocked, whereas a dramatic increase in apoptosis is observed in the meiotic region of the germ line. DNA damage-induced apoptosis is mediated by the same core execution machinery as somatic programmed cell death. However, the upstream components of the pathway are genetically distinct from those involved in the regulation of developmental or physiological programmed cell death. Proteins involved in DNA damage signaling are typically divided into three categories according to their position within the signaling cascade (Figure 1.3). The more upstream components are sensor complexes that localize to the site of damaged DNA and initiate a response to it. Downstream of these lay transducers that relay the initial "damage signal" to various effector molecules by triggering a phosphorylation cascade. The latter ones will elicit specific biological responses such as the already mentioned repair processes, cell cycle arrest, apoptosis as well as changes in the transcriptional pattern of key genes.

In *C. elegans* germ cell apoptosis can be triggered using various types of exogenous genotoxic agents such as ionizing radiation, UV light, alkylating agents and chemotherapeutic drugs. Screens for mutants defective in the DNA damage responses led to the discovery of three genes *hus-1* (Hofmann et al., 2002), *mrt-2* (Ahmed and Hodgkin, 2000) and *rad-5*/*clk-2* (Ahmed et al., 2001), all of which are essential for DNA damage-induced cell cycle arrest and apoptosis. Additionally loss of function mutations in these genes have been reported to result in increased embryonic lethality (Ahmed et al., 2001; Ahmed and Hodgkin, 2000). Six years ago, *cep-1*, the *C. elegans* p53 homolog, was identified using sensitive database algorithms (Derry et al., 2001; Schumacher et al., 2001). Mutations in *cep-1* completely block ionizing radiation- and UV-C-induced apoptosis. Interestingly, CEP-1 seems to be dispensable for cell cycle arrest upon ionizing radiation (Derry et al., 2001) but not upon UV-C (Stergiou et al., 2007), unlike the situation in mammals where p53 plays a

key checkpoint role. Despite this difference, the discovery of *cep-1* together with previous work from the Hengartner lab have revealed a striking similarity of the events that follow DNA damage in worms and higher organisms. In both cases conserved checkpoint proteins activate CEP-1/p53 upon genotoxic stress which will, in turn, activate the transcription of BH3-only pro-apoptotic factors *egl-1* and *ced-13* in *C. elegans* (Hofmann et al., 2002; Schumacher et al., 2005), or PUMA and Noxa in mammals (Nakano and Vousden, 2001; Oda et al., 2000).

Recent studies from the Hengartner lab have revealed an additional layer of complexity in DNA damage responses. Stergiou and colleagues carried out an elegant genetic analysis of the cellular responses to UV-C light in the *C. elegans* germ line and identified several genes regulating the apoptotic response or cell cycle arrest (Stergiou et al., 2007). Intriguingly, many of these genes act in a signaling pathway that partially overlaps with, but is distinct from, the pathway that is activated in response to ionizing radiation. Moreover, this study identified a novel critical role of the Nucleotide Excision Repair (NER) pathway, known to be involved in the recognition and repair of UV-C induced lesions (pyrimidine dimmers and 6-4-Pps), in promoting apoptosis and cell cycle arrest. While the exact mode of action of NER in this context is not well understood all these findings argue for a stimulus-dependent role of repair components in regulating major cellular decisions and unravel the fine balance that exists between repair and apoptosis.

The complexity of the yet simple worm pathways activated upon DNA damage doesn't stop here. The sequencing of the *C. elegans* genome has revealed that a surprisingly large proportion of genes relevant for human disease have nematode counterparts. Several of these are functional orthologs of genes commonly mutated in human cancers such as *bcr-1*/BRCA1 (mutated in early onset and ovarian cancer), *abl-1*/ABL (mutated in chronic myeloid leukemia) and *lin-35*/pRB (retinoblastoma protein) to name only a few. These observations combined with the worm's simple genetics and its great potential in drug screens and high-throughout studies render *C. elegans* a very promising tool to study DNA damage responses.

1.3.5 Other pathways mediating germ line apoptosis

Recently a stress-induced pathway mediating germ cell apoptosis was defined (Salinas et al., 2006). Salinas and coworkers have studied the effect of different types of stress, such as starvation, oxidative and osmotic stress and heat-shock, on germ cell apoptosis and investigated the genetic requirements for this process. They found out that stress induced apoptosis is regulated by an *egl-1*- and *p53*-independent mechanism which is probably similar to physiological germ cell death. The authors also showed that the MAPKKs MEK-1 and the SEK-1 are essential for cell death mediated by oxidative, osmotic and heat shock stress but not for starvation suggesting that different types of environmental stress can activate different signaling pathways. Despite a very superficial characterization of the pathways involved, this study is the first systematic effort to decipher the mechanisms that activate germ cell death in response to stress that do not cause DNA damage.

Germ cell apoptosis can also be induced in response to pathogen infection via an *egl-1*-dependent pathway. The best-studied example is during infection by Salmonella bacteria. Salmonella kills *C. elegans* over the course of several days by a mechanism involving a persistent colonization of the worm's intestine and this infection has been associated with increased levels of germ cell apoptosis (Aballay and Ausubel, 2001; Aballay et al., 2000). Interestingly, *ced-3* and *ced-4* mutants which are defective for programmed cell death are also hyper-susceptible to Salmonella-mediated cell killing suggesting that in this case germ cell apoptosis plays a protective role against pathogen infection (Aballay and Ausubel, 2001). Work from the same group has also implicated a p38-mitogen-activated protein kinase (MAPK) pathway, comprising PMK-1 (MAPK), and the more upstream components SEK-1 (MAPKK) and NSY-1 (MAPKKK) in Salmonella-mediated cell death (Aballay et al., 2003; Kim et al., 2002). Activation of this signaling cascade culminates in transcriptional upregulation of *egl-1*, which in turn triggers apoptosis via a well-established mechanism. Much less is known, in contrast, about the signals generated during infection and which activate these pathways to finally trigger apoptosis in the *C. elegans* germ line. Since infection seems to be confined in the intestine it has been posited that virulence factors trigger the production of somatic signals that are transmitted in the germ line to activate apoptosis. The nature of this signals and the

mechanism by which killing germ cells protects against infection remain to be determined.

Studies of innate immunity in *C. elegans* have demonstrated that the activation of apoptosis downstream of a p38 MAPK signaling cascade, an important feature of innate immune signaling pathways, has been conserved between nematodes and mammals. They also rose for the first time the exciting possibility that programmed cell death in the germ line might be influenced, to a certain extent, by events originating in somatic tissues.

1.4 APOPTOTIC CELL CORPSE ENGULFMENT

Upon activation of apoptosis, dying cells are rapidly removed from the surrounding tissues either by professional phagocytes in higher organisms or, as is the case in *C. elegans*, by neighboring cells of different types. Engulfment is an essential process that occurs throughout life in multi-cellular animals as part of development, homeostasis and wound healing (Henson and Hume, 2006; Kawane et al., 2006; Scott et al., 2001; Wu et al., 2006). In mammals failure to dispose of apoptotic cell corpses can lead to exposure of autoantigens and it has been found to be the cause of many pathologies, such as lupus erythematosus and chronic polyarthritis (Franz et al., 2006; Gaipl et al., 2006; Kawane et al., 2006).

Despite the lack of professional phagocytic cells apoptotic cell corpse engulfment in *C. elegans* is a highly efficient process, as dying cells are internalized and mostly digested within less than one hour. Previous genetic studies in the nematode have led to the identification of at least seven major genes, *ced-1, -2, -5, -6, -7, -10* and *ced-12*, responsible for the engulfment of apoptotic cells (Ellis et al., 1991; Gumienny et al., 2001; Hedgecock et al., 1983; Wu et al., 2001; Zhou et al., 2001). In these mutants, cells deaths occur normally, but many of the dying cells fail to be engulfed and persist in the animal for several hours. These persistent cell corpses, that have the appearance of flat refractile disks, can be easily observed and quantitated using Nomarski optics.

Most of these genes do not seem to be absolutely essential for engulfment. Mutations in *ced-1, -2, -5, -6, -7,* and *ced-12* considerably delay the process of engulfment, but eventually most cell corpses disappear suggesting that engulfment of

dying cells is not completely abrogated in these mutants. Indeed, even in the strongest alleles, less than 30% of the embryonic programmed cell deaths are still visible as corpses at hatching (Hengartner, 1997).

Analysis of all the possible double mutant combinations among these seven engulfment genes together with biochemical studies have placed these genes into two partially redundant genetic groups, that define two partially redundant molecular pathways (Figure 1.4). Double mutants with mutations belonging to the same group usually exhibit the phenotype of the stronger single mutant, while double mutants carrying mutations in genes belonging to different pathways display a greatly increased, ideally additive, engulfment defect.

Interestingly, all the *C. elegans* engulfment genes have functional homologs in higher vertebrates, suggesting that the mechanisms mediating cell corpse removal are evolutionary conserved. Thus, studies of apoptotic cell corpse engulfment in the worm might help us to gain significant insights into the mechanisms mediating and regulating apoptotic corpse removal in higher organisms.

1.4.1 The ced-1, -6. -7 pathway

The first pathway consists of the genes *ced-1*, *ced-6* and *ced-7. ced-1* encodes a large transmembrane protein containing several extracellular EGF-repeats, a single transmembrane domain, and an intracellular carboxy-terminal candidate signaling domain. Mosaic analysis has demonstrated that the activity of CED-1 is required in the phagocyte rather than in the dying cell. Because fluorescently tagged CED-1 fusion proteins have been shown to be recruited around dying cells very early during engulfment, it has been proposed that CED-1 probably acts as a receptor that recognizes and binds dying cells. However, the nature of its ligand on the surface of the apoptotic cell remains elusive. The intracellular domain of CED-1 is not important for localization of CED-1 around apoptotic corpses but is important for CED-1 function *in vivo*. Structure-function analysis has revealed that it contains at least two motifs essential for engulfment: NPXY (Asn-Pro_any amino acid-Tyr) and YXXL (Tyr-any amino acid-any amino acid-Leu). Both motifs contain Tyrosine residues that can be phosphorylated and the NPXY motif has been shown to bind CED-6 via its phosphotyrosine-binding domain (PTB) (see below).

The exact mammalian homolog of CED-1 has been the subject of controversy. Three different candidates have been proposed so far based on sequence similarity, domain content and interaction studies: SREC (Scavenger Receptor from Endothelial Cells) which contains an extracellular domain similar to that of CED-1 but has no similarity to the intracellular domain, CD91 also known as LRP (LDL receptor-related protein) has a C-terminal region similar to the cytoplasmic domain of CED-1 but lacks similarity to the extracellular domain and mEFG10 which has an overall similar predicted domain structure. CD91(LRP) was also found to physically interact with the same proteins as CED-1, CED-6 and its human counterpart, and this interaction was dependent on the NPXY motif of either CED-1 or CD91.

ced-6 codes for an adaptor protein with a PTB domain, a central leucine zipper domain promoting homodimerization and a proline-rich region that contains several putative SH3-binding sites (Liu and Hengartner, 1998). Similar to CED-1, mosaic analysis indicates that CED-6 acts in the engulfing cells. Several lines of evidence suggest that CED-6 acts downstream of CED-1 to transduce signals from the CED-1 receptor which will result in cytoskeletal remodeling. Overexpression of CED-6 is able to partially rescue the engulfment defect of *ced-1* and *ced-7* mutants suggesting that *ced-6* acts genetically downstream of these two genes. This is further supported by cell biology studies showing that loss of *ced-6* function doesn't affect CED-1 clustering around corpses. CED-6::YFP is also recruited around corpses in *ced-1* dependent manner and at the same time as CED-1 suggesting a direct interaction between these two molecules *in vivo* (Kinchen et al., 2005). Last but not least, CED-6 has been shown to bind to the NPXY motif of CED-1 via its PTB domain.

The human functional homolog of *C. elegans* CED-6 is hCED-6 or GULP. Overexpression of GULP has been shown to promote engulfment in mammalian cell culture (Su et al., 2002) and in *ced-6* mutant worms suggesting that it can substitute for functional CED-6. Additionally GULP, which also possesses a PTB domain and a leucine zipper region, binds to both *C. elegans* CED-1 and CD91(LRP) proteins in a NPXY-dependent manner. Both CED-6 and GULP are believed to act as adaptor proteins ensuring the signal transduction from the CED-1 receptor to other intracellular signaling molecules, the nature of which remains to be determined.

The last gene in this pathway, *ced-7*, encodes for a transmembrane transporter of the ABC superfamily (Wu and Horvitz, 1998a). ABC transporters catalyze the

translocation of different types of molecules (e.g. lipids, proteins, sugars) across the plasma membrane by hydrolyzing ATP. Interestingly, *ced-7* is the only *C. elegans* engulfment gene that has been found to function in both the apoptotic and the engulfing cell.

The mammalian homolog of CED-7, ABCA1 is required for apoptotic cell corpse removal in mouse and is highly expressed in macrophages engaged in engulfment demonstrating that the function of *ced-7* is conserved across species (Hamon et al., 2000; Luciani and Chimini, 1996). The function of CED-7/ABCA1, however, is currently not very well understood. It has been hypothesized that ABCA1 might play a role in modulating the distribution of phosphatidylserine (PS) on the outer leaflet of the plasma membrane. PS exposure is a well-known marker of apoptotic cells and has been proposed to function as an eat me signal to promote engulfment (Fadok et al., 2001; Fadok et al., 1992). By analogy *C. elegans* CED-7 might also act in a similar way but direct testing is needed to validate this theory. Interestingly, Zhou and co-workers reported that in *ced-7* mutants CED-1::GFP fails to properly localize around apoptotic cell corpses suggesting that CED-7 cooperates with CED-1 in the recognition of apoptotic corpses. The lack of proper CED-1 clustering around cell corpses in *ced-7(lf)* mutants has been somehow controversial since our lab has been unable to reproduce this observation (Kinchen JM and Hengartner MO, unpublished observations).

1.4.2 The ced-2, -5, -12 pathway

The second pathway mediating apoptotic cell corpse engulfment is better characterized and consists of *ced-2*, *ced-5* and *ced-12*. Loss of function mutations in these genes result not only in defects in cell corpse clearance but also in a characteristic distal tip cell (DTC) migration defect phenotype, indicating that the products of these genes also control cell morphology. Similar to *ced-1* and *ced-6*, mosaic analysis has shown that the products of *ced-2*, *ced-5* and *ced-12* are exclusively required in the engulfing cells.

ced-2 encodes for a small adaptor protein which contains a N-terminal SH2 (Src-homology 2) and two SH3 (Src-homology 3) domains (Reddien and Horvitz, 2000) and is similar to mammalian CrkII, a protein involved in the regulation of cell

shape and cell motility (Klemke et al., 1998). By analogy it has been hypothesized that in *C. elegans* CED-2 might act to modulate the shape of the membrane during apoptotic cell corpse engulfment. CED-5 is a member of the CDM protein family that also comprises human DOCK180 and DOCK4 and the Drosophila Myoblast City. Both CED-5 and DOCK180 are very big proteins and contain an SH3 domain at their N-terminus, followed by a large central region containing a DOCKER domain, and a C-terminal Proline Rich Domain (PRD). Biochemical studies have shown that the DOCKER domain can act as novel type of guanine nucleotide exchange factor (GEF) for Rac (Brugnera et al., 2002), while the PRD is believed to be involved in effector protein binding. The last member of this pathway, CED-12 contains a PH domain and a proline-rich candidate SH3 binding domain, both of which are required for efficient engulfment; it is homologous to three human, ELMO1, ELMO2 and ELMO3, and one Drosophila, dCED-12, proteins, all of which share the same domain content (Gumienny et al., 2001; Wu et al., 2001; Zhou et al., 2001).

How do all these players function to control apoptotic cell corpse engulfment? Interaction studies, primarily relying on yeast two hybrid experiments, have demonstrated that the SH3 domain of CED-2 interacts which the PRD of CED-5, resulting in the recruitment of CED-5 to cell membranes (Reddien and Horvitz, 2000). Additionally, CED-5 has been shown to bind to the PRD of CED12 via its the N-terminal SH3 domain (Gumienny et al., 2001; Wu et al., 2001; Zhou et al., 2001). Finally, all three proteins have been found to interact simultaneously *in vitro* suggesting that they act as a tripartite complex (Wu et al., 2001; Zhou et al., 2001). Biochemical studies, performed with cell lines, have shown that DOCK180 and ELMO1, the mammalian counterparts of CED-5 and CED-12 respectively, can act synergistically to promote GTP loading of Rac1; this suggests a similar mode of action for CED-5 and CED-12 during engulfment in the worm (Brugnera et al., 2002; Gumienny et al., 2001). Additionally, all three CrkII, DOCK180 and ELMO have been shown to act cooperatively to promote Rac activation and engulfment in mammalian cells (Albert et al., 2000; Gumienny et al., 2001) suggesting a strong conservation of the function of the *ced-2*/*ced-5*/*ced-12* pathway across phyla.

What lies upstream of the CED-2:CED-5:CED-12 complex? Recent studies combining assays in both a cell culture system and in *C. elegans* have revealed the existence of a conserved UNC-73/TRIO-MIG-2/RhoG signaling module acting

upstream of CED-12 to regulate engulfment (deBakker et al., 2004). In this study, the authors focused their attention on the N-terminal region of CED-12 and in particular on a stretch of Armadillo repeats (ARM) which appeared to be conserved from worms to mammals. Overexpression studies demonstrated that these repeats are essential for efficient engulfment because they physically bind RhoG/MIG-2, a member of the Rho family of GTPases, which seemed to be necessary for the assembly and the activation of the CED-2/CED-5/CED-12 complex. The authors then examined the function of TRIO/UNC-73, a known GEF for RhoG, and found that it was also required for efficient engulfment in both the nematode and the mammalian system. In summary deBakker and colleagues propose a model where CED-12/ELMO plays a central role in orchestrating the activity of two GEFs, UNC-73/TRIO and CED-5/Dock180, and of their respective substrates, the small GTPases RhoG/MIG-2 and Rac1/CED-10, all of which work synergistically to promote engulfment.

Studies of mammalian integrins have suggested a role for these molecules as receptors, acting upstream of the CrkII-DOCK180 complex and leading to Rac1 activation (Albert et al., 2000). However, none of the three integrin subunits in the worm has been implicated in apoptotic cell clearance so far (Gumienny et al., 2001; Wu et al., 2001). Thus, the major receptor activating the *ced-2, -5, -12* pathway remains to be discovered.

1.4.3 ced-10 acts downstream of both engulfment pathways

CED-10 is homologous to the mammalian GTPase Rac1 and is a member of the family of Rho/Rac/Cdc42 small GTPases, a subgroup of the Ras superfamily. Members of the Rho/Rac/Cdc42 family are involved in the control of cell morphology via regulation of the cytoskeleton in several different biological contexts, such as axon guidance, lamelipodia and filopodia formation as well as phagocytosis of opsonized particles in mammals (Hall, 1998; Hall and Nobes, 2000). Loss of CED-10 function impairs apoptotic cell corpse engulfment in the worm but also leads to a variety of defects in cell migration, including the migration of DTCs, axon outgrowth and morphogenetic movements during early embryonic development (Kishore and Sundaram, 2002; Lundquist et al., 2001; Reddien and Horvitz, 2000; Steven et al., 1998). These observations implicate CED-10 in the regulation of cytoskeleton in

response to a variety of extracellular stimuli. Further, they suggest that CED-10 and Rac1 might share similar functions and define an *in vivo* role for Rac proteins in the removal of apoptotic cells.

Initial genetic studies have placed *ced-10* in the *ced-2*, *ced-5*, *ced-12* pathway for engulfment based on double mutant analysis and overexpression experiments, which were not complete (Ellis et al., 1991; Reddien and Horvitz, 2000). However, to date genetic and cell biology studies, which were carried out with a recently isolated *ced-10* null allele, have placed CED-10/Rac downstream of both pathways revealing that signaling through the *ced-1*, *-6*, *-7* pathway also culminates in activation of this GTPase (Kinchen et al., 2005). In this study, Kinchen and coworkers elegantly showed that loss of function mutations in *ced-1*, *ced-6* and *ced-7* abrogate polymerization of actin around apoptotic germ cell corpses and that overexpression of *ced-10* rescues the engulfment defects of these mutants. These observations were further supported by double mutant analysis using a *ced-10* null, which suggested that *ced-10* acts genetically downstream of both pathways. The discrepancies between the results of Kinchen et al. and previously published studies and can be attributed to the use of weak *ced-10* alleles by Ellis et al. as well as and Reddien and Horvitz, which did not completely eliminate gene function.

A hallmark of the mode of action of GTPases is their ability to cycle between a GTP-bound/active and GDP-bound/inactive state. Regulatory proteins known as GEFs (Guanine nucleotide exchange factors) and GAPs (GTPase activating proteins) can shift the balance towards one way or another, by increasing affinity for the GTP or activating the GTPase activity respectively. The mechanism by which the *ced-2*, *-5, -12* pathway activates CED-10 has been relatively well-defined. As mentioned before, biochemical studies have suggested that the CED-5/Dock180:CED-12/ELMO complex (Gumienny et al., 2001; Wu and Horvitz, 1998b; Wu et al., 2001; Zhou et al., 2001) acts as an unconventional GEF to facilitate GTP loading, and thus activation of, CED-10. In contrast, it is currently unclear how signaling through the *ced-1*, *-6*, *-7* pathway impacts on CED-10 activity especially in the absence of a functional GEF in this pathway. Future experiments should focus on understanding how this is accomplished.

1.4.4 The dynamin case

Work from Zheng Zhou's laboratory has led to the identification of a novel player in apoptotic cell corpse engulfment. In a recent study, Yu and co-workers reported that *dyn-1*, which encodes the only *C. elegans* homolog of mammalian dynamins, acts downstream of CED-1 to mediate internalization and degradation of cell corpses (Yu et al., 2006). Dynamins are large GTPases that belong to a heterogeneous protein superfamily consisting of classical dynamins, dynamin-like and several other proteins (for review see Praefcke and McMahon, 2004). The distinction between all these classes of proteins relies on their domain content and only classical dynamins, such as DYN-1 and mammalian dynamins 1, 2 and 3, have the following five domains: a GTPase domain at the N-terminus, a middle domain, a PH domain, a GED and a C-terminal PRD ensuring the binding of effector proteins.

Previous screens for engulfment genes were designed in such a way that allowed the isolation of viable mutants only. In order to identify engulfment genes with other essential functions, Yu et al. screened for mutants exhibiting defects cell corpse clearance and an arrest during embryogenesis. From this screen, fourteen of the isolated mutants had lesions within the *dyn-1* coding region, most of them clustering in the GTPase domain, suggesting a crucial, and novel, function for this gene in engulfment. In *C. elegans*, loss of DYN-1 function has been previously associated with defects in synaptic vesicle recycling (Clark et al., 1997), clathrin-mediated endocytosis (Sato et al., 2006) as well as with defects in cytokinesis (Thompson et al., 2002). Importantly, in their study, Yu et al. provide evidence that the newly identified function of *dyn-1* during engulfment is independent of its role in endocytosis.

Localization studies showed that DYN-1 is recruited to extending pseudopods where it colocalized with the CED-1 receptor. Double mutant analysis was also used to place *dyn-1* genetically downstream of the ced-1, ced-6, ced-7 pathway and this result was further supported by cell biology studies demonstrating that recruitment of DYN-1 to the sites of engulfment was dependent on these genes. Interestingly, according to this study, in the absence of functional DYN-1 a large percentage of

corpses are still engulfed but persist inside the phagocytes suggesting that DYN-1 also functions at a step after phagosome closure, probably during corpse digestion.

To further characterize the function of DYN-1 in corpse clearance Yu et al. used an endosome marker and monitored the recruitment of vesicles at the site of engulfment. The authors showed that endosomes, which normally cluster at engulfment sites, fail to do so in *dyn-1* mutant animals, suggesting that DYN-1 controls the recruitment/delivery of endocytic vesicles to the site of engulfment as well as their fusion with the plasma membrane. This has been hypothesized to serve two purposes: delivery of membrane to allow for pseudopod extension and delivery of factors that will lead to corpse degradation within the phagolysosome.

Yu and colleagues performed a comprehensive analysis of DYN-1 function during phagocytosis of apoptotic cells in *C. elegans* and speculated that the mode of action of dynamins in engulfment is conserved. In Chapter 3 of this thesis, Dr. Jason Kinchen and myself provide our personal version of the role of dynamins in both the nematode and in mammalian cells. Despite some similarities with the results of Yu et al., our work demonstrates that the primary conserved function of dynamin is to regulate entry of the newly formed phagosome in the degradative pathway and not to ensure membrane delivery. Additionally, our cell biology and DYN-1 localization studies showed that mutations in either engulfment pathway compromise recruitment of DYN-1 around apoptotic cells, suggesting that *dyn-1* functions downstream of both engulfment pathways. Our work on *dyn-1* prompted us to investigate further the pathways mediating corpse degradation in *C. elegans*, which resulted in the discovery of the core components of a conserved pathway mediating phagosome maturation.

Dynamin proteins are known to be mechanistically involved in vesicle fission by assembling in a compact ring structure around the neck of endocytic vesicles and then using their GTPase to expand like a spring and detach the vesicles from the plasma membrane. The results described here suggest that dynamin can additionally promote vesicle fusion and/or could participate in active transport of vesicle along cytoskeletal tracks. Biochemical studies of the function of dynamins in the context of engulfment should help us understand its exact mode of action.

1.4.5 Phosphatidylserine exposure and engulfment

Phosphatidylserine (PS) is a normal, although quantitatively minor, constituent of cellular membranes. In living cells, PS is normally asymmetrically distributed in the plasma membrane so that essentially all of the PS is restricted to the cytosolic inner leaflet. During apoptosis this asymmetry collapses and PS becomes exposed on the cell surface where it is thought to act as one of the major "eat-me" signals, which allow recognition of the apoptotic cell by the phagocytes.

Previous work has suggested that PS, once exposed on the surface of the cell, is recognized by the phosphatidylserine receptor (PSR), a protein expressed in most phagocytes and which has been shown to specifically bind to PS *in vitro* (Fadok et al., 2000). In support of this model, disruption of the *Ptdsr* gene in mice and a deletion in the single *C. elegans* phosphatidylserine receptor homolog, *psr-1,* have been reported to result in increased numbers of non-phagocytosed corpses (Hong et al., 2004; Li et al., 2003; Wang et al., 2003). Double mutant analysis complemented by physical interaction studies, have placed *psr-1* in the *ced-2*/*ced-5*/*ced-12* pathway leading to the hypothesis that PSR-1 could be one of the receptors activating this pathway in the nematode; the extremely mild engulfment defects of *psr-1* mutant worms observed by Wang and coworkers, suggest, however, that PSR-1 is not the major receptor upstream of *ced-2, -5, -12*.

Intriguingly, the role of PSR in apoptotic cell clearance has recently been questioned. An independently generated strain of *Ptdsr* knockout mouse did not display any defects in engulfment of dead cells, but rather, increased perinatal lethality accompanied by severe differentiation defects in many tissues (Bose et al., 2004; Williamson and Schlegel, 2004). These observations clearly show that the putative phosphatidylserine receptor has other essential functions during early development. Also, analysis of at least two *C. elegans psr-1* deletion alleles (including the allele used by Wang and coworkers) by the Hengartner laboratory didn't confirm the presence of persistent cell corpses compromising the suggested role of *psr-1* in apoptotic cell clearance (Zullig et al., 2007). Last but not least, an increasing amount of evidence suggests that the PS receptor is localized in the nucleus, rather than on the plasma membrane, challenging the view that it acts as a receptor (Clissold and Ponting, 2001; Cui et al., 2004; Savill et al., 2003). It is thus unclear whether this protein plays any role during engulfment of apoptotic cells.

Similar to *psr-1*, *nex-1* is another *C. elegans* candidate engulfment gene identified on the basis of protein sequence homology to a protein involved in mammalian engulfment. NEX-1 is homologous to annexin I, a PS-binding protein, which has been shown to translocate from the cytosol to the outer leaflet of the plasma membrane of dying cells (Arur et al., 2003). Mammalian annexin I colocalizes with exposed PS and is required for efficient clustering of PS receptor around apoptotic cells. RNAi-mediated knockdown of both annexin I and of the *C. elegans* homolog, *nex-1,* interferes with engulfment in a cell culture system and in the worm, respectively. Putative *nex-1* deletion mutants, however, do not display a persistent cell corpse phenotype (Reddien and Horvitz, 2004). Perhaps the deletion does not fully eliminate the activity of NEX-1 or maybe the effect of RNAi is other than simply reducing *nex-1* function. Thus, the role of *nex-1* in the worm remains somewhat ambiguous.

Which molecules are mediating PS exposure? Recently, three independent studies tried to address this question using *C. elegans* as a model system (Venegas and Zhou, 2007; Wang et al., 2007; Zullig et al., 2007). All these studies established relatively elegant, but quite artificial, tools to monitor PS exposure and screened for genes which would interfere with this process. Three genes were proposed to mediate PS exposure in *C. elegans*: *scrm-1* (scramblase-1) and *plsc-1*/*scrm-3* (phospholipid scramblase-1), two putative phospholipid scramblases, and *tat-1,* which codes for a transbilayer amphipathic transporter. Curiously, not only all these three studies identified different genes but, depending on the study, different results were obtained for the same candidates. The reason for these discrepancies is currently not known. Although it is likely that a cell possesses several different ways to expose PS, this doesn't explain why there is no overlap between the different genes identified by these studies. It would be interesting to compare the results obtained for each candidate using all the three different PS-exposure reporter systems available.

1.4.6 Phagosome maturation in C. elegans

While several players regulating the early steps of corpse recognition and internalization have been characterized (Gardai et al., 2006; Reddien and Horvitz, 2004), the molecules and mechanisms relevant to the subsequent processing of

internalized corpses are poorly defined. In Chapter 3 I report the identification and the characterization of a novel pathway for the processing of internalized apoptotic cells in *C. elegans* and in mammals. Using a series of targeted or unbiased reverse genetic screens we identified over a dozen of genes with previously uncharacterized role in engulfment. Using cell biology, genetics and biochemical studies we ordered these genes in a linear and conserved pathway mediating phagosome maturation (Figure 1.1). This is the first study in the worm of the complex sequence of events occurring after internalization of apoptotic corpses inside the phagocyte and it has shown that *C. elegans* is an attractive model system to study these processes.

1.4.7 Open questions

Over the last 15 years intensive studies of apoptotic cell corpse engulfment in *C. elegans*, but also in other organisms, have significantly enhanced our understanding of this complex process. However, many genes involved in engulfment remain to be identified as illustrated by the numerous gaps that exist in the current model for engulfment. Which is the major receptor that activates the CED-2, -5, -12 pathway? What is the nature of the ligands on the surface of the dying cell that activate each one of the engulfment pathways? How does CED-6 transduce signals to activate CED-10? Once CED-10 is activated how does it drive pseudopod extension? How important is the contribution of PS exposure in phagocytosis and what is the precise role of the PS receptor? These are only some of the questions that need to find an answer within the next few years.

1.5 APOPTOTIC DNA DEGRADATION

Apoptotic cell death is defined by a series of morphological changes of cells such as cytoplasmic shrinkage, condensation and fragmentation of nuclei, and blebbing of the plasma membranes (Kerr et al., 1972). An additional hallmark of apoptosis is the degradation of chromosomal DNA of dying cells into a ladder of characteristic oligonucleosomal-length fragments (Wyllie, 1980). In mammals many enzymes and factors have been proposed to function in apoptotic DNA degradation including, DNaseI, DNaseII, DNase gamma, cyclophilin, caspase-activated DNAse (CAD, also known as DFF40) and the mitochondrial endonuclease G (reviewed by

(Nagata, 2005; Samejima and Earnshaw, 2005). All these players are organized into two independent degradation systems: a cell autonomous system that functions in dying cells and non-autonomous system which takes place in phagocytes after engulfment of the dying cell (Nagata, 2005).

C. elegans NUC-1 (*nuc*lease abnormal-1) was the first worm nuclease involved in DNA degradation during apoptotic cell death and was discovered more than 30 years ago (Sulston, 1976). Loss of NUC-1 function results in the accumulation of TUNEL-positive nuclei in mutant embryos indicating that NUC-1 acts to resolve 3'OH DNA breaks (labelled by TUNEL) generated during apoptosis (Wu et al., 2000). Additionally, *nuc-1* mutants fail to digest the DNA of ingested bacteria in the intestine and exhibit increased numbers of Syto-11 positive pycnotic bodies, due to the inability of engulfing cells to degrade DNA derived from postembryonic cell deaths. Loss of NUC-1 activity, however, has no effect on the number and the kinetics of embryonic cell deaths, or on apoptotic cell corpse engulfment suggesting that NUC-1 is dispensable for cell killing (Hedgecock et al., 1983; Parrish and Xue, 2003; Wu et al., 2000).

The *nuc-1* locus encodes an acid-dependent nuclease similar to mammalian DNase II (Hevelone and Hartman, 1988; Lyon et al., 2000; Wu et al., 2000). Studies of DNaseII mutants in *C. elegans*, Drosophila and mouse have suggested that this enzyme acts primarily within the phagolysosome during engulfment-mediated DNA degradation (Kawane et al., 2003; Krieser et al., 2002; Wu et al., 2000). A handful of genetic evidence implies, however, that NUC-1 might also act during cell-autonomous DNA fragmentation in the worm. More experiments, such as mosaic analysis or tissue-specific phenotypic rescues, are needed in order to clearly define whether this is the case.

More recent genetic and biochemical studies in *C. elegans* have led to the discovery of numerous genes involved in apoptotic DNA degradation (Table 1.1). These comprise six cell death related nucleases (*crn* genes), *cyp-13* (cyclophilin-13) as well as *cps-6* (ced-3 protease suppressor-6) (Parrish et al., 2001; Parrish and Xue, 2003). CPS-6, which was among the first molecules identified to affect DNA degradation in the worm, encodes the nematode homologue of mitochondrial endonuclease G, a protein normally involved in mitochondrial replication. It has been show to cooperate with WAH-1 (worm AIF homolog-1), the worm homolog of

apoptosis-inducing factor (AIF) to promote DNA degradation, but also cell killing in both the nematode and mammalian systems (Li et al., 2001; Parrish et al., 2001; Wang et al., 2002).

Parrish and Xue, who studied the role of most of the aforementioned factors in DNA degradation using reverse genetic approaches, also showed that there are at least two cell autonomous DNA degradation pathways. RNAi against *crn* genes results in an accumulation of TUNEL-positive cells in *C. elegans* embryos and with the exception of *crn-6(RNAi)* and *nuc-1(lf)* in a delay of cell death and inhibition of cell killing in sensitized backgrounds. Additionally, reduction of the activity of *crn-2* and *crn-3* by RNAi, but not of any other *crn* nucleases enhances the TUNEL phenotype of the *cps-6* mutants, suggesting that *crn-2* and *crn-3* likely act in a pathway different from that of *cps-6* and the rest of the *crn* genes. This genetic approach was nicely complemented by biochemical studies which demonstrated that several of these nucleases assemble to form a multi-enzyme complex known as the degradosome (Parrish et al., 2001; Parrish and Xue, 2003); this complex contains CPS-6 and WAH-1 along with 6 other cell death related nucleases all of which contribute to cell-autonomous apoptotic DNA cleavage. CRN-2 /CRN-3, are not part of this complex further supporting the view that they function as standalone players in a different DNA fragmentation pathway which is parallel to the degradosome.

Unlike all the other nucleases NUC-1 and CRN-6 seem to be dispensable for programmed cell death and are believed to function during the later stages of the apoptotic program. Even though CRN-6 is also homologous to DNaseII, its inhibition by RNAi doesn't result in neither an accumulation of bacterial DNA in the worm's intestine nor in the appearance of pycnotic bodies, suggesting that, unlike NUC-1, *crn* nucleases are specifically involved in DNA degradation during programmed cell death.

All these studies have revealed a surprising degree of complexity and identified a variety of different molecules, which assemble into sophisticated systems to regulate apoptotic DNA fragmentation. While cell autonomous-DNA degradation is not essential for cell death, processing of cell corpses by the phagocytes especially during development is critical for life in higher organisms. DNA degradation has also been proposed to act to eliminate viral or other harmful DNA, to amplify other death signals as part of a signaling pathway that connects to DNA damage and repair, and to

prevent self-immunization with DNA which a potent auto-antigen. Future work should focus on elucidating the mechanisms accomplishing each one of these different roles.

1.6 FUTURE PERSPECTIVES

Genetic studies in *C. elegans* have been instrumental in the identification of a cell death machinery which has been found to be surprisingly well conserved from worms to mammals. The recent discoveries of the *C. elegans* p53 homolog, *cep-1,* as well as of the, so far overlooked, role of mitochondria in worm apoptosis clearly demonstrate that there are plenty of things we still ignore about *C. elegans* programmed cell death. Increasing efforts to complement the traditional genetic methodology with cell biology, biochemistry and notably large-scale systems biology approaches will certainly continue to enhance our understanding of the biology of apoptosis and of *C. elegans* as a model organism.

1.7 REFERENCES

Aballay, A., and Ausubel, F. M. (2001). Programmed cell death mediated by ced-3 and ced-4 protects Caenorhabditis elegans from Salmonella typhimurium-mediated killing. Proc Natl Acad Sci U S A *98*, 2735-2739.

Aballay, A., Drenkard, E., Hilbun, L. R., and Ausubel, F. M. (2003). Caenorhabditis elegans innate immune response triggered by Salmonella enterica requires intact LPS and is mediated by a MAPK signaling pathway. Curr Biol *13*, 47-52.

Aballay, A., Yorgey, P., and Ausubel, F. M. (2000). Salmonella typhimurium proliferates and establishes a persistent infection in the intestine of Caenorhabditis elegans. Curr Biol *10*, 1539-1542.

Acehan, D., Jiang, X., Morgan, D. G., Heuser, J. E., Wang, X., and Akey, C. W. (2002). Three-dimensional structure of the apoptosome: implications for assembly, procaspase-9 binding, and activation. Mol Cell *9*, 423-432.

Adams, J. M., and Cory, S. (2001). Life-or-death decisions by the Bcl-2 protein family. Trends Biochem Sci *26*, 61-66.

Adrain, C., Creagh, E. M., and Martin, S. J. (2001). Apoptosis-associated release of Smac/DIABLO from mitochondria requires active caspases and is blocked by Bcl-2. Embo J *20*, 6627-6636.

Ahmed, S., Alpi, A., Hengartner, M. O., and Gartner, A. (2001). C. elegans RAD-5/CLK-2 defines a new DNA damage checkpoint protein. Curr Biol *11*, 1934-1944.

Ahmed, S., and Hodgkin, J. (2000). MRT-2 checkpoint protein is required for germ line immortality and telomere replication in C. elegans. Nature *403*, 159-164.

Albert, M. L., Kim, J. I., and Birge, R. B. (2000). alphavbeta5 integrin recruits the CrkII-Dock180-rac1 complex for phagocytosis of apoptotic cells. Nat Cell Biol *2*, 899-905.

Alnemri, E. S., Livingston, D. J., Nicholson, D. W., Salvesen, G., Thornberry, N. A., Wong, W. W., and Yuan, J. (1996). Human ICE/CED-3 protease nomenclature. Cell *87*, 171.

Arur, S., Uche, U. E., Rezaul, K., Fong, M., Scranton, V., Cowan, A. E., Mohler, W., and Han, D. K. (2003). Annexin I is an endogenous ligand that mediates apoptotic cell engulfment. Dev Cell *4*, 587-598.

Bloss, T. A., Witze, E. S., and Rothman, J. H. (2003). Suppression of CED-3-independent apoptosis by mitochondrial betaNAC in Caenorhabditis elegans. Nature *424*, 1066-1071.

Boag, P. R., Nakamura, A., and Blackwell, T. K. (2005). A conserved RNA-protein complex component involved in physiological germ line apoptosis regulation in C. elegans. Development *132*, 4975-4986.

Boise, L. H., Gonzalez-Garcia, M., Postema, C. E., Ding, L., Lindsten, T., Turka, L. A., Mao, X., Nunez, G., and Thompson, C. B. (1993). bcl-x, a bcl-2-related gene that functions as a dominant regulator of apoptotic cell death. Cell *74*, 597-608.

Bose, J., Gruber, A. D., Helming, L., Schiebe, S., Wegener, I., Hafner, M., Beales, M., Kontgen, F., and Lengeling, A. (2004). The phosphatidylserine receptor has essential functions during embryogenesis but not in apoptotic cell removal. J Biol *3*, 15.

Bossy-Wetzel, E., Newmeyer, D. D., and Green, D. R. (1998). Mitochondrial cytochrome c release in apoptosis occurs upstream of DEVD-specific caspase activation and independently of mitochondrial transmembrane depolarization. Embo J *17*, 37-49.

Boyd, J. M., Gallo, G. J., Elangovan, B., Houghton, A. B., Malstrom, S., Avery, B. J., Ebb, R. G., Subramanian, T., Chittenden, T., Lutz, R. J., and et al. (1995). Bik, a novel death-inducing protein shares a distinct sequence motif with Bcl-2 family proteins and interacts with viral and cellular survival-promoting proteins. Oncogene *11*, 1921-1928.

Brugnera, E., Haney, L., Grimsley, C., Lu, M., Walk, S. F., Tosello-Trampont, A. C., Macara, I. G., Madhani, H., Fink, G. R., and Ravichandran, K. S. (2002). Unconventional Rac-GEF activity is mediated through the Dock180-ELMO complex. Nat Cell Biol *4*, 574-582.

Budihardjo, I., Oliver, H., Lutter, M., Luo, X., and Wang, X. (1999). Biochemical pathways of caspase activation during apoptosis. Annu Rev Cell Dev Biol *15*, 269-290.

Cain, K., Bratton, S. B., Langlais, C., Walker, G., Brown, D. G., Sun, X. M., and Cohen, G. M. (2000). Apaf-1 oligomerizes into biologically active approximately 700-kDa and inactive approximately 1.4-MDa apoptosome complexes. J Biol Chem *275*, 6067-6070.

Chen, F., Hersh, B. M., Conradt, B., Zhou, Z., Riemer, D., Gruenbaum, Y., and Horvitz, H. R. (2000). Translocation of C. elegans CED-4 to nuclear membranes during programmed cell death. Science *287*, 1485-1489.

Chinnaiyan, A. M., Chaudhary, D., O'Rourke, K., Koonin, E. V., and Dixit, V. M. (1997a). Role of CED-4 in the activation of CED-3. Nature *388*, 728-729.

Chinnaiyan, A. M., O'Rourke, K., Lane, B. R., and Dixit, V. M. (1997b). Interaction of CED-4 with CED-3 and CED-9: a molecular framework for cell death. Science *275*, 1122-1126.

Chittenden, T., Harrington, E. A., O'Connor, R., Flemington, C., Lutz, R. J., Evan, G. I., and Guild, B. C. (1995). Induction of apoptosis by the Bcl-2 homologue Bak. Nature *374*, 733-736.

Choi, S. S., Park, I. C., Yun, J. W., Sung, Y. C., Hong, S. I., and Shin, H. S. (1995). A novel Bcl-2 related gene, Bfl-1, is overexpressed in stomach cancer and preferentially expressed in bone marrow. Oncogene *11*, 1693-1698.

Church, D. L., Guan, K. L., and Lambie, E. J. (1995). Three genes of the MAP kinase cascade, mek-2, mpk-1/sur-1 and let-60 ras, are required for meiotic cell cycle progression in Caenorhabditis elegans. Development *121*, 2525-2535.

Clark, S. G., Shurland, D. L., Meyerowitz, E. M., Bargmann, C. I., and van der Bliek, A. M. (1997). A dynamin GTPase mutation causes a rapid and reversible temperature-inducible locomotion defect in C. elegans. Proc Natl Acad Sci U S A *94*, 10438-10443.

Clissold, P. M., and Ponting, C. P. (2001). JmjC: cupin metalloenzyme-like domains in jumonji, hairless and phospholipase A2beta. Trends Biochem Sci *26*, 7-9.

Conradt, B. (2001). Cell engulfment, no sooner ced than done. Dev Cell *1*, 445-447.

Conradt, B., and Horvitz, H. R. (1998). The C. elegans protein EGL-1 is required for programmed cell death and interacts with the Bcl-2-like protein CED-9. Cell *93*, 519-529.

Conradt, B., and Horvitz, H. R. (1999). The TRA-1A sex determination protein of C. elegans regulates sexually dimorphic cell deaths by repressing the egl-1 cell death activator gene. Cell *98*, 317-327.

Conus, S., Rosse, T., and Borner, C. (2000). Failure of Bcl-2 family members to interact with Apaf-1 in normal and apoptotic cells. Cell Death Differ *7*, 947-954.

Crittenden, S. L., Troemel, E. R., Evans, T. C., and Kimble, J. (1994). GLP-1 is localized to the mitotic region of the C. elegans germ line. Development *120*, 2901-2911.

Cui, P., Qin, B., Liu, N., Pan, G., and Pei, D. (2004). Nuclear localization of the phosphatidylserine receptor protein via multiple nuclear localization signals. Exp Cell Res *293*, 154-163.

deBakker, C. D., Haney, L. B., Kinchen, J. M., Grimsley, C., Lu, M., Klingele, D., Hsu, P. K., Chou, B. K., Cheng, L. C., Blangy, A., *et al.* (2004). Phagocytosis of apoptotic cells is regulated by a UNC-73/TRIO-MIG-2/RhoG signaling module and armadillo repeats of CED-12/ELMO. Curr Biol *14*, 2208-2216.

Derry, W. B., Putzke, A. P., and Rothman, J. H. (2001). Caenorhabditis elegans p53: role in apoptosis, meiosis, and stress resistance. Science *294*, 591-595.

Deveraux, Q. L., and Reed, J. C. (1999). IAP family proteins--suppressors of apoptosis. Genes Dev *13*, 239-252.

Earnshaw, W. C., Martins, L. M., and Kaufmann, S. H. (1999). Mammalian caspases: structure, activation, substrates, and functions during apoptosis. Annu Rev Biochem *68*, 383-424.

Ellis, H. M., and Horvitz, H. R. (1986). Genetic control of programmed cell death in the nematode C. elegans. Cell *44*, 817-829.

Ellis, R. E., and Horvitz, H. R. (1991). Two C. elegans genes control the programmed deaths of specific cells in the pharynx. Development *112*, 591-603.

Ellis, R. E., Jacobson, D. M., and Horvitz, H. R. (1991). Genes required for the engulfment of cell corpses during programmed cell death in Caenorhabditis elegans. Genetics *129*, 79-94.

Fadok, V. A., Bratton, D. L., Rose, D. M., Pearson, A., Ezekewitz, R. A., and Henson, P. M. (2000). A receptor for phosphatidylserine-specific clearance of apoptotic cells. Nature *405*, 85-90.

Fadok, V. A., de Cathelineau, A., Daleke, D. L., Henson, P. M., and Bratton, D. L. (2001). Loss of phospholipid asymmetry and surface exposure of phosphatidylserine is required for phagocytosis of apoptotic cells by macrophages and fibroblasts. J Biol Chem *276*, 1071-1077.

Fadok, V. A., Voelker, D. R., Campbell, P. A., Cohen, J. J., Bratton, D. L., and Henson, P. M. (1992). Exposure of phosphatidylserine on the surface of apoptotic lymphocytes triggers specific recognition and removal by macrophages. J Immunol *148*, 2207-2216.

Fesik, S. W., and Shi, Y. (2001). Structural biology. Controlling the caspases. Science *294*, 1477-1478.

Frank, S., Gaume, B., Bergmann-Leitner, E. S., Leitner, W. W., Robert, E. G., Catez, F., Smith, C. L., and Youle, R. J. (2001). The role of dynamin-related protein 1, a mediator of mitochondrial fission, in apoptosis. Dev Cell *1*, 515-525.

Franz, S., Gaipl, U. S., Munoz, L. E., Sheriff, A., Beer, A., Kalden, J. R., and Herrmann, M. (2006). Apoptosis and autoimmunity: when apoptotic cells break their silence. Curr Rheumatol Rep *8*, 245-247.

Gaipl, U. S., Sheriff, A., Franz, S., Munoz, L. E., Voll, R. E., Kalden, J. R., and Herrmann, M. (2006). Inefficient clearance of dying cells and autoreactivity. Curr Top Microbiol Immunol *305*, 161-176.

Gardai, S. J., Bratton, D. L., Ogden, C. A., and Henson, P. M. (2006). Recognition ligands on apoptotic cells: a perspective. J Leukoc Biol *79*, 896-903.

Gartner, A., Milstein, S., Ahmed, S., Hodgkin, J., and Hengartner, M. O. (2000). A conserved checkpoint pathway mediates DNA damage--induced apoptosis and cell cycle arrest in C. elegans. Mol Cell *5*, 435-443.

Glucksmann, A. (1950). Cell deaths in normal vertebrate ontogeny. Biol Rev, Cambridge Philos Soc *26*, 59-86.

Gross, A., McDonnell, J. M., and Korsmeyer, S. J. (1999). BCL-2 family members and the mitochondria in apoptosis. Genes Dev *13*, 1899-1911.

Gumienny, T. L., Brugnera, E., Tosello-Trampont, A. C., Kinchen, J. M., Haney, L. B., Nishiwaki, K., Walk, S. F., Nemergut, M. E., Macara, I. G., Francis, R., *et al*. (2001). CED-12/ELMO, a novel member of the CrkII/Dock180/Rac pathway, is required for phagocytosis and cell migration. Cell *107*, 27-41.

Gumienny, T. L., Lambie, E., Hartwieg, E., Horvitz, H. R., and Hengartner, M. O. (1999). Genetic control of programmed cell death in the Caenorhabditis elegans hermaphrodite germ line. Development *126*, 1011-1022.

Hall, A. (1998). Rho GTPases and the actin cytoskeleton. Science *279*, 509-514.

Hall, A., and Nobes, C. D. (2000). Rho GTPases: molecular switches that control the organization and dynamics of the actin cytoskeleton. Philos Trans R Soc Lond B Biol Sci *355*, 965-970.

Hall, D. H., Winfrey, V. P., Blaeuer, G., Hoffman, L. H., Furuta, T., Rose, K. L., Hobert, O., and Greenstein, D. (1999). Ultrastructural features of the adult hermaphrodite gonad of Caenorhabditis elegans: relations between the germ line and soma. Dev Biol *212*, 101-123.

Hamon, Y., Broccardo, C., Chambenoit, O., Luciani, M. F., Toti, F., Chaslin, S., Freyssinet, J. M., Devaux, P. F., McNeish, J., Marguet, D., and Chimini, G. (2000). ABC1 promotes engulfment of apoptotic cells and transbilayer redistribution of phosphatidylserine. Nat Cell Biol *2*, 399-406.

Han, J., Sabbatini, P., and White, E. (1996). Induction of apoptosis by human Nbk/Bik, a BH3-containing protein that interacts with E1B 19K. Mol Cell Biol *16*, 5857-5864.

Hanahan, D., and Weinberg, R. A. (2000). The hallmarks of cancer. Cell *100*, 57-70.

Haraguchi, M., Torii, S., Matsuzawa, S., Xie, Z., Kitada, S., Krajewski, S., Yoshida, H., Mak, T. W., and Reed, J. C. (2000). Apoptotic protease activating factor 1 (Apaf-1)-independent cell death suppression by Bcl-2. J Exp Med *191*, 1709-1720.

Hasegawa, E., Karashima, T., Sumiyoshi, E., and Yamamoto, M. (2006). C. elegans CPB-3 interacts with DAZ-1 and functions in multiple steps of germ line development. Dev Biol *295*, 689-699.

Hausmann, G., O'Reilly, L. A., van Driel, R., Beaumont, J. G., Strasser, A., Adams, J. M., and Huang, D. C. (2000). Pro-apoptotic apoptosis protease-activating factor 1 (Apaf-1) has a cytoplasmic localization distinct from Bcl-2 or Bcl-x(L). J Cell Biol *149*, 623-634.

Hedgecock, E. M., Sulston, J. E., and Thomson, J. N. (1983). Mutations affecting programmed cell deaths in the nematode Caenorhabditis elegans. Science *220*, 1277-1279.

Hegde, R., Srinivasula, S. M., Ahmad, M., Fernandes-Alnemri, T., and Alnemri, E. S. (1998). Blk, a BH3-containing mouse protein that interacts with Bcl-2 and Bcl-xL, is a potent death agonist. J Biol Chem *273*, 7783-7786.

Hengartner, M. O. (1997). Cell Death. In C. elegans II, D. L. Riddle, T. Blumenthal, B. J. Meyer, and J. R. Priess, eds. (New York, Cold Spring Harbor Press), pp. 383-416.

Hengartner, M. O., Ellis, R. E., and Horvitz, H. R. (1992). Caenorhabditis elegans gene ced-9 protects cells from programmed cell death. Nature *356*, 494-499.

Hengartner, M. O., and Horvitz, H. R. (1994). C. elegans cell survival gene ced-9 encodes a functional homolog of the mammalian proto-oncogene bcl-2. Cell *76*, 665-676.

Henson, P. M., and Hume, D. A. (2006). Apoptotic cell removal in development and tissue homeostasis. Trends Immunol *27*, 244-250.

Hevelone, J., and Hartman, P. S. (1988). An endonuclease from Caenorhabditis elegans: partial purification and characterization. Biochem Genet *26*, 447-461.

Hirsh, D., Oppenheim, D., and Klass, M. (1976). Development of the reproductive system of Caenorhabditis elegans. Dev Biol *49*, 200-219.

Hoeppner, D. J., Hengartner, M. O., and Schnabel, R. (2001). Engulfment genes cooperate with ced-3 to promote cell death in Caenorhabditis elegans. Nature *412*, 202-206.

Hofmann, E. R., Milstein, S., Boulton, S. J., Ye, M., Hofmann, J. J., Stergiou, L., Gartner, A., Vidal, M., and Hengartner, M. O. (2002). Caenorhabditis elegans HUS-1 is a DNA damage checkpoint protein required for genome stability and EGL-1-mediated apoptosis. Curr Biol *12*, 1908-1918.

Hofmann, K., Bucher, P., and Tschopp, J. (1997). The CARD domain: a new apoptotic signalling motif. Trends Biochem Sci *22*, 155-156.

Hong, J. R., Lin, G. H., Lin, C. J., Wang, W. P., Lee, C. C., Lin, T. L., and Wu, J. L. (2004). Phosphatidylserine receptor is required for the engulfment of dead apoptotic cells and for normal embryonic development in zebrafish. Development *131*, 5417-5427.

Horvitz, H. R., Shaham, S., and Hengartner, M. O. (1994). The genetics of programmed cell death in the nematode Caenorhabditis elegans. Cold Spring Harb Symp Quant Biol *59*, 377-385.

Hsu, S. Y., Kaipia, A., McGee, E., Lomeli, M., and Hsueh, A. J. (1997). Bok is a pro-apoptotic Bcl-2 protein with restricted expression in reproductive tissues and heterodimerizes with selective anti-apoptotic Bcl-2 family members. Proc Natl Acad Sci U S A *94*, 12401-12406.

Hsu, S. Y., Lin, P., and Hsueh, A. J. (1998). BOD (Bcl-2-related ovarian death gene) is an ovarian BH3 domain-containing proapoptotic Bcl-2 protein capable of dimerization with diverse antiapoptotic Bcl-2 members. Mol Endocrinol *12*, 1432-1440.

Hu, Y., Ding, L., Spencer, D. M., and Nunez, G. (1998). WD-40 repeat region regulates Apaf-1 self-association and procaspase-9 activation. J Biol Chem *273*, 33489-33494.

Huang, D. C., and Strasser, A. (2000). BH3-Only proteins-essential initiators of apoptotic cell death. Cell *103*, 839-842.

Hubbard, E. J., and Greenstein, D. (2000). The Caenorhabditis elegans gonad: a test tube for cell and developmental biology. Dev Dyn *218*, 2-22.

Inohara, N., Ding, L., Chen, S., and Nunez, G. (1997). harakiri, a novel regulator of cell death, encodes a protein that activates apoptosis and interacts selectively with survival-promoting proteins Bcl-2 and Bcl-X(L). Embo J *16*, 1686-1694.

Inohara, N., Gourley, T. S., Carrio, R., Muniz, M., Merino, J., Garcia, I., Koseki, T., Hu, Y., Chen, S., and Nunez, G. (1998). Diva, a Bcl-2 homologue that binds directly to Apaf-1 and induces BH3-independent cell death. J Biol Chem *273*, 32479-32486.

Irmler, M., Hofmann, K., Vaux, D., and Tschopp, J. (1997). Direct physical interaction between the Caenorhabditis elegans 'death proteins' CED-3 and CED-4. FEBS Lett *406*, 189-190.

Jagasia, R., Grote, P., Westermann, B., and Conradt, B. (2005). DRP-1-mediated mitochondrial fragmentation during EGL-1-induced cell death in C. elegans. Nature *433*, 754-760.

James, C., Gschmeissner, S., Fraser, A., and Evan, G. I. (1997). CED-4 induces chromatin condensation in Schizosaccharomyces pombe and is inhibited by direct physical association with CED-9. Curr Biol *7*, 246-252.

Jiang, X., and Wang, X. (2000). Cytochrome c promotes caspase-9 activation by inducing nucleotide binding to Apaf-1. J Biol Chem *275*, 31199-31203.

Karashima, T., Sugimoto, A., and Yamamoto, M. (2000). Caenorhabditis elegans homologue of the human azoospermia factor DAZ is required for oogenesis but not for spermatogenesis. Development *127*, 1069-1079.

Karbowski, M., and Youle, R. J. (2003). Dynamics of mitochondrial morphology in healthy cells and during apoptosis. Cell Death Differ *10*, 870-880.

Kawane, K., Fukuyama, H., Yoshida, H., Nagase, H., Ohsawa, Y., Uchiyama, Y., Okada, K., Iida, T., and Nagata, S. (2003). Impaired thymic development in mouse embryos deficient in apoptotic DNA degradation. Nat Immunol *4*, 138-144.

Kawane, K., Ohtani, M., Miwa, K., Kizawa, T., Kanbara, Y., Yoshioka, Y., Yoshikawa, H., and Nagata, S. (2006). Chronic polyarthritis caused by mammalian DNA that escapes from degradation in macrophages. Nature *443*, 998-1002.

Kayne, P. S., and Sternberg, P. W. (1995). Ras pathways in Caenorhabditis elegans. Curr Opin Genet Dev *5*, 38-43.

Kerr, J. F., Wyllie, A. H., and Currie, A. R. (1972). Apoptosis: a basic biological phenomenon with wide-ranging implications in tissue kinetics. Br J Cancer *26*, 239-257.

Kiefer, M. C., Brauer, M. J., Powers, V. C., Wu, J. J., Umansky, S. R., Tomei, L. D., and Barr, P. J. (1995). Modulation of apoptosis by the widely distributed Bcl-2 homologue Bak. Nature *374*, 736-739.

Kim, D. H., Feinbaum, R., Alloing, G., Emerson, F. E., Garsin, D. A., Inoue, H., Tanaka-Hino, M., Hisamoto, N., Matsumoto, K., Tan, M. W., and Ausubel, F. M. (2002). A conserved p38 MAP kinase pathway in Caenorhabditis elegans innate immunity. Science *297*, 623-626.

Kimble, J., and Ward, S. (1988). Germ-line development and fertilization. In The nematode Caenorhabditis elegans, W. W. a. t. C. o. C. e. researchers, ed. (New York, Cold Spring Harbor Laboratory), pp. 191-213.

Kinchen, J. M., Cabello, J., Klingele, D., Wong, K., Feichtinger, R., Schnabel, H., Schnabel, R., and Hengartner, M. O. (2005). Two pathways converge at CED-10 to mediate actin rearrangement and corpse removal in C. elegans. Nature *434*, 93-99.

Kishore, R. S., and Sundaram, M. V. (2002). ced-10 Rac and mig-2 function redundantly and act with unc-73 trio to control the orientation of vulval cell divisions and migrations in Caenorhabditis elegans. Dev Biol *241*, 339-348.

Klemke, R. L., Leng, J., Molander, R., Brooks, P. C., Vuori, K., and Cheresh, D. A. (1998). CAS/Crk coupling serves as a "molecular switch" for induction of cell migration. J Cell Biol *140*, 961-972.

Kluck, R. M., Bossy-Wetzel, E., Green, D. R., and Newmeyer, D. D. (1997). The release of cytochrome c from mitochondria: a primary site for Bcl-2 regulation of apoptosis. Science *275*, 1132-1136.

Kozopas, K. M., Yang, T., Buchan, H. L., Zhou, P., and Craig, R. W. (1993). MCL1, a gene expressed in programmed myeloid cell differentiation, has sequence similarity to BCL2. Proc Natl Acad Sci U S A *90*, 3516-3520.

Krieser, R. J., MacLea, K. S., Longnecker, D. S., Fields, J. L., Fiering, S., and Eastman, A. (2002). Deoxyribonuclease IIalpha is required during the phagocytic phase of apoptosis and its loss causes perinatal lethality. Cell Death Differ *9*, 956-962.

Kritikou, E. A., Milstein, S., Vidalain, P. O., Lettre, G., Bogan, E., Doukoumetzidis, K., Gray, P., Chappell, T. G., Vidal, M., and Hengartner, M. O. (2006). C. elegans

GLA-3 is a novel component of the MAP kinase MPK-1 signaling pathway required for germ cell survival. Genes Dev *20*, 2279-2292.

Kumar, S., Kinoshita, M., Noda, M., Copeland, N. G., and Jenkins, N. A. (1994). Induction of apoptosis by the mouse Nedd2 gene, which encodes a protein similar to the product of the Caenorhabditis elegans cell death gene ced-3 and the mammalian IL-1 beta-converting enzyme. Genes Dev *8*, 1613-1626.

Lettre, G., Kritikou, E. A., Jaeggi, M., Calixto, A., Fraser, A. G., Kamath, R. S., Ahringer, J., and Hengartner, M. O. (2004). Genome-wide RNAi identifies p53-dependent and -independent regulators of germ cell apoptosis in C. elegans. Cell Death Differ *11*, 1198-1203.

Li, L. Y., Luo, X., and Wang, X. (2001). Endonuclease G is an apoptotic DNase when released from mitochondria. Nature *412*, 95-99.

Li, M. O., Sarkisian, M. R., Mehal, W. Z., Rakic, P., and Flavell, R. A. (2003). Phosphatidylserine receptor is required for clearance of apoptotic cells. Science *302*, 1560-1563.

Li, P., Nijhawan, D., Budihardjo, I., Srinivasula, S. M., Ahmad, M., Alnemri, E. S., and Wang, X. (1997). Cytochrome c and dATP-dependent formation of Apaf-1/caspase-9 complex initiates an apoptotic protease cascade. Cell *91*, 479-489.

Lin, E. Y., Orlofsky, A., Wang, H. G., Reed, J. C., and Prystowsky, M. B. (1996). A1, a Bcl-2 family member, prolongs cell survival and permits myeloid differentiation. Blood *87*, 983-992.

Liu, Q. A., and Hengartner, M. O. (1998). Candidate adaptor protein CED-6 promotes the engulfment of apoptotic cells in C. elegans. Cell *93*, 961-972.

Liu, Q. A., and Hengartner, M. O. (1999). The molecular mechanism of programmed cell death in C. elegans. Ann N Y Acad Sci *887*, 92-104.

Luciani, M. F., and Chimini, G. (1996). The ATP binding cassette transporter ABC1, is required for the engulfment of corpses generated by apoptotic cell death. Embo J *15*, 226-235.

Lundquist, E. A., Reddien, P. W., Hartwieg, E., Horvitz, H. R., and Bargmann, C. I. (2001). Three C. elegans Rac proteins and several alternative Rac regulators control

axon guidance, cell migration and apoptotic cell phagocytosis. Development *128*, 4475-4488.

Lyon, C. J., Evans, C. J., Bill, B. R., Otsuka, A. J., and Aguilera, R. J. (2000). The C. elegans apoptotic nuclease NUC-1 is related in sequence and activity to mammalian DNase II. Gene *252*, 147-154.

Martinou, I., Fernandez, P. A., Missotten, M., White, E., Allet, B., Sadoul, R., and Martinou, J. C. (1995). Viral proteins E1B19K and p35 protect sympathetic neurons from cell death induced by NGF deprivation. J Cell Biol *128*, 201-208.

Maurer, C. W., Chiorazzi, M., and Shaham, S. (2007). Timing of the onset of a developmental cell death is controlled by transcriptional induction of the C. elegans ced-3 caspase-encoding gene. Development *134*, 1357-1368.

Metzstein, M. M., Stanfield, G. M., and Horvitz, H. R. (1998). Genetics of programmed cell death in C. elegans: past, present and future. Trends Genet *14*, 410-416.

Miura, M., Zhu, H., Rotello, R., Hartwieg, E. A., and Yuan, J. (1993). Induction of apoptosis in fibroblasts by IL-1 beta-converting enzyme, a mammalian homolog of the C. elegans cell death gene ced-3. Cell *75*, 653-660.

Moriishi, K., Huang, D. C., Cory, S., and Adams, J. M. (1999). Bcl-2 family members do not inhibit apoptosis by binding the caspase activator Apaf-1. Proc Natl Acad Sci U S A *96*, 9683-9688.

Nagata, S. (2005). DNA degradation in development and programmed cell death. Annu Rev Immunol *23*, 853-875.

Nakano, K., and Vousden, K. H. (2001). PUMA, a novel proapoptotic gene, is induced by p53. Mol Cell *7*, 683-694.

Navarro, R. E., Shim, E. Y., Kohara, Y., Singson, A., and Blackwell, T. K. (2001). cgh-1, a conserved predicted RNA helicase required for gametogenesis and protection from physiological germ line apoptosis in C. elegans. Development *128*, 3221-3232.

Nicholson, D. W., and Thornberry, N. A. (1997). Caspases: killer proteases. Trends Biochem Sci *22*, 299-306.

O'Connor, L., Strasser, A., O'Reilly, L. A., Hausmann, G., Adams, J. M., Cory, S., and Huang, D. C. (1998). Bim: a novel member of the Bcl-2 family that promotes apoptosis. Embo J *17*, 384-395.

Oda, E., Ohki, R., Murasawa, H., Nemoto, J., Shibue, T., Yamashita, T., Tokino, T., Taniguchi, T., and Tanaka, N. (2000). Noxa, a BH3-only member of the Bcl-2 family and candidate mediator of p53-induced apoptosis. Science *288*, 1053-1058.

Oltvai, Z. N., Milliman, C. L., and Korsmeyer, S. J. (1993). Bcl-2 heterodimerizes in vivo with a conserved homolog, Bax, that accelerates programmed cell death. Cell *74*, 609-619.

Ottilie, S., Wang, Y., Banks, S., Chang, J., Vigna, N. J., Weeks, S., Armstrong, R. C., Fritz, L. C., and Oltersdorf, T. (1997). Mutational analysis of the interacting cell death regulators CED-9 and CED-4. Cell Death Differ *4*, 526-533.

Parrish, J., Li, L., Klotz, K., Ledwich, D., Wang, X., and Xue, D. (2001). Mitochondrial endonuclease G is important for apoptosis in C. elegans. Nature *412*, 90-94.

Parrish, J. Z., and Xue, D. (2003). Functional genomic analysis of apoptotic DNA degradation in C. elegans. Mol Cell *11*, 987-996.

Praefcke, G. J., and McMahon, H. T. (2004). The dynamin superfamily: universal membrane tubulation and fission molecules? Nat Rev Mol Cell Biol *5*, 133-147.

Puthalakath, H., and Strasser, A. (2002). Keeping killers on a tight leash: transcriptional and post-translational control of the pro-apoptotic activity of BH3-only proteins. Cell Death Differ *9*, 505-512.

Qin, H., Srinivasula, S. M., Wu, G., Fernandes-Alnemri, T., Alnemri, E. S., and Shi, Y. (1999). Structural basis of procaspase-9 recruitment by the apoptotic protease-activating factor 1. Nature *399*, 549-557.

Rabizadeh, S., LaCount, D. J., Friesen, P. D., and Bredesen, D. E. (1993). Expression of the baculovirus p35 gene inhibits mammalian neural cell death. J Neurochem *61*, 2318-2321.

Ray, C. A., Black, R. A., Kronheim, S. R., Greenstreet, T. A., Sleath, P. R., Salvesen, G. S., and Pickup, D. J. (1992). Viral inhibition of inflammation: cowpox virus encodes an inhibitor of the interleukin-1 beta converting enzyme. Cell *69*, 597-604.

Reddien, P. W., Cameron, S., and Horvitz, H. R. (2001). Phagocytosis promotes programmed cell death in C. elegans. Nature *412*, 198-202.

Reddien, P. W., and Horvitz, H. R. (2000). CED-2/CrkII and CED-10/Rac control phagocytosis and cell migration in Caenorhabditis elegans. Nat Cell Biol *2*, 131-136.

Reddien, P. W., and Horvitz, H. R. (2004). The engulfment process of programmed cell death in caenorhabditis elegans. Annu Rev Cell Dev Biol *20*, 193-221.

Reed, J. C., Jurgensmeier, J. M., and Matsuyama, S. (1998). Bcl-2 family proteins and mitochondria. Biochim Biophys Acta *1366*, 127-137.

Robertson, A. M., and Thomson, J. N. (1982). Morphology of programmed cell death in the ventral nerve cord of Caenorhabditis elegans. J Embryol Exp Morph *67*, 89-100.

Rospert, S., Dubaquie, Y., and Gautschi, M. (2002). Nascent-polypeptide-associated complex. Cell Mol Life Sci *59*, 1632-1639.

Saffman, E. E., and Lasko, P. (1999). Germ line development in vertebrates and invertebrates. Cell Mol Life Sci *55*, 1141-1163.

Saleh, A., Srinivasula, S. M., Acharya, S., Fishel, R., and Alnemri, E. S. (1999). Cytochrome c and dATP-mediated oligomerization of Apaf-1 is a prerequisite for procaspase-9 activation. J Biol Chem *274*, 17941-17945.

Salinas, L. S., Maldonado, E., and Navarro, R. E. (2006). Stress-induced germ cell apoptosis by a p53 independent pathway in Caenorhabditis elegans. Cell Death Differ *13*, 2129-2139.

Salvesen, G. S., and Dixit, V. M. (1997). Caspases: intracellular signaling by proteolysis. Cell *91*, 443-446.

Salvesen, G. S., and Dixit, V. M. (1999). Caspase activation: the induced-proximity model. Proc Natl Acad Sci U S A *96*, 10964-10967.

Samejima, K., and Earnshaw, W. C. (2005). Trashing the genome: the role of nucleases during apoptosis. Nat Rev Mol Cell Biol *6*, 677-688.

Sato, K., Sato, M., Audhya, A., Oegema, K., Schweinsberg, P., and Grant, B. D. (2006). Dynamic regulation of caveolin-1 trafficking in the germ line and embryo of Caenorhabditis elegans. Mol Biol Cell *17*, 3085-3094.

Savill, J., Gregory, C., and Haslett, C. (2003). Cell biology. Eat me or die. Science *302*, 1516-1517.

Schedl, T. (1997). Developmental genetics of the germ-line. In C. elegans II, D. L. Riddle, T. Blumenthal, B. J. Meyer, and J. Priess, eds. (New Work, Cold Spring Harbor Laboratory), pp. 241-269.

Schumacher, B., Hofmann, K., Boulton, S., and Gartner, A. (2001). The C. elegans homolog of the p53 tumor suppressor is required for DNA damage-induced apoptosis. Curr Biol *11*, 1722-1727.

Schumacher, B., Schertel, C., Wittenburg, N., Tuck, S., Mitani, S., Gartner, A., Conradt, B., and Shaham, S. (2005). C. elegans ced-13 can promote apoptosis and is induced in response to DNA damage. Cell Death Differ *12*, 153-161.

Scott, R. S., McMahon, E. J., Pop, S. M., Reap, E. A., Caricchio, R., Cohen, P. L., Earp, H. S., and Matsushima, G. K. (2001). Phagocytosis and clearance of apoptotic cells is mediated by MER. Nature *411*, 207-211.

Seshagiri, S., and Miller, L. K. (1997). Caenorhabditis elegans CED-4 stimulates CED-3 processing and CED-3-induced apoptosis. Curr Biol *7*, 455-460.

Shaham, S. (1998). Identification of multiple Caenorhabditis elegans caspases and their potential roles in proteolytic cascades. J Biol Chem *273*, 35109-35117.

Shaham, S., and Horvitz, H. R. (1996a). An alternatively spliced C. elegans ced-4 RNA encodes a novel cell death inhibitor. Cell *86*, 201-208.

Shaham, S., and Horvitz, H. R. (1996b). Developing Caenorhabditis elegans neurons may contain both cell-death protective and killer activities. Genes Dev *10*, 578-591.

Shaham, S., Reddien, P. W., Davies, B., and Horvitz, H. R. (1999). Mutational analysis of the Caenorhabditis elegans cell-death gene ced-3. Genetics *153*, 1655-1671.

Shi, Y. (2002). Mechanisms of caspase activation and inhibition during apoptosis. Mol Cell *9*, 459-470.

Song, Q., Kuang, Y., Dixit, V. M., and Vincenz, C. (1999). Boo, a novel negative regulator of cell death, interacts with Apaf-1. Embo J *18*, 167-178.

Spector, M. S., Desnoyers, S., Hoeppner, D. J., and Hengartner, M. O. (1997). Interaction between the C. elegans cell-death regulators CED-9 and CED-4. Nature *385*, 653-656.

Srinivasula, S. M., Ahmad, M., Fernandes-Alnemri, T., and Alnemri, E. S. (1998). Autoactivation of procaspase-9 by Apaf-1-mediated oligomerization. Mol Cell *1*, 949-957.

Stergiou, L., Doukoumetzidis, K., Sendoel, A., and Hengartner, M. O. (2007). The nucleotide excision repair pathway is required for UV-C-induced apoptosis in Caenorhabditis elegans. Cell Death Differ *14*, 1129-1138.

Steven, R., Kubiseski, T. J., Zheng, H., Kulkarni, S., Mancillas, J., Ruiz Morales, A., Hogue, C. W., Pawson, T., and Culotti, J. (1998). UNC-73 activates the Rac GTPase and is required for cell and growth cone migrations in C. elegans. Cell *92*, 785-795.

Strasser, A., O'Connor, L., and Dixit, V. M. (2000). Apoptosis signaling. Annu Rev Biochem *69*, 217-245.

Su, H. P., Nakada-Tsukui, K., Tosello-Trampont, A. C., Li, Y., Bu, G., Henson, P. M., and Ravichandran, K. S. (2002). Interaction of CED-6/GULP, an adapter protein involved in engulfment of apoptotic cells with CED-1 and CD91/low density lipoprotein receptor-related protein (LRP). J Biol Chem *277*, 11772-11779.

Sulston, J. E. (1976). Post-embryonic development in the ventral cord of Caenorhabditis elegans. Philos Trans R Soc Lond B Biol Sci *275*, 287-297.

Sulston, J. E., Albertson, D. G., and Thomson, J. N. (1980). The Caenorhabditis elegans male: postembryonic development of nongonadal structures. Dev Biol *78*, 542-576.

Sulston, J. E., and Horvitz, H. R. (1977). Post-embryonic cell lineages of the nematode, Caenorhabditis elegans. Dev Biol *56*, 110-156.

Sulston, J. E., Shierenberg, E., White, J. G., and Thomson, N. (1983). The embryonic cell lineage of the nematode Caenorhabditis elegans. Dev Biol *100*, 64-119.

Thompson, H. M., Skop, A. R., Euteneuer, U., Meyer, B. J., and McNiven, M. A. (2002). The large GTPase dynamin associates with the spindle midzone and is required for cytokinesis. Curr Biol *12*, 2111-2117.

Thomson, C. (1995). Apoptosis in the pathogenesis and treatment of disease. Science *267*, 1456-1462.

Thornberry, N. A., and Lazebnik, Y. (1998). Caspases: enemies within. Science *281*, 1312-1316.

Trent, C., Tsuing, N., and Horvitz, H. R. (1983). Egg-laying defective mutants of the nematode Caenorhabditis elegans. Genetics *104*, 619-647.

Truman, J. (1984). Cell death in invertebrate nervous systems. Ann Rev Neurosci *7*, 171-188.

Tsujimoto, Y., Yunis, J., Onorato-Showe, L., Erikson, J., Nowell, P. C., and Croce, C. M. (1984). Molecular cloning of the chromosomal breakpoint of B-cell lymphomas and leukemias with the t(11;14) chromosome translocation. Science *224*, 1403-1406.

van Loo, G., Saelens, X., van Gurp, M., MacFarlane, M., Martin, S. J., and Vandenabeele, P. (2002). The role of mitochondrial factors in apoptosis: a Russian roulette with more than one bullet. Cell Death Differ *9*, 1031-1042.

Venegas, V., and Zhou, Z. (2007). Two Alternative Mechanisms That Regulate the Presentation of Apoptotic Cell Engulfment Signal in Caenorhabditis elegans. Mol Biol Cell *18*, 3180-3192.

Wang, K., Yin, X. M., Chao, D. T., Milliman, C. L., and Korsmeyer, S. J. (1996). BID: a novel BH3 domain-only death agonist. Genes Dev *10*, 2859-2869.

Wang, L., Miura, M., Bergeron, L., Zhu, H., and Yuan, J. (1994). Ich-1, an Ice/ced-3-related gene, encodes both positive and negative regulators of programmed cell death. Cell *78*, 739-750.

Wang, X., Wang, J., Gengyo-Ando, K., Gu, L., Sun, C. L., Yang, C., Shi, Y., Kobayashi, T., Mitani, S., Xie, X. S., and Xue, D. (2007). C. elegans mitochondrial factor WAH-1 promotes phosphatidylserine externalization in apoptotic cells through phospholipid scramblase SCRM-1. Nat Cell Biol *9*, 541-549.

Wang, X., Wu, Y. C., Fadok, V. A., Lee, M. C., Gengyo-Ando, K., Cheng, L. C., Ledwich, D., Hsu, P. K., Chen, J. Y., Chou, B. K., *et al.* (2003). Cell corpse engulfment mediated by C. elegans phosphatidylserine receptor through CED-5 and CED-12. Science *302*, 1563-1566.

Wang, X., Yang, C., Chai, J., Shi, Y., and Xue, D. (2002). Mechanisms of AIF-mediated apoptotic DNA degradation in Caenorhabditis elegans. Science *298*, 1587-1592.

Williamson, P., and Schlegel, R. A. (2004). Hide and seek: the secret identity of the phosphatidylserine receptor. J Biol *3*, 14.

Wu, D., Wallen, H. D., and Nunez, G. (1997). Interaction and regulation of subcellular localization of CED-4 by CED-9. Science *275*, 1126-1129.

Wu, Y., Tibrewal, N., and Birge, R. B. (2006). Phosphatidylserine recognition by phagocytes: a view to a kill. Trends Cell Biol *16*, 189-197.

Wu, Y. C., and Horvitz, H. R. (1998a). The C. elegans cell corpse engulfment gene ced-7 encodes a protein similar to ABC transporters. Cell *93*, 951-960.

Wu, Y. C., and Horvitz, H. R. (1998b). C. elegans phagocytosis and cell-migration protein CED-5 is similar to human DOCK180. Nature *392*, 501-504.

Wu, Y. C., Stanfield, G. M., and Horvitz, H. R. (2000). NUC-1, a caenorhabditis elegans DNase II homolog, functions in an intermediate step of DNA degradation during apoptosis. Genes Dev *14*, 536-548.

Wu, Y. C., Tsai, M. C., Cheng, L. C., Chou, C. J., and Weng, N. Y. (2001). C. elegans CED-12 acts in the conserved crkII/DOCK180/Rac pathway to control cell migration and cell corpse engulfment. Dev Cell *1*, 491-502.

Wyllie, A. H. (1980). Glucocorticoid-induced thymocyte apoptosis is associated with endogenous endonuclease activation. Nature *284*, 555-556.

Xue, D., and Horvitz, H. R. (1995). Inhibition of the Caenorhabditis elegans cell-death protease CED-3 by a CED-3 cleavage site in baculovirus p35 protein. Nature *377*, 248-251.

Xue, D., Shaham, S., and Horvitz, H. R. (1996). The Caenorhabditis elegans cell-death protein CED-3 is a cysteine protease with substrate specificities similar to those of the human CPP32 protease. Genes Dev *10*, 1073-1083.

Yang, E., Zha, J., Jockel, J., Boise, L. H., Thompson, C. B., and Korsmeyer, S. J. (1995). Bad, a heterodimeric partner for Bcl-XL and Bcl-2, displaces Bax and promotes cell death. Cell *80*, 285-291.

Yang, X., Chang, H. Y., and Baltimore, D. (1998). Essential role of CED-4 oligomerization in CED-3 activation and apoptosis. Science *281*, 1355-1357.

Yoshida, H. (2003). The role of Apaf-1 in programmed cell death: from worm to tumor. Cell Struct Funct *28*, 3-9.

Yu, X., Odera, S., Chuang, C. H., Lu, N., and Zhou, Z. (2006). C. elegans Dynamin mediates the signaling of phagocytic receptor CED-1 for the engulfment and degradation of apoptotic cells. Dev Cell *10*, 743-757.

Yuan, J., and Horvitz, H. R. (1992). The Caenorhabditis elegans cell death gene ced-4 encodes a novel protein and is expressed during the period of extensive programmed cell death. Development *116*, 309-320.

Yuan, J., Shaham, S., Ledoux, S., Ellis, H. M., and Horvitz, H. R. (1993). The C. elegans cell death gene ced-3 encodes a protein similar to mammalian interleukin-1 beta-converting enzyme. Cell *75*, 641-652.

Yuan, J., and Yankner, B. A. (2000). Apoptosis in the nervous system. Nature *407*, 802-809.

Yuan, J. Y., and Horvitz, H. R. (1990). The Caenorhabditis elegans genes ced-3 and ced-4 act cell autonomously to cause programmed cell death. Dev Biol *138*, 33-41.

Zhou, Z., Caron, E., Hartwieg, E., Hall, A., and Horvitz, H. R. (2001). The C. elegans PH domain protein CED-12 regulates cytoskeletal reorganization via a Rho/Rac GTPase signaling pathway. Dev Cell *1*, 477-489.

Zou, H., Henzel, W. J., Liu, X., Lutschg, A., and Wang, X. (1997). Apaf-1, a human protein homologous to C. elegans CED-4, participates in cytochrome c-dependent activation of caspase-3. Cell *90*, 405-413.

Zou, H., Li, Y., Liu, X., and Wang, X. (1999). An APAF-1.cytochrome c multimeric complex is a functional apoptosome that activates procaspase-9. J Biol Chem *274*, 11549-11556.

Zullig, S., Neukomm, L. J., Jovanovic, M., Charette, S. J., Lyssenko, N. N., Halleck, M. S., Reutelingsperger, C. P., Schlegel, R. A., and Hengartner, M. O. (2007). Aminophospholipid translocase TAT-1 promotes phosphatidylserine exposure during C. elegans apoptosis. Curr Biol *17*, 994-999.

FIGURE 1.1 The genetic pathway for programmed cell death in *C. elegans*

Programmed cell death in *C. elegans* proceeds via a genetic pathway, which was found to be conserved across a wide range of species, including mammals. This pathway can be broken down into three major steps: the induction and execution of the death program, the phagocytosis and removal of the apoptotic cell, and finally the degradation of the DNA of the apoptotic corpse. In reality these steps are far from being discrete as more and more evidence suggest that they present significant overlap (see text for details). Engulfment can be further subdivided into two different processes - the recognition and the internalization of the dead cell and a series of complex events which initiate the ingestion of the apoptotic corpse, commonly refered to as phagosome maturation. While the decision to die and the induction of the apoptotic program require cell type specific signals, the core killing machinery (*egl-1, ced-9, ced-4* and *ced-3*) and the factors mediating cell corpse engulfment (*ced-1, ced-2, ced-5, ced-6, ced-7, ced-10,* and *ced-12*) operate independently of the cell type.

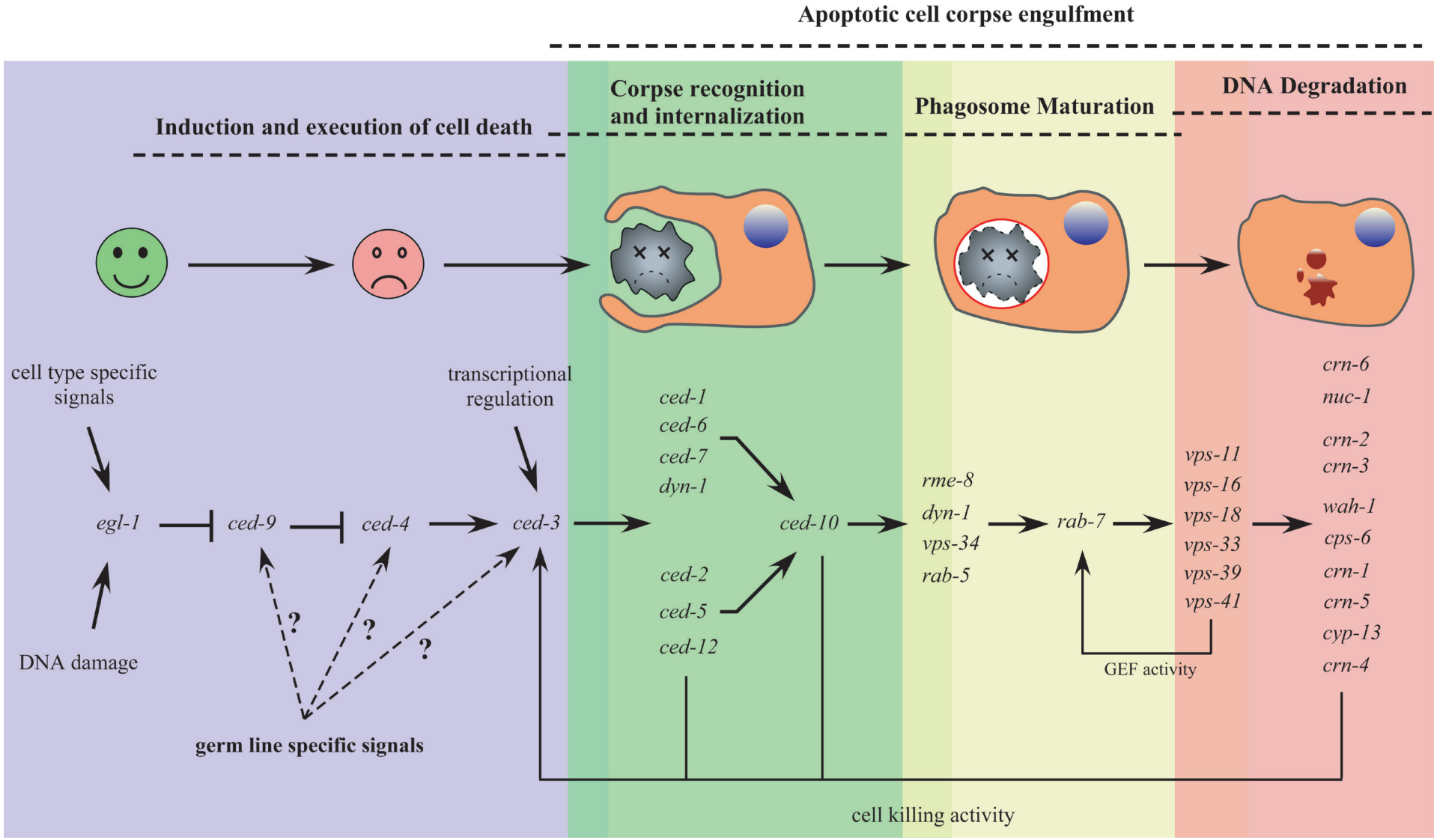
Apoptotic cell corpse engulfment
Induction and execution of cell death
Corpse recognition and internalization
Phagosome Maturation
DNA Degradation
cell type specific signals
transcriptional regulation
egl-1
ced-9
ced-4
ced-3
DNA damage
germ line specific signals
?
?
?
ced-1
ced-6
ced-7
dyn-1
ced-2
ced-5
ced-12
ced-10
rme-8
dyn-1
vps-34
rab-5
rab-7
vps-11
vps-16
vps-18
vps-33
vps-39
vps-41
GEF activity
crn-6
nuc-1
crn-2
crn-3
wah-1
cps-6
crn-1
crn-5
cyp-13
crn-4
cell killing activity

Table 1.1 List of genes involved in programmed cell death in *C. elegans* and function, where known.

Gene Name	Homologue/Function	Reference
Factors involved in apoptotic cell death		
ced-3	Caspase orthologue, promotes apoptosis by cleaving specific substrates	Yuan et al., 1993
ced-4	APAF1 homologue, promotes apoptosis by assisting CED-3 activation	Yuan and Horvitz, 1992 Zou et al., 1997
ced-9	Bcl-2 orthologue, prevents apoptosis by sequestrating CED-4 on the mitochondrial membrane	Hengartner et al. 1992; Hengartner and Horvitz, 1994
egl-1	BH3-only domain containing protein, promotes apoptosis by displacing CED-4 from CED-9	Conradt and Horvitz, 1998
icd-1	βNAC, localizes on mitochondria, involved in *ced-3* -independent cell death	Bloss et al., 2003
Factors involved in germ cell death		
gla-1/cpb-3	cytoplasmic polyadenylation element binding protein	Boag et al., 2005
gla-3	TIS-11 like protein	Kritikou et al., 2006
cgh-1	DEAD-box RNA helicase	Navarro et al. 2001
daz-1	RNA binding, required for progression of meiosis during oogenesis	Karashima et al., 2000
car-1	RNA binding protein, orthologous to human LSM14A and LSM14B	Boag et al., 2005
R05D3.4	predicted E3 ubiquitin ligase	Lettre et al., 2004
pmk-3	p38 MAP kinase	Lettre et al., 2004
Factors involved in apoptotic cell corpse engulfment		
ced-1	transmembrane receptor, homologous to SREC, LR91/LRP	Zhou et al., 2001
ced-6	adaptor protein, interacts with the cytoplasmic tail of CED-1	Liu and Hengartner, 1998
ced-7	ABC transporter. required for CED-1 localization around apoptotic cells	Wu and Horvitz, 1998a
ced-2	CrkII homolog, adaptor protein	Reddien and Horvitz, 2000
ced-5	Dock180 homolog, large docking protein, acts as a RacGEF to regulate CED-10 activity	Wu and Horvitz, 1998b
ced-10	Rac1 homolog, small GTPase involved in membrane movements	Reddien and Horvitz, 2000
ced-12	ELMO homolog, acts as a RacGEF to regulate CED-10 activity	Gumienny et al., 2001
nex-1	annexin I homolog, binds to PS	Arur et al. 2003
mig-2	RhoG homolog, small GTPase regulates CED-12-mediated Rac activation	deBakker et al., 2004
unc-73	Trio homolog, exhibitis GEF towards MIG-2/RhoG	deBakker et al., 2004
psr-1	putative PS receptor	Wang et al., 2003
tat-1	aminophospholipid translocase, promotes PS exposure during apoptosis	Zullig et al., 2007
scrm-1	phospholipid scramblase, promotes PS exposure during apoptosis	Wang et al., 2007
plsc-1/scrm-3	phospholipid scramblase, promotes PS exposure during apoptosis	Venegas and Zhou, 2007
dyn-1	Dynamin, large GTPase required for internalization/phagosome maturation	Yu et al. 2006
Factors involved in apoptotic DNA degradation		
nuc-1	Dnase II homologue, required for the resolution of TUNEL(+) ends	Wu et al., 2000
wah-1	Apoptosis Inducing Factor homolog	Wang et al., 2002
cps-6	EndoG homologue	Parrish et al., 2001
crn-1	Fen1 homologue, 5'-3' exonuclease	Parrish et al., 2003
crn-2	homologous to the magnesium-dependent TatD nuclease of E. coli	Parrish and Xue, 2003
crn-3	homologous to the 100 kDa polymyositis/scleroderma autoantigen (PM/Scl-100), a ribonuclease component of the exosome	Parrish and Xue, 2003
crn-4	homologous to a famiula of 3'-5' exonucleases including ribonuclease T and the epsilon sunit of DNA polymerase III	Parrish and Xue, 2003
crn-5	exosomal 3'-5' exoribonuclease complex, subunit Rrp46	Parrish and Xue, 2003
crn-6	DNase II homologue	Parrish and Xue, 2003
cyp-13	cyclophilin, exhibits nuclease activity in vitro	Parrish and Xue, 2003

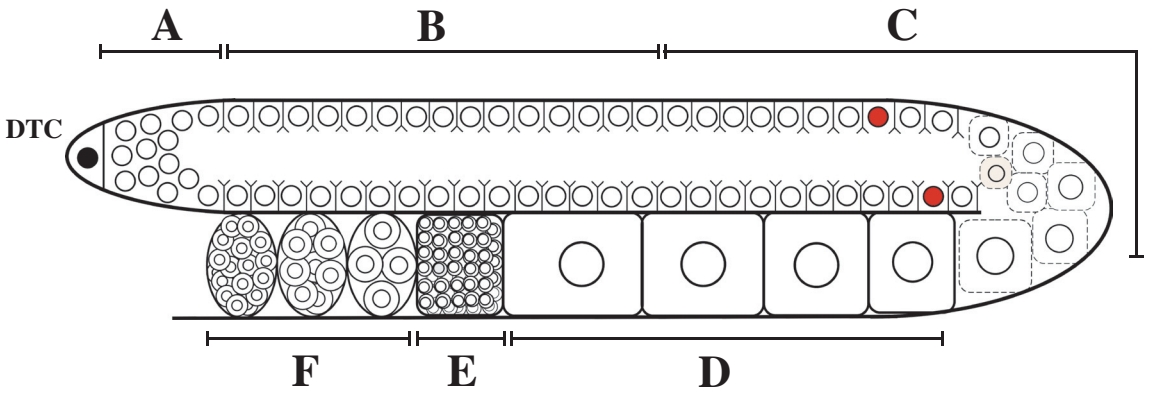

FIGURE 1.2 Cartoon of the *C. elegans* adult hermaphrodite germ line

The *C. elegans* adult hermaphrodite germ line consists of two symmetrical U-shaped tubes whose proximal ends are linked to a common uterus. The distal region of the gonad is capped by a distal tip cell (DTC) which is responsible for maintaining the stem cell potential of neighboring mitotic germ cells (A). As germ cells moveout of the distal mitotic zone they enter the transition zone (B) where they progress into the pachytene stage of meiotic prophase I. When cells exit from the pachytene stage (C), they become competent to undergo apoptosis (red nuclei); apoptotic cells are removed by the somatic sheath cells which encasse the gonad and are not shownhere. Surviving germ cells enlarge and cellularize to become oocytes arrested at the diakinesis stage (D). Upon activation, mature oocytes progress through the spermatheca (E), where they are fertilized. The resulting eggs transit into the uterus (F), where they wait to be laid through the vulva.

FIGURE 1.3 DNA damage response pathways

Cells are under the constant threat of DNA damaging agents such as, ionizing radiation, oxygen radicals, ormonofunctional alkylating agents, the action of which can cause different types of DNA lesions. To preserve the integrity of their genomes, higher organisms have developed sophisticated systems able to recognize and repair the damaged DNA, or when the damage is irreparable to initate apoptosis. Proteins involved in DNA damage signaling are typically divided into three categories according to their position within the signaling cascade. The more upstream components are sensor complexes that localize to the site of damage and initiate a response to it (HUS-1, MRT-2 and XPA-1). Downstream of these lay transducers (ATM-1, ATL-1, CHK-1 and CHK-2) that relay the resulting signal to various effector molecules by triggering a phosphorylation cascade. Once activated, effectors (CEP-1) will elicit specific biological responses such as repair processes, cell cycle arrest or apoptosis.

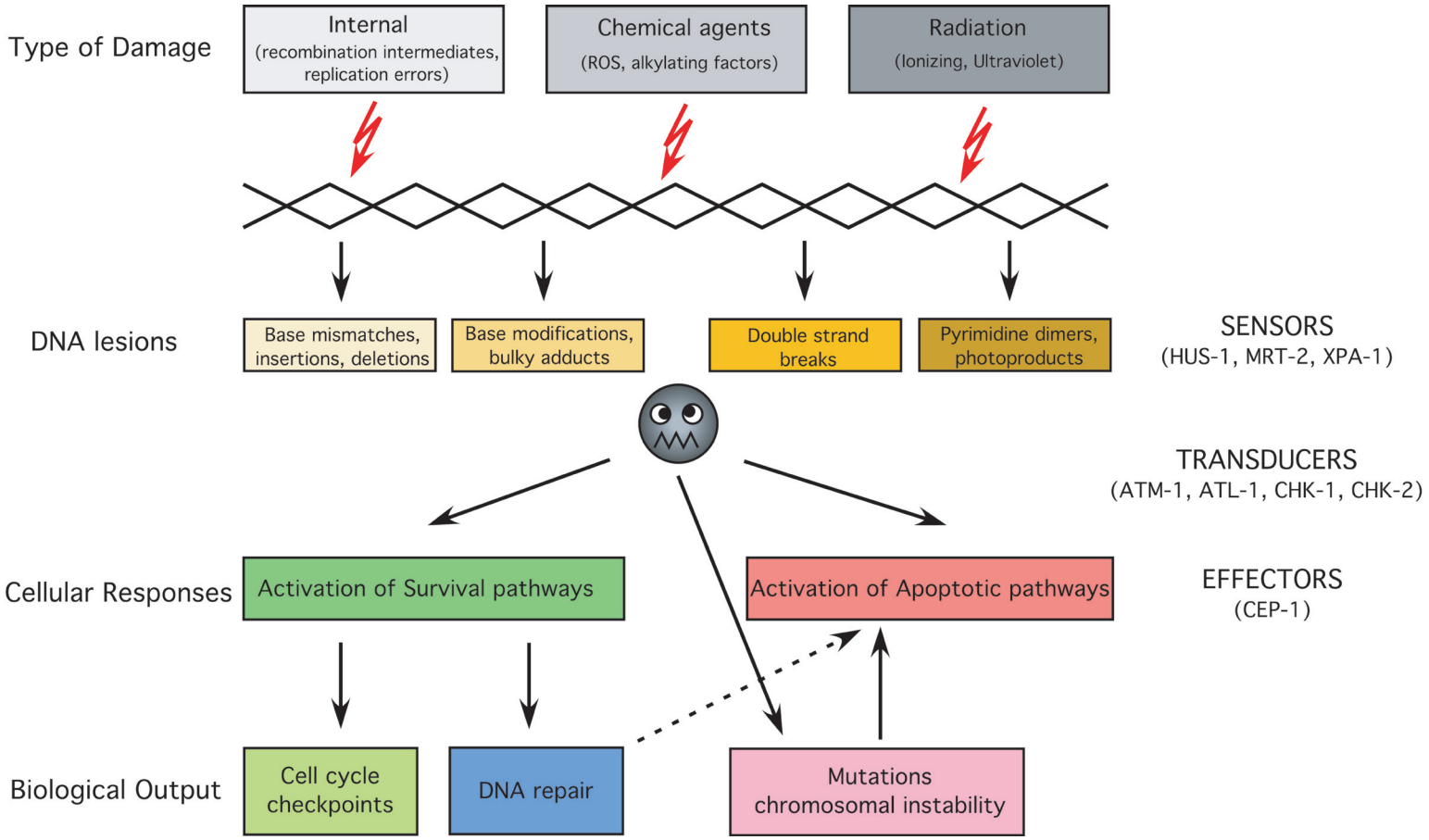
Type of Damage
Internal
(recombination intermediates, replication errors)
Chemical agents
(ROS, alkylating factors)
Radiation
(Ionizing, Ultraviolet)
DNA lesions
Base mismatches, insertions, deletions
Base modifications, bulky adducts
Double strand breaks
Pyrimidine dimers, photoproducts
SENSORS
(HUS-1, MRT-2, XPA-1)
TRANSDUCERS
(ATM-1, ATL-1, CHK-1, CHK-2)
Cellular Responses
Activation of Survival pathways
Activation of Apoptotic pathways
EFFECTORS
(CEP-1)
Biological Output
Cell cycle checkpoints
DNA repair
Mutations chromosomal instability

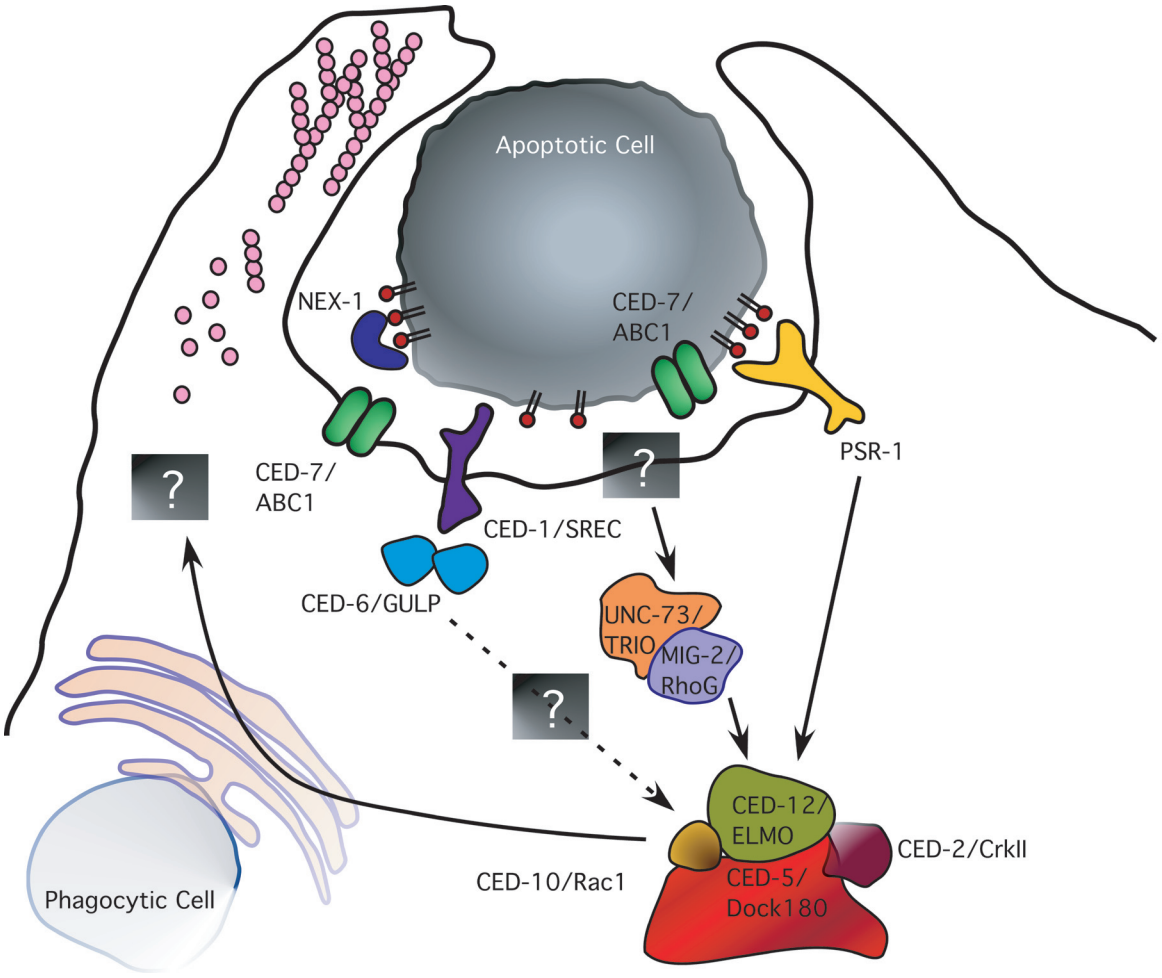

FIGURE 1.4 Pathways controlling apoptotic cell corpse engulfment in *C. elegans*

Previous studies have led to the identification of at least two partially redundant genetic pathways mediating engulfment of apoptotic cells in *C. elegans*. The first pathway consists of *ced-1, -6* and *-7* and the second of the *ced-2, -5* and *-12* genes. Recent studies have shown that *ced-10*, which codes for the small GTPase Rac, acts downstream of both pathways to mediate cytoskeletal rearrengements leading to corpse internalization. In the last few years, several new players have been discovered either via reverse genetics (NEX-1 and PSR-1) or by homology (UNC-73 and MIG-2). All these genes, however, do not represent the full complement of factors controlling cell corpse clearance; some of the key unknown players are depicted by colored boxes with question marks (see text for details).

CHAPTER 2

DESIGNING A REVERSE GENETICS SCREEN FOR GENES CONTROLLING APOPTOTIC CELL CORPSE ENGULFMENT

CHAPTER 2

DESIGNING A REVERSE GENETIC SCREEN FOR GENES CONTROLLING APOPTOTIC CELL CORPSE ENGULFMENT

2.1 ABSTRACT

This chapter summarizes my efforts to design and set up a systematic functional genomic approach for the identification of novel genes involved in apoptotic cell corpse engulfment. Here, I describe the proof of principle as well as the rationale of the screen and I briefly go through a series of control experiments, which constitute the groundwork of what finally became a "half genome-wide" RNAi screen. I report that RNAi by feeding against known engulfment genes results in a weak engulfment defect in the *C. elegans* germ line, in wild type worms. This weak effect is amplified in mutants exhibiting increased levels of germ cell apoptosis, such as *gla-3(op216)* and is sufficient to suppress actin polymerization around dead cells as well as staining of the latter ones by the vital dye Acridine Orange. This entire chapter also serves as a detailed introduction to Chapter 3 where I present an in depth analysis of several of the novel engulfment genes we identified, and in particular of *dyn-1,* the *C. elegans* dynamin homolog.

2.2 INTRODUCTION

Despite the considerable wealth of knowledge about the molecular mechanisms controlling the first steps of programmed cell death (Adams, 2003; Meier et al., 2000; Metzstein et al., 1998; Shi, 2002), comparatively little is known about the mechanisms that control apoptotic cell corpse engulfment. Genetic studies to date have identified in the nematode two evolutionarily conserved signaling pathways linked to the recognition and internalization of apoptotic cells. The first pathway is composed of CED-2/CrkII (Reddien and Horvitz, 2000), an adaptor protein, as well as of CED-5/Dock180 (Wu and Horvitz, 1998b) and CED-12/ELMO (Gumienny et al., 2001; Wu et al., 2001; Zhou et al., 2001a), which exhibit a bipartite GEF activity towards CED-10/Rac1 (Brugnera et al., 2002). In the second pathway,

CED-1/LRP/MEGF10 (Hamon et al., 2006; Su et al., 2002; Zhou et al., 2001b) and CED-7/ABCA1/ABCA7 (Jehle et al., 2006; Luciani and Chimini, 1996; Wu and Horvitz, 1998a), two transmembrane proteins that may mediate recognition of the apoptotic cell, and CED-6/GULP (Liu and Hengartner, 1998; Su et al., 2002), an adaptor protein, also signal to CED-10/Rac during engulfment (Henson, 2005; Kinchen and Hengartner, 2005). How these two signaling pathways cooperate to promote engulfment and subsequent degradation of the apoptotic cell is currently not well understood.

In *C. elegans*, most of our current knowledge of apoptotic cell corpse clearance comes from a handful of genetic screens that required the animals homozygous for engulfment mutations to be viable (Ellis et al., 1991). These screens might have therefore missed important regulators of engulfment with essential functions, notably during early embryonic development, since mutations in such genes would most likely result in early lethality. A way to identify such engulfment genes with pleiotropic functions would, thus, be to design and perform genetic screens allowing the recovery of homozygous lethal mutations exhibiting engulfment defects. Alternatively, other strategies, such as RNAi-based reverse genetic screens where only a partial knockdown of gene expression can be achieved, might be very useful to identify novel engulfment genes with other, essential functions.

The RNAi method has several key advantages over the classic forward approach for probing gene function. While both approaches can be used to screen an entire genome for genes involved in a particular biological process, RNAi is considerably less time-consuming than classic forward genetic screens. This is primarily due to the fact that forward screens require the positional cloning of genes, which is often a slow and laborious process. In contrast, the use of RNAi allows one to link automatically any mutant phenotype to a known sequence, and thus to avoid mapping and cloning of the newly identified genes. Another characteristic of RNAi is that it leads in most cases to a knock-down, rather than a knockout, of gene expression thereby resulting in weak and partial loss-of-function phenotypes. This, together with the experimental possibility in *C. elegans* to control the developmental stage at which RNAi can be applied make this technique an attractive tool to uncouple early and late functions of genes during development.

For all the reasons described above, I decided to give the RNAi strategy a try. This chapter essentially describes all the backstage work of such an RNAi-based reverse genetic screen for novel genes involved in apoptotic cell clearance, but which could possibly have additional, essential functions. The work described here kept me busy for roughly the first six months of my Ph.D.

2.3 RESULTS

2.3.1 RNAi by feeding can be used to confirm the function of engulfment genes in C. elegans

RNAi is currently the simplest and most efficient method for inactivating genes in *C. elegans* and, within the last few years, it has become an increasingly important reverse-genetics tool for probing gene function. This technique rapidly produces gene-specific loss-of-function or hypomorphic phenotypes, based on observation of knockdown of many genes in *C. elegans* (Hong et al., 1998). RNAi of target genes can be achieved by microinjection of dsRNA into the *C. elegans* gonad, by soaking animals in a dsRNA-containing solution or by feeding worms with bacteria engineered to produce high levels of dsRNA (Timmons et al., 2001; Timmons and Fire, 1998). Microinjection was thought to be the most efficient of these three methods but recently developed optimized protocols allow RNAi by ingestion of dsRNA-expressing bacteria to be at least as effective as RNAi by injection of dsRNA (Kamath et al., 2001). The major advantage of RNAi by feeding over injection is that it is considerably less labour-intensive, allowing the performance of RNAi on thousands of worms with little effort. The second, and perhaps the most important, advantage of this method is the availability of several bacterial RNAi libraries (Kamath et al., 2003; Rual et al., 2004) covering the largest part of the *C. elegans* genome. The construction of these libraries has revolutionized the *C. elegans* world since it opened the way to several large scale screening projects, covering many different aspects of worm biology.

My initial ambition was to examine whether we could exploit the numerous advantages of the feeding RNAi technique to elucidate the mechanisms of apoptotic cell corpse clearance. I soon realized that this was a rather daunting task since, back then, several members of the lab were convinced that genes controlling engulfment

were refractory to RNAi. Previous work in the Hengartner lab has, indeed, suggested that RNAi against genes involved in engulfment has little or no effect during embryogenesis (Hengartner MO, personal communication).

The first step I took was to extensively optimize the RNAi conditions, in order to test whether I could obtain relevant phenotypes for all the currently known engulfment genes. For this, I decided to focus not on embryonic tissues, which have been traditionally used in all previous genetic screens for engulfment mutants, but on the adult hermaphrodite germ line. I chose to work with the germ line for two major reasons: first, because RNAi has been shown to be particularly efficient in this tissue (Maine, 2001) and second because engulfed germ cells can be stained with the vital day Acridine Orange (the practical importance of this is discussed below). To test whether an efficient knockdown of the engulfment genes can be achieved, I cloned all the appropriate RNAi constructs and performed time-course analysis upon RNAi by feeding, scoring germ cell corpses by DIC microscopy. RNAi was essentially performed as previously described (Kamath et al., 2003; Lettre et al., 2004), though several parameters such as the temperature, the incubation time of RNAi plates upon seeding and the IPTG concentration were changed, in order to establish a consensus set of experimental conditions resulting in a persistent cell corpse phenotype for all, or most of, the currently know engulfment players. However, since engulfment genes are very different in terms of protein size, protein structure, and therefore protein stability, I wasn't expecting them all to be efficiently inactivated by RNAi. Indeed, despite an extensive optimization I failed to discover conditions allowing an efficient knock-down of *ced-2* and, to a certain extent, of *ced-12,* even though a mild accumulation of germ cell corpses was observed at late timepoints. For all the other engulfment genes, however, I did observe a statistically significant increase in the number of apoptotic germ cells, suggestive of a persistent cell corpse phenotype (Figure 2.1).

To further support this finding, I used a YFP::actin fusion, a very useful tool the Hengartner lab has established to monitor *in vivo* the reorganization of the actin cytoskeleton around the apoptotic cell during engulfment of dead germ cells. This results in the appearance of fluorescent halos, which are easy to quantify using high-power fluorescence microscopy. Previous work from the Hengartner lab has also shown that in engulfment mutants polymerization of actin around the apoptotic cell

corpse fails to occur, suggesting that engulfment genes are required for this process (Kinchen et al., 2005). Quantification of the number of fluorescent actin rings under DIC upon RNAi against known engulfment players revealed that actin polymerization around apoptotic corpses was significantly decreased (Figure 2.2). This decrease in the number of actin haloes and the concomitant increase in the number of apoptotic germ cells strongly indicate that engulfment is efficiently abrogated by feeding RNAi.

2.3.2 Designing a RNAi-based high-throughput screen

Having obtained relevant RNAi phenotypes I was then interested in establishing a high-throughput approach, allowing me to screen several hundreds of genes a day. To do this, I used the vital dye AO, an intercalating agent that binds nucleic acids and has been previously used successfully in Drosophila to specifically stain apoptotic cells in live animals (Abrams et al., 1993; White et al., 1994). Previous work from the Hengartner lab established that, in *C. elegans* AO preferentially stains engulfed apoptotic germ cells (Milstein S., 2001) providing a very useful tool for monitoring both programmed cell death and engulfment in the germ line, under a standard epifluorescence stereoscope. However, since wild type worms stain very poorly with AO, due to the very low levels of germ cell death, I chose to use a mutant (*gla–3*) exhibiting increased levels of endogenous germ cell apoptosis and therefore increased levels of AO staining (Kritikou et al., 2006). The rationale of the screen was that since the engulfment mutants fail to stain with AO, the phenotype one would have to screen for, upon RNAi, is the suppression of the AO staining. Using this strategy I would bypass the need to quantify the refractile apoptotic bodies under DIC optics upon RNAi-mediated knock down of each gene. With AO one can screen up to 300 genes in roughly 3 hours. To screen the same number of genes using DIC optic one would need 25 hours, considering a 5 min average slide preparation and scoring time.

I also performed a series of control experiments to assess whether RNAi against known engulfment genes was able to decrease or to completely suppress the elevated levels of AO staining of *gla-3* mutants. Using the same RNAi conditions as before I was successful in suppressing the AO staining of germ cell corpses upon RNAi-mediated inactivation of most of the currently known engulfment genes in the

gla-3 background. To quantify this effect I estimated the percentage of animals that do not stain with AO (Fig 3a and 3b). As expected, RNAi against *ced-1*, *ced-5*, *ced-6* and *ced-10* was found to be fully penetrant whereas a significantly weaker effect was observed for *ced-2* and *ced-12*, consistently with the results obtained previously. This macroscopic suppression of the AO staining correlates with a decrease in the number of AO positive apoptotic corpses, quantified under DIC optics (Figure 2.3c). To further prove that this suppression of AO staining was due to a defect in engulfment I repeated all the assays I performed for wild type worms, in the *gla-3* background. In these mutants, RNAi against known engulfment genes gave rise to a dramatic increase in the number of refractile germ cell corpses and a strong suppression of actin polymerization around dead germ cells, confirming that the suppression of AO staining observed was due to a defect in apoptotic corpse clearance (Table 2.1).

Although AO staining is currently the fastest tool for monitoring apoptosis in the *C. elegans* germ-line, its accuracy and reproducibility have proven to be questionable. Previous work from our lab established that the percentage of false positives (i.e. worms that have apoptotic corpses but fail to stain) is approximately 5%. In order to estimate the percentage of false positives and, in parallel, assess the reproducibility of the AO staining, all the genes that we identified after the primary screen were rescreened at least 2 more times. Additionally, to eliminate genes that reduce the number of apoptotic cells in the germ line (either directly or indirectly) we compared our candidates to the results of other RNAi screens (Bieri et al., 2007) and removed candidates whose knockdown has been reported to result in delayed development or germ line defects such as sterility (Figure 2.4).

Finally, candidate genes for which RNAi resulted in a reproducible suppression of the AO staining were confirmed by observing the appearance and number of apoptotic corpses in the hermaphrodite gonad, using DIC optics. Although DIC is time-consuming compared to AO staining, it is the most accurate way to survey programmed cell death; it allows to directly observe the apoptotic corpses in the hermaphrodite gonad, making it possible to perform a quantitative analysis of programmed cell death (Figure 2.4).

2.3.3. Estimation of the screening efficiency in the gla-3 background

Using the strategy described above, Johann Almendinger (a former diploma and current PhD student) and myself systematically inactivated approximately 10.000 genes corresponding to chromosomes I, III, IV and X using the RNAi feeding library built by the Ahringer lab (Kamath and Ahringer, 2003; Kamath et al., 2003). The library consists of 16757 bacterial strains, each individual bacterial clone being able to synthesize dsRNA designed to inactivate a single gene. This corresponds to approximately 86% of the 19427 current predicted genes in *C. elegans,* with similar coverage across each chromosome.

Early in the screening process I was interested in determining the effectiveness of the screen in the specific genetic background used, namely *gla-3(op216).* I, thus, examined whether I could identify correctly both the known loss-of-function phenotypes of previously studied loci and the previously reported RNAi phenotypes (Kamath et al., 2003) for the same loci (Figure 2.5). To do this, I decided to focus on a small number of post-embryonic phenotypes that were directly associated with a partial or complete suppression of the AO staining and/or led to morphological defects that could be scored easily and unambiguously at the young adult stage (the stage at which I would screen for an engulfment defect). In order to simplify subsequent data processing I defined the following phenotypic classes: the Germ Line Defective (**GLD**) class, consisting of phenotypes associated with major germ-line-related developmental defects, such as complete lack of germ-line or any abnormal gonad morphology associated with sterility; the Growth Defective (**Gro**) class consisting of slow or arrested post-embryonic growth at a post-L1 stage; the Larval defective class (**Larv**) consisting of arrested post-embryonic growth at the L1 stage or larval lethality; and finally, the Morphology Defective (**Morph**) class comprising animals that have a protruding vulva (*Pvl*) or animals whose body size is smaller than wild-type worms (*Sma*). This analysis was carried out using a small dataset from an initial pilot screen where only chromosome III was screened.

For 45% of the loci studied, the phenotypes detected in my screen were the same as both the known loss-of-function phenotype and the RNAi phenotype previously reported (Figure 2.5). Moreover, for 21% of the mutationally defined loci the expected phenotype was not observed but this finding was consistent with previous RNAi experiments, where no RNAi phenotype was reported either. Finally,

the screen failed to detect any of the expected mutant or RNAi phenotypes for 17% of previously characterized genes. The screen was more efficient in detecting GLD and Larv phenotypes, probably because they lead to a complete suppression of the AO staining and are easily detected under an epifluorescence stereoscope. Consistent with this observation, a previously published RNAi screen (Kamath et al., 2003) report that RNAi is more efficient in detecting sterile or larval lethal phenotypes than other post-embryonic defects. In addition, even if the detection efficiency of phenotypes associated with a developmental delay or a defective morphology was relatively low, it was comparable to the efficiency of other RNAi screens (Kamath et al., 2003). Together, all these findings suggest that in *gla–3(op216)* animals RNAi-mediated inactivation of genes is at least as effective as in wild-type worms. Moreover, this analysis revealed no synthetic phenotypes specific to the *gla-3* background, since the RNAi phenotypes obtained were similar to those obtained with wild-type worms.

2. 3.4. Screening of chromosomes I, III, IV and X

Upon systematic inactivation of 9215 genes we identified 60 candidate genes for which RNAi reproducibly results in partial or complete suppression of AO staining. This corresponds to less than 1% of the subset of the library screened. Knockdown of a subset of candidates increased numbers of refractile cell corpses in the gonad (the complete candidate list can be found in chapter 3 as Supplementary Table S1). Interestingly, among these candidate genes are *ced-1*, located on chromosome I, *ced-6*, located on chromosome III and *ced-5*, located on chromosome IV, three already characterized engulfment genes. These three engulfment genes are the only ones for which RNAi clones exist in the RNAi library (Kamath et al., 2003) and, thus, their successful recovery from a blind unbiased screen validates our screening strategy.

2.3.4.1. The Arp2/3 complex and engulfment in C. elegans

In our screen we identified two members of the Arp2/3 complex in *C. elegans*, *arx-3* and *arx-5* (Sawa et al., 2003); Arp2/3 is known to play a key role during actin reorganization and corpse removal in mammalian systems (Tosello-Trampont et al., 2003). I found that RNAi against *arx-3* and *arx-5* results in a dramatic increase in the

number of germ cell corpses and a strong suppression of actin polymerization around dying germ cells suggesting that the function of this complex in apoptotic cell corpse clearance is conserved in *C. elegans* (Figure 2.6). As expected, RNAi-mediated knockdown of several subunits of the complex gave a similar phenotype (data not shown). The known catalytic function of this complex as well as its proven involvement in engulfment and phagocytosis in other systems make Arp2/3 an ideal candidate acting downstream of CED-10/Rac1 to mediate membrane extension. However, the molecular link between activation of the latter and Arp2/3 remains to be determined, since RNAi experiments targeting most of the known regulators of this complex did not result in an engulfment defect (data not shown).

2.3.4.2. Discovery of genes controlling late steps of the engulfment process

Among the candidate genes identified was also the *C. elegans* homologue of Vps34, a phosphoinositide-3-kinase, which has been proposed to function in maturation of phagosomes into acidic lysosomes in macrophages (Vieira et al., 2001). This suggests that our screen could isolate not only genes involved in early steps of engulfment – such as recognition of the dying cell and extension of pseudopods around it - but also genes controlling events downstream of corpse internalization. Indeed, several lines of experimental evidence indicate that, in *C. elegans, vps-34* acts at a late step during engulfment, after the corpse has been completely internalized. *vps-34(RNAi)* results in increased numbers of AO negative germ cell corpses without significantly affecting actin polymerization around dying cells suggesting that, in this case, the corpses are normally internalized but persist inside the phagocyte (see Chapter 3 for more details). By homology, several other genes which we identified may also play a role during later steps of the engulfment process (Bieri et al., 2007). These include *phi-25,* encoding a protein homologous to human vacuolar protein-associating protein 4B, *dyci-1* encoding for a dynein intermediate chain, *rab-10,* encoding for a small GTPase of the Ras superfamily, *vha-15*, encoding for a vacuolar ATPase and *rme-8,* a DnaJ-domain protein involved in endosomal trafficking. In this category of genes belongs another one of our candidates *dyn-1,* the only *C. elegans* dynamin homolog. The discovery of all these genes, believed to control late events during the process of engulfment, has prompted us to further investigate the mechanisms involved in phagosome maturation in the worm. The role of several of

these genes in regulating phagosome maturation has been experimentally addressed and will be discussed in more details in the Chapter 3.

2.4 DISCUSSION

Here I describe a reverse genetics approach aiming to identify novel players of apoptotic cell clearance in *C. elegans*. We screened 9215 genes and we identified 60 genes for which RNAi reproducibly resulted in suppression of AO staining of apoptotic germ cell corpses. While for a subset of these genes we did observe an increase in the number of germ cell corpses (e.g. *dyn-1* and *vps-34*) for several others we found no significant difference in the number of corpses upon RNAi treatment. Knockdown of these genes might only slightly delay the engulfment process rather than blocking it. Alternatively some of these genes might be important only for acridine orange staining but not for engulfment *per se*, although these two processes seem so far to be tightly interconnected.

Our screen has also proven to be very efficient in identifying genes required for late steps of the engulfment process, after completion of the sequence of events (corpse recognition, membrane extension and membrane closure) leading to corpse internalization. Interestingly, several of these genes have been previously known to be important for endocytic traffic in *C. elegans* suggesting that there is a point of convergence between the pathways mediating apoptotic cell corpse engulfment and endocytosis. While this seems to be a rather trivial conclusion the reality is far from being that simple. First, not all the genes involved in endocytosis play a role in apoptotic cell corpse clearance. As an example, loss of function mutations in *rme-1* and *rme-2*, which play key roles in receptor-mediated endocytosis in the nematode (Grant and Hirsh, 1999; Grant et al., 2001; Lin et al., 2001) have no engulfment defect, suggesting that these genes are not important for corpse removal (Chapter 3, supplementary Table S4). Second, depending on the biological context, either endocytosis or engulfment, the same protein might be subject to different types of regulation. This concept is nicely illustrated in the case of RAB-5, a small GTPase of the Ras superfamily, which plays a key role in membrane traffic during endocytosis. RAB-5, which is a well-known early endosome marker, is also recruited around apoptotic corpses both in *C. elegans* and in a cell culture system, suggesting that this

molecule also plays a conserved role in the maturation of the phagosome during apoptotic cell corpse engulfment. In the context of endocytosis, the activity of Rab5 is known to be regulated by the GEF Rabex5 (Sato et al., 2005) and this mode of regulation is conserved in *C. elegans* where loss of function mutations in *rme-6*, the Rabex5 homolog, are associated with endocytic defects. These mutations however have no effect on apoptotic cell corpse clearance suggesting that in this case the activity of RAB-5 has to be regulated by a different player (Chapter 3, supplementary Table S4). This will be discussed in more details in the following chapter where I will present strong evidence about the involvement of Rab GTPases in cell corpse engulfment.

My initial idea to use an RNAi-based strategy as a way to obtain a controlled reduction of function rather than a strong loss-of-function has led to the identification of several novel engulfment genes that have additional essential functions. Loss of function mutations, or even reduction of function be means of RNAi, of subunits of the Arp2/3 complex (Sawa et al., 2003), *dyn-1* (Clark et al., 1997; Thompson et al., 2002), *vps-34* (Bieri et al., 2007) or *rme-8* (Zhang et al., 2001) have been shown to result in embryonic or early larval lethality. Such genes have been missed during previous genetic screens that required animals homozygous for engulfment mutations to be viable. Thus, even though further analysis of our candidates was somehow limited by the availability of conditional mutants, the RNAi approach described here has proven to be a valuable tool in deciphering the mechanisms of apoptotic cell corpse clearance.

The design of our screen was such that we were also expecting to pull out genes acting as suppressors of *gla-3*-mediated germ line apoptosis. Even though for some of our candidates we did observe slightly lower numbers of germ cell corpses compared to *gla-3* alone it is unclear whether this reflects an apoptotic suppression or arises as a secondary consequence of slight growth-related or germ line defects. As a result, it is at present unclear whether in our list there is a hidden clue which will elucidate the mechanism by which *gla-3* triggers germ cell death (see manuscript in chapter 4 for more details). A comprehensive analysis of all the candidate genes resulting in lower number of germ cell corpses need to be performed to address this question.

This RNAi screen provided us with a significant number of interesting candidates, and has opened several new doors in the *C. elegans* biology of apoptotic cell corpse engulfment. However it is unlike that these genes represent the full complement of the factors involved in corpse clearance. So the question that arises is "how are we going too find *even more* new genes"? After spending several months setting up this RNAi screen and after having screened several thousands of RNAi clones I believe we have reached the limits of this approach in terms of sensitivity. I'm convinced that the most efficient way to identify the remaining missing links would be to follow custom-tailored candidate-based approaches or focus more on either forward or reverse modifier screens. Two graduate students in the Hengartner lab, Johann Amendinger and Sérgio Pinto, have already started working in this direction under my guidance. They used bioinformatics approaches to selectively define a subset of potentially interesting genes based on their functional domain content and constructed a mini-RNAi library containing approximately 500 clones. The next step will be to specifically inactivate each one of these genes using RNAi by feeding in several different mutant backgrounds and screen for genes that either suppress or re-allow AO staining of germ cell corpses. This new approach has already started yielding very exciting results!

2.5 METHODS

2.5.1 General methods and strains

Methods for culturing *C. elegans* have been described by Brenner (Brenner, 1974). All mutant strains used in these study were grown at 20°C and were derived from the wild type variety Bristol N2. Mutations used were as follows: LGI: *gla-3(op216),* and *LGIV opIs110[Plim-7::yfp::act-5]*. Unless noted otherwise mutations were previously described (Bieri et al., 2007)

2.5.2 Screening using RNAi by feeding

RNAi by feeding was performed as described (Kamath et al., 2001; Lettre et al., 2004) with the following modifications. Plates containing NGM-agarose supplemented with 2mM IPTG ("RNAi plates") were inoculated with 300mL of bacterial cultures grown 8-12h for each targeted gene. Between 30 and 60 synchronized L1 stage worms where placed on each RNAi plate and left for 72h at 20°C. The following dsRNA-synthesizing bacteria were used as positive controls for each RNAi experiment: *ced-3(RNAi)* resulting in complete suppression of germ line apoptosis, *bir-1(RNAi)* giving rise to high embryonic lethality *unc-22(RNAi)* exhibiting an uncoordinated phenotype. In most cases, the RNAi phenotypes of these genes were found to be fully penetrant. Worms fed with bacteria carrying the RNAi vector (L4440) without any insert or with an insert originating from the coding sequence of GFP, referred to as *GFP(RNAi)*, were used as the reference strain.

In order to estimate the relative number of corpses after knock-down of each targeted gene, young adult worms were stained with Acridine Orange (AO; Molecular Probes, Eugene, OR), a vital dye that preferentially stains apoptotic germ cells (Milstein S, 2001). Staining with AO was performed as follows. 0.5 mL of a solution of AO in M9 buffer (0.02mg/mL) was directly added to each RNAi plate and worms were stained for 1 to 1.5 hours at room temperature, avoiding light exposure. During this time worms ingested the dye while eating dsRNA-expressing *E. coli*. Worms were washed off RNAi plates with 300mL M9 buffer and transferred onto fresh OP50-seeded plates. In order to reduce non-specific background staining in the intestine and the germ line, worms were allowed to destain for 30 min before observation, avoiding light exposure.

Phenotypic analysis was carried out by inspecting worms under a dissecting microscope, equipped with standard epifluorescence filters.

2.5.3 DIC microscopy and cell corpse counts

For the Nomarski analysis animals were placed on 4% agar slides in a drop of M9 salt solution containing either 30 mM NaN_3 (Hodgkin, 1980) or 3-5mM levamisole (Sigma) and mounted under a coverslip for observation. For most animals observed only one gonad arm was scored, as the other arm was usually concealed by the intestine. For each targeted gene associated with a suppression of the AO staining the average corpse number with the standard deviation (s.d) were determined using the Excel program (Microsoft).

2.5.4. Photography

Pictures were captured using a ORCA-ER digital CCD camera on a Leica DM-RA research microscope and processed using OpenLab software and Photoshop (Adobe).

2.5.5. Bioinformatic analyses and categorization of genes

To corroborate that the RNAi phenotypes observed were the result of the inactivation of the corresponding genes each candidate RNAi clone was sequenced. Additionaly, to confirm that the RNAi phenotypes were due to the inactivation of a single gene candidate RNAi clones were compared with the database of strains that are predicted to hit more than one gene (Kamath et al., 2003). Clones that were found to cross-react with more than one genes were excluded.

Candidate genes were grouped into functional classes as previously described (Kamath et al., 2003). Briefly these functional classes are: (1) DNA metabolism (synthesis, replication and structure), (2) RNA metabolism (general transcription machinery, splicing, processing, RNA binding and regulation of chromatin), (3) Protein metabolism (translation, degradation and folding) (4) Metabolism, including energy production and intermediary metabolism, (5) Cell-cycle and chromosome dynamics, (6) Cellular structure, including cell junction/adhesion, cytoskeleton, ion

channels, protein sorting, vesicle regulation and cell polarity, (7) Gene specific transcription, (8) Signaling, including kinases, phosphatases and components of signal transduction pathways and (9) Viral, referring to retroviral and transposon-derived sequences. Genes which could not be unambiguously assigned to one of the above functional classes, either because they have motives for which there is insufficient information to assign a function to or because they don't have any significant matches in any other organisms, were placed into the "unknown" functional class.

2.5.6. Plasmid construction and cloning

Genomic fragments corresponding to *ced-2*, *ced-7, ced-10*, and *ced-12* loci were amplified by PCR from N2 genomic DNA using primers sets designed by the Ahringer lab (Kamath et al., 2003). The sizes of amplicons were as follows: 917 bp for *ced-2*, 2247 bp for *ced-7*, 2385 bp for *ced-10*, and 969 bp for *ced-12*.

All fragments were cloned in PCR2.1-TOPO vector (Invitrogen) and their ends were sequenced to ensure that there were no mutations. Inserts were then excised from the corresponding plasmids using EcoRI and subcloned in the L4440 RNAi vector using the same enzyme. For *ced-7* the size of the EcoRI insert was 1471 bp since the PCR product contained two additional EcoRI restriction sites.

Recombinant plasmids were then transformed into HT115(DE3) to generate the corresponding feeding RNAi clones.

2.6. REFERENCES

Abrams, J. M., White, K., Fessler, L. I., and Steller, H. (1993). Programmed cell death during Drosophila embryogenesis. Development *117*, 29-43.

Adams, J. M. (2003). Ways of dying: multiple pathways to apoptosis. Genes Dev *17*, 2481-2495.

Bieri, T., Blasiar, D., Ozersky, P., Antoshechkin, I., Bastiani, C., Canaran, P., Chan, J., Chen, N., Chen, W. J., Davis, P., *et al.* (2007). WormBase: new content and better access. Nucleic Acids Res *35*, D506-510.

Brenner, S. (1974). The genetics of Caenorhabditis elegans. Genetics *77*, 71-94.

Brugnera, E., Haney, L., Grimsley, C., Lu, M., Walk, S. F., Tosello-Trampont, A. C., Macara, I. G., Madhani, H., Fink, G. R., and Ravichandran, K. S. (2002). Unconventional Rac-GEF activity is mediated through the Dock180-ELMO complex. Nat Cell Biol *4*, 574-582.

Clark, S. G., Shurland, D. L., Meyerowitz, E. M., Bargmann, C. I., and van der Bliek, A. M. (1997). A dynamin GTPase mutation causes a rapid and reversible temperature-inducible locomotion defect in C. elegans. Proc Natl Acad Sci U S A *94*, 10438-10443.

Ellis, R. E., Jacobson, D. M., and Horvitz, H. R. (1991). Genes required for the engulfment of cell corpses during programmed cell death in Caenorhabditis elegans. Genetics *129*, 79-94.

Grant, B., and Hirsh, D. (1999). Receptor-mediated endocytosis in the Caenorhabditis elegans oocyte. Mol Biol Cell *10*, 4311-4326.

Grant, B., Zhang, Y., Paupard, M. C., Lin, S. X., Hall, D. H., and Hirsh, D. (2001). Evidence that RME-1, a conserved C. elegans EH-domain protein, functions in endocytic recycling. Nat Cell Biol *3*, 573-579.

Gumienny, T. L., Brugnera, E., Tosello-Trampont, A. C., Kinchen, J. M., Haney, L. B., Nishiwaki, K., Walk, S. F., Nemergut, M. E., Macara, I. G., Francis, R., *et al.* (2001). CED-12/ELMO, a novel member of the CrkII/Dock180/Rac pathway, is required for phagocytosis and cell migration. Cell *107*, 27-41.

Hamon, Y., Trompier, D., Ma, Z., Venegas, V., Pophillat, M., Mignotte, V., Zhou, Z., and Chimini, G. (2006). Cooperation between Engulfment Receptors: The Case of ABCA1 and MEGF10. PLoS ONE *1*, e120.

Henson, P. M. (2005). Engulfment: ingestion and migration with Rac, Rho and TRIO. Curr Biol *15*, R29-30.

Hong, Y., Roy, R., and Ambros, V. (1998). Developmental regulation of a cyclin-dependent kinase inhibitor controls postembryonic cell cycle progression in Caenorhabditis elegans. Development *125*, 3585-3597.

Jehle, A. W., Gardai, S. J., Li, S., Linsel-Nitschke, P., Morimoto, K., Janssen, W. J., Vandivier, R. W., Wang, N., Greenberg, S., Dale, B. M., *et al.* (2006). ATP-binding cassette transporter A7 enhances phagocytosis of apoptotic cells and associated ERK signaling in macrophages. J Cell Biol *174*, 547-556.

Kamath, R. S., and Ahringer, J. (2003). Genome-wide RNAi screening in Caenorhabditis elegans. Methods *30*, 313-321.

Kamath, R. S., Fraser, A. G., Dong, Y., Poulin, G., Durbin, R., Gotta, M., Kanapin, A., Le Bot, N., Moreno, S., Sohrmann, M., *et al.* (2003). Systematic functional analysis of the Caenorhabditis elegans genome using RNAi. Nature *421*, 231-237.

Kamath, R. S., Martinez-Campos, M., Zipperlen, P., Fraser, A. G., and Ahringer, J. (2001). Effectiveness of specific RNA-mediated interference through ingested double-stranded RNA in Caenorhabditis elegans. Genome Biol *2*, RESEARCH0002.

Kinchen, J. M., Cabello, J., Klingele, D., Wong, K., Feichtinger, R., Schnabel, H., Schnabel, R., and Hengartner, M. O. (2005). Two pathways converge at CED-10 to mediate actin rearrangement and corpse removal in C. elegans. Nature *434*, 93-99.

Kinchen, J. M., and Hengartner, M. O. (2005). Tales of cannibalism, suicide, and murder: Programmed cell death in C. elegans. Current Topics in Developmental Biology *65*, 1-45.

Kritikou, E. A., Milstein, S., Vidalain, P. O., Lettre, G., Bogan, E., Doukoumetzidis, K., Gray, P., Chappell, T. G., Vidal, M., and Hengartner, M. O. (2006). C. elegans GLA-3 is a novel component of the MAP kinase MPK-1 signaling pathway required for germ cell survival. Genes Dev *20*, 2279-2292.

Lettre, G., Kritikou, E. A., Jaeggi, M., Calixto, A., Fraser, A. G., Kamath, R. S., Ahringer, J., and Hengartner, M. O. (2004). Genome-wide RNAi identifies p53-dependent and -independent regulators of germ cell apoptosis in C. elegans. Cell Death Differ *11*, 1198-1203.

Lin, S. X., Grant, B., Hirsh, D., and Maxfield, F. R. (2001). Rme-1 regulates the distribution and function of the endocytic recycling compartment in mammalian cells. Nat Cell Biol *3*, 567-572.

Liu, Q. A., and Hengartner, M. O. (1998). Candidate adaptor protein CED-6 promotes the engulfment of apoptotic cells in C. elegans. Cell *93*, 961-972.

Luciani, M. F., and Chimini, G. (1996). The ATP binding cassette transporter ABC1, is required for the engulfment of corpses generated by apoptotic cell death. Embo J *15*, 226-235.

Maine, E. M. (2001). RNAi As a tool for understanding germline development in Caenorhabditis elegans: uses and cautions. Dev Biol *239*, 177-189.

Meier, P., Finch, A., and Evan, G. (2000). Apoptosis in development. Nature *407*, 796-801.

Metzstein, M. M., Stanfield, G. M., and Horvitz, H. R. (1998). Genetics of programmed cell death in C. elegans: past, present and future. Trends Genet *14*, 410-416.

Reddien, P. W., and Horvitz, H. R. (2000). CED-2/CrkII and CED-10/Rac control phagocytosis and cell migration in Caenorhabditis elegans. Nat Cell Biol *2*, 131-136.

Rual, J. F., Ceron, J., Koreth, J., Hao, T., Nicot, A. S., Hirozane-Kishikawa, T., Vandenhaute, J., Orkin, S. H., Hill, D. E., van den Heuvel, S., and Vidal, M. (2004). Toward improving Caenorhabditis elegans phenome mapping with an ORFeome-based RNAi library. Genome Res *14*, 2162-2168.

Sato, M., Sato, K., Fonarev, P., Huang, C. J., Liou, W., and Grant, B. D. (2005). Caenorhabditis elegans RME-6 is a novel regulator of RAB-5 at the clathrin-coated pit. Nat Cell Biol *7*, 559-569.

Sawa, M., Suetsugu, S., Sugimoto, A., Miki, H., Yamamoto, M., and Takenawa, T. (2003). Essential role of the C. elegans Arp2/3 complex in cell migration during ventral enclosure. J Cell Sci *116*, 1505-1518.

Shi, Y. (2002). Mechanisms of caspase activation and inhibition during apoptosis. Mol Cell *9*, 459-470.

Su, H. P., Nakada-Tsukui, K., Tosello-Trampont, A. C., Li, Y., Bu, G., Henson, P. M., and Ravichandran, K. S. (2002). Interaction of CED-6/GULP, an adapter protein involved in engulfment of apoptotic cells with CED-1 and CD91/low density lipoprotein receptor-related protein (LRP). J Biol Chem *277*, 11772-11779.

Thompson, H. M., Skop, A. R., Euteneuer, U., Meyer, B. J., and McNiven, M. A. (2002). The large GTPase dynamin associates with the spindle midzone and is required for cytokinesis. Curr Biol *12*, 2111-2117.

Timmons, L., Court, D. L., and Fire, A. (2001). Ingestion of bacterially expressed dsRNAs can produce specific and potent genetic interference in Caenorhabditis elegans. Gene *263*, 103-112.

Timmons, L., and Fire, A. (1998). Specific interference by ingested dsRNA. Nature *395*, 854.

Tosello-Trampont, A. C., Nakada-Tsukui, K., and Ravichandran, K. S. (2003). Engulfment of apoptotic cells is negatively regulated by Rho-mediated signaling. J Biol Chem *278*, 49911-49919.

Vieira, O. V., Botelho, R. J., Rameh, L., Brachmann, S. M., Matsuo, T., Davidson, H. W., Schreiber, A., Backer, J. M., Cantley, L. C., and Grinstein, S. (2001). Distinct roles of class I and class III phosphatidylinositol 3-kinases in phagosome formation and maturation. J Cell Biol *155*, 19-25.

White, K., Grether, M. E., Abrams, J. M., Young, L., Farrell, K., and Steller, H. (1994). Genetic control of programmed cell death in Drosophila. Science *264*, 677-683.

Wu, Y. C., and Horvitz, H. R. (1998a). The C. elegans cell corpse engulfment gene ced-7 encodes a protein similar to ABC transporters. Cell *93*, 951-960.

Wu, Y. C., and Horvitz, H. R. (1998b). C. elegans phagocytosis and cell-migration protein CED-5 is similar to human DOCK180. Nature *392*, 501-504.

Wu, Y. C., Tsai, M. C., Cheng, L. C., Chou, C. J., and Weng, N. Y. (2001). C. elegans CED-12 acts in the conserved crkII/DOCK180/Rac pathway to control cell migration and cell corpse engulfment. Dev Cell *1*, 491-502.

Zhang, Y., Grant, B., and Hirsh, D. (2001). RME-8, a conserved J-domain protein, is required for endocytosis in Caenorhabditis elegans. Mol Biol Cell *12*, 2011-2021.

Zhou, Z., Caron, E., Hartwieg, E., Hall, A., and Horvitz, H. R. (2001a). The C. elegans PH domain protein CED-12 regulates cytoskeletal reorganization via a Rho/Rac GTPase signaling pathway. Dev Cell *1*, 477-489.

Zhou, Z., Hartwieg, E., and Horvitz, H. R. (2001b). CED-1 is a transmembrane receptor that mediates cell corpse engulfment in C. elegans. Cell *104*, 43-56.

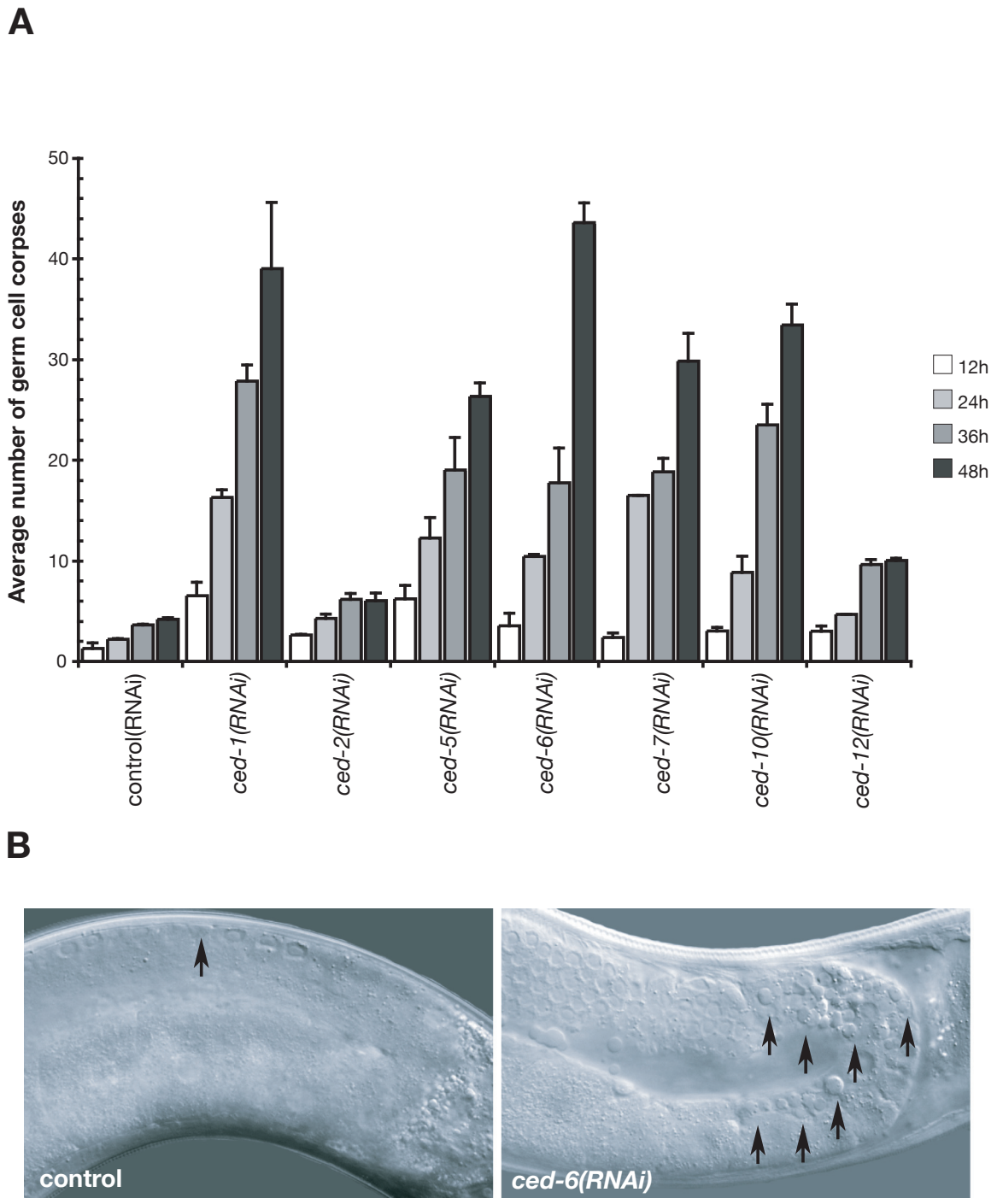

FIGURE 2.1 RNAi phenocopies weak loss of function mutations in engulfment genes

(A) Synchronized wild type worms were fed with bacteria expressing dsRNA against *ced-1, ced-2, ced-5, ced-6, ced-7, ced-10* and *ced-12* as described in materials and methods. Apoptotic corpses were scored using DIC optics at 12, 24, 36 and 48 after the L4/adult molt. Data shown represent the average of the mean of at least two independent experiments (n=10-15 per experiment). Errors bars represent the SD. (B) Representative DIC photomicrographs of wild type control and wild type worms fed with RNAi bacteria targeting *ced-6*, 36h post L4/adult molt. Arrows indicate areas with apoptotic corpses.

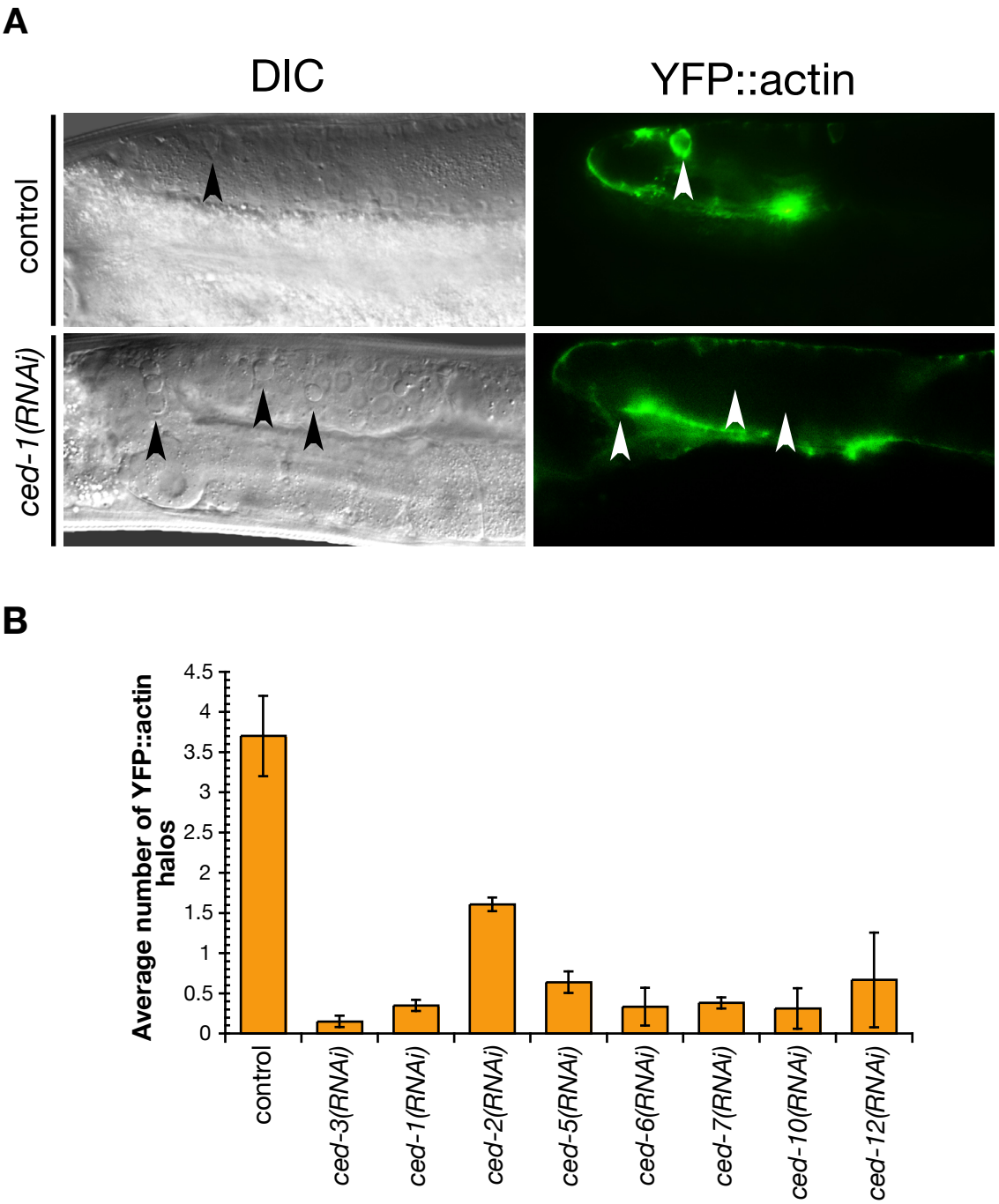

FIGURE 2.2 RNAi against known engulfment genes abrogates actin polymerization around apoptotic germ cell corpses

(A) DIC and fluorescence pictures of wild type control and *ced-1(RNAi)* treated animals carrying the *opIs110[Plim 7::yfp::act-5]*, 24h post L4/adult molt. The *opIs110* transgene expresses YFP-tagged actin in the somatic sheath cells, which highlights corpses in the process of being engulfed. Arrowheads indicate apoptotic cells or YFP::actin halos.
(B) Synchronized wild type worms carrying the *opIs110*transgene were scored by fluorescence microscopy for recruitment of YFP::actin around apoptotic germ cell corpses upon RNAi against *ced-1, ced-2, ced-5, ced-6, ced-7, ced-10* and *ced-12*. Data shown represent the average of the mean of at least three independent experiments (n=10-15 per experiment). Errors bars represent the SD.

FIGURE 2.3 RNAi against known engulfment genes suppresses AO staining of germ cell corpses in the *gla-3(op216)* background

(A) Fluorescence pictures of *gla-3(op216)* control and *ced-1(RNAi)*, *ced-2(RNAi)*, *ced-6(RNAi)* and *ced-10(RNAi)*-treated worms stained with Acridine Orange, 24h post L4/adult molt. RNAi against *ced-3* suppresses germ cell death and was used as a negative control for AO staining. Arrowheads indicate areas exhibiting intense AO staining. The asterisk indicates the *C. elegans* spermatheca, which occasionally stains intensely with AO. (B) Synchronized *gla-3(op216)* worms fed with RNAibacteria targeting *ced-1, ced-2, ced-5, ced-6, ced-7, ced-10* and *ced-12* were stained with Acridine Orange. The penetrance of the suppression of AO staining was then estimated by counting AO positive vs AO negative worms. (C) Synchronized *gla-3(op216)* worms fed with RNAi bacteria targeting *ced-1, ced-2, ced-5, ced-6, ced-7, ced-10* and *ced-12* were stained with Acridine Orange and then the number of AO positive germ cell corpses was determined using fluorescence microscopy, 24h post L4/adult molt. Data shown represent the average of the mean of at least three independent experiments (n=10-15 per experiment). Errors bars represent the SD.

A

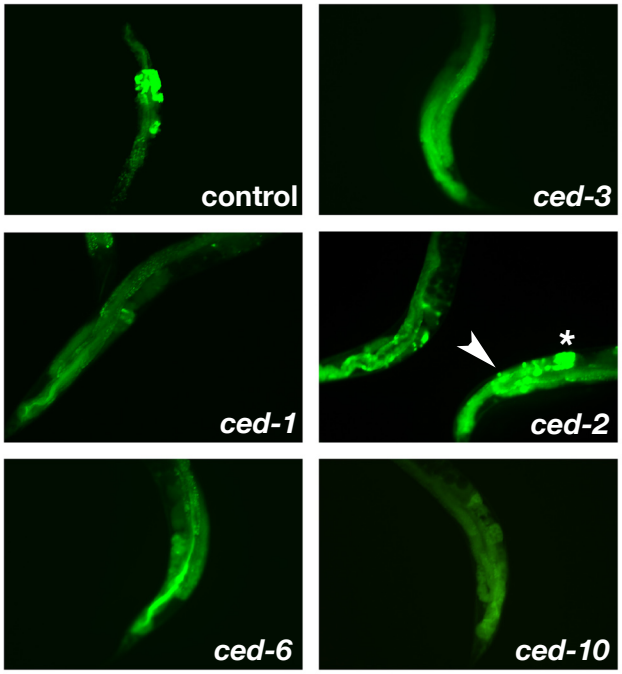

B

Genotype	AO+ worms	AO- worms	*n*
gla-3 ced-1(RNAi)	0	149	149
gla-3;ced-2(RNAi)	88	55	143
gla-3;ced-5(RNAi)	18	166	184
gla-3;ced-6(RNAi)	1	155	156
gla-3;ced-7(RNAi)	81	82	163
gla-3;ced-10(RNAi)	2	135	137
gla-3 ced-12(RNAi)	15	65	80
gla-3;GFP(RNAi) control	98	8	106

C

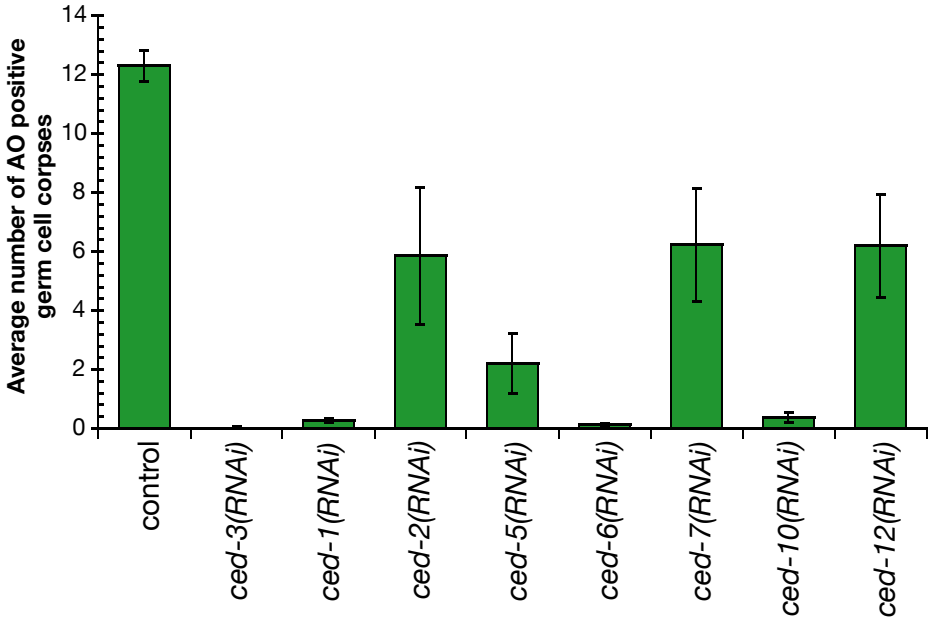

Table 2.1 RNAi against engulfment genes results in increased number of germ cell corpses and a strong suppression of actin halos in the *gla-3* background

Genotype	DIC	YFP::actin	n
gla-3(lf);ced-3(RNAi)	0.1 ± 0.1	-	30
gla-3(lf);control(RNAi)	8.7 ± 1.7	-	30
gla-3(lf);ced-1(RNAi)	26.6 ± 6.1	-	30
gla-3(lf);ced-2(RNAi)	13.0 ± 2.0	-	23
gla-3(lf);ced-5 (RNAi)	19.4 ± 4.3	-	30
gla-3(lf);ced-6(RNAi)	20.3 ± 3.6	-	29
gla-3(lf);ced-7(RNAi)	29.8 ± 2.2	-	20
gla-3(lf);ced-10(RNAi)	33.1 ± 3.9	-	23
gla-3(lf);ced-12(RNAi)	10.1 ± 4.8	-	20
gla-3(lf);opIs110;ced-3(RNAi)	0	0	23
gla-3(lf);opIs110;control(RNAi)	11.0 ± 1.6	7.0 ± 1.4	23
gla-3(lf);opIs110;ced-1(RNAi)	36.1 ± 2.3	0.4 ± 0.1	20
gla-3(lf);opIs110;ced-2(RNAi)	18.5 ± 6.0	5.3 ± 0.5	36
gla-3(lf);opIs110;ced-5(RNAi)	28.7 ± 3.7	0.6 ± 0.4	20
gla-3(lf);opIs110;ced-6(RNAi)	26.5 ± 3.0	0.4 ± 0.3	20
gla-3(lf);opIs110;ced-7(RNAi)	21.2 ± 3.5	1.1 ± 0.2	34
gla-3(lf);opIs110;ced-10(RNAi)	31.8 ± 3.1	0.3 ± 0.2	36
gla-3(lf);opIs110;ced-12(RNAi)	17.7 ± 3.3	5.7 ± 2.5	20

Synchronized *gla-3(op216)* worms with or without the *opIs110[Plim 7::ypf::act-5]* transgene were fed with RNAi bacteria targeting *ced-1, ced-2, ced-5, ced-6, ced-7, ced-10* and *ced-12* . The number of apoptotic cells and the number of YFP:actin halos were then determined using DIC and fluorescence microscopy, 24h post L4/adult molt. Data shown represent the average of the mean of at least two independent experiments (n=10-15 per experiment) +/- SD.

FIGURE 2.4 Schematic representation of the screening strategy

Worms were fed bacteria expressing dsRNA at the L1 larval stage, then stained with Acridine Orange once they reached adulthood. AO negative candidates were rescreened at least 3 times and only candidates for which RNAi resulted in a reproducible suppression of AO staining were analysed further. These candidates were then compared to the results of previous RNAi screens to exclude false negatives due to sterility or other gonadal or growth defects. Finally. refractile cell corpses were scored in the 12h-hour adult hermaphrodite gonad using DIC microscopy.

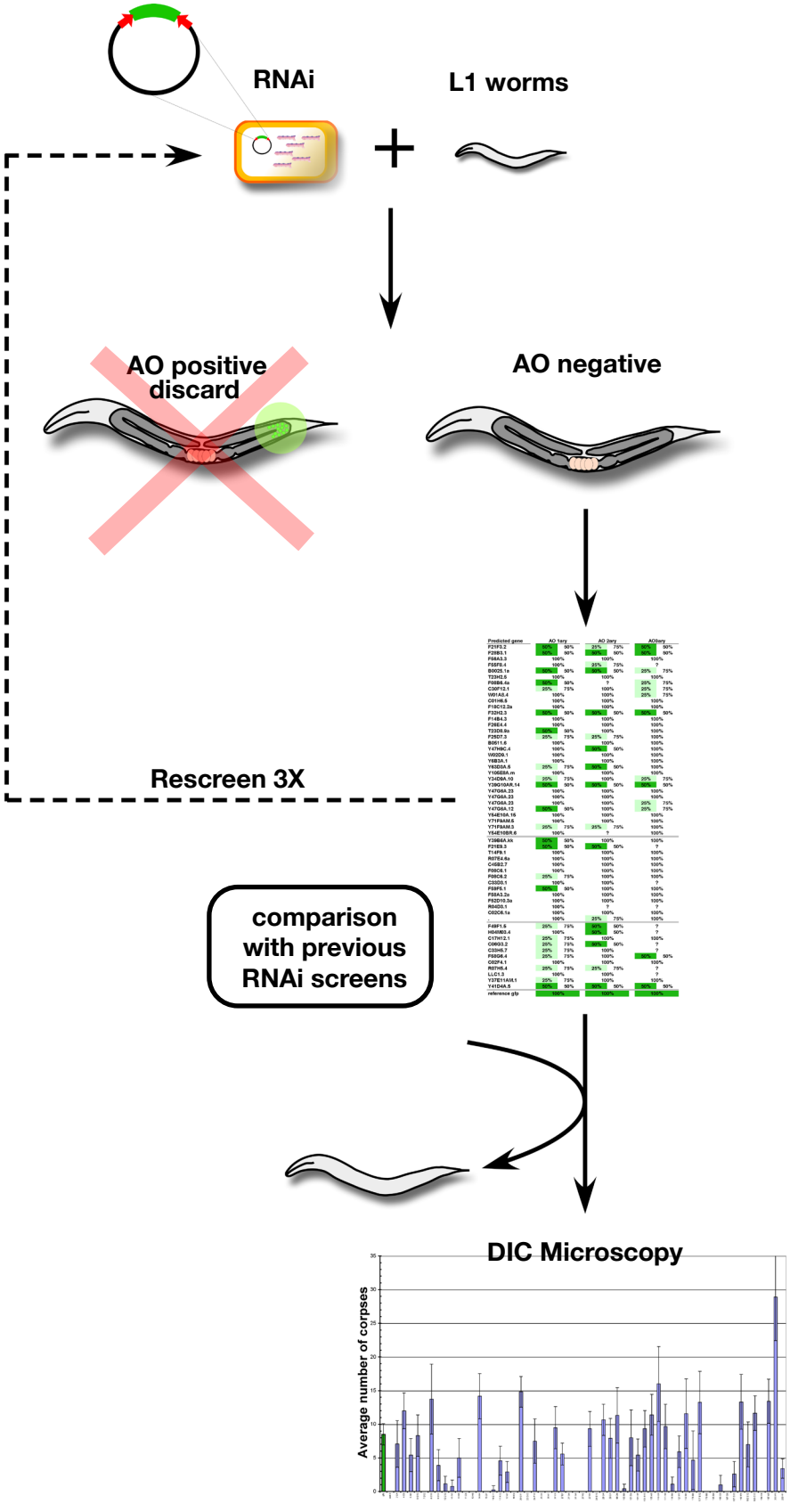
RNAi
L1 worms
AO positive
discard
AO negative
Rescreen 3X
comparison
with previous
RNAi screens
DIC Microscopy
Average number of corpses

FIGURE 2.5 Effectiveness of the screen in identifying correctly loss of function phenotypes

(A) RNAi phenotypes were compared with those of genes that have known loss-of-function phenotypes and with the previously reported RNAi phenotypes of the same loci. Phenotypic classes were defined as described in the text and Methods. "Known mutant phenotype" gives the published phenotype for the indicated gene, "Known RNAi phenotype" denotes the published RNAi phenotype (Kamath et al., 2003), (-) no phenotype was detected, (4) a phenotype was detected, "Hit" means that an RNAi phenotype was obtained, "Pub M" denotes that the RNAi phenotype matched the published mutant phenotype, "Pub R" denotes that the RNAi phenotype matched the published RNAi phenotype. (B) Pie chart illustrates the effectiveness of the screen in identifying known phenotypes. "RNAi + Mutant" (green) denotes the percentage of genes for which the phenotype observed was the same both as the mutant and the RNAi phenotype previously reported, "RNAi" (yellow) is the percentage of genes for which the phenotype detected was the same as the RNAi phenotype previously reported, "Mutant" (purple) denotes the percentage of genes for which the phenotype detected matched the known mutant phenotype, "No match" is the percentage of genes for which no phenotype was obtained. "ND" non determined. (C) Comparison of the effectiveness of the screen with previously reported RNAi screens in identifying known loss-of-function phenotypes. "RNAi phenotype detected" gives the number of genes for which a phenotype was obtained in my screen that matched the mutant phenotype, "RNAi phenotype reported" gives the number of genes for which the RNAi phenotype published matched the mutant phenotype (Kamath et al., 2003). Percentages are given as the percentage of total number of genetic loci with a known mutant phenotype (29).

A

Locus	Predicted Gene	Known Mutant Phenotype	Known RNAi Phenotype	RNAi Phenotype GlDe	GroDe	MorphDe	LarvDe	Result Hit	Pub M	Pub R
arf-1	B0336.2	Emb/Ste	Emb, Ste, Unc, Pvl, Rup	✓	-	✓	-	✓	✓	✓
clk-1	ZC395.2	Gro	-	-	-	-	-	-	-	✓
cyk-1	F11H8.4	Emb/Ste	Emb, Adl, Rup, Clr	-	-	-	-	-	-	-
daf-4	C05D2.1a	Sma, Egl	-	-	-	-	-	-	-	✓
egl-45	C27D11.1	Ste, Egl	Ste, Sck, Egl	ND	ND	ND	ND	ND	ND	ND
fem-2	T19C3.8	Ste	-	-	-	-	-	-	-	✓
glp-1	F02A9.6	Emb/Ste	Emb, Ste, Stp	✓	-	-	-	✓	✓	✓
gro-1	ZC395.6	Gro	-	-	-	-	-	-	-	-
hmg-1.2	F47D12.4a	Ste,Pvl, Rup	Stp	✓	-	✓	-	✓	✓	✓
ina-1	F54G8.3	Pvl	Rup	ND	ND	ND	ND	ND	ND	ND
let-756	C05D11.4	Lvl, Gro, Clr, Pvl, Egl, Unc	-	-	-	-	-	-	-	✓
mab-21	F35G12.6	Emb, Sma, Unc	-	-	-	-	-	-	-	✓
mev-1	T07C4.7	wk Ste, Gro	Emb, Ste, Gro	✓	✓	-	-	✓	✓	✓
mpk-1	F43C1.2a	Emb/Ste, Vul, Egl	Emb, Ste	ND	ND	ND	ND	ND	ND	ND
mup-4	K07D8.1	wk Emb, Lvl, Prz	Adl, Prz, Sck	-	-	-	✓	✓	✓	-
ncc-1	T05G5.3	Emb/Ste, Unc, Dpy, Big hea	Emb, Ste	✓	-	-	-	✓	✓	✓
nob-1	Y75B8A.2a	Emb/Lvl, Bmd	Emb, Bmd	-	-	-	-	-	-	-
pal-1	C38D4.6	Emb/Ste, Bmd, Sck	Emb	-	-	-	-	-	-	-
pat-3	ZK1058.2	Emb, Lvl	Ste, Adl, Sck, Unc	✓	-	-	✓	✓	✓	✓
pat-4	C29F9.7	Emb, Lvl	Emb, Ste, Unc, Prz, Lvl	-	-	-	✓	✓	✓	✓
pha-1	Y48A6C.5	Lvl	-	-	-	-	✓	✓	✓	-
rsp-8	C18D11.4	Emb/Ste, Gro	Gro	-	✓	-	-	✓	✓	✓
sma-2	ZK370.2	Sma	-	-	-	-	-	-	-	✓
sma-3	R13F6.9	Gro, Sma	Sma	-	-	-	-	-	-	-
sma-4	R12B2.1	Sma	Sma, Dpy	-	-	✓	-	✓	✓	✓
tbg-1	F58A4.8	Emb/Ste	Emb, Ste	✓	-	-	-	✓	✓	✓
unc-32	ZK637.8a	Emb, Ste, Unc	Ste, Pvl, Sck	✓	-	✓	-	✓	✓	✓
vha-1	R10E11.8	Emb/Ste	Emb, Ste, Sck	✓	-	-	✓	✓	✓	✓
vha-2	R10E11.2	Ste	Ste, Sck	ND	ND	ND	ND	ND	ND	ND

B

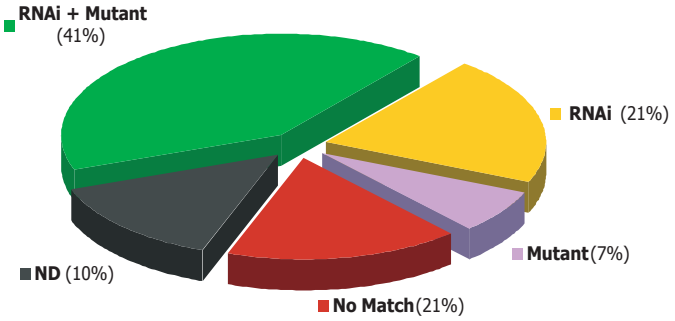

C

Phenotype	Genetic loci on chromosome III	RNAi phenotype detected	RNAi phenotype reported
Sterile	**14**	**9** (64%)	**10** (71%)
Developmental Delay	**6**	**2** (33%)	**2** (33%)
Larval Lethal	**6**	**4** (67%)	**1** (17%)
Morphology Defect	**8**	**2** (25%)	**2** (25%)
All phenotypes	**34**	**17** (50%)	**15** (44%)

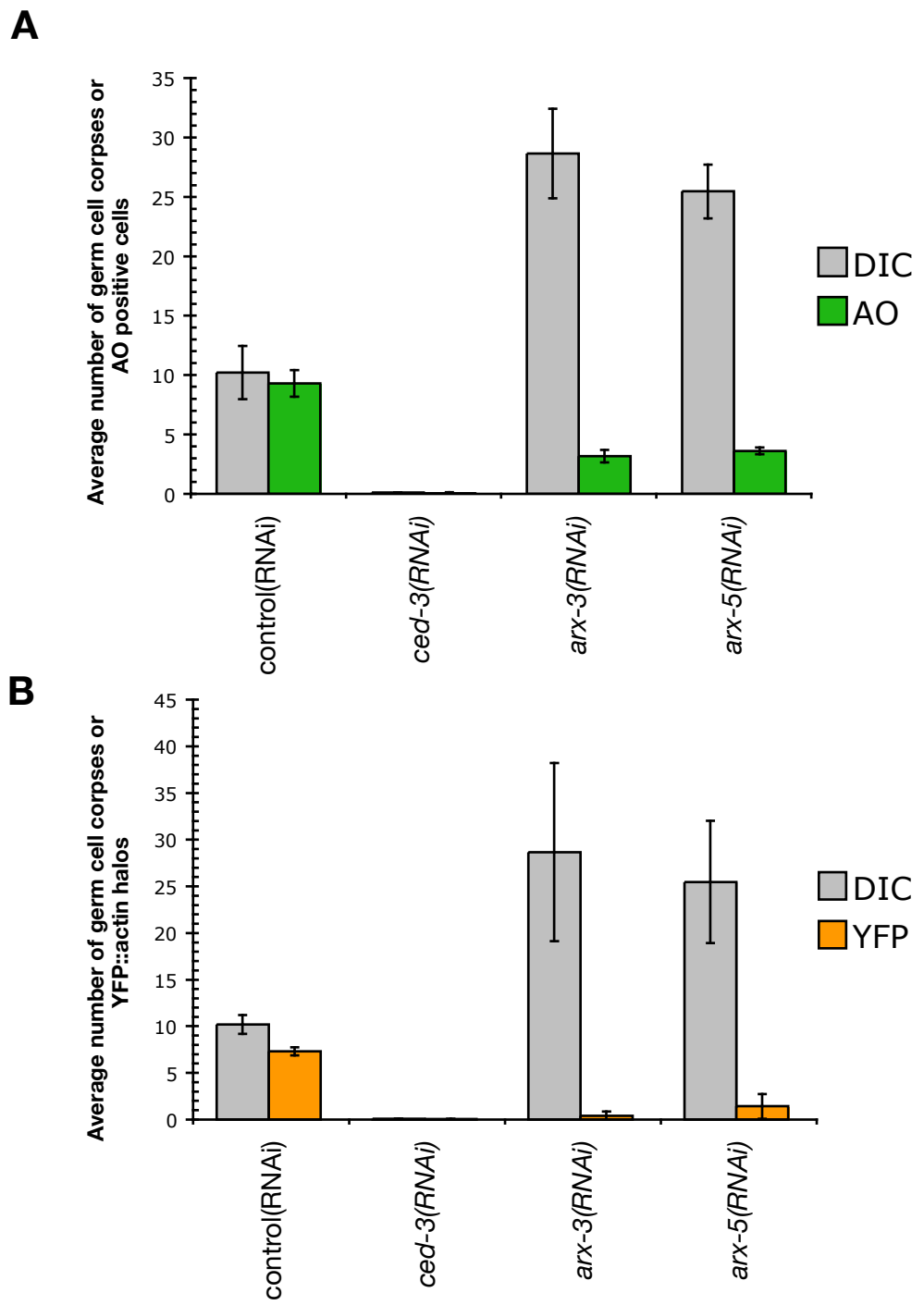

FIGURE 2.6 RNAi against subunits of the Arp2/3 complex results in an engulfment defect

(A) Synchronized *gla-3(op216)* worms fed with RNAi bacteria targeting *arx-3* and *arx-5* were stained with Acridine Orange and then scored by fluorescence microscope for AO positive germ cell corpses,24h post L4/adult molt. Data shown represent the average of the mean of at least three independent experiments (n=10-15 per experiment). Errors bars represent the SD. RNAi against *ced-3* suppresses germ cell death and was used as a negative control for AO staining. (B) Synchronized *gla-3(op216)* worms carrying the *opIs110[Plim 7::ypf::act-5]* transgene were scored by fluorescence microscopy for recruitment of YFP::actin around apoptotic germ cell corpses upon RNAi of *arx-3* and *arx-5*.Data shown represent the average of the mean of at least three independent experiments (n=10-15 per experiment). Errors bars represent the SD.

CHAPTER 3

A NOVEL PATHWAY FOR PHAGOSOME MATURATION DURING ENGULFMENT OF APOPTOTIC CELLS

CHAPTER 3

A NOVEL PATHWAY FOR PHAGOSOME MATURATION DURING ENGULFMENT OF APOPTOTIC CELLS

3.1 PREFACE

In this chapter I describe a collaborative effort aiming to understand the pathways mediating phagosome maturation in both *C. elegans* and in mammalian cells. This work was initiated by some key candidate genes we identified by an unbiased RNAi screen described in the previous chapter, and was complemented by several additional candidate-based approaches aiming to uncover more components of the pathway. A combination of genetics, cell biology and cell culture experiments allowed us to assemble a linear pathway for phagosome maturation during engulfment of apoptotic cells. At the end of the chapter I include some additional results regarding the identification of a factor which might link pseudopod extension with phagosome maturation.

Dr. Jason Kinchen (University of Virginia, Charlottesville) performed all the cell culture experiments (Figures 5, 6 and 7), as well as the *C. elegans* experiments depicted in Figure 2 and Table 1. I designed and set up the unbiased RNAi screen which led to the identification of *dyn-1*, *vps-34* and *rme-8* (Figure 3); Johann Almendinger screened chromosomes I, IV and X while I screened chromosome III. Additionally, I constructed the RAB-5 and RAB-7 reporters and generated the corresponding transgenic animals where I studied the recruitment of these endocytic markers around corpses. I carried out the genetic characterization of *rab-7*, *dyn-1* and *vps-34* with Johann's help (Figure 1, 3 and Figure 7). Dr. Lilli Stergiou constructed a set of YFP- or CFP-tagged *dyn-1* reporter constructs and, together, we generated the corresponding transgenic animals. Lilli also acted as an independent observed blindly confirming several of our scores. Jason wrote the first draft of the manuscript, which we then edited together. Finally, all the experiments reported in the manuscript that follows were designed by Jason and myself.

A novel pathway for phagosome maturation during engulfment of apoptotic cells

Jason M. Kinchen[1*], Kimon Doukoumetzidis[2,3,*], Johann Almendinger[2,3], Lilli Stergiou[2], Annie Tosello-Trampont[1], Costi D. Sifri[4], Michael O. Hengartner[2,†], and Kodi S. Ravichandran[1,†]

[1] Beirne Carter Center for Immunology Research, University of Virginia, Charlottesville, VA 22908
[2] Institute of Molecular Biology and [3]PhD program in Molecular Life Sciences, University of Zurich, CH-8057, Zurich, Switzerland
[4] Department of Internal Medicine, University of Virginia, Charlottesville VA 22908
*, † These authors contributed equally to this work

Running Title: A novel, conserved pathway for phagosome maturation
Word count:
Abstract: 313 words
Manuscript: 4,943
Methods: 1,082
Number of References: 71
---

†Corresponding authors:

Kodi S. Ravichandran
Beirne Carter Center for Immunology Research
University of Virginia
Charlottesville, VA 22908
Phone: 434-243-6093
Fax: 434-924-1221

Michael O. Hengartner
Institute of Molecular Biology
University of Zurich
Winterthurerstrasse 190
8057 Zurich
Switzerland
Phone: ++41 44 635 3140
Fax: ++41 44 635 6861

The efficient removal of apoptotic cells is critical for the physiological well-being of the organism[1-4]. While several players regulating the early steps of corpse recognition and internalization have been characterized[5], the molecules and mechanisms relevant to the subsequent processing of the internalized corpses are poorly understood. Here, we identify a novel pathway for the processing of internalized apoptotic cells in *C. elegans* and in mammals. First, we show that Rab5 and Rab7 are sequentially recruited to phagosomes containing apoptotic corpses as they mature within the phagocytes. After defining a genetic requirement for both Rab5 and Rab7 during processing of internalized corpses, we used a series of targeted genetic screens to identify players that regulate the recruitment or retention of Rab5 and Rab7 to phagosomes. While seven members of the HOPS complex (a Rab7 activator/effector complex) were required for Rab7 localization or retention on phagosomes containing apoptotic corpses, surprisingly, none of the known guanine nucleotide exchange factors (GEFs) linked to Rab5 regulation were relevant for processing of apoptotic cell corpses. To identify additional factors that might regulate Rab5 during phagosome maturation, we undertook an unbiased reverse genetic screen and identified 61 genes potentially required for corpse removal. We performed in-depth analysis of two candidate genes, *vps-34* and *dyn-1/dynamin*, whose disruption resulted in the accumulation of internalized, but undegraded, corpses within abnormal phagosomes that are defective in Rab5 recruitment. Using a series of genetic and biochemical experiments, we ordered these proteins in a pathway, with DYN-1 functioning upstream of VPS-34, in the recruitment/retention of Rab5 to the nascent phagosome. Further, we identified a novel biochemical complex containing Vps34, dynamin and Rab5, providing a mechanism for Rab5 recruitment to the phagosome. Since the inability to properly process apoptotic cells has been linked to autoimmune disease[4,6], our work identifies new evolutionarily conserved players influencing this process and provides insights into the control of corpse processing in phagocytes.

Removal of apoptotic cells (engulfment) can be broken down into a series of steps, comprising recognition, internalization, phagosome maturation and finally lysosomal

degradation of the apoptotic cell by the phagocyte; engulfment is an essential process that occurs throughout life in multi-cellular animals as part of development, homeostasis and wound healing[1-4,7,8]. In mammals, impaired clearance of apoptotic cell corpses can lead to exposure of autoantigens, resulting in onset of autoimmune diseases, such as systemic lupus erythematosus and chronic polyarthritis[4,9,10]. Modulation of the engulfment process is therefore a potential therapeutic target in these conditions. One of the fundamental challenges in understanding how defects in engulfment of apoptotic cells translates into diseased states is the identification of critical players involved in corpse removal and how these proteins orchestrate the different stages of engulfment.

The nematode *C. elegans* represents a powerful genetic tool for the study of programmed cell death[11,12]. Large numbers of cells are induced to die during two periods in the life of a worm: during embryonic and larval morphogenesis and during germ cell development[13]. Genetic studies have identified two evolutionarily conserved signaling pathways involved in the recognition and internalization of apoptotic cells. The first pathway includes the adapter protein CED-2/CrkII[14] functioning together with two other proteins, CED-12/ELMO and CED-5/Dock180[15-18], which exhibits GEF activity towards CED-10/Rac1[19]. In the second pathway, two transmembrane proteins, CED-1/LRP1/MEGF10[20-22] and CED-7/ABCA1/ABCA7[23-25], may mediate recognition of the apoptotic cell and function upstream of the adapter protein CED-6/GULP[21,26]; this complex has also been suggested to signal to CED-10/Rac1 during engulfment[27,28]. Activation of CED-10/Rac1 promotes rearrangement of the actin cytoskeleton, permitting pseudopod extension around the apoptotic prey and ultimately internalization of the cell corpse into a membrane bound phagosome[29,30]. Studies in mammalian cells

and in model organisms have shed light on the early steps of engulfment, such as the recognition and internalization of dying cells, but the identities of proteins required for subsequent steps, such as the maturation of phagosomes containing apoptotic cells into acidic structures, remains unclear. Proteomic approaches have identified a large number of phagosome-associated proteins, which can be found on membrane adjacent to phagocytosed particles[31]; how these candidates function in phagosome maturation and processing remains to be determined.

Here, we identify a novel pathway for the maturation of internalized apoptotic cell corpses. First, we show that the GTPases RAB-5 and RAB-7 are required for efficient corpse degradation following internalization, and that RAB-5 and RAB-7 are recruited to phagosomes containing apoptotic cells in a temporally distinct manner. Using a series of targeted and unbiased genetic screens in the nematode *C. elegans*, we identify a number of genes functionally required at various stages during phagosome maturation and order them into a linear pathway. Finally, we show that a dynamin-Vps34 complex is required for efficient Rab5 recruitment or stabilization on the nascent phagosome, providing a mechanism by which internalized apoptotic cells enter the lysosomal network.

Results

RAB-5 and RAB-7 are required for efficient phagosome maturation

The *C. elegans* adult hermaphrodite gonad is composed of two U-shaped tubes joined at a central uterus; germ cell nuclei sharing a common cytoplasm line the periphery of the tube, forming a large syncytium[32]. When germ cells die, they cellularize away from the common syncytium and condense, generating cell corpses that appear as 'refractile' bodies by differential interference contrast (DIC) microscopy[33]. Apoptotic germ cells are rapidly recognized and internalized by the surrounding gonadal sheath cells that encase the germ line[33]; little is known regarding the ultimate fate of internalized corpses in *C. elegans*.

To better understand maturation of apoptotic cell-containing phagosomes, we first addressed the importance of the small GTPases Rab5 and Rab7, which have been shown to localize to phagosomes containing internalized bacteria[34]. We generated transgenic worms expressing CFP::RAB-5 or YFP::RAB-7 and assayed their localization around apoptotic cells in the adult hermaphrodite gonad; apoptotic germ cells could be readily visualized inside RAB-5 or RAB-7 staining structures (**Figure 1, a-h**). RAB-5 preferentially localized around early, uncondensed cell corpses, when cells are being actively internalized[29] (**Supplementary Figure S1**). CFP::RAB-5 did not colocalize with YFP::actin around the apoptotic cell (data not shown), suggesting RAB-5 is recruited following corpse internalization and actin disassembly. Further, RAB-5-positive phagosomes weakly stained with SYTO dyes, which we have previously shown stains engulfed apoptotic cells in acidic lysosomal structures[29,35] (**Figure 1**, **c,** quantitated in **t**). In comparison, YFP::RAB-7 localized around late stage,

highly-refractile apoptotic cell corpses (**Figure 1q,** quantitated in **t**), most of which stained brightly with SYTO dyes (**Figure 1**, **g**). Multiple corpses were occasionally observed within RAB-5 or RAB-7 staining structures, suggesting that phagosomes may fuse following corpse recognition and internalization (**Figure 1, a-h, asterisks**). The recruitment of RAB-5 and RAB-7 around apoptotic cells was severely compromised in worms deficient in *ced-1* or *ced-5,* which represent members of two partially redundant pathways required for corpse phagocytosis*,* thus definitively placing RAB-5 and RAB-7 recruitment to the phagosome at a step downstream of corpse internalization (**Figure 1, i-p, quantitated in Table S2a**).

Even though RAB-5 and RAB-7 were recruited to phagosomes, the functional requirement for these proteins in corpse removal was not known. RNA interference (RNAi) directed against *rab*-5 or *rab-7* resulted in accumulation of refractile corpses in the adult hermaphrodite gonad (**Table 1**, **Figure 1, r, s**). Further, in *rab-7(RNAi)* worms, phagosomes containing apoptotic cells were arrested at the RAB-5-positive stage (**Figure 2**, **g**) suggesting that RAB-5 functions upstream of RAB-7 in a linear pathway for phagosome maturation. While refractile cell corpses in *rab-5(RNAi)* and *rab-7(RNAi)* most likely arose due to defects in phagosome maturation, increased numbers of refractile cell corpses could have been the result of increased physiological cell death or decreased corpse internalization. To discriminate between these possibilities, we used a YFP::actin transgenic strain to monitor corpse internalization (and indirectly programmed cell death) in the gonad; numbers of cells undergoing internalization in *rab-5* and *rab-7* deficient worms was similar to wild type, suggesting that the increased corpse number is due to defects in phagosome maturation (see **Supplementary Figure S1**). Taken together, these data place RAB-5 downstream of

corpse internalization and upstream of RAB-7 (**Figure 1t**), and suggest that both of these GTPases are critical for proper clearance of apoptotic cells *in vivo*.

A targeted screen for players thought to regulate RAB-5 and RAB-7 reveals a linear pathway for phagosome maturation

We next used a candidate gene approach to identify genes that would regulate both RAB-5 and RAB-7 signaling during cell corpse clearance. Mammalian and yeast Rab5 GTP exchange factors (GEFs), which promote cycling of GTPases from the GDP to GTP-bound conformation, all share a canonical Vps9 domain[36]. There are three Vps9-domain containing proteins in the nematode, *rme-6, rabx-5,* and *tag-333*[37]. Among them, RME-6 and RABX-5 are both homologues of mammalian RabEx-5 and have been shown to be redundantly required for receptor-mediated endocytosis[38]. Surprisingly, neither the single mutants *rme-6*, *rabx-5* or *tag-333* nor the triple mutant *rme-6(b1014); tag-333(gk431); rabx-5(RNAi)* worms showed any defects in corpse removal, suggesting that this class of proteins is not required for RAB-5 function during apoptotic cell clearance. However, we did see decreased embryonic viability associated with *rme-6; rabx-5* doubly deficient worms[38] (unpublished observations), suggesting that knockdown of *rabx-5* was efficient.

We then asked whether RAB-5 effectors, which are thought to bind activated, GTP-bound RAB-5, play a role in apoptotic cell clearance. Analysis of worms harboring mutants of the nematode homologues of the FYVE-domain containing RAB-5 effectors EEA1 (EEA-1) and Rabenosyn-5 (RABS-5) had no obvious defects in corpse degradation, although the same mutant strains have previously been shown to display defects during endocytosis in the nematode[39-41] (**Table 1**). EEA-1 and RABS-5 are

hypothesized to function as a tethering complex during a 'concentrating' stage of endocytosis, where multiple vesicles have been reported to fuse into RAB-5 positive structures[42]. To address the importance of fusion events during corpse clearance, we scored worms deficient in the ATPase NSF-1, the nematode homologue of N-ethylmaleimide-sensitive factor (NSF) and a key component of the vesicular fusion machinery on early endosomes[43]. Loss of NSF-1 does not result in increased corpse number (**Table 1**), suggesting that a concentrating step is dispensable for efficient corpse degradation. It is notable thatr *nsf-1(RNAi)* resulted in significant embryonic lethality as previously reported (data not shown) [44], suggesting that knockdown was efficient under these conditions.

It was possible that an alternate FYVE or PX-domain-containing protein (both of which bind to endosomal structures) would be involved in RAB-5 function during corpse removal. There are 14 FYVE-domain containing proteins and 12 PX-domain containing proteins in the nematode genome[37]. Analysis of worms with disruptions in the 14 FYVE domain-containing proteins (either existing mutants in seven genes, or RNAi mediated knockdown of the other seven candidates) showed no obvious defect in corpse removal in the germ line. Knockdown of two of the twelve PX-domain containing proteins, sorting nexins encoded by *Y116A8c.26* and *F17H10.3*, resulted in increased numbers of germ cell corpses. However, the defects we observed in *Y116A8c.26(RNAi)* and *F17H10.3(RNAi)* were relatively weak (either due to redundancy of gene function or RNAi efficiency), and we did not see a clear effect on RAB-5 or RAB-7 recruitment to the phagosome (data not shown). We propose that the two sorting nexins may play a redundant role for RAB-5 or RAB-7 recruitment to the

phagosome or may affect an aspect of phagosome maturation unrelated to RAB-5 or RAB-7 recruitment or release.

We next tested genes potentially regulating RAB-7 function. The HOPS complex is a GEF/effector complex which acts on RAB-7 during endocytosis and is composed of the products of seven genes – *vps-11, vps-16, vps-18, vps-33, vps-41,* and *vps-45*[45]. RNAi directed against each of these genes resulted in the accumulation of refractile apoptotic cells (**Figure 2, a-f, Table 1**). Since the number of cells undergoing internalization in the gonad, as measured by YFP::actin staining, was similar to wild type (**Supplementary Figure S1**), these refractile corpses likely represent internalized but undegraded apoptotic cells. To place these genes within the pathway for phagosome maturation, we assayed RAB-5 and RAB-7 recruitment to the phagosome (**Figure 2, g, h-s**). Interestingly we found that RNAi mediated disruption of five of the members of the VPS/HOPS complex, *vps-11, vps-16, vps-18, vps-33* and *vps-41* results in apoptotic cells arrested in RAB-7-positive phagosomes; these genes are likely not needed for RAB-5 release from the phagosome or for subsequent RAB-7 recruitment, but rather play a role in further maturation of RAB-7-positive phagosomes.

Two additional HOPS complex members, *vps-41* and *vps-45*, function at different stages of maturation. VPS-45 is a member of the family of proteins (Sec1 homologues) that mediate targeting of vesicles in the lysosomal degradation pathway. Knockdown of *vps-45* showed only a mild increase in the number of RAB-7 or RAB-5 phagosomes, suggesting that VPS-45 might be dispensable for RAB-5/RAB-7 recruitment and resolution, perhaps functioning in the transition from RAB-7 to LMP-1 (LAMP-1) positive lysosomes. Additionally, *vps-41(RNAi)* resulted in a mild increase in the

number of RAB-5-positive phagosomes, suggesting VPS-41 may influence RAB-5 release from the phagosome. These data further extended our linear pathway for phagosome maturation, with HOPS complex members functioning at multiple steps of RAB-5/RAB-7 function (**Figure 2, t**).

An unbiased genetic screen identifies additional genes required for efficient corpse removal

In our targeted gene analyses above, we were unable to identify upstream regulators of RAB-5 function that would be required for maturation of apoptotic cell-containing phagosomes. We thus undertook an unbiased, reverse genetic screen[35] to systematically identify genes involved in both corpse internalization and processing during germ cell apoptosis. We previously showed that the vital dye acridine orange selectively stains internalized apoptotic cell corpses at late stages of degradation[29,35] (**Figure 3**, **a-d**). Corpses in *rab-7(RNAi)* worms, which are arrested in RAB-5(+) phagosomes, weakly stained with acridine orange (**Figure 3, j**, **m**), suggesting that RAB-5(+) phagosomes are acidified. Using a feeding RNAi library[46], we screened for genes on chromosomes I, III, IV and X that suppress acridine orange staining of apoptotic cells in the adult hermaphrodite gonad (see Methods)

By design, we expected to identify candidates whose disruption caused defects in programmed cell death or corpse recognition/internalization (which in turn, would manifest as a decrease in the number of AO positive corpses) in addition to candidates whose disruption caused defects in phagosome maturation or acidification of phagosomes and phagolysosomes (candidates most relevant to this manuscript). Following elimination of all genes previously shown to cause developmental delay or

sterility[37], we identified 61 genes whose knockdown reproducibly resulted in decreased AO staining (**Figure 3e**, **Supplementary Table S1**). In addition to the known genes required for corpse recognition (*ced-1*) and internalization (*ced-5* and *ced-6*) present in the RNAi library[46] we also identified components of the Arp2/3 complex in *C. elegans*, *arx-3* and *arx-5*[47]. The Arp2/3 complex plays a key role during actin reorganization and corpse removal in mammalian systems[48]; we posit that inactivation of the Arp2/3 complex in *C. elegans* similarly interferes with actin-dependent corpse internalization. Additionally, we identified *wip-1* and C24A1.3 (a tyrosine kinase), which may regulate activity of the small GTPase Cdc42 during corpse removal.

Analysis of the remaining candidates suggested that we indeed identified genes in most of these predicted classes. Homologues of several candidates, *phi-25, dyci-1, rab-10,* and *rme-8,* suggest theses genes may play a role during corpse processing and phagosome maturation[37]. Further, we isolated *vha-15*, a vacuolar ATPase, which may be required for acidification of the lysosome and hence onset of AO staining. Interestingly, included among our candidates that caused defects in phagosome maturation were the nematode homologue of Vps34 and dynamin[49], which we chose to characterize further. Disruption of VPS-34 (nematode homologue of Vps34) or DYN-1 (the nematode homologue of dynamin) resulted in increased numbers of undegraded refractile corpses; we decided to focus on DYN-1 for further study, as corpses in *dyn-1(lf)* worms appeared arrested in abnormal phagosome structures and a role for dynamin in phagosome maturation had yet to be described.

DYN-1 functions upstream of VPS-34 during phagosome maturation

Dynamins belong to a family of large GTPases that have been linked to both organization of the actin cytoskeleton[50] and internalization of antibody-opsonized cells[51]. Dynamin has been shown to form an endogenous complex with Arp2/3 and other actin binding proteins[50]; however the exact function of dynamin during remodeling of the actin cytoskeleton during engulfment is unknown[52]. Additionally, dynamin plays a key role in receptor-mediated endocytosis and protein trafficking[52]. In the nematode, DYN-1 is also involved in cytokinesis and is required for synaptic vesicle transport[49,53]. Mammalian Vps34 has been proposed to function in maturation of phagosomes into acidic lysosomes, suggesting that VPS-34 may also be a key regulator of phagosome maturation[54].

dyn-1(RNAi) and a temperature-sensitive mutation, *dyn-1(ky51)*[49], resulted in an accumulation of refractile corpses in the adult hermaphrodite gonad (**Figure 3f**, **g** and **Supplementary Table S1**, **S2b**). To further investigate the role of DYN-1 in engulfment, we generated YFP- or CFP-tagged DYN-1 constructs and assayed localization of DYN-1 during corpse removal. We detected enrichment of DYN-1 in punctate structures surrounding early apoptotic cells at the stage during which active phagocytosis occurs[29] (**Figure 3**, **l-m, Supplementary Figure S2**). These DYN-1::CFP structures colocalized with the YFP::actin meshwork that forms around early apoptotic cells (**Figure 3**, **v**) during corpse internalization. We could not detect enrichment of DYN-1 adjacent to the apoptotic cell in *ced-1* mutant worms (**Figure 3, n, o** and **Supplementary Figure S2**), further suggesting DYN-1 is recruited at a stage following corpse recognition. Finally, in *ced-5* or *ced-6* mutant worms (**Figure 3, p, q**), and other genetic backgrounds deficient for corpse internalization (**Supplementary Figure S2)**,

DYN-1 enrichment adjacent to apoptotic cells was also greatly decreased compared to wild type, suggesting that DYN-1 is recruited to the apoptotic cell following recognition and at a late stage during or following internalization of the corpse. DYN-1 recruitment to apoptotic corpses was transient; SYTO41-positive late apoptotic cell corpses fail to stain with DYN-1 (**Figure 3, w-z**), suggesting DYN-1 is rapidly removed from the phagosome membrane following corpse internalization and actin disassembly.

We next asked whether DYN-1 functions upstream or downstream of VPS-34. In *vps-34(RNAi)* worms, DYN-1::YFP is still efficiently recruited to apoptotic corpses (**Figure 3, r-u**), suggesting that DYN-1 likely functions upstream of VPS-34 during engulfment. We also assessed DYN-1 localization after disruption of RME-8, another candidate that was isolated in the screen as having increased numbers of refractile corpses in the gonad. *rme-8* was initially identified in a screen for genes defective in receptor-mediated endocytosis; RME-8 localizes to the early endosome, though its exact mechanism of function is unknown[55-57]. In *rme-8(b1023ts)* worms, DYN-1::YFP was efficiently recruited around corpses as well, suggesting that DYN-1 may function between corpse internalization and an early phagosome structure.

DYN-1 is required for the processing of corpses following engulfment

One of the best known roles for dynamin during endocytosis is in pinching of vesicles from the plasma membrane (membrane scission) [52]; a similar but phenotypically distinct process occurs when the phagocytic cup fully extends around the apoptotic cell and must fuse to completely encompass the apoptotic cell. To further test whether apoptotic cells are engulfed in *dyn-1(ky51)* mutant worms and to monitor phagocytic cup closure, we tested transgenic *dyn-1(ky51)* worms expressing CED-1::GFP and

YFP::CED-6, which are enriched at the cell membrane around apoptotic cells during corpse internalization[20,29]. Both CED-1::GFP and YFP::CED-6 were efficiently recruited around apoptotic cells in *dyn-1(ky51)* mutant worms (**Figure 4, a-d** quantitated in **Supplementary Table S3**), and the phagocytic cup appeared to be completely closed around the apoptotic cell (**Figure 4, d, inset**), suggesting DYN-1 is not required for pseudopod extension. In wild-type worms, CED-1 is rapidly removed from the phagosome following corpse internalization (**Figure 4b**)[20,29]. However, in *dyn-1(ky51)* mutants the total number of CED-1- and CED-6-staining cells was increased compared to wild type, consistent with early defects in phagosome maturation (**Figure 4, d** and **Supplementary Table S3**).

To address the mechanism by which increased refractile corpses are generated (apoptotic, internalization, or maturation defect), we assayed corpse internalization in *dyn-1(ky51*) mutant worms using a YFP::actin transgene. Worms deficient in DYN-1 showed similar numbers of corpses undergoing internalization as wild type nematodes (**Figure 4, e**-**h**, quantitated in **k**). In contrast, internalization was not seen in *ced-1(lf)* (**Figure 4, i, j**), which has previously been linked to actin rearrangement during corpse recognition[29]. Taken together, we conclude that the refractile corpses in *dyn-1(ky51)* mutant worms were arrested in phagosomes at a stage following corpse internalization.

In a recent report, Yu *et al.* showed that approximately 40% of the corpses present in the gonad of *dyn-1(RNAi)* worms persist un-engulfed[58]. However, our studies suggested no defect in corpse internalization *per se* but instead a key role for DYN-1 during phagosome maturation after corpse internalization. Based on additional studies (see **Supplemental Figure S3**), we conclude that the discrepancy likely reflects

differences in experimental conditions, more specifically the duration of DYN-1 inactivation (12-24 hour in our experiments versus 42-hours in those of Yu *et al*.). At these later timepoints, we detect gross defects in the actin cytoskeleton, suggesting that dynamin plays a primary role in phagosome maturation, and a secondary role in maintenance of the actin cytoskeleton; thus, to avoid potential unintended secondary defects, we have performed all our nematode assays here at the 12-hour adult stage following *dyn-1(ky51)* inactivation (**Supplementary Figure S3**).

Dynamin function during phagosome maturation is evolutionarily conserved

We next addressed the role of dynamin in phagosome maturation in the mammalian context. There are three mammalian dynamins: *dynamin-2* is ubiquitously expressed, while *dynamin-1* and *dynamin-3* show a more restricted expression (brain and testes, respectively[59]). Since most cell types possess the ability to engulf, we chose to focus on the role of *dynamin-2*. In both J774 macrophages and NIH3T3 fibroblasts (models for professional and nonprofessional phagocytes, respectively) we observed recruitment of endogenous dynamin around apoptotic cells (**Figure 5, a-h**) with kinetics similar to those observed for actin polymerization (**Figure 5o, Supplementary Figure S4**). Observed dynamin staining originated from phagocytes and not from targets being engulfed, as apoptotic cells not undergoing internalization showed no obvious dynamin staining (**Figure 5, a, b, arrowhead**). Recruitment of dynamin into the phagocytic cup was also specific and not due to a general recruitment of proteins involved in actin organization or proteins involved in endocytosis, as cortactin, a dynamin-interacting protein[52], was excluded from the phagocytic cup (**Supplementary Figure S5**).

To better address dynamin localization within the phagocytic cup, we acquired confocal z-stacks and reconstructed xz- or yz-planes. In the absence of phagocytic cup formation, bound apoptotic cells (at either 4 ˚C or 37 ˚C) showed no observable dynamin staining (**Supplementary Figure S4**). Apoptotic cells being internalized by phagocytes showed punctate staining within the phagocytic cup (**Figure 5, j-l, m, n**). Dynamin staining appeared to be excluded from the leading edge, suggesting that dynamin is likely not involved in membrane extension around the apoptotic cell. Consistent with these observations, we could not detect any defect in internalization using either a dominant negative $Dyn2^{K44A}$ construct, which has impaired GTPase activity[60], or siRNA mediated knockdown of dynamin (**Supplementary Figure S6**). As in the nematode, dynamin recruitment during engulfment was transient, as staining was rapidly lost from the phagosome following corpse internalization (**Figure 5o** and **Supplementary Figure S4**).

We next addressed whether the role of mammalian dynamin, similar to DYN-1 in *C. elegans*, would also regulate phagosome maturation. We assessed acidification of phagosomes containing apoptotic thymocytes in NIH/3T3 cells in which dynamin function was impaired. While apoptotic cells appear to be internalized normally, corpses within cells expressing dominant negative $Dyn2^{K44A}$ or treated with *dyn2* siRNA did not mature into acidic endosomes, as determined by Lysotracker Red staining (**Figure 6a-h**, quantitated in **u**, **v**). This phenotype was unlikely due to general defects in endocytosis, as $Dyn2^{siRNA}$ did not produce abnormal clathrin pits (**Supplementary Figure S6**). Taken together, these data suggested a critical role for mammalian dynamin during phagosome maturation after internalization of apoptotic cells. Since this function of dynamin appeared to be at roughly a step when Rab5 localization to the

phagosome would occur, this suggested an exciting possibility that dynamin and/or Vps34 could provide the missing upstream link to Rab5 recruitment/retention to nascent phagosomes during apoptotic cell processing.

Dynamin plays an evolutionarily conserved role in recruitment/retention of Rab5

Phagosomes in dynamin-deficient cells appear arrested in abnormal, unacidified lysosomal structures. Unlike control transfected NIH/3T3 cells, in which Rab5 was efficiently recruited to apoptotic cell-containing phagosomes (**Figure 6**, **m-p,** quantitated in **w**), NIH/3T3 cells transfected with dominant negative $Dyn2^{K44A}$ showed a significant decrease in the percent of apoptotic cells in Rab5-positive phagosomes ($p < 0.001$) (**Figure 6**, **q-t**, **w**). This suggests that dynamin is required for efficient maturation of a nascent phagosome containing internalized apoptotic cells into Rab5-positive phagosomes. Consistent with this hypothesis, cells expressing dominant negative $Rab5^{S34N}$ had decreased numbers of internalized apoptotic cells staining with Lysotracker Red (**Figure 6, i-l**, quantitated in **u**), confirming that phagosomes must become Rab5-positive before they can acidify.

We next asked whether decreased DYN-1 function in the nematode would similarly lead to impaired RAB-5 or RAB-7 recruitment. In *dyn-1(ky51)* worms at the nonpermissive temperature, phagosomal RAB-5 staining was decreased, suggesting a defect in recruitment of RAB-5 to the maturing phagosome (**Figure 7, e, f,** quantitated in **q**). In addition, phagosomes in *dyn-1(ky51)* mutant worms were abnormally large compared to those seen in wild-type worms (**Figure 7, e** vs. **a**, **arrowheads,** quantitated in **s**); these enlarged phagosomes resemble structures observed in mammalian cells that are the result of abnormal fusion events[61]. In contrast,

uninternalized cell corpses in *ced-1* or *ced-5* mutant worms did not show a similar increase in corpse volume (**Figure 7s**, **Supplementary Figure S8**). RAB-7 halos were also greatly decreased in *dyn-1(ky51)* mutant worms, consistent with a block in phagosome maturation (**Figure 7, g, h**). It is noteworthy that RAB-5 and RAB-7 positive endosomes, likely resulting from receptor-mediated endocytosis, appeared normal (**Supplementary Figure S9**), suggesting a more stringent requirement for DYN-1 in the recruitment of RAB-5 and RAB-7 to phagosomes containing apoptotic cells. Taken together, these data suggest a specific and evolutionarily conserved role for dynamin homologues in regulation of phagosomes containing apoptotic cells upstream of RAB-5.

A Dynamin-Vps34-Rab5 complex controls the maturation of nascent phagosomes

Since our DYN-1::YFP localization studies (**Figure 3**, **s**) suggested that DYN-1 might function upstream of RME-8 or VPS-34, we next looked at recruitment of RAB-5 in *vps-34*-or *rme-8* deficient nematodes (Figure 7, I-j). Knockdown of *vps-34* or *rme-8* also resulted in defects in RAB-5 recruitment or stabilization on the nascent phagosomes (**Figure 7**, **r**), similar to *dyn-1(ky51*) mutant worms. This suggested that DYN-1, RME-8 and VPS-34 function at a step upstream of RAB-5 recruitment to the nascent phagosome. However, how these proteins might function together to mediate RAB-5 recruitment was unclear.

Mammalian Vps34 has previously been shown to bind Rab5[62]; thus, it was possible that Vps34 served as the link between dynamin and Rab5. Interestingly, we identified a dynamin:Vps34 complex that was specifically co-immunoprecipitated from transiently

transfected cells (**Figure 7, t**). Under these conditions Vps34 did not associate with other proteins involved in the engulfment of apoptotic cells, such as Dock180 (**Figure 7**, **t**). Further, we were also able to detect a biochemical complex containing the three proteins dynamin, Vps34, and Rab5 (**Figure 7, u)**. Since dynamin did not interact with Rab5 in the absence of Vps34, this suggested a bridging role for Vps34 in linking dynamin and Rab5, consistent with our studies suggesting that DYN-1 functions upstream of VPS-34. These data also provided a biochemical explanation for our results linking dynamin and Vps34 to recruitment or stabilization of Rab5 on phagosomes containing apoptotic cells (**Figure 7, e-l)**. Taken together, our genetic, cell biological and biochemical data suggest a linear pathway for phagosome maturation during engulfment apoptotic cells wherein DYN-1/dynamin functions together with VPS-34 to control early stages of phagosome maturation (**Figure 7**, **w**).

Discussion

While previous studies in both the mammalian and nematode have focused on recognition and internalization of apoptotic cells, further processing of the internalized corpses has been poorly understood. In this work, through the complementary use of targeted and unbiased functional genetic screens, along with biochemical studies, we define components of a novel, evolutionarily conserved pathway for phagosome maturation following internalization of apoptotic cells. We first identify a critical role for the small GTPases RAB-5 and RAB-7 in maturation of phagosomes containing apoptotic cells. Next, we used a targeted genetic screen followed by an unbiased genome-wide screen to identify multiple components both upstream and downstream of RAB-5 and RAB-7. DYN-1 and VPS-34 were among 61 genes identified using the genome-wide screen. Through additional in-depth studies in both worms and

mammals, we now describe a novel role for dynamin after internalization of the corpse and upstream of VPS-34, RME-8 and RAB-5 distinct from the role of dynamin previously recognized in vesicle scission and maintenance of the actin cytoskeleton[52]. Moreover, using a series of biochemical studies, we have also identified a novel protein complex containing dynamin, Vps34 and Rab5, providing a mechanism for recruitment/stabilization of Rab5 on the nascent phagosome. However, it is still unknown whether defects in dynamin inhibit Rab5 recruitment to the phagosome, or are required to stabilize Rab5 following recruitment. Although our genetic studies clearly suggest a role for RME-8 at a step upstream of Rab5 recruitment, how RME-8 functions with VPS-34 and RAB-5 during phagosome maturation remains to be determined.

It has been loosely assumed that once the corpse is internalized, phagosomes containing the 'apoptotic cargo' would feed into a common endocytic machinery. Our work clearly highlights several features of phagosome maturation during apoptotic cell clearance that are distinct from fluid phase endocytosis. For example, worms deficient in *rme-1* and *rme-2*, which play key roles during fluid-phase endocytosis in the nematode, are not required for efficient removal of apoptotic cell corpses in the gonad (**Supplementary Table S6**). With respect to dynamin and DYN-1, the role during phagosome maturation seems to be as a signal transduction molecule and distinct from DYN-1 function during endocytosis. Moreover, knockdown of *nsf-1*, which regulates fusion pore formation in yeast and mammalian cells and is required for proper receptor-mediated endocytosis, did not inhibit corpse removal, supporting our model for conversion of phagosomes from DYN-1 to RAB-5 to RAB-7 positive structures. These results, combined with our other observations that the Rab5 GEFs *rme-6* and *rabx-5*

are not required for corpse clearance, suggest that fluid-phase endocytosis and apoptotic cell clearance not only use distinct internalization processes but likely use different post-internalization maturation pathways.

In both mammalian cells and in *C. elegans*, a feedback regulation between internalization and degradation of the apoptotic cell corpse have been implied[6,63-66]. However, the protein machinery that connects these events is unknown. Here, we have identified dynamin, which is recruited to the phagocytic cup during the internalization step of engulfment, but whose function is required later for maturation of the internalized corpse into an acidic, Lysotracker/SYTO staining compartment. We also identified several homologues of sorting nexins in our screen, including *lst-4*, which appears to function in the internalization phase of corpse removal (data not shown). Intriguingly, *dyn-1* mutants also show a potential feedback into corpse internalization (see below), and *lst-4* may represent a point of intersection between internalization of apoptotic cells and their degradation.

In addition to a simple 'garbage disposal' function, phagosome maturation is essential for the proper function of the cellular immune system. Apoptotic cells are not trafficked into MHC class II-containing phagosomes[67], and the inability to properly degrade apoptotic cells has also been linked to autoimmune disease; this opens the possibility that blocking corpse degradation via the 'standard' pathway results in inappropriate presentation of antigens derived from apoptotic cells[4]. Thus, the components of the phagosome maturation pathway described here, along with several previously unrecognized players identified through the reverse genetic screens in *C. elegans* (**Supplementary Table 1**) may allow further characterization of the process of

apoptotic cell clearance with significant implications for tolerance to apoptotic cell-derived self antigens and autoimmunity.

Acknowledgements

The authors would like to thank members of the Ravichandran and Hengartner laboratories for helpful input and suggestions on this manuscript. We would also like to thank Dorothy Schafer for dynamin plasmids, David Castle and Jim Casanova for the GFP-Rab5 expression constructs and Lukas Neukomm for providing pLN022 and pLN019 plasmids. Some strains used in this work were obtained from the *Caenorhabditis* Genetics Center (CGC). This work was supported by grants from the National Institutes of Health (USA) to KSR, and from the EU Project Apoclear, the Ernst Hadorn Foundation, the University of Zurich and the Swiss National Science Foundation to MOH. JMK is an Arthritis Foundation Postdoctoral Fellow.

Methods

Nematode Strains and Reagents

Nematode strains were cultivated as previously described[12]. Mutations used were as follows: *LGI: gla-3(op216), ced-12(k149), ced-1(e1735); LGIII: ced-6(n1813), ced-7(n1996); LGIV: ced-2(n1994), ced-10(n3246), opIs110[P_{lim-7}::yfp::act-5]; LGV: bcIs39[P_{lim-7}::ced-1::gfp]*, *LGX: dyn-1(ky51). opIs160[P_{ced-6}::yfp::ced-6; unc-119(+)],* Integration sites of *opIs220[P_{eft-3}::dyn-1::yfp;unc-119(+)], opIs223[P_{eft-3}::yfp::rab-7;unc-119(+)] and opIs282[P_{ced-1}::yfp::rab-5; unc-119(+)]* were not mapped. Unless noted otherwise mutations were previously described[37]. *opEx1278[P_{eft-3}::yfp::rab-7; unc-119(+)]*, *opEx1279[P_{eft-3}::cfp::rab-5; unc-119(+)], opEx1304[P_{ced-1}::yfp::rab-5; unc-119(+)] and opEx1303[P_{ced-1}::yfp::rab-7; unc-119(+)]* are extrachromosomal arrays.

Reagents used in this study were Alexa-647 phalloidin, Hoechst 33342, SYTO41, SYTO59, acridine orange (Invitrogen), anti-FLAG M2 (Sigma), anti-clathrin light chain CON-1, anti-cortactin, anti-dynamin-2 C-18, anti-HA F-7 (Santa Cruz), anti-dynamin Hudy1 (Upstate), Alexa 488, 555 anti-mouse, and Alexa 555 anti-rabbit (Invitrogen); all secondary antibodies were highly cross-adsorbed to minimize cross reactivity between species. Plasmids pcDNA-HA-Dyn2^{WT} and pcDNA-HA-Dyn2^{K44A} were a gift from Dorothy Schaffer, and pGreen Lantern-Rab5^{S34N} and pGreen Lantern–Rab5^{Q67L} was a gift of Jim Casanova.

Reverse genetic screening

Feeding RNAi was performed as described[46] with the following modifications. Plates containing NGM-agarose and 1-2mM IPTG ("RNAi plates") were inoculated with 300 mL of appropriate bacterial cultures (transformed with constructs for generation of double stranded RNA under the control of the T7 promoter) were incubated for 8-12 hours before addition of worms. Between 30 and 60 synchronized *gla-3(op216)* L1 stage worms (which was used to increase the number of apoptotic germ cells) were placed on each RNAi plate and left for 72h at 20°C. Worms on plates were then stained with Acridine Orange[35] and scored for percent of worms showing AO staining of apoptotic cell corpses under an M^{2}Bio epifluorescence dissecting microscope (Zeiss). Candidate genes were grouped into functional classes as previously described[46]. To eliminate genes that reduce the number of apoptotic cell corpses in the germ line (either directly or indirectly), we compared our candidates to the results of other RNAi screens and removed candidates whose knockdown resulted in delayed morphogenesis or sterility. Number of germ cell corpses was then scored by DIC microscopy for each candidate where possible (**Supplementary Table S1**).

The following dsRNA-synthesizing bacteria were used as positive controls for each RNAi experiment: *bir-1(RNAi),* which gives rise to high embryonic lethality, *unc-22(RNAi),* which results in an Uncoordinated phenotype, and *ced-3(RNAi)*, which potently suppresses germ cell apoptosis. Worms fed with HT115(DH3) bacteria transformed with the original L4440 RNAi vector containing no insert were used as a reference strain.

DIC and Fluorescence microscopy (Nematode)

Worms were placed on 2% agarose pads in M9, anaesthetized with 3-5mM levamisole (Sigma) and mounted under a cover slip for observation using a Leica DM-RA or Zeiss Axiovert 200 microscope equipped with DIC (Nomarski) optics and standard epifluorescence with filtersets appropriate for visualization of YFP, CFP/SYTO 41, SYTO 59 or GFP. Images were false-colored in OpenLab or Adobe Photoshop 7.0, which was also used to optimize brightness/contrast.

Staining of worms with Acridine Orange (Molecular Probes) was performed as previously described[29]. To visualize engulfed cells, gonads were dissected in PBS supplemented with 12.5□M of SYTO 41 or SYTO 59, then incubated in the dark for 10 minutes prior to observation.

Synchronization and C. elegans *phagocytosis assays*

To score apoptotic corpses in the hermaphrodite germ line, clean worms were synchronized by picking hermaphrodites at the L4 larval stage (Christmas tree vulva). These worms were incubated for 24 hours at 20 °C then scored for persistent cell corpses and fluorescent halos where appropriate. Inactivation of DYN-1 in *dyn-1(ky51)* mutant worms occurs in less than a minute following shift to the nonpermissive temperature[49]. For all experiments using the temperature sensitive *dyn-1(ky51)* allele worms were shifted to 25 °C as L4s and scored after 12, 24 and 36 hours for persistent cell corpses and fluorescent haloes. At the nonpermissive temperature, *dyn-1(ky51)* mutants exhibits pleiotropic phenotypes and only worms exhibiting a gonad morphology as close to wild-type as possible were chosen for scoring. For all experiments using the temperature sensitive *rme-8(b1023)* worms were grown at 15°C and were shifted to 25°C as L4s. For most animals only one gonad arm was scored, as the other arm was concealed by the intestine.

Immunofluorescence in mammalian cells

Cells were incubated overnight in Lipofectamine 2000 as previously described[68], then washed and incubated in DMEM + 10% serum ~8 hours before engulfment assay was conducted. For siRNA experiments, cells were transfected using Amaxa program U-30 and Kit R for NIH/3T3 cells or T-21 and Kit V for J774 macrophages (Amaxa, Germany) with an siRNA SMARTpool containing 4 siRNAs targeting mouse *dynamin-2* (Dharmacon cat # M-044919-01), *elmo1* (M-041254-00) or a noncoding SMARTpool (Dharmacon cat # D-001206-13) using 1.2 mg of total siRNA (0.3 mg of each individual siRNA) as previously described[69], then incubated 48 hours to recover.

Images were acquired using a Zeiss 510-UV laser scanning confocal microscope with 405, 488, 543, and 633 lasers (Zeiss AG, Germany). For z reconstruction experiments, confocal z sections were acquired every 0.3 mm; z-axis was reconstructed in LSM and subsequently deconvolved.

Apoptotic thymocytes were generated as previously described[70]; apoptotic thymocytes (5×10^5 cells per condition) were added to NIH/3T3 cells in 4-well Labtek II culture chambers followed by a brief centrifugation to pellet cells onto the slide. Of the cells that bind to the phagocyte monolayer, ~98% are apoptotic by anti-active caspase-3 staining (data not shown). Thymocytes were allowed to be engulfed for 30 minutes; unbound apoptotic thymocytes were gently washed off DMEM + 10% FBS, and then

subsequently incubated for 2 hours. For Lysotracker staining, cells were incubated with apoptotic cells in DMEM + 10% FBS containing 1/10,000 dilution of Lysotracker Red. Cells were then fixed with 3% paraformaldehyde (Sigma) in PBS for 30 minutes, permeabilized with 0.1% Triton X-100 (Sigma) and blocked with 5% milk that had been clarified by high speed centrifugation. Antibody staining was then done as previously described[68].

Generation of transgenic nematodes

Low copy transgenic worms were obtained by microparticle bombardment in a Biolistic PDS-1000 (Bio-Rad) transformation as previously described[71]. *unc-119* was used as a transformation marker. *opIs220 [P_{eft-3}::dyn-1::yfp]* was found to rescue the temperature sensitive persistent cell corpse phenotype of the *dyn-1(ky51)* mutants. For *opEx1278 [P_{eft-3}::yfp::rab-7]* and *opEx1279 [P_{eft-3}::cfp::rab-5]* we observed an accumulation of the fluorescent proteins into vesicular structures suggesting that the fusion proteins are functional (**Supplementary Figure S11**). Similar vesicular structures were observed in worms carrying *opEx1304[P_{ced-1}::yfp::rab-5; unc-119(+)], opEx1303[P_{ced-1}::yfp::rab-7; unc-119(+)] or opIs282[P_{ced-1}::yfp::rab-5; unc-119(+)].*

Immunoprecipitations

293T cells were transiently transfected with 2 mg of each appropriate constructs. After 36 h, the cells were lysed (in 1% Triton X-100, 50mM Tris and 150mM NaCl) and immunoprecipitated using anti-FLAG (clone M2, Sigma) or anti-GFP (B-2, Santa Cruz) antibody directly coupled to sepharose.

The authors declare no competing financial interests.

Correspondence and requests for materials should be addressed to ravi@virginia.edu (mammalian) or Michael.Hengartner@molbio.unizh.ch (nematode).

References

1. Scott, R. S. et al. Phagocytosis and clearance of apoptotic cells is mediated by MER. *Nature* **411**, 207-11 (2001).
2. Savill, J. & Fadok, V. Corpse clearance defines the meaning of cell death. *Nature* **407**, 784-8 (2000).
3. Hanayama, R., Miyasaka, K., Nakaya, M. & Nagata, S. MFG-E8-dependent clearance of apoptotic cells, and autoimmunity caused by its failure. *Curr Dir Autoimmun* **9**, 162-72 (2006).
4. Kawane, K. et al. Chronic polyarthritis caused by mammalian DNA that escapes from degradation in macrophages. *Nature* **443**, 998-1002 (2006).
5. Gardai, S. J., Bratton, D. L., Ogden, C. A. & Henson, P. M. Recognition ligands on apoptotic cells: a perspective. *J Leukoc Biol* **79**, 896-903 (2006).
6. Schrijvers, D. M., De Meyer, G. R., Kockx, M. M., Herman, A. G. & Martinet, W. Phagocytosis of apoptotic cells by macrophages is impaired in atherosclerosis. *Arterioscler Thromb Vasc Biol* **25**, 1256-61 (2005).
7. Henson, P. M. & Hume, D. A. Apoptotic cell removal in development and tissue homeostasis. *Trends Immunol* **27**, 244-50 (2006).
8. Wu, Y., Tibrewal, N. & Birge, R. B. Phosphatidylserine recognition by phagocytes: a view to a kill. *Trends Cell Biol* **16**, 189-97 (2006).
9. Franz, S. et al. Apoptosis and autoimmunity: when apoptotic cells break their silence. *Curr Rheumatol Rep* **8**, 245-7 (2006).
10. Gaipl, U. S. et al. Inefficient clearance of dying cells and autoreactivity. *Curr Top Microbiol Immunol* **305**, 161-76 (2006).
11. Horvitz, H. R. Worms, life, and death (Nobel lecture). *Chembiochem* **4**, 697-711 (2003).
12. Brenner, S. The genetics of *Caenorhabditis elegans*. *Genetics* **77**, 71-94 (1974).
13. Lettre, G. & Hengartner, M. O. Developmental apoptosis in *C. elegans*: a complex CEDnario. *Nat Rev Mol Cell Biol* **7**, 97-108 (2006).
14. Reddien, P. W. & Horvitz, H. R. CED-2/CrkII and CED-10/Rac control phagocytosis and cell migration in *Caenorhabditis elegans*. *Nat Cell Biol* **2**, 131-6 (2000).
15. Wu, Y. C. & Horvitz, H. R. *C. elegans* phagocytosis and cell-migration protein CED-5 is similar to human DOCK180. *Nature* **392**, 501-4 (1998).
16. Wu, Y. C., Tsai, M. C., Cheng, L. C., Chou, C. J. & Weng, N. Y. *C. elegans* CED-12 acts in the conserved crkII/DOCK180/Rac pathway to control cell migration and cell corpse engulfment. *Dev Cell* **1**, 491-502 (2001).
17. Zhou, Z., Caron, E., Hartwieg, E., Hall, A. & Horvitz, H. R. The *C. elegans* PH domain protein CED-12 regulates cytoskeletal reorganization via a Rho/Rac GTPase signaling pathway. *Dev Cell* **1**, 477-89 (2001).
18. Gumienny, T. L. et al. CED-12/ELMO, a novel member of the CrkII/Dock180/Rac pathway, is required for phagocytosis and cell migration. *Cell* **107**, 27-41 (2001).
19. Brugnera, E. et al. Unconventional Rac-GEF activity is mediated through the Dock180-ELMO complex. *Nat Cell Biol* **4**, 574-82 (2002).
20. Zhou, Z., Hartwieg, E. & Horvitz, H. R. CED-1 is a transmembrane receptor that mediates cell corpse engulfment in *C. elegans*. *Cell* **104**, 43-56 (2001).

21. Su, H. P. et al. Interaction of CED-6/GULP, an adapter protein involved in engulfment of apoptotic cells with CED-1 and CD91/low density lipoprotein receptor-related protein (LRP). *J Biol Chem* **277**, 11772-9 (2002).
22. Hamon, Y. et al. Cooperation between Engulfment Receptors: The Case of ABCA1 and MEGF10. *PLoS ONE* **1**, e120 (2006).
23. Luciani, M. F. & Chimini, G. The ATP binding cassette transporter ABC1, is required for the engulfment of corpses generated by apoptotic cell death. *Embo J* **15**, 226-35 (1996).
24. Wu, Y. C. & Horvitz, H. R. The *C. elegans* cell corpse engulfment gene ced-7 encodes a protein similar to ABC transporters. *Cell* **93**, 951-60 (1998).
25. Jehle, A. W. et al. ATP-binding cassette transporter A7 enhances phagocytosis of apoptotic cells and associated ERK signaling in macrophages. *J Cell Biol* **174**, 547-56 (2006).
26. Liu, Q. A. & Hengartner, M. O. Candidate adaptor protein CED-6 promotes the engulfment of apoptotic cells in *C. elegans*. *Cell* **93**, 961-72 (1998).
27. Henson, P. M. Engulfment: ingestion and migration with Rac, Rho and TRIO. *Curr Biol* **15**, R29-30 (2005).
28. Kinchen, J. M. & Hengartner, M. O. Tales of cannibalism, suicide, and murder: Programmed cell death in *C. elegans*. *Current Topics in Developmental Biology* **65**, 1-45 (2005).
29. Kinchen, J. M. et al. Two pathways converge at CED-10 to mediate actin rearrangement and corpse removal in *C. elegans*. *Nature* **434**, 93-9 (2005).
30. Kinchen, J. M. & Ravichandran, K. S. Journey to the grave: signaling events regulating removal of apoptotic cells. *J Cell Sci* **120**, 2143-9 (2007).
31. Stuart, L. M. et al. A systems biology analysis of the Drosophila phagosome. *Nature* **445**, 95-101 (2007).
32. Hall, D. H. et al. Ultrastructural features of the adult hermaphrodite gonad of *Caenorhabditis elegans*: relations between the germ line and soma. *Dev Biol* **212**, 101-23 (1999).
33. Gumienny, T. L., Lambie, E., Hartwieg, E., Horvitz, H. R. & Hengartner, M. O. Genetic control of programmed cell death in the *Caenorhabditis elegans* hermaphrodite germline. *Development* **126**, 1011-22 (1999).
34. Gruenberg, J. & van der Goot, F. G. Mechanisms of pathogen entry through the endosomal compartments. *Nat Rev Mol Cell Biol* **7**, 495-504 (2006).
35. Lettre, G. et al. Genome-wide RNAi identifies p53-dependent and -independent regulators of germ cell apoptosis in *C. elegans*. *Cell Death Differ* **11**, 1198-203 (2004).
36. Carney, D. S., Davies, B. A. & Horazdovsky, B. F. Vps9 domain-containing proteins: activators of Rab5 GTPases from yeast to neurons. *Trends Cell Biol* **16**, 27-35 (2006).
37. Bieri, T. et al. WormBase: new content and better access. *Nucleic Acids Res* **35**, D506-10 (2007).
38. Sato, M. et al. *Caenorhabditis elegans* RME-6 is a novel regulator of RAB-5 at the clathrin-coated pit. *Nat Cell Biol* **7**, 559-69 (2005).
39. Andrews, R. & Ahringer, J. Asymmetry of Early Endosome Distribution in *C. elegans* Embryos. *PLoS ONE* **2**, e493 (2007).

40. Gengyo-Ando, K. et al. The SM protein VPS-45 is required for RAB-5-dependent endocytic transport in *Caenorhabditis elegans*. *EMBO Rep* **8**, 152-7 (2007).
41. Hayakawa, A. et al. The WD40 and FYVE domain containing protein 2 defines a class of early endosomes necessary for endocytosis. *Proc Natl Acad Sci U S A* **103**, 11928-33 (2006).
42. Rink, J., Ghigo, E., Kalaidzidis, Y. & Zerial, M. Rab conversion as a mechanism of progression from early to late endosomes. *Cell* **122**, 735-49 (2005).
43. Haas, A. NSF--fusion and beyond. *Trends Cell Biol* **8**, 471-3 (1998).
44. Fraser, A. G. et al. Functional genomic analysis of *C. elegans* chromosome I by systematic RNA interference. *Nature* **408**, 325-30 (2000).
45. Grosshans, B. L., Ortiz, D. & Novick, P. Rabs and their effectors: achieving specificity in membrane traffic. *Proc Natl Acad Sci U S A* **103**, 11821-7 (2006).
46. Kamath, R. S. et al. Systematic functional analysis of the *Caenorhabditis elegans* genome using RNAi. *Nature* **421**, 231-7 (2003).
47. Sawa, M. et al. Essential role of the *C. elegans* Arp2/3 complex in cell migration during ventral enclosure. *J Cell Sci* **116**, 1505-18 (2003).
48. Tosello-Trampont, A. C., Nakada-Tsukui, K. & Ravichandran, K. S. Engulfment of apoptotic cells is negatively regulated by Rho-mediated signaling. *J Biol Chem* **278**, 49911-9 (2003).
49. Clark, S. G., Shurland, D. L., Meyerowitz, E. M., Bargmann, C. I. & van der Bliek, A. M. A dynamin GTPase mutation causes a rapid and reversible temperature-inducible locomotion defect in *C. elegans*. *Proc Natl Acad Sci U S A* **94**, 10438-43 (1997).
50. Krueger, E. W., Orth, J. D., Cao, H. & McNiven, M. A. A dynamin-cortactin-Arp2/3 complex mediates actin reorganization in growth factor-stimulated cells. *Mol Biol Cell* **14**, 1085-96 (2003).
51. Gold, E. S. et al. Dynamin 2 is required for phagocytosis in macrophages. *J Exp Med* **190**, 1849-56 (1999).
52. Orth, J. D. & McNiven, M. A. Dynamin at the actin-membrane interface. *Curr Opin Cell Biol* **15**, 31-9 (2003).
53. Thompson, H. M., Skop, A. R., Euteneuer, U., Meyer, B. J. & McNiven, M. A. The large GTPase dynamin associates with the spindle midzone and is required for cytokinesis. *Curr Biol* **12**, 2111-7 (2002).
54. Vieira, O. V. et al. Distinct roles of class I and class III phosphatidylinositol 3-kinases in phagosome formation and maturation. *J Cell Biol* **155**, 19-25 (2001).
55. Chang, H. C., Hull, M. & Mellman, I. The J-domain protein Rme-8 interacts with Hsc70 to control clathrin-dependent endocytosis in Drosophila. *J Cell Biol* **164**, 1055-64 (2004).
56. Girard, M., Poupon, V., Blondeau, F. & McPherson, P. S. The DnaJ-domain protein RME-8 functions in endosomal trafficking. *J Biol Chem* **280**, 40135-43 (2005).
57. Zhang, Y., Grant, B. & Hirsh, D. RME-8, a conserved J-domain protein, is required for endocytosis in *Caenorhabditis elegans*. *Mol Biol Cell* **12**, 2011-21 (2001).
58. Yu, X., Odera, S., Chuang, C. H., Lu, N. & Zhou, Z. C. elegans Dynamin mediates the signaling of phagocytic receptor CED-1 for the engulfment and degradation of apoptotic cells. *Dev Cell* **10**, 743-57 (2006).

59. Urrutia, R., Henley, J. R., Cook, T. & McNiven, M. A. The dynamins: redundant or distinct functions for an expanding family of related GTPases? *Proc Natl Acad Sci U S A* **94**, 377-84 (1997).
60. Reubold, T. F. et al. Crystal structure of the GTPase domain of rat dynamin 1. *Proc Natl Acad Sci U S A* **102**, 13093-8 (2005).
61. Duclos, S. et al. Rab5 regulates the kiss and run fusion between phagosomes and endosomes and the acquisition of phagosome leishmanicidal properties in RAW 264.7 macrophages. *J Cell Sci* **113 Pt 19**, 3531-41 (2000).
62. Shin, H. W. et al. An enzymatic cascade of Rab5 effectors regulates phosphoinositide turnover in the endocytic pathway. *J Cell Biol* **170**, 607-18 (2005).
63. Wu, Y. C., Stanfield, G. M. & Horvitz, H. R. NUC-1, a *caenorhabditis elegans* DNase II homolog, functions in an intermediate step of DNA degradation during apoptosis. *Genes Dev* **14**, 536-48 (2000).
64. Parrish, J. Z. & Xue, D. Functional genomic analysis of apoptotic DNA degradation in C. elegans. *Mol Cell* **11**, 987-96 (2003).
65. Krieser, R. J. et al. Deoxyribonuclease IIalpha is required during the phagocytic phase of apoptosis and its loss causes perinatal lethality. *Cell Death Differ* **9**, 956-62 (2002).
66. Erwig, L. P. et al. Differential regulation of phagosome maturation in macrophages and dendritic cells mediated by Rho GTPases and ezrin-radixin-moesin (ERM) proteins. *Proc Natl Acad Sci U S A* **103**, 12825-30 (2006).
67. Blander, J. M. & Medzhitov, R. Regulation of phagosome maturation by signals from toll-like receptors. *Science* **304**, 1014-8 (2004).
68. Grimsley, C. M., Lu, M., Haney, L. B., Kinchen, J. M. & Ravichandran, K. S. Characterization of a novel interaction between ELMO1 and ERM proteins. *J Biol Chem* **281**, 5928-37 (2006).
69. Tosello-Trampont, A. C. et al. Identification of two signaling submodules within the CrkII/ELMO/Dock180 pathway regulating engulfment of apoptotic cells. *Cell Death Differ* (2007).
70. Tosello-Trampont, A. C., Brugnera, E. & Ravichandran, K. S. Evidence for a conserved role for CRKII and Rac in engulfment of apoptotic cells. *J Biol Chem* **276**, 13797-802 (2001).
71. Praitis, V., Casey, E., Collar, D. & Austin, J. Creation of low-copy integrated transgenic lines in *Caenorhabditis elegans*. *Genetics* **157**, 1217-26 (2001).

Figure 1. RAB-5 and RAB-7 are required for efficient corpse clearance.

Bright field images represent DIC micrographs. Arrows and arrowheads indicate apoptotic germ cells or protein localized around apoptotic germ cells in dissected gonads. Chart shows number of halos normalized to corpse number; Error bars represent s.e.m. n>10 animals for each condition. Size bar, 10 μm.

(**a**-**h**) In wild-type worms, CFP::RAB-5 (**a-d**) and YFP::RAB-7 (**e**-**h**) highlight SYTO-positive, late stage internalized germ cell corpses (**d**, **h**, arrowheads) as well as corpses that stain weakly with SYTO dyes (**d**, arrow). Occasionally, more than one corpse can be seen inside RAB-5 or RAB-7 positive structures (**d, h,** asterisks). RAB-5 and RAB-7 stain discrete stages during corpse engulfment, with RAB-5 preferentially localizing around early corpses and RAB-7 localizing around late apoptotic cell corpses (**q, Supplementary Figure S8**).

(**i-p**) Mutation of either *ced-1* or *ced-5* severely reduces recruitment of CFP::RAB-5 (**j**, **l**) and YFP::RAB-7 (**m**, **p**) around apoptotic cell corpses (**l, k, m, o,** arrowheads). Quantitated data are presented in Supplementary Table S2a.

(**r**, **s**) RNA interference against either *rab-5* (**r**) or *rab-7* (**s**) resulted in increased numbers of undegraded refractile corpses in the adult hermaphrodite gonad. *rab-5(RNAi)* resulted in incompletely penetrant larval arrest; animals scored represent escapers that grew into adults.

Kinchen and Doukoumetzidis et al, Figure 1

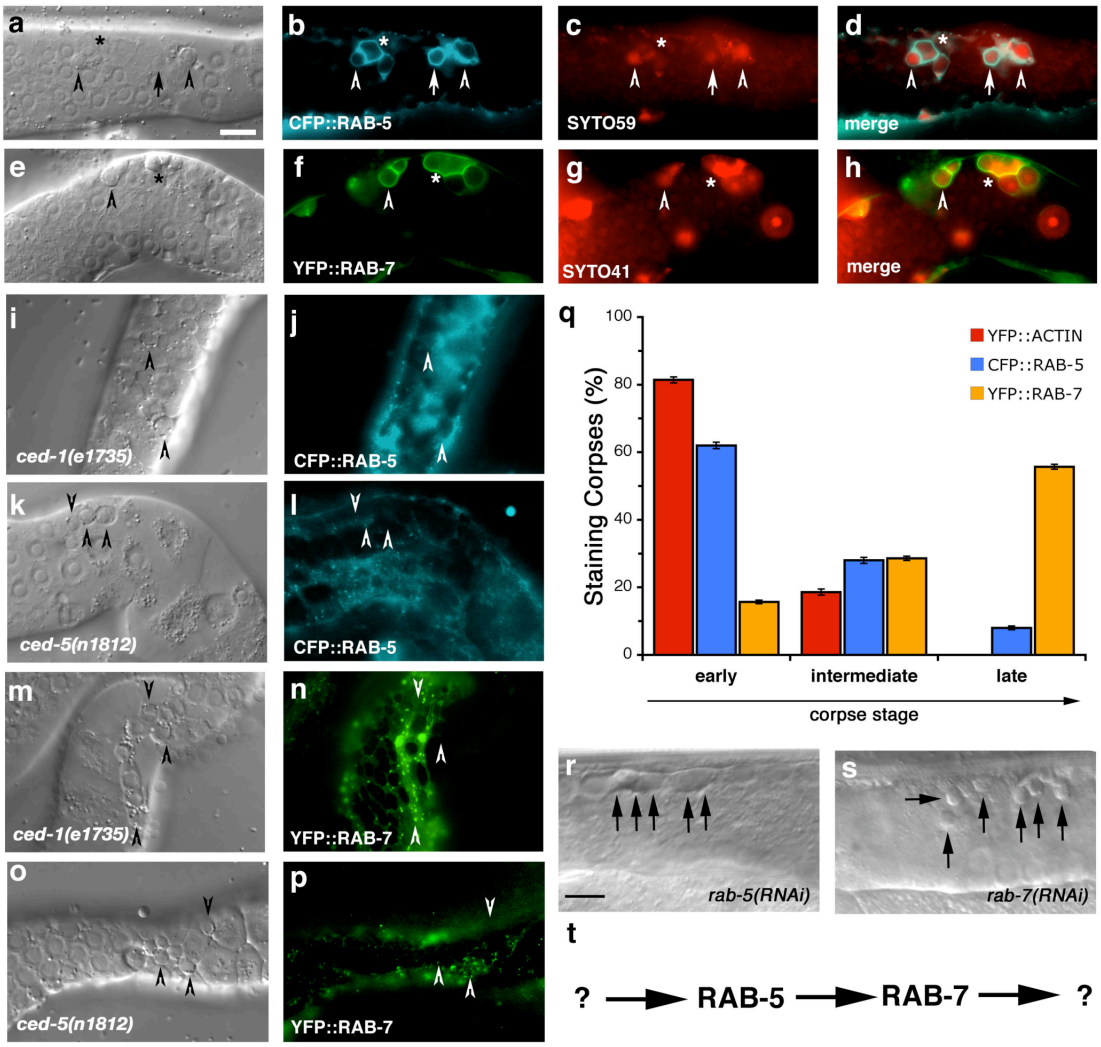

Figure 2. The HOPS complex functions downstream of RAB-7 during phagosome maturation.

Bright field images represent DIC micrographs. Arrows and arrowheads indicate apoptotic germ cells or protein localized around apoptotic germ cells; asterisks represent RAB-7 staining phagosomes that contain non-refractile, partially degraded apoptotic cells. Chart shows number of halos ± s.d. Size bar represents 10 μm.

(**a-f)** RNA interference against members of the HOPS complex resulted in increased numbers of undegraded, refractile cell corpses in the gonad.

(**g-s**) While number of RAB-5-positive phagosomes (**i**,**m**,**q**) were similar to control RNAi treated nematodes (**i**), the number of RAB-7-positive phagosomes (**k**,**o**,**s**) were increased compared to control (**k**). Data was quantitated in (**g**).

(**t**) Genetic pathway for phagosome maturation.

Kinchen and Doukoumetzidis et. al., Figure 2

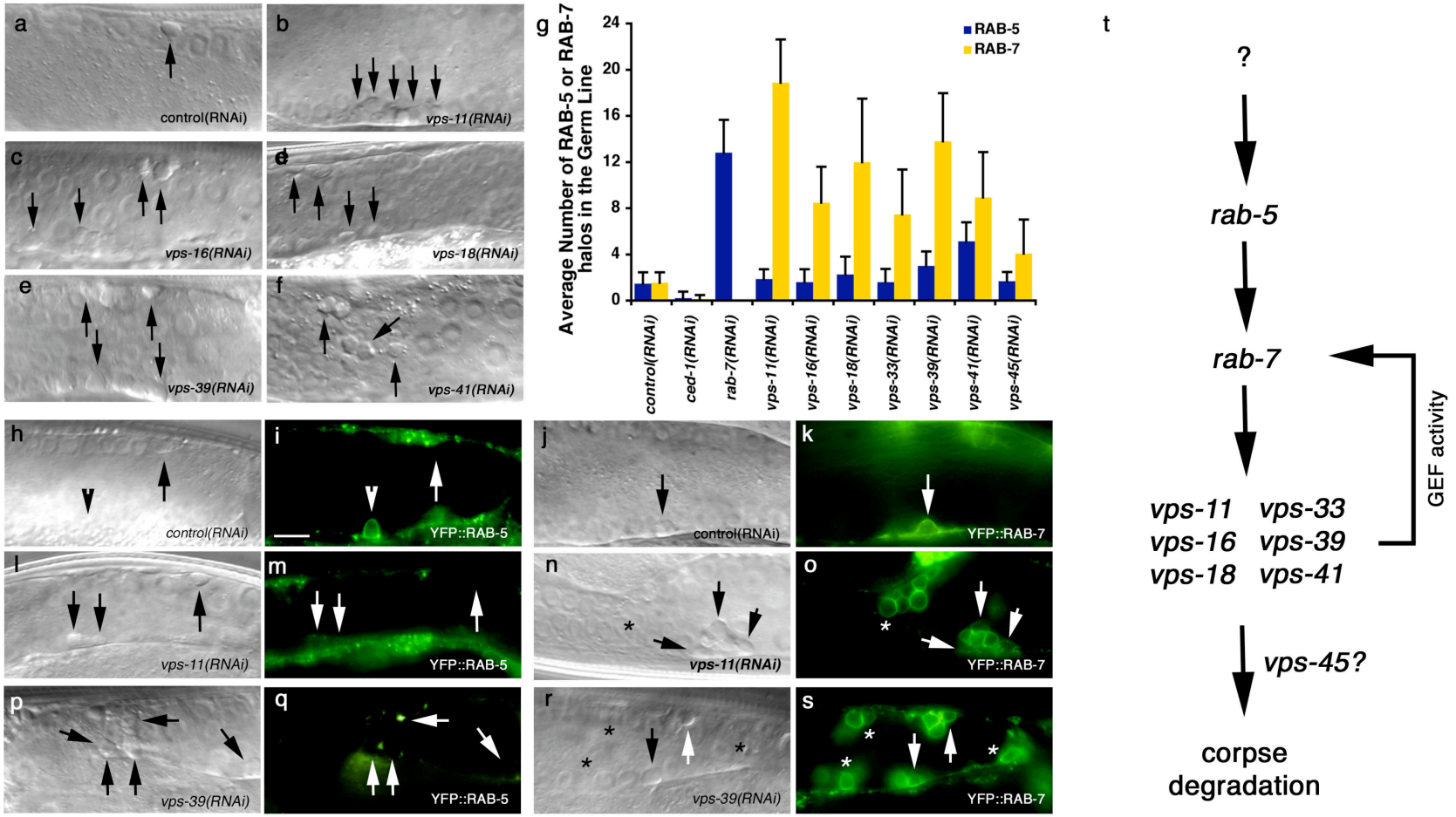

Figure 3. A reverse genetic screen identifies DYN-1, which is required for efficient corpse removal and localizes around apoptotic cells in the adult hermaphrodite gonad.

Bright field images represent DIC micrographs. Arrows/arrowheads indicate refractile cell corpses in the DIC images or the indicated protein for localization around apoptotic cells in the fluorescence images. *dyn-1(ky51*) mutant worms are shown at the nonpermissive temperature. Scale bar, 10 □m.

(**a**-**d**) In wild-type worms (**a, b**), acridine orange (AO) preferentially stains engulfed apoptotic cells present in acidic compartments. In worms mutant for genes required for efficient removal of apoptotic cells, refractile cell corpses persist but do not stain with AO [*ced-1(e1735),* **c, d**].

(**e**) Schematic of reverse genetic screen. Worms were fed bacteria expressing dsRNA as at the L1 larval stage, then stained with AO as adults. AO negative candidates were then compared to previous RNAi screens to exclude false negatives due to sterility or other gonadal defects. Genes identified were assigned to categories based on proposed function (e.g., cell architecture). Finally, refractile cell corpses were scored in the 12-hour adult hermaphrodite gonad by DIC microscopy (**Supplementary Table 1**).

(**f-k**) Inactivation of candidate genes identified in the screen, e.g. *dyn-1(ky51)* (**f**, **g**) and *vps-34(RNAi)* (**h**, **i**) showed persistent corpses without AO staining (**g**, **i**, arrowheads). *rab-7(RNAi)* showed corpses arrested in AO-staining phagosomes (**j, k**).

(**l-u**) DYN-1 is recruited around the apoptotic cell during phagocytosis (**l, m**, arrowhead), but not when the engulfment process is disrupted, as in *ced-1* (**n, o**) and *ced-5* (**p, q**) deficient worms. In *vps-34* (**r**, **s**) and *rme-8* (**t**, **u**) deficient worms, DYN-1 is still recruited, suggesting DYN-1 functions upstream of (or in parallel to) VPS-34 and RME-8 during corpse removal.

(**v**) DYN-2 is recruited to the phagocytic cup and associated with early phagosomes. DYN-1::CFP colocalizes with YFP::actin around early/intermediate stage apoptotic cell corpses (**v** and the appropriate subpanels).
(**w**-**z**) DYN-1 is recruited around SYTO 41-negative (early) apoptotic cell corpses (w, x, **z,** overlay, inset**,** arrow) and is not present on late, SYTO41-positive corpses (**y,** overlay, inset, arrowhead). SYTO 41, like acridine orange, preferentially stains late-stage, internalized apoptotic cells.

Kinchen & Doukoumetzidis et al. Figure 3

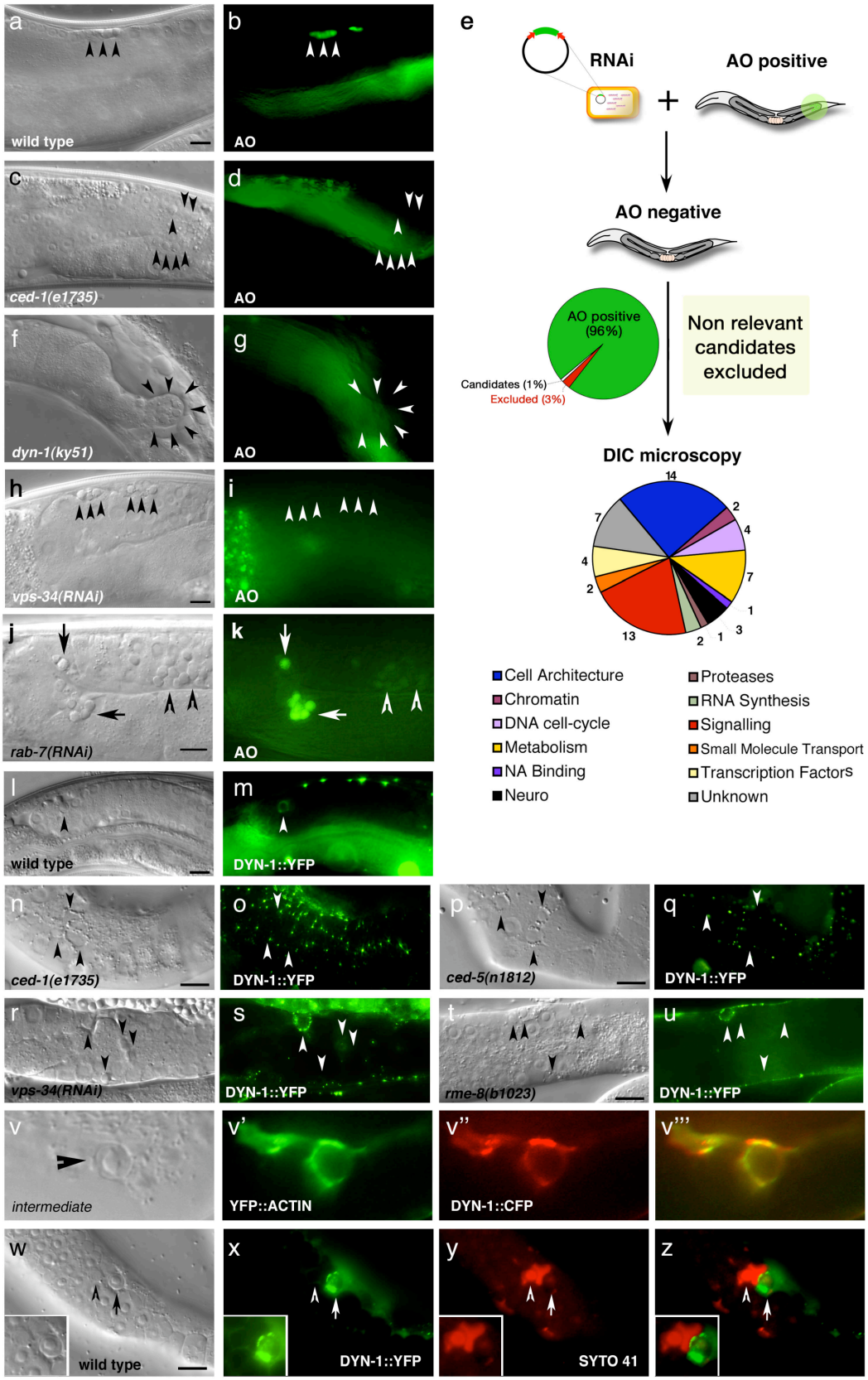

Figure 4. Apoptotic cells are efficiently internalized in *dyn-1* mutant worms

Bright field images represent DIC micrographs. Arrows, arrowheads indicate apoptotic cells. Scale bar, 10 □m. Error bars represent s.d.

(**a-j)** Both CED-1::GFP recruitment, which marks the phagocytic cup (**b,** inset), and actin reorganization (**e**, arrows) during engulfment appear normal in *dyn-1(ky51)* worms at the non-permissive temperature (**d**, **h,** arrows), while *ced-1(e1735)* mutant worms display a severe defect in actin polymerization and internalization of the apoptotic cell (**j**, arrows). Residual staining in the sheath cells represents cortical actin filaments or G-actin.

(**k**) Quantitation of YFP::Actin (*opIs110*) recruitment around apoptotic germ cells during corpse internalization.

Kinchen and Doukoumetzidis et al, Figure 4

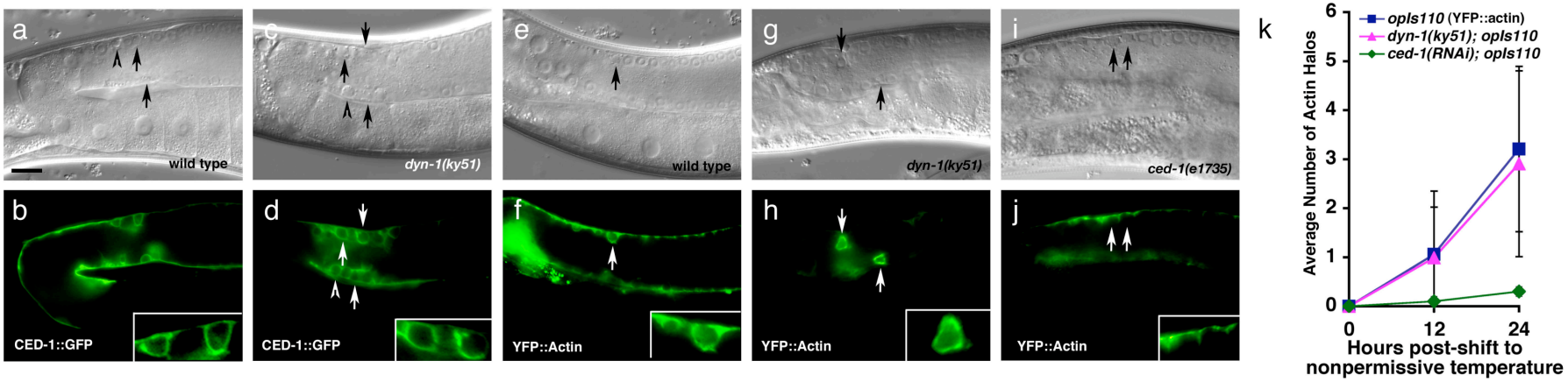

Figure 5. Dynamin in phagocytes is recruited around apoptotic cells coincident with corpse internalization.

CFSE/TAMRA stains the cytoplasm of apoptotic cells, frequently resulting in a lunette of staining around the nucleus. Arrows and asterisks indicate apoptotic cells. Scale bar, 10 μm. Error bars represent s.d.

(**a-h**) J774 macrophages (**a-d)** or NIH/3T3 fibroblasts (**e-h**) were incubated with apoptotic thymocytes or apoptotic Jurkat cells, respectively, and localization of endogenous dynamin (green) and polymerized actin (red) were monitored. Dynamin was recruited to the phagocytic cup with actin in J774 (15 min) (**d**, merge) and NIH/3T3 cells (30 min) (**h,** merge) (indicated by arrow), but was not recruited around bound apoptotic cells (**d**, arrowhead).

(**i-n**) Confocal z-sections were reconstructed to generate yz planes (**m, n**). J774 macrophages incubated with apoptotic cells at 4 ˚C did not show phagocytic cup formation or enrichment of endogenous dynamin around the apoptotic cell (**Supplementary Figure S2**). Cells incubated at 37 ˚C showed dynamin localized in the phagocytic cup (**m**, arrowhead and **n**, camera lucida) adjacent to the apoptotic cell in a punctate pattern (**j**, **k**, inset). Dotted lines (**l**) indicate plane of yz reconstruction.

(**o**) Time course of endogenous dynamin recruitment around the apoptotic cell corpse in J774 macrophages. Cells that had bound apoptotic cells were scored positive for dynamin recruitment if a “halo” of dynamin was seen to surround the apoptotic cell. 4 ˚C, *n=100* (4 experiments); 37 ˚C, *n=200* (8 experiments).

Kinchen and Doukoumetzidis et al, Figure 5

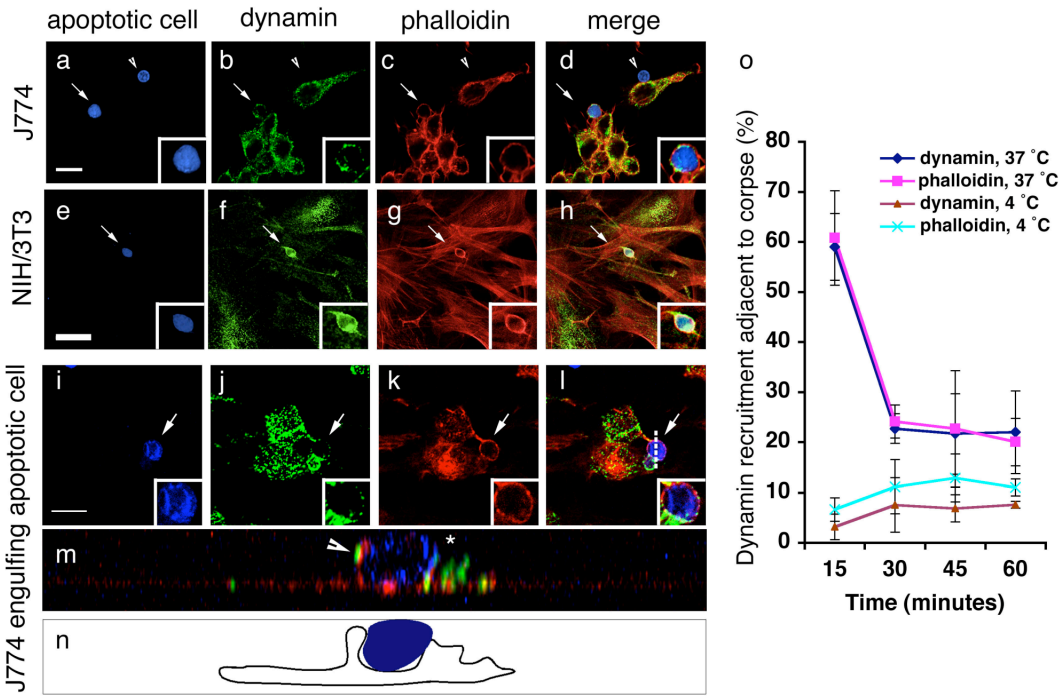

Figure 6. Dynamin is required for maturation of engulfed apoptotic cells into Rab5-coated endosomes.

Arrows and arrowheads indicate apoptotic cells or protein recruited around engulfed apoptotic cells in phagosomes. Neither $Dyn2^{K44A}$ nor $Dyn2^{RNAi}$ had any obvious effect on staining of endogenous endosomal/lysosomal structures with Lysotracker Red or Rab5. Error bars represent s.d. Scale bar, 10 □m.

(**a-l**) NIH/3T3 fibroblasts transfected with GFP (**a-d**), HA-$Dyn2^{K44A}$ (**e-h**), or GFP-$Rab5^{S34N}$ (**i-l**) were incubated with apoptotic thymocytes in the presence of Lysotracker Red to determine the efficiency of phagosome maturation. In the majority of GFP-transfected cells, internalized apoptotic thymocytes (arrows) co-stained with Lysotracker red (**d**, inset); cells transfected with $Dyn2^{K44A}$ (**h**, **i)** or $Rab5^{S34N}$ (**l**, inset) showed decreased numbers of engulfed thymocytes co-staining with Lysotracker. Apoptotic cells incubated at 4 ˚C with phagocytes did not stain strongly with Lysotracker Red (**u**, **Supplementary Figure S7**). HA-$Dyn2^{K44A}$ expressing cells were stained with anti-HA and an Alexa 488-conjugated secondary antibody for visualization of transfected cells.

(**m-t**) Apoptotic cells were incubated with NIH/3T3 fibroblasts, transfected with either GFP alone (as control) or HA-$Dyn2^{K44A}$ and the localization of endogenous Rab5 was monitored. The majority of engulfed apoptotic thymocytes inside GFP-transfected cells were in endosomes coated with Rab5 (**o,** arrowheads**, p**, inset). In $Dyn2^{K44A}$ transfected cells, phagosome maturation was disrupted and decreased numbers of engulfed thymocytes were in Rab5 coated endosomes (**t**, arrowhead, inset). Apoptotic cells incubated at 4 ˚C with phagocytes did not stain strongly for Rab5 (**w**, **Supplementary Figure S7**)

(**u**) Quantitation of experiment shown in (**a-l**). 4 ˚C *n*=20 (2 experiments), 37 ˚C, *n=60* (3 experiments).

(v) NIH/3T3 fibroblasts were electroporated with a control siRNA or *dynamin-2* (*dyn2*) siRNA and assayed as in (**a-l**). $Dyn2^{siRNA}$ cells showed decreased co-localization with Lysotracker as compared to $control^{siRNA}$ cells. *n=50* (2 experiments).

(**w**) Quantitation of experiment shown in (**m-t**). 4 ˚C *n*=20 (2 experiments), 37 ˚C, *n=60* (4 experiments).

Kinchen and Doukoumetzidis et al, Figure 6

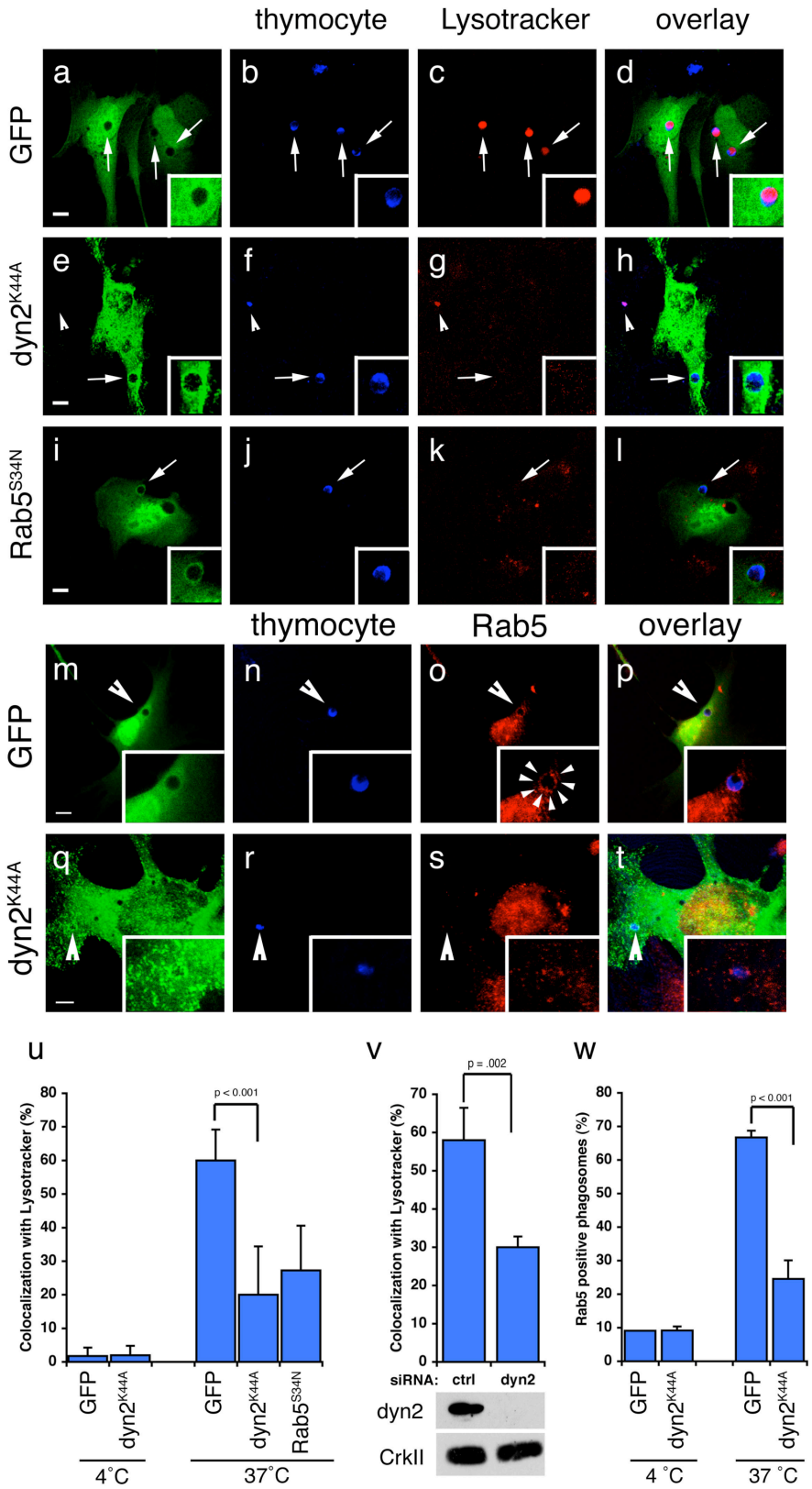

Figure 7. DYN-1 is required for efficient recruitment of RAB-5 and RAB-7 to phagosomes containing engulfed apoptotic cells in the *C. elegans* gonad.

Bright field images represent DIC micrographs. Arrows and arrowheads indicate apoptotic germ cells or protein localized around apoptotic germ cells. *dyn-1(ky51*) worms are shown at the nonpermissive temperature (25 ˚C) unless otherwise stated. Scale bar, 10 □m. *n > 10* for each transgenic. Error bars represent s.e.m.

Compared to wild type (**a-d**), CFP::RAB-5 (**e, f**) and YFP::RAB-7 (**g,h**) halos are decreased in the gonad of *dyn-1(ky51)* mutant worms (**f**, **h**, arrowheads) ; quantitated data is presented in (**q**). Further, phagosomes appear larger in *dyn-1(ky51)* mutant worms (**e, g**, arrowhead and volume quantitated in **s**). Nematodes deficient in *vps-34* (**i-l**) or *rme-8* (**m-p**) showed similar decreases in the number of RAB-5 or RAB-7 corpses (quantitated in **r**).

(**t, u**) Vps34 interacts specifically with HA-dynamin-2 (but not HA-tagged Dock180) (**t**). Vps34 and Dyn2 also form a complex with Rab5 when co-expressed in 293T cells (**u**).

(**v**) Potential model for dynamin function. In wild-type cells, DYN-1/dynamin is recruited around the apoptotic cell during corpse engulfment. We propose that DYN-1 recruits/stabilizes RAB-5 on the nascent phagosomes via its interaction with the PtdIsn(3)-Kinase VPS-34.

(**w**) Genetic pathway for the engulfment of apoptotic cell corpses in the nematode.

Kinchen and Doukoumetzidis et al, Figure 7

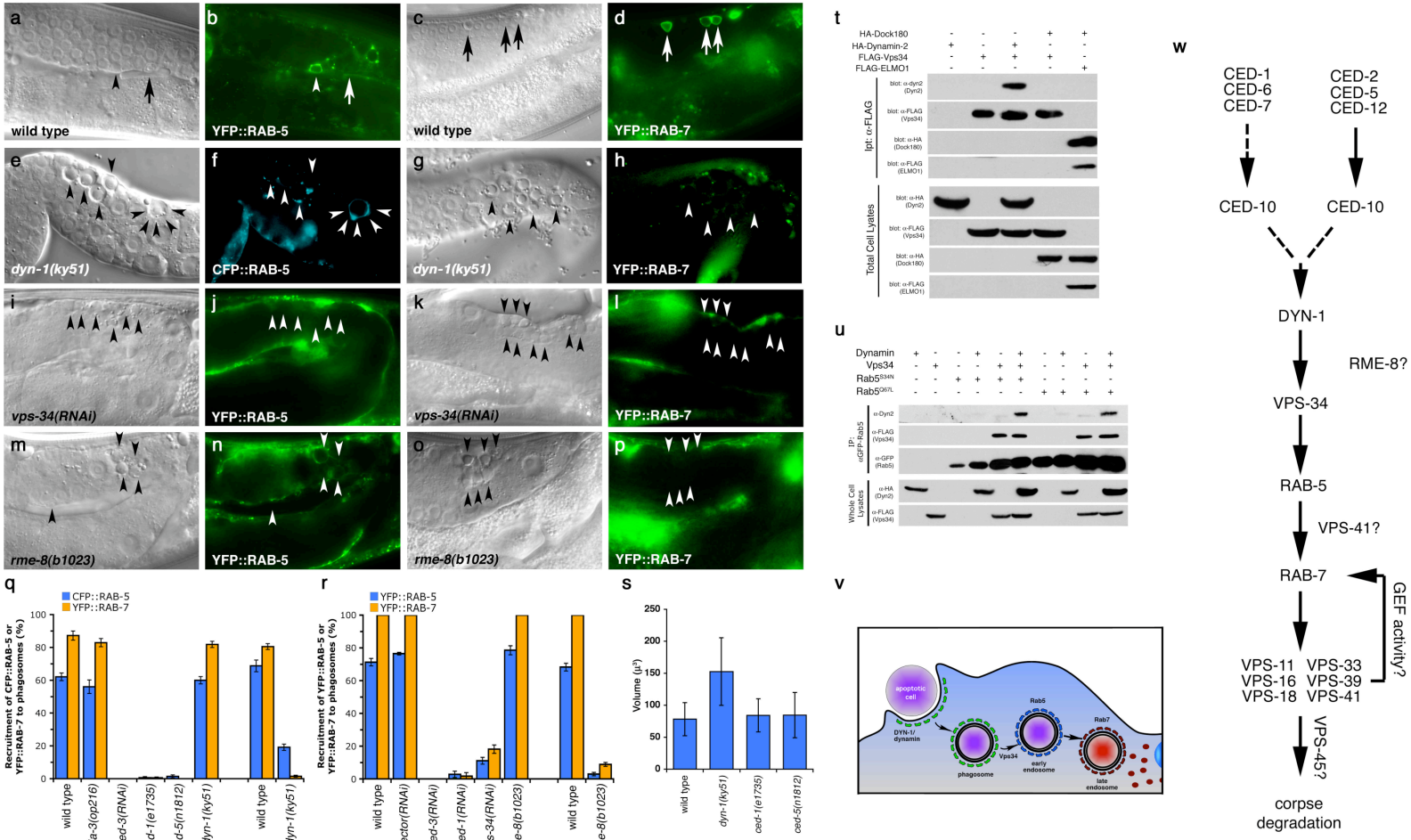

Table 1. A targeted screen identifies genes required for phagosome maturation

Genotype	Corpse Number (DIC)	*n*
wild type	2.3 ± 0.7	10
ced-1(e1735)	18.2 ± 4.4	10
ced-1(RNAi)	11.2 ± 3.1	10
rab-5(RNAi)	10.1 ± 4.6	30
rab-7(RNAi)	25.4 ± 9.3	30
vps-34(RNAi)	8.4 ± 2.1	30
nsf-1(RNAi)	1.5 ± 0.8	15
Rab5 GEFs (Vps9-domain containing proteins)		
tag-333(gk431) (RIN2)	1.6 ± 0.7	20
rme-6(b1014) (RabEx-5)	2.1 ± 0.9	10
rabx-5(RNAi)	1.8 ± 0.9	30
rabx-5(tm512)	1.5 ± 0.8	20
rme-6(b1014); rabx-5(RNAi)	2.0 ± 0.9	10
tag-333(gk431); rme-6(b1014)	1.4 ± 1.0	20
tag-333(gk431); rme-6(b1014); rabx-5(RNAi)	1.5 ± 0.7	15
VPS/HOPS complex		
vps-11(RNAi)	10.8 ± 2.6	25
vps-16(RNAi)	13.7 ± 3.8	30
vps-18(RNAi)	12.7 ± 4.1	30
vps-33(RNAi)	6.1 ± 2.4	30
vps-39(RNAi)	11.8 ± 4.2	40
vps-41(RNAi)	13.1 ± 7.0	30
vps-45(RNAi)	11.4 ± 5.3	40
FYVE-domain containing proteins		
aka-1(ok707) (SARA)	1.4 ± 0.7	20
rabs-5(ok1513) (Rabenosyn-5)	1.1 ± 0.9	20
VT23B5.2(ok912) (BWF1)	1.4 ± 0.9	20
eea-1(ok1040) (EEA1)	1.8 ± 0.9	30
tag-77(gk206) (FGD6)	1.5 ± 0.7	20
mtm-6(ok330) (MTM6)	1.3 ± 0.8	20
exc-5(rh232) (FGD1)	1.2 ± 1.1	20
ZK632.12(RNAi) (Pafin2)	2.1 ± 1.1	30
hgrs-1(RNAi) (HRS)	1.7 ± 1.5	20
lst-2(RNAi) (LZ-FYVE)	1.8 ± 1.1	30
F22G12,4(RNAi) (Rabankyrin)	2.3 ± 1.0	20
mtm-3(RNAi) (MTM3)	1.9 ± 0.9	30
wdfy-2(RNAi) (WDFY2)	2.4 ± 2.1	20
ppk-3(RNAi) (PIP5K)	2.3 ± 1.7	30
PX-domain containing proteins		
Y116A8c.26(RNAi) (sorting nexin 13)	7.4 ± 3.4	45
F17H10.3 (RNAi) (sorting nexin 17)	6.5 ± 2.8	39
lst-4(RNAi) (sorting nexin 18)	8.0 ± 2.7	30
F55C5.7(RNAi) (ribosomal S6 kinase)	2.5 ± 2.2	35
F13E9.1(RNAi) (Nischarin)	2.5 ± 1.3	15
F25H2.2 (RNAi) (sorting nexin 27)	2.3 ± 1.1	15
tag-157(RNAi) (sorting nexin 12)	2.7 ± 2.7	25
Y59A8b.22\(RNAi) (sorting nexin 5)	2.1 ± 1.0	15
Y48E1b.14(RNAi) (sorting nexin 14)	2.3 ± 1.6	15
snx-1(RNAi) (sorting nexin 1)	1.4 ± 0.8	15
pld-1(RNAi) (phospholipase D)	1.7 ± 1.0	15
F39B1.1(RNAi) (PI3KC2a)	1.5 ± 0.7	15

Number of refractile cell corpses were scored in the 12-hour adult hermaphrodite gonad. Whether a particular gene was analyzed through the use of existing mutant strains or through RNAi is indicated. Mammalian homologue is shown in parentheses next to gene name (when different from nematode name). *rab-5* worms arrest during larval development; worms scored represent escapees. Data shown is average ± s.d. Mutations used were backcrossed at least twice.

Supplementary Methods

Mammalian phagocytosis assay

J774 macrophages were transiently transfected in triplicate with the indicated plasmids (with GFP) in a 24-well plate or were electroporated with siRNA (see Methods) [2]. Approximately 24 hours after transfection, the cells were incubated with 1 x 10^6 TAMRA-labeled apoptotic cells (approximately 10 cells per phagocyte plated) in DMEM + 10% FBS (Cellgro). After three hours, the wells were then washed with PBS + 0.5% BSA + 1 % NaN_3 and removed from the plate with 1x Trypsin-EDTA. Cells were then stained with anti-CD3ε (UCH-T1) PE-Cy5 (Santa Cruz) and read immediately on a FACS-Caliber flow cytometer (BD Biosystems). Data was analyzed using FlowJo (TreeStar, Inc). As shown previously[2], the majority of double positive cells scored in the FACS assay represents particles engulfed by transfected cells or particles in the process of internalization, and do not represent cells simply bound to the cell surface. For siRNA experiments, J774 macrophages were stained with CFSE to differentiate phagocyte and apoptotic cell populations; for transfected cells, phagocytes were recognized by GFP fluorescence. For transfected cells, ~150,000 events were acquired; for siRNA-treated cells, ~50,000 events were acquired.

Plasmid construction

Genomic fragments corresponding to *dyn-1*, *rab-5* and *rab-7* loci were amplified by PCR from N2 genomic DNA using primers (Supplementary Table S6) that added an AscI site upstream and an FseI site downstream of the coding sequence (AscI - FseI cassette). All three AscI - FseI cassettes were cloned in the pCR2.1-TOPO vector (Invitrogen) and sequenced to ensure fidelity. Each cassette was then excised using AscI - FseI and placed under the control of the ubiquitously expressed *eft-3* promoter.

For *dyn-1*, a genomic fragment predicted to encode both protein isoforms was cloned into pLN022yfp upstream of *yfp* to generate pLS37 or into pLN022cfp upstream of *cfp* to generate pLS50. For *rab-5* and *rab-7,* the amplified genomic regions were cloned into pLN019 and then tagged at the N-terminus of the protein with *cfp* or *yfp* to generate pKD47 and pKD38 respectively.

Supplementary References

1. Kamath, R. S. et al. Systematic functional analysis of the *Caenorhabditis elegans* genome using RNAi. *Nature* **421**, 231-7 (2003).
2. Tosello-Trampont, A. C., Brugnera, E. & Ravichandran, K. S. Evidence for a conserved role for CRKII and Rac in engulfment of apoptotic cells. *J Biol Chem* **276**, 13797-802 (2001).

Kinchen and Doukoumetzidis et al, Supplementary Figure S1

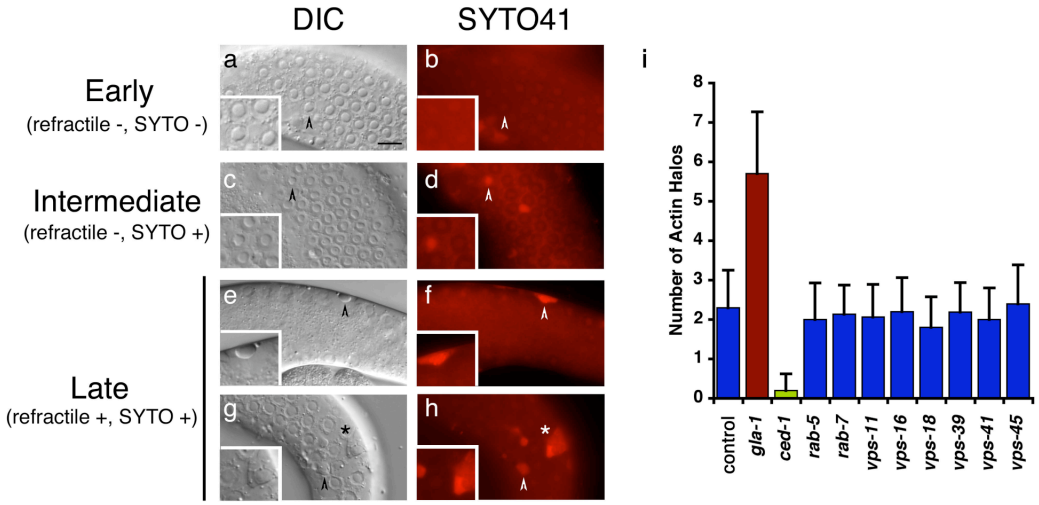

Supplementary Figure S1. Stages of engulfment and actin dynamics.

Arrowheads point to apoptotic cells. Asterisk indicates apoptotic cells potentially sharing lysosomal structures. Scale bar, 10 μm.

(**a**-**h**) In Figure 1, CFP::RAB-5, YFP::RAB-7, and YFP::Actin halos are normalized to the number of early, intermediate, and late cell corpses, 'Early' apoptotic cells in the gonad begin as non-refractile SYTO41 negative bodies. After some time, these corpses progress to the 'intermediate stage' staining weakly with SYTO41 (but are still non-refractile). Finally, 'late' apoptotic cells are refractile and stain strongly with SYTO41 (**e**, **f**, **g, h**). Occasionally, multiple apoptotic cells can be seen in a single SYTO41-staining lysosome (**g**, **h**, asterisk).

(**i**) Actin is enriched at the membrane as the phagocyte extends its membrane around the apoptotic cell corpse; this makes actin an excellent readout to identify different defects in cell corpse removal. Increased apoptosis, such as that found in *gla-1(RNAi)* worms, results in increased numbers of actin halos in the gonad (**I**, **red bar**). Defects in corpse internalization, such as that in *ced-1(RNAi)* worms (**I**, **green bar**) results in decreased numbers of actin halos as cell corpse engulfment (and actin recruitment) are impaired. In worms treated with RNAi against *rab-5* or *rab-7*, or the HOPS complex, numbers of actin halos were similar to control, suggesting that corpses are efficiently engulfed in these backgrounds (**I**, **blue bars**).

Kinchen and Doukoumetzidis et al, Supplementary Figure S2

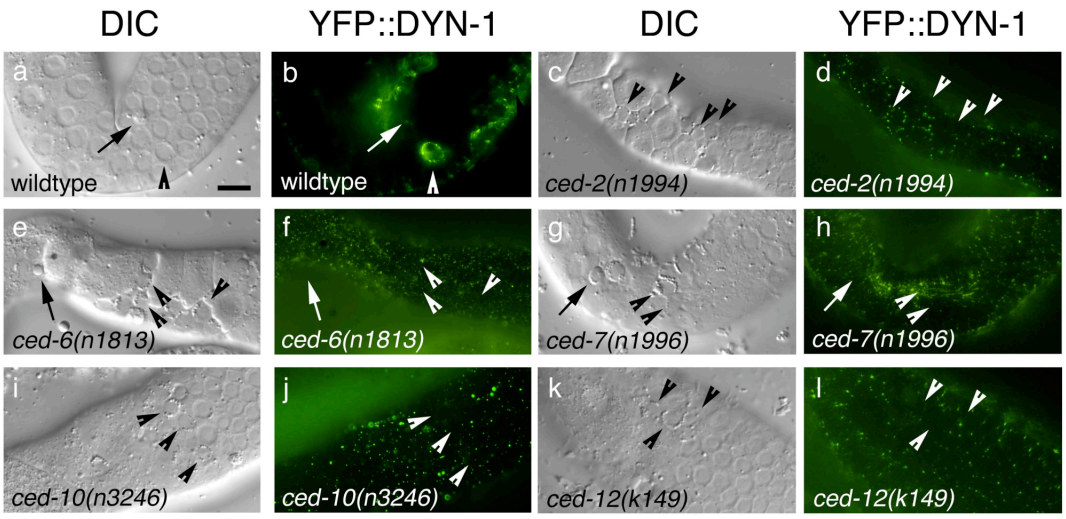

Supplementary Figure S2. DYN-1::YFP requires CED-2, CED-6, CED-7, CED-10, and CED-12 for appropriate localization in the germ line.

Arrowheads indicate early apoptotic cells; arrows indicate late, highly refractile apoptotic cells. Scale bar, 10 μm.

DYN-1::YFP is recruited around early apoptotic cells in wild-type worms (**a**, **b**, arrowheads) but not around late, highly refractile apoptotic cells (**a**, **b** arrow). In worms mutant for *ced-2* (**c**, **d**), *ced-6* (**e**, **f**), *ced-7* (**g**, **h**), *ced-10* (**i**, **j**) and *ced-12* (**k**, **l**) DYN-1 is not recruited around the apoptotic cell (arrows, arrowheads).

Kinchen and Doukoumetzidis et al, Supplementary Figure S3

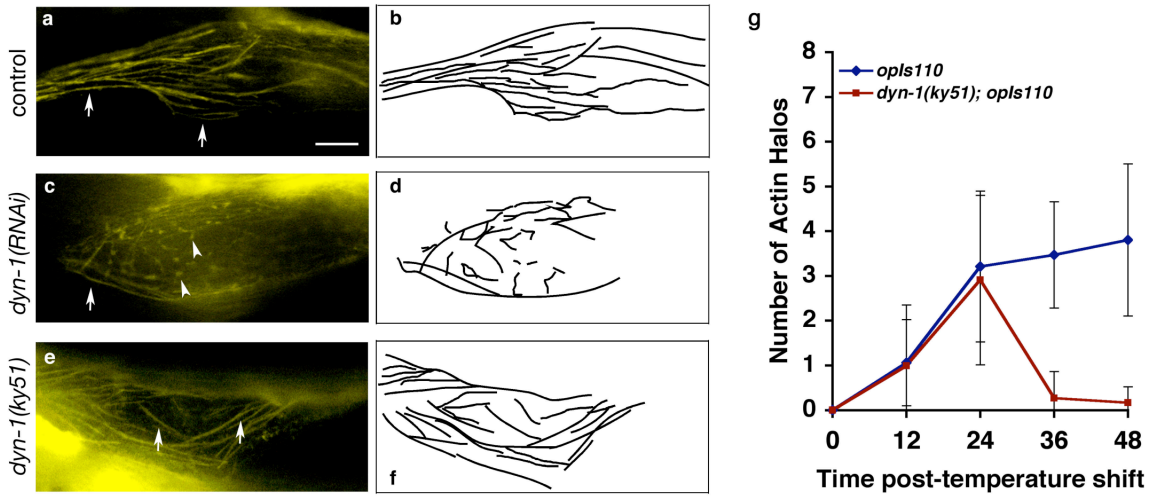

Supplementary Figure S3. Actin fibers become disorganized at late stages following DYN-1 inactivation.

Arrows and arrowheads indicate actin fibers in the gonad. Camera lucida (**b**, **d**, **f**) is shown next to appropriate immunofluorescence image (**a**, **c**, **e**). Scale bar, 10 μm.

We use a relatively short-term inactivation (24 hour) of a temperature-sensitive *dyn-1* allele for our experiments; those of Yu *et al.* used 42-hour gene inactivation by RNA interference. To address whether this may be the source of the discrepancy between these two studies, we asked whether phagocytic defects accumulated in the gonad over time. At late stages, we saw gross distortion of gonad structure and disorganization of the actin stress fibers; actin stress fibers tend to run longitudinally in the proximal gonad in wild type worms (**a, b**). However, *dyn-1(RNAi)* worms show distorted, disoriented actin fibers (**c, d**); in *dyn-1(ky51)* mutant worms, the actin fiber pattern appears as wild type (**e, f**). In fact, we did observe a potential phagocytic defect following long-term inactivation of DYN-1 in older adult gonads (**g**), both in *dyn-1(ky51)* (**g**) and *dyn-1(RNAi)* worms (not shown), as measured by decreased numbers of observed actin halos (data not shown). However, we believe that these defects in internalization represent *dyn-1* role in maintenance of the actin cytoskeleton rather than a primary role for dynamin in corpse internalization. Thus, in our experiments throughout the manuscript, we have chosen to use this time point to avoid potential secondary effects.

Kinchen and Doukoumetzidis et al, Supplementary Figure S4

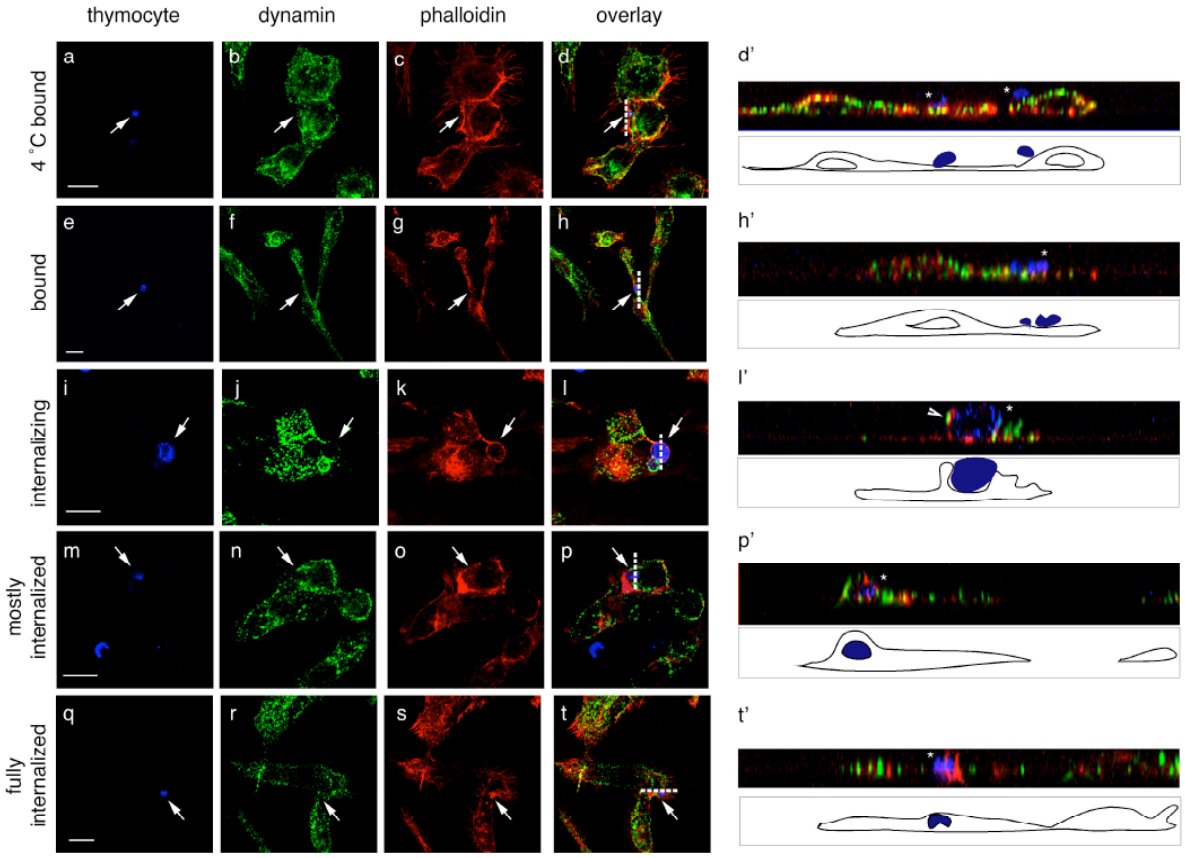

Supplementary Figure S4. Dynamin is recruited around the apoptotic cell during the internalization process.

Arrows and asterisks indicate apoptotic cells. For yz and xz reconstructions, a camera lucida tracing is included beneath the reconstruction. Scale bar, 10 μm. Dotted line indicates plane of z section.

Apoptotic cells were incubated with J774 macrophages at either 4 ˚C (**a-d, d'**) or at 37 ˚C (**e-t, h', l', p', t'**) to monitor localization of dynamin during corpse internalization. Dynamin did not localize around cells bound to the surface of macrophages (**a-h**, arrows and **d'**, **h'** yz reconstruction), but was localized around apoptotic cells during pseudopod extension by the phagocytic cell (**i-p**, arrows and **l', p'**, yz reconstruction). In reconstructed sections, dynamin staining can be seen in the phagocytic cup (**l'**, arrowhead) but appears excluded from the leading edge. Following internalization, dynamin staining is quickly lost (**q-t**, arrow and **t'**, xz reconstruction, asterisk).

Kinchen and Doukoumetzidis et al, Supplementary Figure S5

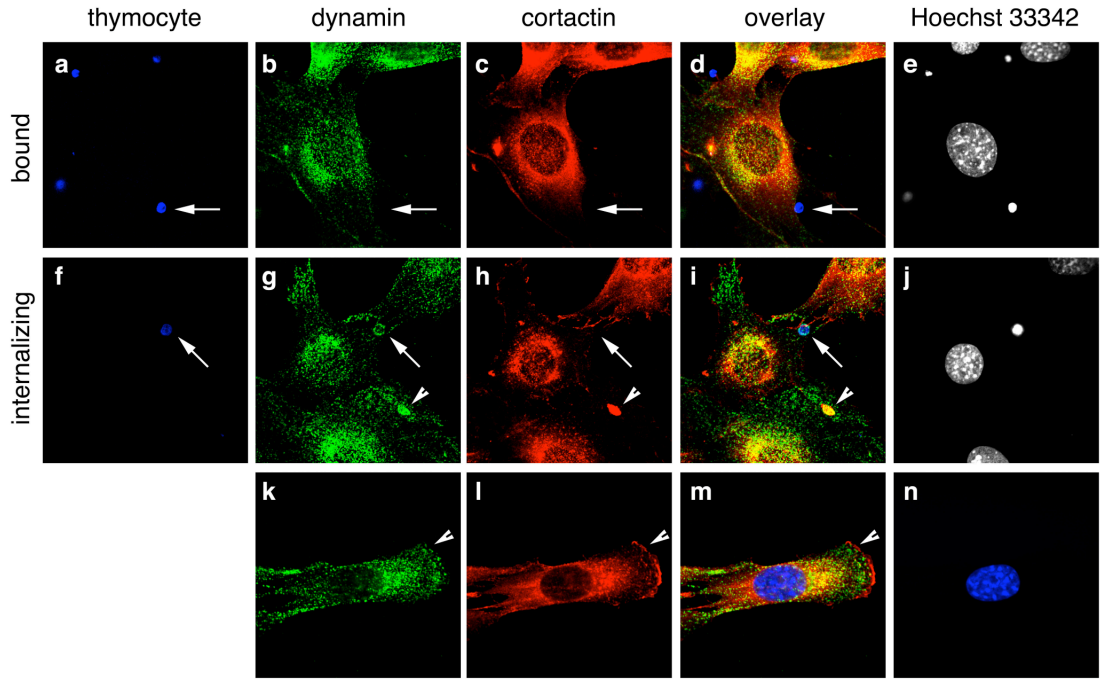

Supplementary Figure S5. Dynamin, but not the dynamin-interacting protein cortactin, is recruited to the phagocytic cup during internalization of the apoptotic cell.

Scale bar, 10 μm.

Endogenous dynamin was recruited to the phagocytic cup around cells being engulfed (**f-j,** arrow) whereas dynamin is not recruited to bound apoptotic cells (**a**-**e**). Endogenous cortactin could not be detected in the phagocytic cup (**f-j**) but did colocalize with endogenous dynamin in dorsal ruffle structures (**i**, arrowhead) but not in lamellipodia (**k**-**m**). Arrows indicate apoptotic cells. Arrowheads indicate membrane ruffles.

Supplementary Figure S6. Dynamin plays no detectable role in the internalization of apoptotic cells by J774 macrophages.

Scale bar, 10 μm. Arrows and arrowheads point to clathrin pits associated with endocytosed vesicles. Asterisk marks the location of Golgi body when visible in the confocal section. Data shown represent averages ± s.d.

Phagocytes were incubated with apoptotic Jurkat cells and subsequently stained cells with a fluorescently conjugated anti-CD3 antibody (see Supplementary Methods). If the phagocytic cup were still open, the anti-CD3 antibody would be free to diffuse and stain the apoptotic cell.

(**a**-**c**) J774 macrophages were transfected with control non-coding siRNA or siRNA targeting either *dynamin-2* (*dyn2*) or *elmo1* (*elmo*). Phagocytes were incubated with apoptotic Jurkat cells and subsequently stained with anti-CD3 to monitor closure of the phagocytic cup. *elmo1* knockdown decreased the efficiency of phagocytosis as well as of the membrane closure compared to control siRNA (**a, b**); there was no effect of siRNA against *dyn2*. Representative Western blot and quantitation of knockdown are shown in (**c**).

(**d**-**f**) J774 macrophages were transfected with GFP, dominant negative $Dyn2^{K44A}$, or dominant negative Rac^{T17N} and assayed as in (**a**-**c**). Western blot shows that all the transfected proteins were expressed (**f**).

It was possible that we were not getting strong enough inhibition of dynamin activity. To test this, NIH/3T3 cells (**a**-**n**) or J774 macrophages (**o**-**t**) were transfected with GFP (**a**-**d, o**-**q**) or HA-$Dyn2^{K44A}$ (**e**-**h, r**-**t**) to monitor phenotypes associated with inhibition of endocytosis. Consistent with previous observations, cells expressing $Dyn2^{K44A}$ accumulated abnormal clathrin-coated pit structures (**f**, arrowheads and **s**, arrows) when compared to GFP-transfected cells (**b**, arrowheads and **s**, arrows). By contrast, treatment of cells with *dyn2* siRNA causes a partial loss-of-function phenotype, without accumulation of endocytic intermediates [$dyn2^{siRNA}$ (**l**-**n**), arrowheads compared to control siRNA (**i**-**k**), arrowheads].

Kinchen and Doukoumetzidis et al, Supplementary Figure S6

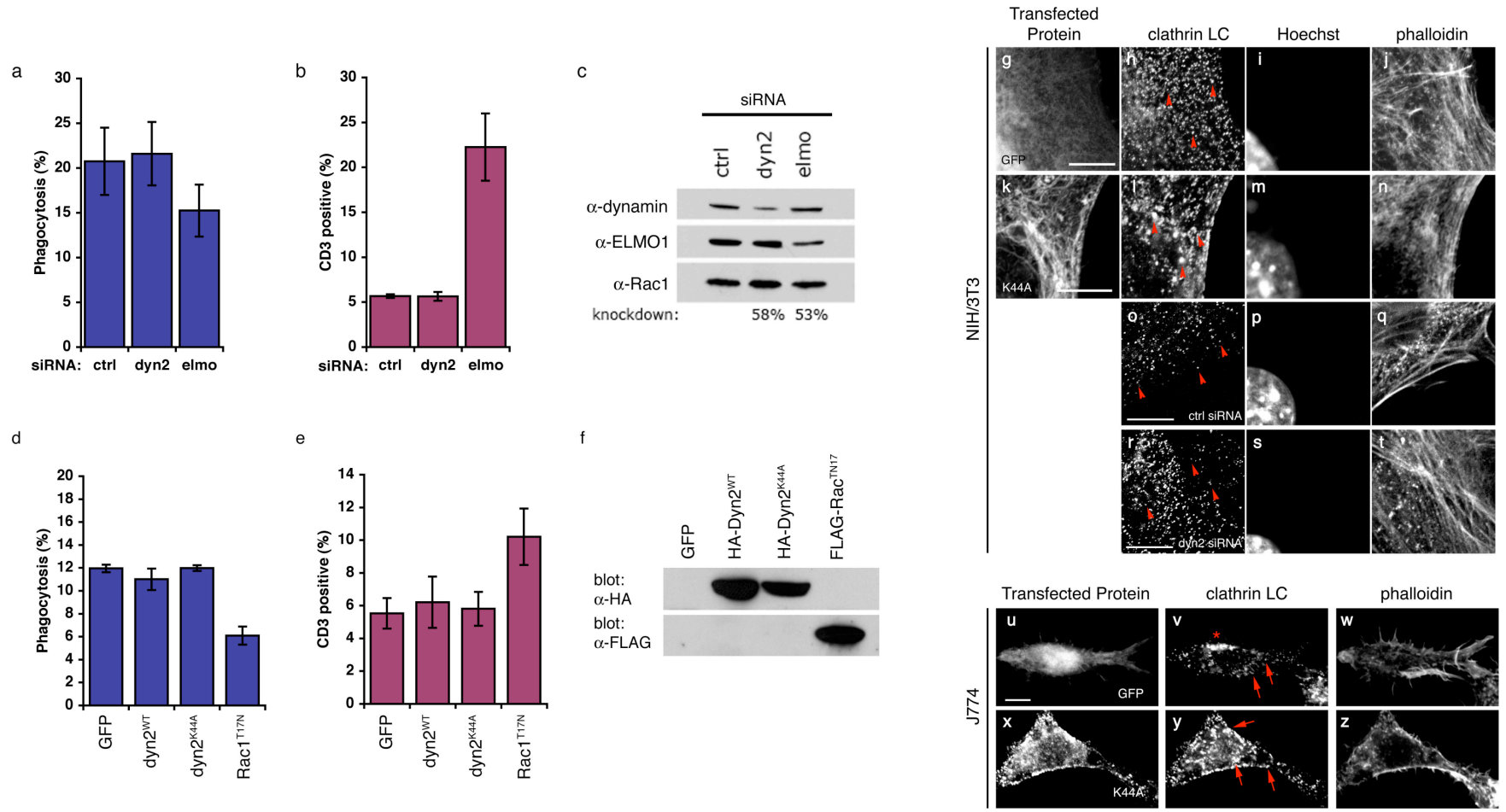

Kinchen and Doukoumetzidis et al, Supplementary Figure S7

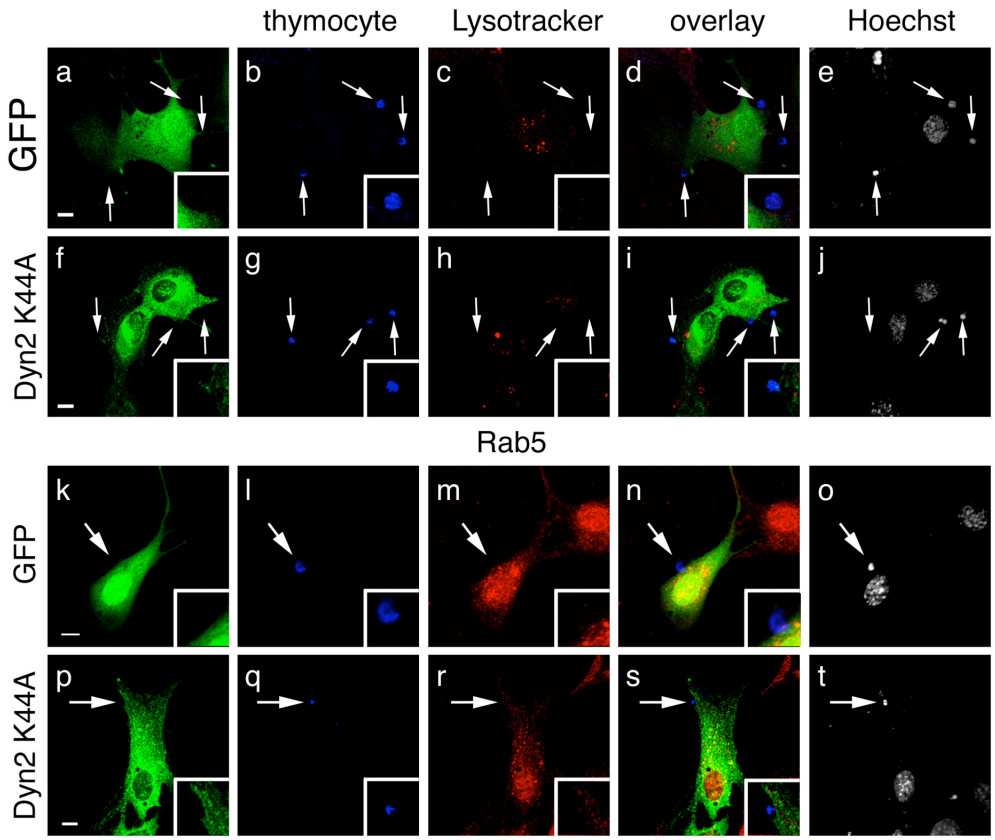

Supplementary Figure S7. Apoptotic cells incubated with phagocytes at 4 ˚C do not stain with Lysotracker Red or Rab5.

Scale bar, 10 μm.

NIH/3T3 cells incubated with apoptotic thymocytes (**b**, **g**, **l**, **p**, arrows) at 4 ˚C were stained with Lysotracker Red (**a**-**j**) or stained for endogenous Rab5 (**k**-**t**). Cells transfected with GFP (**a**, **k**) or dyn2^{K44A} (**k**, **p**) did not acquire Lysotracker Red staining (**c**, **h**, arrows, inset) or Rab5 staining (**m**, **r**, arrows, inset). Hoechst 33342 staining is additionally shown to indicate the position of the apoptotic cell nucleus (**e**, **j**, **o**, **t**, arrows). This control experiment was performed to ensure specificity of Lysotracker and Rab5 staining observed at 37˚C incubation as shown in Figure 3 of the manuscript.

Kinchen and Doukoumetzidis et al, Supplementary Figure S8

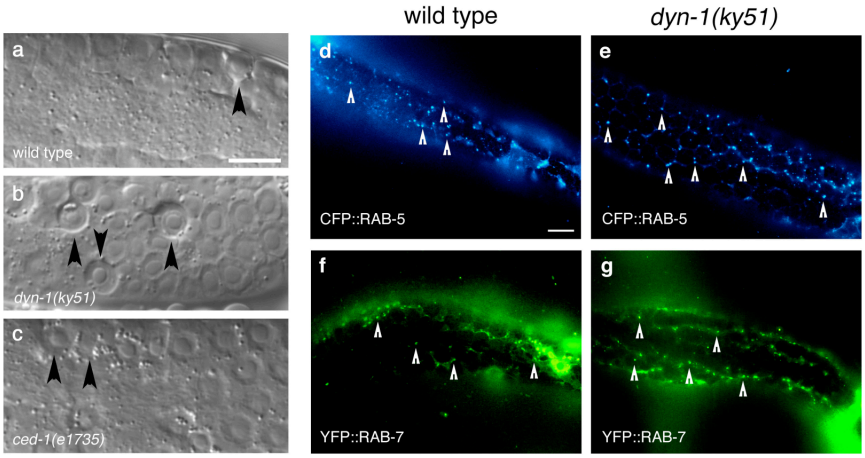

Supplementary Figure S8. Loss of *dyn-1* function results in a defect in phagosome maturation, but endosomes generated by receptor-mediated endocytosis appear unaffected.

Arrows indicate refractile cell corpses or reporter proteins as indicated. Scale bar, 10 μm.

Phagosomes containing internalized apoptotic cells in *dyn-1(ky51)* mutant worms are larger than those found in wild type worms (**a, b**, arrowheads). Persistent uninternalized apoptotic cells in *ced-1* worms are similar to wild type (**c**). Images were quantitated using Openlab software. Quantitation is shown in **Figure 4w**. Arrowheads point to early apoptotic cells. Scale bar, 10 μm.

No decrease was detected in RAB-5 and RAB-7 staining vesicular structures in the 12-hour adult hermaphrodite gonad (arrowheads) in wild type (**d**, **f**) versus *dyn-1(ky51)* mutant worms (**e**, **g**) at the nonpermissive temperature (25 ˚C).

Supplementary Table S1. Candidate engulfment genes suppress Acridine Orange staining of apoptotic cells in the adult hermaphrodite gonad.

Data shown in 'AO Staining' column represents the fraction of worms that were AO positive (green) or AO negative (white), with the approximate penetrance of the phenotype listed. Genes were tested on three independent experiments conducted on different days to rigorously test for reproducibility. ND, not done (due to gonadal defects). Worms were staged and corpse scored as described in Methods. *n,* number of worms scored. Data shown represents average ± s.d.

Acridine orange (AO) selectively labels engulfed apoptotic germ cells. Candidate engulfment genes were identified in a feeding RNAi screen for genes, which when knocked down result in reduced AO staining in adult hermaphrodite gonads. *gla-3(op216)* mutant worms were used to increase the number of apoptotic cell corpses so that acridine orange (AO) staining could be viewed under a dissecting microscope. Identified candidates were compared to those isolated in previous screens. Candidate genes whose knockdown resulted in sterility and growth defects, which in turn could reduce the number of AO positive cells without influencing corpse removal, were excluded from further analyses and are not shown. Genes are grouped by proposed function (as identified in WormBase) as previously described[1]; genes required for actin dynamics are included in 'cell architecture.' Number of apoptotic germ cell corpses was quantitated in *gla-3(op216)* mutant worms grown on bacteria expressing the indicated construct.

Supplementary Table S1. List of candidates isolated from unbiased reverse genetic screen shown in Figure 3.

Gene Model	Locus	Description	Chromosome	Refractile Corpses (DIC)	*n*	AO staining Exp.1	Exp.2	Exp.3
	gfp			8.6 ± 1.6	36	100%	100%	100%
	ced-3			0.1 ± 0.3	36	100%	100%	100%
Cell Architecture								
Y6B3A.1		Guanine nucleotide exchange factor	I	12.9 ± 5.4	36	100%	100%	100%
T23H2.5	*rab-10*	Rab-like GTPase	I	3.9 ± 2.3	12	100%	100%	100%
Y63D3A.5	*tfg-1*	Unnamed protein	I	n.d.		25% 75%	50% 50%	100%
Y71F9AM.5	*nxt-1*	RNA export factor NXT1	I	n.d.		100%	100%	100%
F08B6.4	*unc-87*	required to maintain the structure of myofilaments	I	7.3 ± 6.8	24	50% 50%	n.d.	25% 75%
F56A3.3	*npp-6*	Nuclear pore complex Nup160 compoent	I	n.d.		100%	100%	100%
F18C12.2	*rme-8*	Endocytosis function (maturation)?	I	n.d.		100%	100%	100%
Y34D9A.10	*phi-25*	Vacuolar protein sorting-associated protein 4B	I	9.5 ± 3.1	12	25% 75%	100%	25% 75%
F56A3.3	*npp-6*	Nuclear pore complex, Nup160 component	I	n.d.		100%	100%	100%
F18C12.2	*rme-8*	Endocytosis protein RME-8, contains DnaJ domain	I	n.d.		100%	100%	100%
Y79H2A.6	*arx-3*	Actin-related protein Arp2/3 complex, subunit ARPC1/p41-ARC	III	28.3 ± 10,0	24	25% 75%	25% 75%	100%
Y37D8A.1	*arx-5*	Actin-related protein Arp2/3 complex, subunit ARPC3	III	25.0 ± 9.0	24	100%	25% 75%	100%
T26A5.9	*dlc-1*	Member of the Dynein Light Chain gene class	III	9.5 ± 3.5	16	100%	100%	25% 75%
C02F4.1	*ced-5*	homolog of the human protein DOCK180	IV	16.6 ± 5.2	36	100%	100%	100%
C02C6.1	*dyn-1*	Vacuolar sorting protein VPS1	X	27.6 ± 5.6	36	100%	100%	100%
Chromatin								
F25D7.3	*blmp-1*	B Lymphocyte-induced Maturation Protein-1 homolog	I	5.5 ± 3.4	24	25% 75%	25% 75%	100%
C33H5.7		Histone H3 (Lys4) methyltransferase complex and RNA cleavage factor II complex	IV	9.3 ± 2.5	24	25% 75%	100%	n.d.

Gene Model	Locus	Description	Chromosome	Refractile Corpses (DIC)	*n*	AO staining Exp.1		AO staining Exp.2		AO staining Exp.3	
DNA Cell Cycle											
Y39G10AR.14	*mcm-4*	DNA replication licensing factor	I	5.6 ± 1.6	12	50%	50%	50%	50%	50%	50%
Y47G6A.12	*sep-1*	homolog of separase	I	9.3 ± 2.6	12	50%	50%	100%		25%	75%
W02D9.1	*pri-2*	Eukaryotic-type DNA primase, large subunit	I	n.d.		100%		100%		100%	
F32H2.3	*spd-2*	spindle defective	I	13.7 ± 3.7	36	50%	50%	50%	50%	50%	50%
Metabolism											
W01A8.4		ortholog of the NDUFB4/B15 subunit of the mitochondrial NADH dehydrogenase	I	5.0 ± 2.9	12	100%		100%		25%	75%
F25B5.6a		Folylpolyglutamate synthase	III	7.5 ± 2.9	24	100%		100%		100%	
K03H1.1		qrs-2, member of the glutaminyl (Q) tRNA Synthetase gene class	III	8.'0 ± 4.1	15	50%	50%	50%	50%	100%	
LLC1.3		orthologous to the human gene DLD	IV	1.1± 1.1	12	100%		100%		n.d.	
H04M03.4	*glf-1*	UDP-galactopyranose mutase	IV	5.0 ± 4.3	36	100%		50%	50%	n.d.	
F08C6.2		Phosphorylcholine transferase/cholinephosphate cytidylyltransferase	X	2.6 ± 1.9	12	25%	75%	100%		100%	
R04D3.1	*cyp-14A4*	Cytochrome P450 CYP2 subfamily	X	12.8 ± 3.2	24	100%		n.d.		n.d.	
Nuclei Acid Binding											
B0511.6		ATP-dependent RNA helicase pitchoune	I	n.d.		100%		100%		100%	
Neuro											
F21H11.2	*sax-2*	Fry-like conserved proteins	III	9.2 ± 2.1	21	50%	50%	100%		25%	75%
F58G6.6	*del-1*	degenerin-like	IV	9.8 ± 2.5	36	25%	75%	100%		50%	50%
C17H12.1	*dyci-1*	Cytoplasmic dynein intermediate chain	IV	8.0 ± 4.2	12	25%	75%	100%		100%	
Proteases											
F08C6.1	*adt-2*	Disintegrin metalloproteinases with thrombospondin repeats	X	n.d.		100%		100%		100%	

Gene Model	Locus	Description	Chromosome	Refractile Corpses (DIC)	*n*	AO staining Exp.1		AO staining Exp.2		AO staining Exp.3	
RNA Synthesis											
Y54E10BR.6		DNA-directed RNA polymerase subunit E'	I	10.7 ± 2.3	12	100%		n.d.		100%	
F14B4.3		RNA polymerase I, second largest subunit	I	n.d.		100%		100%		100%	
Signaling											
B0025.1	*vps-34*	phosphoinositide 3-kinase	I	13.8 ± 4.3	36	50%	50%	50%	50%	25%	75%
Y47H9C.4	*ced-1*	homologous to human CD91	I	18.7 ± 6.8	36	100%		50%	50%	100%	
F21F3.2		Glycogen synthase kinase-3	I	5.5 ± 2.1	24	50%	50%	25%	75%	50%	50%
F26E4.4		Cell Death Regulator AVEN	I	0.3 ± 0.6	12	100%		100%		100%	
T23D8.9	*sys-1*	Wnt/MAPK pathway transcriptional coactivator	I	4.6 ± 2.2	12	50%	50%	100%		100%	
C28A5.6		Casein kinase (serine/threonine/tyrosine protein kinase)	III	8.7 ± 4.0	21	50%	50%	100%		25%	75%
F56D2.7	*ced-6*	phosphotyrosine-binding (PTB) domain-containing adaptor protein	III	22.0 ± 9.5	24	100%		100%		100%	
R144.4	*wip-1*	WASP-interacting protein	III	11.3 ± 5.9	22	50%	50%	50%	50%	50%	50%
C24A1.3		Tyrosine kinase for activated GTP-bound p21cdc42	III	12.5 ± 2.5	16	100%		100%		50%	50%
Y41D4A.5		Protein Tyrosine phosphatase	IV	10.3 ± 4.2	24	50%	50%	50%	50%	50%	50%
C45B2.7	*ptr-4*	PaTched Related family	X	3.0 ± 2.4	36	100%		100%		100%	
F58A3.2	*egl-15*	Fibroblast/platelet-derived growth factor receptor and related receptor tyrosine kinases	X	11.9 ± 2.8	24	100%		100%		100%	
R07E4.6	*kin-2*	cAMP-dependent protein kinase types I and II, regulatory subunit	X	n.d.		100%		100%		100%	
Small Molecule Transport											
T14F9.1	*vha-15*	Vacuolar H+-ATPase V1 sector, subunit H	X	n.d.		100%		100%		100%	
F59F5.1		Monocarboxylate transporter	X	9.6 ± 5.1	36	50%	50%	100%		100%	

Gene Model	Locus	Description	Chromosome	Refractile Corpses (DIC)	*n*	AO staining Exp.1		AO staining Exp.2		AO staining Exp.3	
Transcription Factors											
F55F8.4	*cir-1*	CBF1-interacting corepressor CIR and related proteins	I	n.d.		100%		25%	75%	n.d.	
C01H6.5	*nhr-23*	Steroid hormone nuclear receptor	I	n.d.		100%		100%		100%	
T26A5.5		F-box protein JEMMA and related proteins with JmjC, PHD, F-box and LRR domains	III	5.5 ±4.0	21	25%	75%	25%	75%	50%	50%
F58A4.7	*hlh-11*	Similar to transcription factor AP-4	III	6.6 ± 4.1	19	100%		100%		n.d.	
Unknown											
C30F12.1		Uncharacterized conserved protein	I	0.8 ± 1.0	12	25%	75%	100%		25%	75%
Y47G6A.29		unknown conserved protein	I	n.d.		100%		100%		100%	
Y55B1BM.1	*stim-1*	mammalian stromal interaction molecule	III	6.8 ± 2.9	23	25%	75%	25%	75%	25%	75%
Y55B1BR.2		unnamed protein	III	7.5 ± 3.6	20	50%	50%	50%	50%	n.d.	
R07H5.4	*sdz-27*	SKN-1 Dependent Zygotic transcript)	IV	12.0 ± 3.5	36	25%	75%	25%	75%	n.d.	
F49F1.5		Secreted surface protein	IV	11.4 ± 3.4	36	25%	75%	50%	50%	n.d.	
F21E9.3		Uncharacterized protein with conserved cysteine	X	11.8 ± 4.2	36	50%	50%	50%	50%	n.d.	

Supplementary Table S2. Recruitment of DYN-1 around apoptotic germ cell corpses requires corpse internalization

Genotype	Refractile Corpses (DIC)	DYN-1::YFP Halos	*n*
wild type	2.7 ± 1.2	-	10
unc-119(ed3)	2.3 ± 1.1	-	10
dyn-1(ky51)	3.1 ± 1.6	-	15
opIs220 [P_{eft-3}::dyn-1::yfp]; dyn-1(ky51)	3.1 ± 1.2	-	15
wild type 25°C	3.4 ± 1.4	-	15
dyn-1(ky51) 25°C	15.9 ± 5.1	-	15
opIs220 [P_{eft-3}::dyn-1::yfp]; dyn-1(ky51) 25°C	3.9 ± 1.0	-	15
unc-119(ed3); opIs220 [P_{eft-3}::dyn-1::yfp]	3.1 ± 1.7	1.8 ± 1.1	22
ced-3(RNAi)	0	-	10
ced-3(RNAi); opIs220 [P_{eft-3}::dyn-1::yfp]	0	0	10
gla-3(op216)	7.2 ± 2.1	-	12
gla-3(op216); opIs220 [P_{eft-3}::dyn-1::yfp]	8.4 ± 2.3	2.8 ± 1.9	17
ced-1(e1735)	17.3 ± 2.7	-	15
ced-1(e1735); opIs220 [P_{eft-3}::dyn-1::yfp]	16.8 ± 2.1	0.1 ± 0.2	21
ced-6(n1813)	17.9 ± 3.3	-	15
ced-6(n1813); opIs220 [P_{eft-3}::dyn-1::yfp]	17.7 ± 3.1	0.3 ± 0.7	20
ced-7(n1996)	16.3 ± 2.3	-	13
ced-7(n1996); opIs220 [P_{eft-3}::dyn-1::yfp]	14.4 ± 2.7	0.2 ± 0.5	23
ced-2(n1994)	11.8 ± 3.5	-	20
ced-2(n1994); opIs220 [P_{eft-3}::dyn-1::yfp]	12.6 ± 4.0	0.2 ± 0.5	20
ced-5(n1812)	14.2 ± 3.0	-	15
ced-5(n1812); opIs220 [P_{eft-3}::dyn-1::yfp]	13.8 ± 2.0	0.1 ± 0.3	20
ced-12(k149)	13.0 ± 2.7	-	15
ced-12(k143); opIs220 [P_{eft-3}::dyn-1::yfp]	12.2 ± 2.6	0.2 ± 0.4	21
ced-10(n3246)	24.9 ± 4.3	-	15
ced-10(n3246); opIs220 [P_{eft-3}::dyn-1::yfp]	22.7 ± 3.9	0.5 ± 0.8	22

Worms were staged and corpses scored as described in Methods. *n,* number of worms scored. *unc-119(+)* is used as marker for transgenics. *ced-3* is the nematode caspase homologue, cell death does not occur in the gonad in *ced-3* deficient worms. Data shown are average ± s.d.

Supplementary Table S3a. Corpses are efficiently recognized and internalized in *dyn-1(ky51)* mutant worms

Genotype	Refractile Corpses (DIC)	CED-1::GFP Halos	*n*
bcIs39[P_{lim-7}::ced-1::gfp]	3.4 ± 1.9	4.1 ± 1.1	14
bcIs39[P_{lim-7}::ced-1::gfp]; dyn-1(ky51)	2.3 ± 0.9	2.9 ± 1.1	14
bcIs39[P_{lim-7}::ced-1::gfp] 25°C	4.6 ± 2.0	4.5 ± 2.5	23
bcIs39[P_{lim-7}::ced-1::gfp]; dyn-1(ky51) 25°C	12.1 ± 3.3	5.5 ± 2.0	14
	Refractile Corpses (DIC)	**YFP::Actin Halos**	
unc-119(ed3); opIs110 [P_{lim-7}::yfp::act-5]	3.9 ± 1.1	2.2 ± 1.1	14
opIs110[P_{lim-7}::yfp::act-5]; dyn-1(ky51)	4.5 ± 1.4	2.0 ± 1.2	14
ced-1(e1735); opIs110 [P_{lim-7}::yfp::act-5]	19.1 ± 5.0	0	15
unc-119(ed3); opIs110 [P_{lim-7}::yfp::act-5] 25°C	4.3 ± 2.2	3.2 ± 1.7	26
opIs110[P_{lim-7}::yfp::act-5]; dyn-1(ky51) 25°C	12.0 ± 4.9	2.9 ± 1.9	26
	Refractile Corpses (DIC)	**YFP::CED-6 Halos**	
unc-119(ed3); opIs160 [P_{ced-6}::yfp::ced-6]	3.0 ± 1.1	2.4 ± 0.8	13
opIs160 [P_{ced-6}::yfp::ced-6]; dyn-1(ky51)	3.1 ± 1.2	2.1 ± 1.0	23
unc-119(ed3); opIs160 [P_{ced-6}::yfp::ced-6] 25°C	3.6 ± 1.7	3.0 ± 1.8	13
opIs160 [P_{ced-6}::yfp::ced-6]; dyn-1(ky51) 25°C	12.9 ± 2.5	6.8 ± 1.9	23

Table S3b. Phagosome closure appears normal in *dyn-1(ky51)* mutant worms

Genotype	Refractile Corpses (DIC)	CED-1::GFP Halos	*n*
bcIs39[P_{lim-7}::ced-1::gfp] 25°C	2.2 ± 1.4	1.6 ± 1.4	13
bcIs39[P_{lim-7}::ced-1::gfp]; dyn-1(ky51) 25°C	2.6 ± 1.9	1.4 ± 1.2	14

Worms were staged and corpse scored as described in Methods. Scores shown in S3b represent average corpses in the medial plane of the gonad to monitor closure of the phagocytic cup. Data shown are average ± s.d.

Supplementary Table S4. Genes required for fluid-phase endocytosis do not accumulate refractile cell corpses.

Genotype	Refractile Corpses (DIC)	*n*
wild type	2.7 ± 1.2	10
rme-1(b1045)	2.2 ± 1.3	12
rme-2(b1008)	3.2 ± 0.9	13
rme-6(1014)	2.4 ± 1.5	13

To rule out an effect of decreased fluid-phase endocytosis in our assays (due to a role of DYN-1 in this process), we tested worms deficient for RME-1/Testin, RME-2/LRP2, and RME-6/Rabex-5, a Guanine Nucleotide Exchange Factor (GEF) for RAB-5. Number of refractile cell corpses was counted in the 12-hour adult hermaphrodite gonad. *n*, number of worms scored. Error represents s.d.

CHAPTER 3

A NOVEL PATHWAY FOR PHAGOSOME MATURATION DURING ENGULFMENT OF APOPTOTIC CELLS

3.3 ADDITIONAL RESULTS

As I mentioned in Chapter 1, classical dynamins, such as DYN-1 and mammalian dynamins 1, 2 and 3, are characterized by the presence of the five following domains: a GTPase domain at the N-terminus which hydrolyses GTP and promotes conformational changes, a middle domain important for oligomerisation, a Pleckstrin Homology (PH) domain mediating binding to phosphoinositides, a GTPase Effector Domain (GED), believed to control the GTP hydrolysis activity, and a C-terminal Proline Rich Domain (PRD) which ensures the binding of effector proteins via their Src Homology 3 (SH3) regions. It is believed that these interactions recruit dynamin to its multiple sites of action in the cell, and, as a result, they are considered to play a very important role in regulating dynamin function.

In order to better understand the mode of action of DYN-1 in apoptotic cell corpse engulfment I performed an additional candidate-based screen using the RNAi methodology. For this, I focused on proteins that could potentially interact with the PRD domain of DYN-1. I first used bioinformatics, with the help of Sergio Pinto, to select all the *C. elegans* genes encoding SH3-containing proteins and found that 62 genes are predicted to code for factors containing such domains (Table 3.1). All the corresponding clones were picked from the RNAi library and sequenced to ensure fidelity. Forty-three clones were found to be correct, while the remaining 19 contained wrong or no inserts or they were not present at all in the Ahringer library. After 2 weeks of intensive cloning I managed to construct 15 of the missing RNAi clones.

To identify potential interaction partners of DYN-1 in the context of cell corpse clearance I performed RNAi against the 58 aforementioned genes. Similar to chapter 2, I utilized the *gla-3* background and chose to assess the suppression of AO staining of germ cell corpses as a criterion for an engulfment defect. RNAi against

only one out of 58 genes I tested, namely *lst-4* (lateral signaling target-4), was found to suppress AO staining and give rise to a very strong persistent cell corpse phenotype in the *C. elegans* germ line (Figure 3.1). *lst-4* encodes a protein homologous to sorting nexins, a diverse group of cellular trafficking proteins that have in common the presence of a specific phospholipid-binding motif, the PhoX (PX) domain. Briefly, these proteins bind to specific phospholipids and play key roles in membrane trafficking and protein sorting (for review see Worby and Dixon, 2002).

LST-4 is homologous to human SH3PX1, also known as SNX9. Although predominantly cytoplasmic, SNX9 has been found to interact with proteins associated with clathrin-coated pits such as the Cdc42-associated tyrosine kinase 2 (ACK2). Importantly, in the context of endocytosis, SNX9 has also been shown to directly bind to and regulate the activity of mammalian dynamins 1 and 2 (Soulet et al., 2005), suggesting that LST-4 might act in a similar way to regulate the function of DYN-1 in *C. elegans*. Importantly, additional studies have demonstrated that SNX9 can also interact with members of the Wiskott-Aldrich syndrome protein family (WASP) (Worby and Dixon, 2002), which are thought to link sites of actin polymerization with components of signal transduction pathways leading to membrane movements or the formation of vesicles. This suggests that SNX9 might function to link the endocytic pathways with the cellular machinery driving polymerization of actin. By analogy, LST-4 might be the factor recruiting dynamin to the pseudopods and coordinating membrane extension with the entry of the newly formed phagosome in the degradative pathway during apoptotic cell clearence. If this is the case then studies of LST-4/SNX9 could allow us to mechanistically link the processes of membrane remodeling and early phagosome formation. Further, they would be an important first step in understanding the feedback mechanisms that abrogate corpse internalization when the, already internalized corpses, cannot be degraded.

3.4 REFFERENCES

Soulet, F., Yarar, D., Leonard, M., and Schmid, S. L. (2005). SNX9 regulates dynamin assembly and is required for efficient clathrin-mediated endocytosis. Mol Biol Cell *16*, 2058-2067.

Worby, C. A., and Dixon, J. E. (2002). Sorting out the cellular functions of sorting nexins. Nat Rev Mol Cell Biol *3*, 919-931.

Table 3.1 *C. elegans* SH3 domain-containing proteins

Gene Model	Locus	RNAi ID	Description (wormbase)	Sequencing
W10C8.1	*ccb-2*	#002F09	L-type voltage-dependent Ca2+ channel, beta subunit	ok
Y44E3A.4	-	#003A03	adaptor protein CMS/SETA	ok
T28F2.5	*ccb-1*	#003B11	beta subunits of dihydropyridine sensitive L-type calcium channels	ok
C50F2.8	-	#003G07	calcium/calmodulin-dependent serine protein kinase/membrane-associated guanylate kinase	ok
F55C7.7	*unc-73*	#004A08	encodes a guanine nucleotide exchange factor (GNEF) similar to the Trio protein	ok
C09D1.1	*unc-89*	#004A11	encodes several protein isoforms variably characterized by the presence or absence of SH3, DH, PH, immunoglobulin and myosin light chain kinase (MLCK)-like protein kinase domains	ok
C34G6.7	*pqn-19*	#008A07	signal transducing adaptor protein STAM/STAM2	ok
C26C6.8	-	#012A02	uncharacterized	ok
F29D10.4	*hum-1*	#014F09	class I unconventional myosin heavy chain	ok
Y106G6H.14	-	#018A10	osteoclast stimulating factor and similar proteins	ok
ZK1151.1	*vab-10*	#020F09	encodes, by alternative splicing, two spectraplakins (VAB-10A and VAB-10B)	ok
F49B2.5	*src-2*	#025G05	protein tyrosine kinase	ok
Y47G6A.5	-	#027G11	protein tyrosine kinase	ok
K07D4.7	*tag-218*	#041F08	putative guanine nucleotide exchange factor TIM, ephexin	ok
M28.7	*nph-1*	#056H01	encodes a novel, SH3 domain-containing protein that is orthologous to mammalian nephrocystin-1	ok
C36E8.4	-	#070A07	uncharacterized conserved protein, contains SH3 and FCH domains	ok
T04C9.1	-	#074F09	orthologous to the human gene GRAF PROTEIN, Oligophrenin-1 and related Rho GTPase-activating proteins	ok
K08E3.3	*toca-2*	#089D03	Cdc42-interacting protein CIP4	ok
K08E3.4	-	#089D04	drebrins and related actin binding proteins	ok
Y55B1BR.4	-	#091D01	calcium/calmodulin-dependent serine protein kinase/membrane-associated guanylate kinase	ok
F58G6.1	-	#108A06	amphiphysin	ok
C02F4.1	*ced-5*	#110C06	homolog of the human protein DOCK180	ok
Y37A1B.15	*gei-18*	#117F11	GEX interacting protein	ok
Y116A8C.36	*itsn-1*	#120E12	encodes a homolog of human NCF1, Intersectin	ok
K11D12.10	*mlk-1*	#137C01	tyrosine kinase specific for activated (GTP-bound) p21cdc42Hs	ok
C01B7.4	*tag-117*	#146B05	calcium/calmodulin-dependent serine protein kinase/membrane-associated guanylate kinase	ok
F46F3.4	*ape-1*	#152G02	encodes an ortholog of inhibitory p53-interacting protein (iASPP)	ok
C46H3.2	-	#177D07	uncharacterized SAM domain protein, Caskin	ok
K10B3.10	*spc-1*	#180E07	encodes the *C. elegans* alpha spectrin ortholog, Ca2+-binding actin-bundling protein (spectrin), alpha chain (EF-Hand protein superfamily)	ok
F35A5.8	*erp-1*	#181G07	homologous to the human gene endophilin B1 (also called SH3GLB1, for SH3 domain GRB2-like endophilin B1)	ok
ZK470.5	*tag-22*	#182C02	encodes a protein with similarity to the human NCK adaptor protein 2	ok
F45E1.7	*sdpn-1*	#188E05	synaptic dynamin binding protein, adaptor protein PACSIN	ok
F41D9.1	-	#189C03	uncharacterized conserved protein, contains TBC, SH3 and RUN domains	ok
C35B8.2	*vav-1*	#190F04	encodes an ortholog of the Vav proto-oncogene, a complex protein with several domains, from N- to C-terminus: a calponin-like actin-binding domain; a RhoGEF/DH domain; a pleckstrin-like domain; a SH2 motif domain; and an SH3 domain	ok
F49E2.2	-	#191B01	uncharacterized protein	ok
F47A4.3	-	#191D10	predicted Rho GTPase-activating protein CdGAPr	ok
M79.1	*abl-1*	#192F12	encodes, by alternative splicing, three isoforms of a Src homology (SH) 2 and 3 domain-containing non-receptor tyrosine kinase orthologous to human ABL1	ok
F17E5.1	*lin-2*	#195G05	encodes a protein belonging to the membrane associated guanylate kinase (MAGUK) family, with several domains (L27, PDZ, SH3, and guanylate kinase) thought to assemble specific multiprotein complexes in particular regions of the cell	ok
F32A5.6	*prx-13*	#049B9	orthologous to the human gene PEX13, a peroxin involved in peroxisome biogenesis	ok
T01E8.3	*plc-3*	#055H8	Phospholipase C	ok
B0336.6	-	#074A11	Abl interactor ortholog, mammalian Abl interactors are associated with synaptosomes, growth cone particles, and macropinocytic vesicles, and may regulate Rac-dependent cytoskeletal reorganization and Abl kinase activity	ok
Y57G11C.24	*eps-8*	#118F3	predicted to encode five protein isoforms with similarity to mouse epidermal growth factor receptor kinase substrate that affects embryonic viability, growth, locomotion, osmoregulation, and larval viability; interacts with GEX-3 in yeast two-hybrid assays	ok
R31.1	*sma-1*	#153B5	encodes a beta-H spectrin	ok
F42H10.3	-	#080B09	Nebulin repeat protein , similar to LASP-1	ok but cross-reactivity
Y41D4B.13	*ced-2*	#122B08	encodes a Src homology (SH) 2 and 3-containing adaptor protein, homologous to human CrkII	cloned
F09E10.8	*toca-1*	#178A05	Cdc42-interacting protein CIP4	cloned
Y37A1B.2	*lst-4*	#117E11	sorting nexin SNX9/SH3PX1 and related proteins	cloned
C14F5.5	*sem-5*	#188D10	encodes a Src homology (SH) domain 2 and 3-containing protein, orthologous to human GRB2	cloned
Y39A3CL.2	*tag-168*	#90E12	peripheral benzodiazepine receptor PRAX-1	not cloned
Y20F4.3	-	not found	uncharacterized	not cloned
Y48G1C.2	*csk-1*	not found	encodes an ortholog of C-terminal Src kinase (Csk)	cloned
C01C7.1	*ark-1*	#115A1	encodes a homolog of the nonreceptor tyrosine kinase ACK which inhibits signalling through the EGF receptor homolog LET-23	cloned
Y92H12A.1	*src-1*	not found	protein tyrosine kinase	not cloned
C10F3.6	*fut-8*	#139B10	encodes a core alpha 1,6-fucosyltransferase	cloned
C25F6.2	*dlg-1*	#184D1	encodes a MAGUK protein, orthologous to Drosophila disks large	cloned
K11E4.4	*tag-207*	#197H6	PAK Guanine nucleotide exchange factor	cloned
B0302.1	*kin-25*	#202H8	encodes a nonreceptor tyrosine kinase that is a member of the Ack subfamily of cytoplasmic tyrosine kinases	cloned
T04D1.3	*unc-57*	#5C11	encodes an ortholog of endophilin A that is required for synaptic vesicle endocytosis	cloned
B0303.7	-	#80F7	sorbin and SH3 domain-containing protein	cloned
Y66H1A.2	-	#92F7	Dolichol-phosphate mannosyltransferase	cloned
Y45F10D.13	*tag-208*	#117D5	uncharacterized	cloned
F19C7.8	-	#97E8	uncharacterized protein	cloned

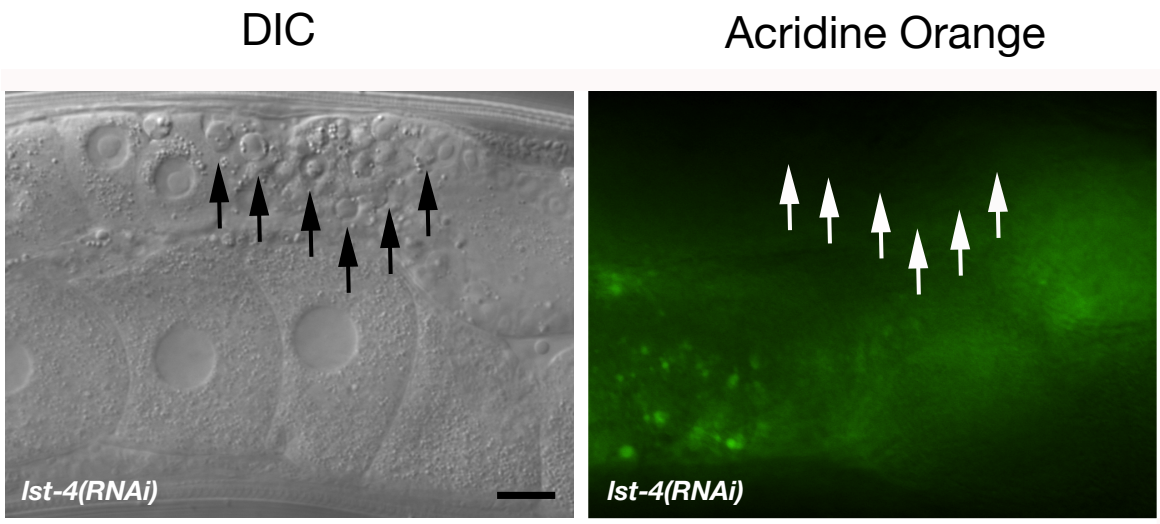

FIGURE 3.1 RNAi against *lst-4* results in a strong engulfment defect in the *C. elegans* germ line

DIC and fluorescence pictures of wild type worms treated with RNAi against *lst-4*, 24h post L4/adult molt. Arrows indicate regions where apoptotic cells accumulate. Note the lack of Acridine Orange staining of germ cell corpses. Scalebar is 10μm.

CHAPTER 4

C. ELEGANS GLA-3 IS A NOVEL COMPONENT OF THE MAP KINASE MPK-1 SIGNALING PATHWAY REQUIRED FOR GERM CELL SURVIVAL

CHAPTER 4

C. ELEGANS GLA-3 IS A NOVEL COMPONENT OF THE MAP KINASE MPK-1 SIGNALING PATHWAY REQUIRED FOR GERM CELL SURVIVAL

4.1 PREFACE

This chapter deals with the identification and characterization of *gla-3*, one the first mutants identified to affect programmed cell death in the *C. elegans* germ line. This work was initiated by Dr S. Milstein several years ago while we was still a graduate student at Cold Spring Harbor Laboratory. He performed the first genetic screen for mutants with increased germ line apoptosis, cloned *gla-1* and *gla-3,* and initiated the genetic characterization of these mutants. The project was then taken over by Dr. Ekaterini Kritikou a post-doctoral fellow in Zurich who pursued the genetic characterization of *gla-3* and established the link with the MAP kinase pathway.

Whereas at the beginning of my Ph.D. I spent some time working on *gla-3*, my contribution to this study is limited to Figure S1. Although a supplementary figure, it helped convincing the reviewers that the increased levels of corpses in *gla-3* mutants were due to increased apoptosis and not to a defect in cell corpse removal.

This study nicely demonstrates that GLA-3 is a novel component of MPK-1 signaling and, as a result, reinforces the hypothesis that germ cell death is tightly linked to the Ras/MAP kinase pathway. It fails, however, to precisely address how *gla-3* regulates apoptosis in the *C. elegans* germ line, despite the fact that this is one of the major mutants known to affect this process. Further studies are needed to elucidate the mechanisms controlling germ cell apoptosis as these continue to remain a mystery.

C. elegans GLA-3 is a novel component of the MAP kinase MPK-1 signaling pathway required for germ cell survival

Ekaterini A. Kritikou,[1,5] Stuart Milstein,[3,5] Pierre-Olivier Vidalain,[3,6] Guillaume Lettre,[1] Erica Bogan,[1,2] Kimon Doukoumetzidis,[1,2] Phillip Gray,[4] Thomas G. Chappell,[4] Marc Vidal,[3] and Michael O. Hengartner[1,7]

[1]Institute of Molecular Biology, University of Zurich, 8057 Zurich, Switzerland; [2]Ph.D. Program in Molecular Life Sciences, University of Zurich, 8057 Zurich, Switzerland; [3]Center for Cancer Systems Biology (CCSB) and Department of Cancer Biology, Dana Farber Cancer Institute and Department of Genetics, Harvard Medical School, Boston, Massachusetts 02115, USA; [4]Invitrogen Corporation, Carlsbad, California 92008, USA

During oocyte development in *Caenorhabditis elegans*, approximately half of all developing germ cells undergo apoptosis. While this process is evolutionarily conserved from worms to humans, the regulators of germ cell death are still largely unknown. In a genetic screen for novel genes involved in germline apoptosis in *Caenorhabditis elegans*, we identified and cloned *gla-3*. Loss of *gla-3* function results in increased germline apoptosis and reduced brood size due to defective pachytene exit from meiosis I. *gla-3* encodes a TIS11-like zinc-finger-containing protein that is expressed in the germline, from the L4 larval stage to adulthood. Biochemical evidence and genetic epistasis analysis revealed that GLA-3 participates in the MAPK signaling cascade and directly interacts with the *C. elegans* MAPK MPK-1, an essential meiotic regulator. Our results show that GLA-3 is a new component of the MAPK cascade that controls meiotic progression and apoptosis in the *C. elegans* germline and functions as a negative regulator of the MAPK signaling pathway during vulval development and in muscle cells.

[*Keywords*: Apoptosis; GLA-3; MAPK signaling; germline development; *C. elegans*]

Supplemental material is available at http://www.genesdev.org.

Received February 24, 2006; revised version accepted June 1, 2006.

Germ stem cells are the precursors to all subsequent generations in a species, and, therefore, germ cell formation is tightly monitored to ensure high-fidelity transfer of the genetic material. Germ cell genome integrity is monitored at several checkpoints, allowing for DNA repair, cell cycle arrest, and apoptosis when required. In mammals, inactivation of genes with checkpoint function frequently results in aberrant cell death and infertility (Lim and Hasty 1996; Bender et al. 2002). Germ cell development is also characterized by either massive waves or low but constant levels of apoptosis that are not caused by genetic defects. For example, >99.9% of oocytes undergo apoptosis in response to hormonal changes that occur at several stages during the female life cycle in mammals (Tilly 2001; Kim and Tilly 2004). Apoptosis is also the fate of ~50% of germ cells undergoing oogenesis in the gonad of *Caenorhabditis elegans* hermaphrodites. (Gumienny et al. 1999). Characterization of the pathways that regulate germ cell death will contribute to our understanding of the cell suicide decision and might allow for more efficient therapeutic manipulation of the apoptotic program.

C. elegans is a good model to study the signaling cascades involved in the decision between germ cell survival and germ cell death (Hengartner 1997; Gumienny et al. 1999). The adult hermaphrodite gonads consist of two U-shaped tubes that are connected at a common uterus. At the distal end of each gonad, mitotic germ stem cells proliferate in response to the Notch ligand LAG-2. Cells beyond the influence of LAG-2 enter meiosis and progress through the pachytene stage of meiosis I; this transition requires activation of the RAS/MAPK (MAP kinase) signaling cascade (Hubbard and Greenstein 2000; Seydoux and Schedl 2001). Following transition through pachytene, germ cells can either enter diakinesis of meiosis I and differentiate into oocytes or undergo apoptosis. We previously suggested that these cell deaths are the result of a physiological, homeostatic control mechanism that limits the number of germ cells permitted to differentiate into oocytes (Gumienny et al. 1999).

[5]These authors contributed equally to this work.
[6]Present address: Laboratoire génomique virale et vaccination, CNRS UMR1930, Institut Pasteur de Paris, 28 Rue du Docteur Roux, Paris, 75724 Cedex 15, France.
[7]Corresponding author.
E-MAIL michael.hengartner@molbio.unizh.ch; FAX 41-44-635-6861.
Article is online at http://www.genesdev.org/cgi/doi/10.1101/gad.384506.

During *C. elegans* somatic development, apoptosis is triggered when the pro-apoptotic BH3-domain-containing protein EGL-1 interacts with the BCL-2 family member CED-9 on the surface of mitochondria. Binding of EGL-1 induces CED-9 to release the sequestered Apaf-1 homolog CED-4, resulting in the formation of a *C. elegans* apoptosome and activation of the caspase CED-3 (Chen et al. 2000; Yan et al. 2004, 2005; for review, see Lettre and Hengartner 2006). We previously showed that germline apoptosis can be induced by both p53-dependent and p53-independent pathways (Lettre et al. 2004). However, whereas DNA damage-induced germline apoptosis depends on the activation of EGL-1, physiological germline apoptosis occurs normally in the absence of EGL-1, indicating that additional regulatory factors are required to trigger the apoptotic cascade in these cells (Gumienny et al. 1999; Gartner et al. 2000).

In an attempt to identify genes that regulate physiological germ cell apoptosis, we performed a forward genetic screen to isolate mutants with increased levels of germline apoptosis. In this paper, we report the cloning and characterization of *gla-3* (germline apoptosis), a gene that encodes a predicted RNA-binding protein of the TIS11 family. Loss of *gla-3* function results in increased germ cell apoptosis and severe defects in oocyte differentiation, which lead to reduced brood size. Biochemical analysis revealed that GLA-3 physically interacts with the *C. elegans* MAPK MPK-1, providing a direct link between the apoptotic process and oogenesis. Furthermore, we show that GLA-3 functions as an inhibitor of the MAPK cascade during vulva formation and in muscle cells. Our findings indicate that GLA-3 is a new component of the MAPK signaling cascade and highlight a molecular link between germ cell survival and pachytene progression in the *C. elegans* germline.

Results

Loss of gla-3 *function results in increased germ cell death*

To identify novel genes involved in the regulation of germ-cell apoptosis, we performed a forward genetic screen to isolate mutations that result in increased germline apoptosis, as described in Materials and Methods. *gla-3* was selected for cloning and further characterization based on the severity of its germline apoptosis phenotype. All three *gla-3* alleles that we analyzed (*op212* and *op216*, isolated in our screen, and *ep312*, generously provided by M. Costa, Exelixis) resulted in increased numbers of germ cell corpses that displayed typical apoptotic morphology (Fig. 1A,B). Because *gla-3* mutants exhibited normal patterns of somatic cell death (data not shown), we conclude that *gla-3* is not a general cell-death regulator.

To investigate whether loss of *gla-3* function results in increased germ cell apoptosis rather than decreased engulfment, we analyzed *gla-3* mutants carrying the integrated transgene *opIs110*, which expresses a YFP-tagged version of cytosolic actin. We previously showed that this YFP::ACT-5 reporter is highly enriched around apoptotic germ cells that are in the process of being engulfed (Kinchen et al. 2005). Whereas inactivation of the engulfment gene *ced-1* largely abolished YFP::actin staining, most apoptotic germ cells in *gla-3(lf); opIs110* (lf, loss of function) animals were surrounded by a YFP::actin halo, indicating that the cells were being engulfed efficiently (Supplemental Fig. 1). These results support our notion that loss of *gla-3* function results in increased germ cell death, rather than decreased cell corpse clearance.

To determine an epistatic relationship between *gla-3* and other components of the apoptotic machinery, we generated strains that contain *gla-3(op212)* and either of the strong loss-of-function mutations *ced-4(n1162)* or *ced-3(n717)*. In both double mutants, germ cell death was completely abrogated, demonstrating that *gla-3(lf)*-induced cell death is apoptotic in nature and that the components of the apoptotic machinery function downstream of *gla-3* (Fig. 1C).

Because germline apoptosis can be mediated by both DNA damage-dependent and -independent mechanisms (Gartner et al. 2000), we carried out epistasis analysis between *gla-3(op212)* and genes that are known to be involved in DNA damage responses. *hus-1(op244)* and *clk-2(mn159*ts*)* mutants are characterized by a complete absence of DNA damage-induced apoptosis, but have nearly normal levels of somatic and germline apoptosis (Ahmed et al. 2001; Hofmann et al. 2002). *gla-3(op212); clk-2(mn159*ts*)* and *hus-1(op244) gla-3(op212)* worms had similar levels of germline apoptosis as *gla-3(op212)* alone, indicating that *gla-3*-induced apoptosis occurs independently of these DNA damage checkpoint genes (Fig. 1D). Because DNA damage-induced apoptosis is dependent on the p53 homolog *cep-1* (Derry et al. 2001; Schumacher et al. 2001), we inactivated *gla-3* using RNA-mediated interference (RNAi) in *cep-1(gk138)* mutants. Consistent with our previous findings (Lettre et al. 2004), we observed similar levels of germline apoptosis in *gla-3(RNAi) cep-1(gk138)* and in *gla-3(RNAi)* alone (Fig. 1E), showing that loss of *gla-3* does not activate a DNA damage apoptotic response.

Finally, we tested the ability of *gla-3* mutants to respond to exogenous DNA damage. We previously showed that ionizing radiation induces apoptosis of meiotic cells and transient cell cycle arrest of the mitotic germ cell population (Gartner et al. 2000). Both apoptosis and cell cycle responses appeared normal in *gla-3(op212)* mutants (Fig. 1D; Supplemental Fig. 2, respectively). These data suggest that the DNA damage response pathways are functional in *gla-3* mutants, and are consistent with a role of *gla-3* in the physiological cell-death pathway.

Identification of mutations in the C. elegans gla-3 *gene*

We genetically mapped *gla-3(op212)* to a 0.36-cM interval, on the right arm of Chromosome I, between the single nucleotide polymorphism markers *pk1058* at 2.31 cM and *opP106* at 2.67 cM, as described in Materials and Methods. We inactivated the 40 genes predicted to reside between these two markers using RNAi, in the hope that knockdown of the relevant gene would phenocopy *gla-*

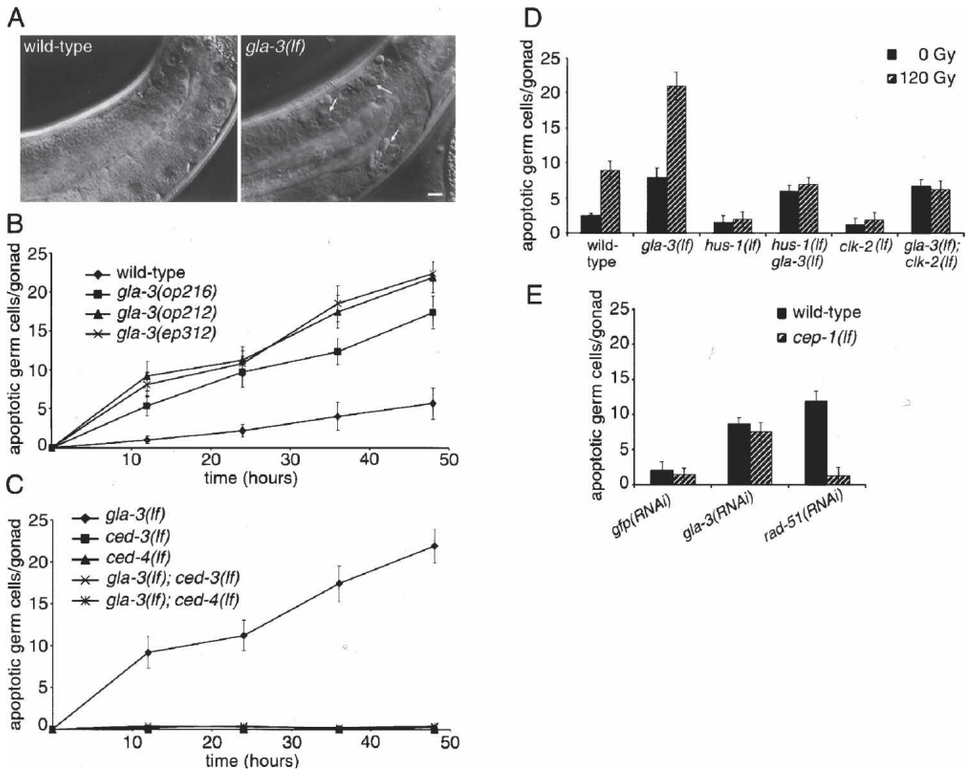

Figure 1. Loss of *gla-3* function results in increased germ cell apoptosis. (*A*) DIC image of wild-type and *gla-3(op212)* adult hermaphrodite gonads. *gla-3(op212)* mutants exhibit an increased number of germ cell corpses (arrows). Anterior is to the *left* and dorsal to the *top*. Scale bar, 8 µm. (*B*) Wild-type and *gla-3(lf)* mutant worms raised at 25°C were synchronized, and germ cell corpses were counted starting at the L4 stage. (*C*) *gla-3(op212)*-induced germ cell death is abrogated in *ced-4(n1162)* and *ced-3(n717)* mutants. (*D*) Mutations in DNA damage checkpoint genes do not abrogate *gla-3(op212)*-induced apoptosis. Synchronized adults (12 h post-L4/adult molt) were irradiated with 120 Gy, and germ cell corpses were counted 24 h later. The following alleles were used: *gla-3(op212)*, *hus-1(op244)*, and *clk-2(mn159*ts*)*. (*E*) *gla-3(RNAi)*-induced apoptosis is not blocked in *cep-1(gk138)* mutants. RNAi-mediated knockdown of the RecA homolog *rad-51*, which results in the accumulation of meiotic intermediates and induces CEP-1-dependent apoptosis (Lettre et al. 2004), was used as a positive control. In panels *B–E*, error bars represent SD from three independent experiments; 20 gonads were scored in each experiment.

3(op212). A single gene, T02E1.3, which encodes two splice variants, gave rise to increased germline apoptosis when inactivated by RNAi. We sequenced T02E1.3 from wild-type, *op212*, and *op216* animals and found a C-to-T transition at position 471 in T02E1.3a (position 574 in T02E1.3b) in *op212*, resulting in a premature stop codon (Fig. 2A), whereas *op216* mutants contain a G-to-A transition in the acceptor splice site of the first intron of T02E1.3a (Fig. 2A). The third allele of *gla-3*, *ep312*, was generated in an independent screen for mutants with increased germline apoptosis in a *cep-1(lf)* mutant background (M. Costa, pers. comm.). *ep312* results in a 265-bp deletion that removes part of the last two exons of *gla-3* and introduces a frameshift at the new junction (Fig. 2A). Based on the strength of its phenotype and the molecular nature of the mutation, we believe *op212* to be a null allele of *gla-3*.

gla-3 *encodes a TIS11-like zinc finger domain protein*

gla-3 encodes a protein that contains two CCCH-like zinc-finger domains (Fig. 2B). This domain is found in a subset of zinc-finger family proteins; its consensus sequence corresponds to C-X_{8-10}-C-X_5-C-X_3-H, where X refers to any amino acid (Varnum et al. 1989). CCCH zinc fingers were first described in the mouse TIS11 protein, where they are responsible for nucleic-acid binding (Varnum et al. 1989; DuBois et al. 1990; Bai and Tolias 1996). Mammalian TIS11-like zinc-finger-containing proteins have been shown to function either as transcription factors or RNA-binding proteins (Taylor et al. 1996; Worthington et al. 2002). Several *C. elegans* genes encoding proteins with TIS11-like zinc-finger domains have been described, including *pie-1*, *mex-1*, *pos-1*, *mex-5*, and *mex-6*, all of which are involved in early blastomere cell-fate determination and germline development (Mello et al. 1996; Guedes and Priess 1997; Tabara et al. 1999; Schubert et al. 2000). In addition, the recently identified TIS11-like proteins OMA-1, OMA-2, and OMA-3 are redundantly required for prophase progression during oocyte maturation (Detwiler et al. 2001; Shimada et al. 2002). GLA-3 is highly similar to these proteins in the CCCH zinc-finger domain (Fig. 2B), but bears no signifi-

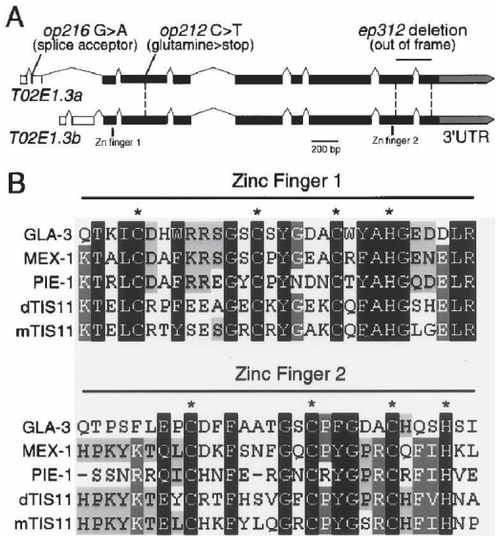

Figure 2. GLA-3 encodes a TIS11-like zinc-finger-containing protein. (*A*) Schematic representation of *gla-3* genomic structure. *T02E1.3* is predicted to have two alternatively spliced forms, which differ in their first two exons. Black boxes indicate exons that are common between *T02E1.3a* and *T02E1.3b;* the gray arrow indicates the 3′-untranslated part of the last exon. White boxes represent alternative 5′-exons that are not shared between the two isoforms. Positions of the *gla-3(op212)*, *gla-3(op216)*, and *gla-3(ep312)* lesions are indicated. Size bar, 200 bp. (*B*) Alignment of the two zinc-finger domains of *C. elegans* GLA-3, MEX-1, PIE-1, *Drosophila melanogaster* dTIS11, and mouse mTIS11. Conserved residues are highlighted in black, dark gray, or light gray, depending on whether five out of five, four out of five, or three out of five proteins possess an identical or similar amino acid at this position. Amino acids that coordinate the zinc atom are marked with asterisks.

cant sequence similarity to other characterized proteins outside of the zinc fingers. Unlike most of the characterized CCCH-zinc-finger-containing proteins in *C. elegans*, the zinc-finger domains in GLA-3 are situated at the two ends of the protein, ~400 amino acids apart.

gla-3 *is expressed in the germline*

We probed a developmental Northern blot from wild-type animals with a probe hybridizing to both *gla-3* transcripts. We found *gla-3* to be expressed in embryos, L4-stage larvae, and adults (Fig. 3A), with the highest expression being in L4 larvae. The predominant developmental difference between an L4 larva and an adult hermaphrodite is the expansion of the germline. To examine the expression of *gla-3* in the adult hermaphrodite germline, we prepared RNA from three temperature-sensitive mutants, defective in various aspects of germline development. At the nonpermissive temperature, *glp-4(bn2*ts*)* mutants produce a somatic gonad that is largely devoid of germ cells (Beanan and Strome 1992), *fem-2(e2105*ts*)* mutants make oocytes but no sperm, and *fem-3(q20*sd*)* mutants make sperm but no oocytes (Barton et al. 1987). We detected *gla-3* expression in all three mutant backgrounds, demonstrating that *gla-3* is expressed in both germline and soma (Fig. 3B). Very low levels of mRNA were observed in *gla-3(op212)* mutants, consistent with the finding that this mutation causes a premature stop, which often results in rapid elimination of the mutant transcript via nonsense-mediated decay (Weischenfeldt et al. 2005).

To investigate the expression pattern of GLA-3 in vivo, we generated strains carrying a GFP reporter driven by the *gla-3* promoter. A 1.5-kb genomic fragment upstream of the *T02E1.3a* ATG was fused to a fragment coding for nuclear localized GFP, and transgenic animals were generated by biolistic transformation (Praitis et al. 2001). GFP expression was observed throughout the germline from the L4 stage onward and in all cells of the early embryo (Fig. 3C), consistent with the *gla-3* mRNA pattern in the developmental Northern blot (Fig. 3A). Interestingly, expression was also observed in muscle cells in threefold stage embryos (Fig. 3C, panel c).

To further investigate temporal and spatial *gla-3* expression, we raised specific polyclonal antibodies against peptides derived from the unique N termini of GLA-3A (T02E1.3a) and GLA-3B (T02E1.3b). Western blot analysis of synchronized wild-type worms revealed that both isoforms are expressed at the L4 and adult stages, whereas no expression was detectable from the L1 to L3 stages, nor in *gla-3(op212)* mutants (Fig. 3D). To examine the expression pattern of GLA-3 in the germline, we investigated the localization of the GLA-3 protein by in situ immunostaining. Consistent with the mRNA expression pattern, GLA-3B was detectable in L4 and adult gonads. The protein was expressed in the mitotic and meiotic zones of the adult germline, and localized to the cytoplasmic compartment, with an enrichment in cortical/submembrane regions (Fig. 3E); a similar pattern of expression was observed with GLA-3A (data not shown). The GLA-3B staining was absent in the gonads of *gla-3(op212)* mutants (Fig. 3E).

Loss of gla-3 *results in impaired oocyte development*

gla-3(lf) mutants were morphologically normal, but exhibited a greatly reduced brood size and a low frequency of embryonic lethality (Table 1). Both defects were milder in *gla-3(op216)* mutants, consistent with the predicted hypomorphic nature of this mutation (which affects only one of the two GLA-3 isoforms). All three mutants showed a further reduction in brood size when raised at high temperature (25°C) (Table 1). Because this reduction was also apparent in the predicted null mutant *gla-3(op212)*, we surmise that loss of *gla-3* function uncovers an intrinsically temperature-sensitive process that is required for oocyte development.

What is the cause of the low brood size in *gla-3* mutants? Sperm in *gla-3(op212)* hermaphrodites and males appeared morphologically normal. We tested the fertility of *gla-3(lf)* sperm by mating *gla-3(lf)* males with *unc-32(e189)* hermaphrodites, and found that the mating efficiency of *gla-3(lf)* males is comparable to that of wild-type animals (Supplemental Table I). Our results indi-

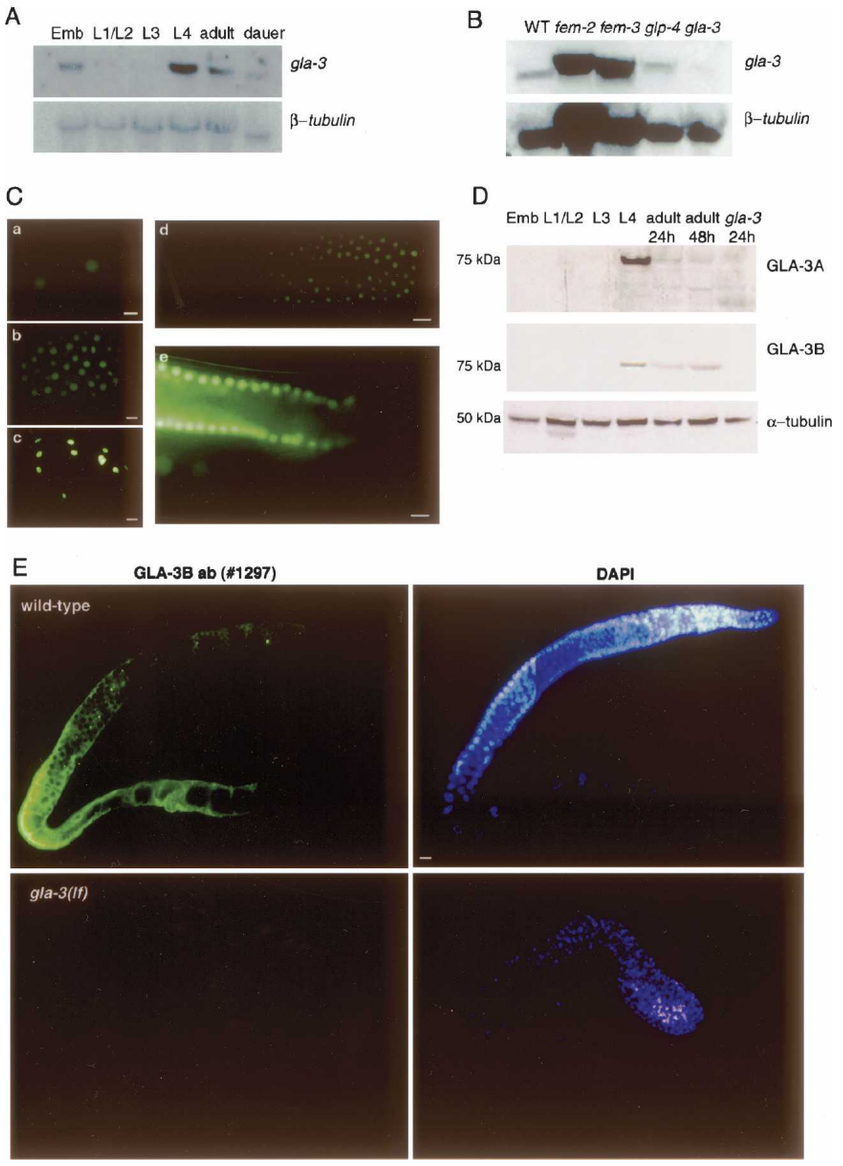

Figure 3. *gla-3* expression is developmentally regulated. (*A*) A Northern blot of total RNA isolated from synchronized wild-type animals was probed with a *gla-3* cDNA as described in Materials and Methods. β-Tubulin was used as a loading control. (*B*) *gla-3* mRNA is present in both germline and soma. Poly(A)$^+$ RNA was extracted from synchronized wild-type, *fem-2(e2105*ts*)* (oocytes only), *fem-3(q20*sd*)* (sperm only), and *glp-4(bn2*ts*)* (no germ cells) adults. β-Tubulin was used as a loading control. (*C*) $P_{gla\text{-}3a}$::*2xNLS*::*gfp* expression in *C. elegans* embryos and germline. Ubiquitous expression was observed in early embryos (*a*,*b*) and in the germline at the L4 larval (*d*) and adult (*e*) stages. Expression was also observed in muscle cells in threefold embryos (*c*). (*D*) Western blot analysis of a developmental time course of wild-type and adult *gla-3(op212)* worms using isoform-specific anti-GLA-3 antibodies. Total protein was extracted as described in Materials and Methods. Twenty micrograms of total protein was loaded per lane; α-tubulin was used as a loading control. (*E*) Localization of GLA-3B in adult hermaphrodite gonads. Gonads were dissected from wild-type and *gla-3(op212)* worms 24 h after the L4/adult molt and were stained with the anti-GLA-3B-specific antibody 1297 and DAPI. Scale bar in *C* and *E*, 8 μm.

cate that the fertility defects in *gla-3(lf)* mutants likely stem from an oogenesis defect.

Consistent with the above conclusion, the gonads of *gla-3(op212)* adult hermaphrodites contained few, abnormally shaped oocytes (Fig. 4A). To examine whether the reduced brood size was the result of excessive apoptosis, we observed gonads of *gla-3(op212); ced-3(n717)* double mutants. Although apoptosis was completely suppressed in these animals (Figs. 1C, 4A), oogenesis was still impaired, indicating that *gla-3* function is necessary for oocyte differentiation rather than germ cell survival per se (Table 1).

To further investigate the oogenesis defect, we stained germ cell nuclei in wild-type and *gla-3(lf)* worms with 4′,6-diamidino-2-phenylindole dihydrochloride (DAPI). In wild-type worms, the transition from mitosis to meiosis occurs at the middle of the distal arm, and pachytene nuclei become visible beyond the transition zone. Oocytes then enter diakinesis in the proximal arm of the gonad, where highly condensed chromosomes can be seen (Fig. 4B). The distal gonads of *gla-3(op212)* mutants were indistinguishable from those of wild-type animals when observed under Nomarski optics or by DAPI staining (Fig. 4A,B). However, only few oocytes developed to the diakinesis stage in the proximal gonads of *gla-3(op212)* adults; detailed analysis revealed that this region was filled mostly with pachytene-stage nuclei (Fig. 4B; data not shown).

Inhibition of apoptosis did not significantly improve the differentiation defects that are caused by loss of *gla-3* function: DAPI staining of *gla-3(op212); ced-3(n717)* double mutants revealed an unusually large number of pachytene-stage nuclei in the proximal arm (Fig. 4; data not shown). The double mutant did contain more diaki-

Table 1. gla-3(lf) *mutants have a reduced brood size and suffer from embryonic lethality*

	Brood size		Survival (%)	
Genotype	20°C (n = 17)	25°C (n = 15)	20°C (n = 20)	25°C (n = 15)
Wild type	259 ± 18	264 ± 23	98 ± 2	99 ± 5
ced-3(n717)	263 ± 22	280 ± 18	98 ± 5	96 ± 6
gla-3(op212)	20 ± 3	5.7 ± 2.1	81 ± 7	75 ± 3
gla-3(ep312)	12 ± 5	4.8 ± 1.4	76 ± 8	72 ± 9
gla-3(op216)	180 ± 25	112 ± 45	95 ± 6	90 ± 4
gla-3(op212); ced-3(n717)	14 ± 3	11 ± 2	85 ± 3	81 ± 5
gla-3(ep312); ced-3(n717)	13 ± 5	10 ± 3	75 ± 10	79 ± 6
gla-3(op216); ced-3(n717)	100 ± 20	53 ± 31	90 ± 8	91 ± 5

Brood size and survival rate were scored as previously described (Hofmann et al. 2002). The data shown are the average ± SD. (n) Number of broods analyzed.

nesis stage oocytes than the *gla-3* single mutant; however, these diakinetic oocytes were misshapen and abnormally small. These results indicate that inhibition of apoptosis allows more female germ cells to enter diakinesis in *gla-3* mutants, but does not rescue the *gla-3(lf)* differentiation defect(s).

Biochemical interaction of GLA-3 and MPK-1 in vitro and in vivo

To identify molecular links between GLA-3 and other proteins involved in oogenesis, we searched the worm interactome (WI5, http://vidal.dfci.harvard.edu/interactomedb) for interaction partners of GLA-3, and found a yeast two-hybrid (Y2H) interaction between GLA-3 and the two isoforms of MPK-1. Using these two MPK-1 isoforms as baits, both GLA-3 isoforms were found as the predominant preys (over 50% of hits) in the AD-cDNA and AD-ORFeome prey libraries (Li et al. 2004; data not shown). MPK-1 is the *C. elegans* homolog of the mammalian ERK1/2 serine/threonine kinases. MPK-1 is required for germline development: In *mpk-1(lf)* mutants, germ cells fail to exit the pachytene stage of meiosis I, resulting in sterility and decreased germ cell apoptosis (Church et al. 1995; Lackner and Kim 1998; Gumienny et al. 1999).

To verify the Y2H result, we performed glutathione-S-transferase (GST) affinity purification experiments in 293T cells transfected with MPK-1 fused to GST and myc-tagged GLA-3. Both isoforms of GLA-3 interacted with both isoforms of MPK-1 (Fig. 5A). To validate the in vitro evidence and show that MPK-1 interacts with GLA-3 in vivo, we immunoprecipitated GLA-3 from *C. elegans* extracts and tested for MPK-1 binding. As illustrated in Figure 5B, MPK-1 could be immunoprecipitated with both isoforms of GLA-3. Our findings show a direct interaction between GLA-3 and MPK-1 in vitro and in vivo, and provide a possible explanation for the germline defects observed in *gla-3(lf)* mutants.

To define the GLA-3 binding interface on MPK-1, we used the reverse Y2H system. We screened a PCR-mutagenized library of *mpk-1* and selected for mutants that could no longer interact with GLA-3. From this set of mutants, we analyzed further those with a single, nonsilent nucleotide change. In total, we identified 20 unique amino acid substitutions that represent 17 different amino acid positions on MPK-1 (Table 2). The majority (nine out of 17) of the amino acid changes that lead to a disruption of the interaction between MPK-1 and GLA-3 clustered to a small region on the surface of MPK-1 (Fig. 6). The region defined by these residues is structurally conserved between MPK-1 and ERK2 and

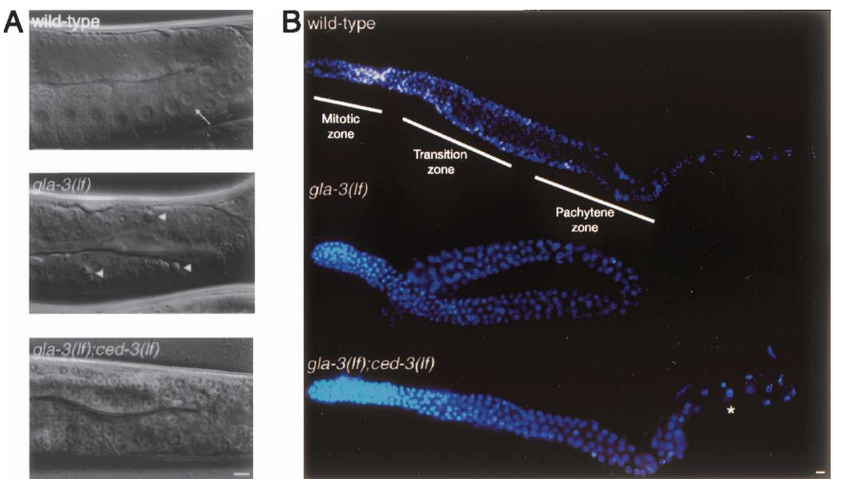

Figure 4. Loss of *gla-3* function results in meiotic arrest during oogenesis. (*A*) Wild-type, *gla-3(op212)*, and *gla-3(op212); ced-3(n717)* adult hermaphrodite animals were examined using DIC microscopy. In wild-type worms, oocytes enter diakinesis in the proximal arm of the gonad (arrow). Arrowheads indicate apoptotic corpses in *gla-3(lf)* animals. (*B*) Images of DAPI-stained gonads from wild-type, *gla-3(op212)*, and *gla-3(op212); ced-3(n717)* adult hermaphrodites. Pachytene nuclei are evident around the bend of the gonad arm. The proximal arm of *gla-3(op212)* mutants contained an excess of pachytene nuclei compared to wild-type worms. The asterisk indicates the first diakinetic nucleus in the proximal arm of *gla-3(lf); ced-3(lf).* Scale bar, 8 µm.

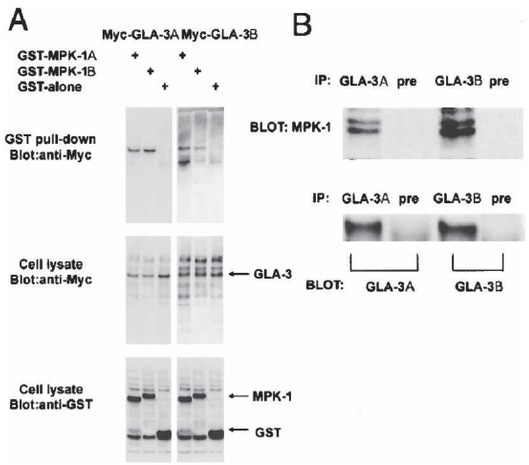

Figure 5. MPK-1 and GLA-3 interact in vitro and in vivo. (*A*) Myc-GLA-3 and GST-MPK-1 interact in 293T cells. 293T cells were transfected with plasmids expressing Myc-tagged GLA-3A or GLA-3B isoforms and GST-MPK-1A or GST-MPK-1B. GST-MPK-1A or GST-MPK-1B was affinity-purified using glutathione beads, and the presence of Myc-GLA-3A or Myc-GLA-3B was detected by immunoblotting using an anti-Myc antibody. (*B*) MPK-1 interacts with GLA-3 in *C. elegans*. Total protein was extracted from synchronized adult hermaphrodites, and immunoprecipitation was performed using anti-GLA-3A or GLA-3B antibodies. Pre-immune serum was used as a control. Immunoprecipitated samples were probed with an antibody against mammalian ERK1/2, which recognizes *C. elegans* MPK-1 (*top* panel) (Lackner and Kim 1998) and with antibodies against GLA-3A or GLA-3B (*bottom* panel).

has been shown to function as a docking site for both regulators and targets of MAPK, such as the phosphatase MKP3 and the kinase ELK1 (Table 2; Zhang et al. 2003). In addition, GLA-3 contains potential MPK-1 binding sites, as defined by a cluster of positive amino acids surrounded by hydrophobic amino acids (Tanoue and Nishida 2002). GLA-3a has one site at position 66–74 (LRKVVRIDR), whereas GLA-3b has two such sites, at positions 66–74 (LRKTKI) and 99–107 (LRKVVRIDE). Taken together, our biochemical and molecular data are consistent with a role of GLA-3 as a regulator or a target of MPK-1 in the *C. elegans* germline.

gla-3 *genetically interacts with components of the MAPK signaling pathway*

Do ras/MAPK pathway genes regulate the apoptotic program? Strong loss-of-function mutations in the *mpk-1* pathway cause a sterile phenotype due to developmental arrest at the pachytene stage of meiosis (Church et al. 1995). We and others have previously shown that pachytene-arrested cells do not undergo apoptosis (Gumienny et al. 1999; Navarro et al. 2001). To address the role of *mpk-1* in *gla-3(lf)*-induced cell death, we performed genetic epistasis analysis between *gla-3* and genes that are known to be involved in the Ras/MAPK pathway. Using the putative null mutation *mpk-1(ga117)* (Lackner and Kim 1998), we found that *gla-3(op212)*-induced apoptosis was completely abrogated in *gla-3(op212); mpk-1(ga117)* double mutants (Fig. 7A). Interestingly, although apoptosis is suppressed, *gla-3* does not rescue the sterile phenotype of *mpk-1(ga117)* (Supplemental Table II). These data demonstrate that *mpk-1* is epistatic to *gla-3*, and that its activation is required for *gla-3(lf)*-induced germ cell death. We then compared the levels of germ cell death in *mpk-1(oz140) ced-9(n2812)* adult hermaphrodites with those in *gla-3(RNAi); mpk-1(oz140) ced-9(n2812)* animals. *ced-9(lf)*-induced and *gla-3(RNAi)*-induced germ cell apoptosis were both completely suppressed in the absence of functional *mpk-1* (Gumienny et al. 1999; Supplemental Table III).

We also analyzed the effect on germline apoptosis of mutants that cause overactivation of MPK-1. We observed no increase in germ cell apoptosis in the ras gain-of-function mutant *let-60(ga89)*. Similarly, *gla-3(op212); let-60(ga89)* double mutants had levels of apoptosis that were comparable to *gla-3(op212)* alone (Fig. 7B). In contrast, inactivation of LIP-1, an MPK-1 phosphatase that functions as a negative regulator of MAPK signaling (Hajnal and Berset 2002), resulted in increased germline apoptosis, with levels comparable to *gla-3* mutants (Fig. 7B). Similarly to *gla-3* mutants, *lip-1(zh15)*-induced germline apoptosis depended on *ced-3* but was *cep-1*-independent (Supplemental Fig. 3), indicating that these two genes might function in the same genetic pathway. Indeed, *gla-3(op212); lip-1(zh15)* double mutants showed only a slight increase in germline apoptosis over the single mutants (Fig. 7B).

lip-1(zh15) mutants display accelerated oocyte devel-

Table 2. *Point mutations in MPK-1 that disrupt interaction with GLA-3*

Position[a]	Hits	Wild type	Mutant	DS[c]
130	1	Ser (TCT)	Pro (CCT)	No
131	1	Ser (TCT)	Phe (TTT)	No
253	14	Asn (AAT)	Asp (GAT)	Yes
391	1	Tyr[b] (TAC)	His (CAC)	Yes
391	1	Tyr[b] (TAC)	Asp (GAC)	Yes
398	3	Leu (CTC)	Pro (CCC)	Yes
410	1	Leu (CTC)	Pro (CCC)	Yes
413	1	Arg[b] (CGT)	His (CAT)	Yes
433	1	Ser (TCT)	Pro (CCT)	No
473	1	Leu (TTG)	Ser (TCG)	No
479	1	Leu (CTC)	Pro (CCC)	Yes
490	1	Cys (TGT)	Ser (AGT)	Yes
491	1	Cys (TGT)	Tyr (TAT)	Yes
497	1	Leu (CTC)	Pro (CCC)	Yes
653	1	Gly (GGA)	Glu (GAA)	No
655	1	Cys (TGT)	Arg (CGT)	No
692	1	Phe (TTC)	Ser (TCT)	No
719	1	Leu (CTC)	Pro (CCC)	No
896	1	Phe (TTC)	Ser (TCC)	No
955	1	Tyr[b] (TAC)	His (CAC)	Yes

[a]Position indicates nucleotide position based on MPK-1 isoform a.
[b]Residues necessary for docking that are identical in MPK-1 and ERK2.
[c]Amino acids that are part of the predicted MPK-1 docking site.

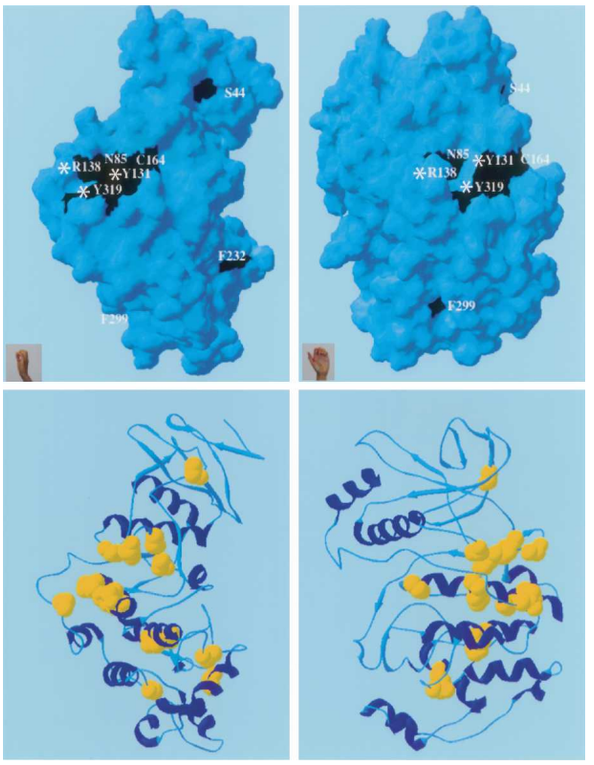

Figure 6. Identification of MPK-1 residues required for the interaction with GLA-3. The reverse two-hybrid system was used to identify residues that are essential for the MPK-1/GLA-3 interaction. Residues, which when altered result in disruption of the interaction, are shown in black in the space-filling model (*top* panels) and in yellow in the ribbon model (*bottom* panels) of MPK-1. Residues with visible surface exposure are noted on the structure, and those that are identical between MPK-1 and its mammalian homolog ERK2 are noted with an asterisk. *Left* and *right* panels represent a 90° rotation of the structure on its axis.

opment due to defective G_2/M-phase arrest (Hajnal and Berset 2002). We scored the number of diakinetic oocytes in the gonads of single and *gla-3(op212); lip-1(zh15)* double mutants and found that the double mutants exhibited decreased numbers of diakinetic oocytes, a phenotype similar to *gla-3(op212)* single mutants (Supplemental Table II). These observations suggest that *gla-3* is epistatic to *lip-1* for germ cell differentiation.

gla-3 *mutations do not result in MPK-1 overactivation*

To test whether loss of *gla-3* function altered the pattern of MPK-1 activation in the germline, we stained dissected gonads with a monoclonal antibody that specifically recognizes the diphosphorylated, activated form of MPK-1 (DP-MPK-1). As previously reported (Miller et al. 2001; Page et al. 2001), MPK-1 was activated in pachytene-stage cells and also, in response to the sperm signal, in the first and sometimes second oocyte proximal to the spermatheca (Supplemental Fig. 4A). The pattern of MPK-1 activation in *gla-3(op212)* mutants was similar to that of wild-type animals, although the DP-MPK-1 staining in the oocytes proximal to the spermatheca was occasionally weaker (Supplemental Fig. 4A), possibly reflecting the abnormal nature of oocytes in *gla-3* mutants.

To further test the hypothesis that GLA-3 might regulate the levels of activated MPK-1, we used an in vitro MPK-1 kinase assay (Alessi et al. 1995; Berset et al. 2001). Using myelin basic protein (MBP) as an MAPK substrate, we found that both *lip-1(zh15)* and *let-60(n1046gf)* animals had higher levels of MAPK enzymatic activity when compared with the wild type (Supplemental Fig. 4B). In contrast, the level of MAPK activity in *gla-3(op212)* and *gla-3(op216)* mutants was similar to the wild type (Supplemental Fig. 4B). Taken together, these data indicate that inactivation of GLA-3 does not directly affect the activation of MPK-1 protein itself.

GLA-3 is a negative regulator of the MAPK signaling pathway in somatic tissues

During *C. elegans* development, LET-60/Ras and MPK-1/MAPK transmit the LIN-3/EGF inductive signal in

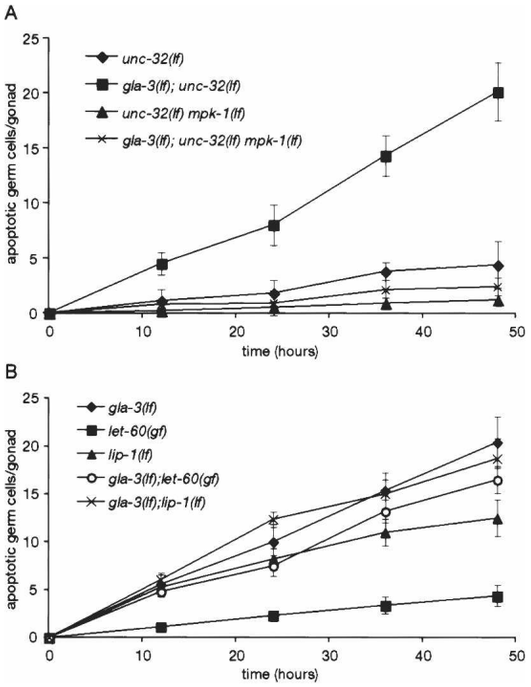

Figure 7. Genetic interactions between *gla-3* and genes involved in Ras/MAPK signaling. (*A*) *unc-32(e189), gla-3(op212); unc-32(e189), unc-32(e189) mpk-1(ga117),* and *gla-3(op212); unc-32(e189) mpk-1(ga117)* animals were synchronized, and germ cell corpses were counted over 48 h starting at the L4 stage. (*B*) Synchronized *gla-3(op212), let-60(ga89), lip-1(zh15), gla-3(op212); let-60(ga89),* and *gla-3(op212); lip-1(zh15)* animals were raised at 25°C, and germline corpses were counted starting at the L4 stage. Error bars represent SD from three independent experiments; 20 gonads were scored in each experiment.

Table 3. gla-3 *is a negative regulator of vulva induction*

Genotype	% Muv	Average P(3–8).p vulval fates	Number of animals
Wild type	0	3.0	75
gla-3(op212)	0	3.0	69
gla-3(op216)	0	3.0	74
*let-60(n1046*sd*)*	80	4.0	54
let-60(ga89)	42	3.5	64
lip-1(zh15)	0	3.0	60
unc-32(e189)	0	3.0	45
unc-32(e189) mpk-1(ga117)	0	0	54
gla-3(op212); let-60(n1046)	97	4.9	48
gla-3(op216); let-60(n1046)	91	5.1	52
gla-3(op212); let-60(ga89)	66	4.5	68
gla-3(op216); let-60(ga89)	63	4.4	84
gla-3(op212); lip-1(zh15)	4.5	3.3	66
gla-3(op216); lip-1(zh15)	3.8	3.1	71
gla-3(op212); unc32(e189) mpk-1(ga117)	0	0	65
gla-3(op216); unc-32(e189) mpk-1(ga117)	0	0	58

vulval precursor cells (VPCs), resulting in vulva formation (Moghal and Sternberg 2003). Loss-of-function mutations in genes that mediate the inductive signaling pathway can lead to a vulvaless (Vul) phenotype due to insufficient induction of VPCs. Conversely, mutations that enhance the inductive signal result in a multivulva (Muv) phenotype, due to hyperinduction of VPCs.

To test the possibility that GLA-3 might also influence MAPK signaling during vulval development, we examined double mutants between *gla-3(lf)* and various mutations that affect vulval induction. In *gla-3(lf)* single mutants, vulval development appeared normal (Table 3). However, loss of *gla-3* function enhanced the multivulva phenotype observed in two different *let-60(gf)* mutants (Table 3), suggesting that GLA-3 might function as an inhibitor of MAPK signaling in VPCs. Similarly, vulval development is normal in *lip-1(lf)* mutants (Berset et al. 2001), whereas double *gla-3(op212); lip-1(zh15)* mutants displayed a weak synthetic Muv phenotype (Table 3). In contrast, the *gla-3* alleles could not suppress the *mpk-1(ga117)* vulvaless phenotype. Taken together, these results indicate that GLA-3 might function as an inhibitor of MAPK signaling during vulval development.

Activation of the Ras/MAPK pathway has also been shown to promote protein degradation in *C. elegans* muscles, leading to a progressive loss of motility (Szewczyk et al. 2002). We therefore investigated whether *gla-3* might influence muscle-protein degradation through its interaction with the Ras/MAPK pathway. Whereas *gla-3* mutants raised at 15°C showed nearly wild-type movement, animals shifted to 25°C at the L4 stage suffered a progressive loss of motility, similar to the defect observed in *let-60(ga89)* mutants (Table 4). The locomotion defect was not significantly enhanced in the *gla-3(lf); let-60(lf)* double mutants, implying that the two genes might affect the same molecular process.

We then monitored protein degradation using an *unc-54::LacZ* transgene that is expressed specifically in body wall and vulval muscles (Zdinak et al. 1997; Szewczyk et al. 2000). This fusion protein is completely stable in well-fed wild-type worms; therefore, any subsequent decline in LacZ activity is the result of protein degradation. Well-fed *gla-3(op212)* mutants exhibited wild-type levels of LacZ activity when grown at 15°C. In contrast, mutants shifted to 25°C at the L4 stage showed a time-dependent loss of reporter activity similar to the loss observed in mutants with an overactivated Ras/MAPK pathway (Fig. 8). Taken together, these observations indicate that GLA-3 might negatively regulate Ras/MAPK-dependent protein degradation in muscle cells.

Discussion

Although much is known about the core apoptotic machinery and the signals that regulate apoptosis during *C. elegans* development (for review, see Lettre and Hengartner 2006), the factors that regulate germline apoptosis are largely unknown. In an attempt to isolate such regu-

Table 4. gla-3(lf) *causes time-dependent loss of mobility*

Genotype	Temp (°C)	Movement rate (waves/min) 0	24	48	72
Wild type	15	98 ± 14	96 ± 12	108 ± 8	103 ± 5
gla-3(op212)	15 → 25		99 ± 8	110 ± 17	102 ± 9
	15	100 ± 8	97 ± 15	93 ± 19	109 ± 8
	15 → 25		78 ± 16	61 ± 10	57 ± 12
gla-3(op216)	15	109 ± 11	103 ± 8	97 ± 5	102 ± 8
	15 → 25		82 ± 7	63 ± 11	60 ± 7
let-60(ga89)	15	100 ± 14	95 ± 15	98 ± 2	101 ± 14
	15 → 25		83 ± 9	56 ± 15	54 ± 10
gla-3(op212); let-60(ga89)	15	90 ± 9	99 ± 11	97 ± 9	89 ± 12
	15 → 25		71 ± 5	54 ± 7	48 ± 11
gla-3(op216); let-60(ga89)	15	96 ± 13	100 ± 7	106 ± 4	94 ± 6
	15 → 25		76 ± 13	62 ± 7	61 ± 4

Data shown are average ± SD from two independent experiments; 15 animals were scored per experiment.

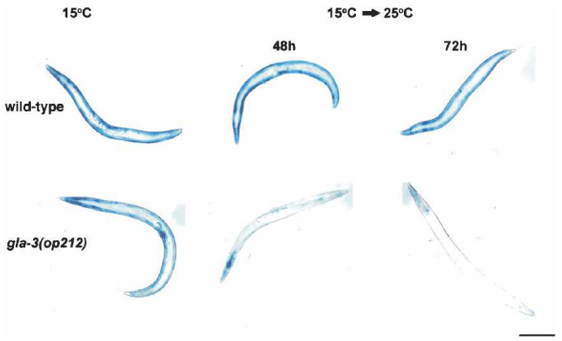

Figure 8. *gla-3(lf)* promotes proteolysis in body wall muscles. Animals were raised at 15°C until the young adult stage (*left* panel), and then shifted to 25°C for 48 or 72 h (*right* panels). β-Galactosidase activity (blue) was measured as described in Materials and Methods. Scale bar, 0.2 mm.

lators, we performed a genetic screen and identified *gla-3*. We found that *gla-3* is important for oocyte differentiation and germ cell survival and encodes a TIS11-like zinc-finger-containing protein. We showed that GLA-3 genetically and physically interacts with the *C. elegans* MAPK MPK-1 and provided evidence to support the notion that GLA-3 might function as a negative regulator of the MAPK pathway in the developing vulva and in muscle cells.

Regulation of germline apoptosis by GLA-3 and other RNA-binding proteins

We showed that *gla-3* has two isoforms, which differ in their two 5′-most exons. Are both isoforms involved in germline apoptosis and oocyte development? Both GLA-3A and GLA-3B are expressed in the germline, and both isoforms interact with MPK-1. Furthermore, the *op216* mutation, which is predicted to affect only GLA-3A, shows weaker defects than the predicted null alleles. Based on these results, we suggest that both isoforms might participate in germline development and apoptosis. However, further work is required to confirm this hypothesis, and to determine whether the isoform-specific N-terminal domains perform distinct functions.

How could GLA-3 regulate germ cell apoptosis? The TIS11-like proteins that have previously been characterized in *C. elegans*, including PIE-1, POS-1 MEX-1, MEX-5, and MEX-6, function in a hierarchical regulatory cascade that controls cell fate during early embryonic development (Schneider and Bowerman 2003). In addition, the combined loss of the TIS11-like proteins, OMA-1 and OMA-2, results in impaired oocyte maturation and female infertility (Detwiler et al. 2001). The mammalian TIS11 zinc-finger-containing protein, tristetraprolin (TTP), is an RNA-binding protein that interacts with 3′-untranslated AU-rich elements of mRNAs and negatively regulates their expression (Lai et al. 1999; Carballo et al. 2000; Cao et al. 2003). Based on the homology between the *C. elegans* and the mammalian TIS11-like proteins, it is possible that PIE-1, POS-1, MEX-1, MEX-5, MEX-6, and GLA-3 exert their functions by acting as mRNA-binding proteins (Barabino et al. 1997; Lai et al. 2000; Worthington et al. 2002).

Inactivation of several RNA-binding proteins, including DAZ-1, CGH-1, CPB-3, and CAR-1, has previously been shown to trigger apoptosis in the *C. elegans* germline (Karashima et al. 2000; Navarro et al. 2001; Lettre et al. 2004; Boag et al. 2005). Similarly to *gla-3*, *daz-1* mutations result in severe oogenic defects due to arrest at the pachytene stage of meiosis I. It is possible that these genes coordinately regulate the synthesis of pro-apoptotic or survival proteins during germline development. Indeed, CGH-1 and CAR-1 interact physically and are components of an evolutionarily conserved RNP complex (Boag et al. 2005). Alternatively, these proteins might function more broadly to promote germline differentiation, and the developmental defects that result from their loss could be the cause of the apoptotic phenotypes observed. Identification of the target mRNAs regulated by these various proteins is required to shed light on this issue.

GLA-3 is a novel component of the MAPK signaling cascade

In addition to its potential function as an RNA-binding protein, GLA-3 also interacts physically with the *C. elegans* MAPK MPK-1 in vitro and in vivo, indicating that GLA-3 might have a role in MPK-1 signaling. In the hermaphrodite germline, activation of the LET-60/MEK-2/MPK-1 signaling pathway is essential for pachytene progression and subsequent entry into diplotene/diakinesis (Church et al. 1995; Lackner and Kim 1998; Miller et al. 2001; Page et al. 2001). Although MPK-1 activation during pachytene progression appears to be transient and tightly regulated (Hajnal and Berset 2002), the nature of the signal that controls its activation and the downstream effectors of MPK-1 remain poorly characterized. Based on its mutant phenotype and its physical interaction with MPK-1, GLA-3 might be directly involved in this process.

Because our expression studies revealed that GLA-3 expression is not restricted to the germline, we also studied the potential role of GLA-3 in MPK-1 signaling in the soma. We found that the absence of *gla-3* resulted in phenotypes consistent with an inappropriate activation of *mpk-1* signaling in both vulval development and protein degradation in body wall muscles. These biochemical and genetic analyses support the idea that GLA-3 functions as a negative component of the Ras/MAPK pathway. However, we were so far unable to detect any change in MPK-1 activity in *gla-3* mutants or worm extracts (Supplemental Fig. 4), suggesting that GLA-3 does not directly regulate MPK-1 activation but, rather, might restrict its access to or interaction with substrates.

Could GLA-3 be a substrate rather than—or in addition to—a regulator of MPK-1? Neither our genetic nor our biochemical data allow us to definitively exclude this possibility. We did not observe any differences in the

GLA-3 protein levels in different mutants of the MAPK pathway by Western blot analysis and in situ immunostaining (Supplemental Fig. 5; data not shown), which indicated that MPK-1 does not directly regulate GLA-3 levels. However, it is possible that MPK-1 phosphorylates GLA-3 and this modification is important for GLA-3 function. Indeed, several kinases, including MAPKMAP kinase 2 (MK2), ERK2, p38, and JNK, can phosphorylate the mammalian TIS11 protein tristetraprolin in response to growth factor or cytokine treatment (Taylor et al. 1995; Mahtani et al. 2001; Chrestensen et al. 2004). Although GLA-3 has several potential MAPK phosphorylation sites, we were unable to determine whether GLA-3 is phosphorylated by MPK-1 in vivo using the antibody that we raised (Supplemental Material 5).

What is the function of GLA-3 in the MAPK signaling pathway?

In *Schizosaccharomyces pombe*, MAPK signaling activity can be regulated through a negative feedback loop that involves Rnc1, a KH-domain-containing RNA-binding protein that stabilizes the Pmp1 phosphatase mRNA (Sugiura et al. 2003). Based on the ability of GLA-3 to bind to MPK-1 and its predicted RNA-binding domains, a similar model could be envisaged in which GLA-3 is activated through interaction with MPK-1, and in response stabilizes mRNAs encoding negative regulators of MPK-1 such as LIP-1.

Materials and methods

Strains, alleles, and genetic analysis

Maintenance and genetic manipulation of *C. elegans* were carried out as described (Brenner 1974). The following mutations and transgenes were used: LG I: *hus-1(op244)*, *gla-3(op212)*, *gla-3(op216)*, *gla-3(ep312)*, *cep-1(gk138)*, *glp-4(bn2*ts*)*; LG II: *lip-1(zh15)*; LG III: *fem-2(e2105*ts*)*, *mpk-1(ga117)*, *mpk-1(oz140)*, *ced-4(n1162)*, *clk-2(mn159*ts*)*, *unc-32(e189)*, *ced-9(n2812)*, *unc-119(ed3)*, *opIs64[$P_{gla\text{-}3a}$::2xNLS::gfp unc-119(+)]*; LG IV: *fem-3(q20*sd*)*, *ced-3(n717)*, *let-60(n1046*gf*)*, *let-60(ga89*gf*)*, *opIs110[$P_{lim\text{-}7}$::yfp::act-5 unc-119(+)]*; LG V: *ccIs55[unc-54::lacZ; sup-7(st5)]*, *gaIs36[HS-mpk-1(+) EF1-D-mek(+) unc-30(+)]*. All mutations are described in WormBase (http://www.wormbase.org). The Bristol strain N2 was used as the wild-type strain. Strains were maintained at 20°C unless stated otherwise. Unless specified otherwise, all phenotypic characterizations were performed on hermaphrodites 24 h post-L4/adult molt. Movement rates were measured as described (Bolanowski et al. 1981).

Isolation of gla-3 *alleles*

gla-3(lf) alleles were isolated in an F_2 screen for mutants with increased germ cell apoptosis. Wild-type animals were mutagenized with ethylmethane sulfonate using a standard protocol (Brenner 1974), and adult F_2 animals with increased apoptotic germ cell corpses were identified with the vital dye acridine orange (AO; Sigma) (Lettre et al. 2004). Two independent alleles (*op212* and *op216*) were isolated from a screen of 45,000 genomes. To eliminate possible additional mutations, each mutant was crossed back to the wild type eight times before subsequent analysis. The *ep312* deletion allele was isolated in a separate screen, performed to identify mutants involved in *cep-1*-independent germ cell apoptosis (M. Costa, pers. comm.).

Cloning of gla-3

The *op212* allele of *gla-3* was mapped near the middle of Chromosome I by two-factor mapping using the marker *dpy-5*. To refine the position of *gla-3*, three-factor mapping was conducted using the following marker combinations: *dpy-5 unc-87*, *dpy-5 unc-29*, and *dpy-24 unc-75*. This analysis placed *gla-3* closer to *unc-29* than *dpy-5*. SNP mapping refined the region to 0.36 cM (roughly 270 kb), which included 40 predicted genes. We then performed RNAi feeding of the 40 genes in this interval. Only inactivation of T02E1.3 resulted in increased germline apoptosis. The molecular changes induced by the *op212*, *op216*, and *ep312* mutations were determined by PCR amplification of the *gla-3* locus from the respective mutants, followed by sequencing of both strands of the amplification product.

RNA interference

Feeding RNAi was performed as previously described (Lettre et al. 2004). Feeding RNAi constructs were obtained either from the Ahringer library (Kamath et al. 2003) or from the ORFeome RNAi collection (Rual et al. 2004), or were generated by subcloning from cDNAs (for *bir-1* and *gfp*).

Germline apoptosis

Apoptotic germ cell corpses were identified and quantitated based on their characteristic morphology under differential interference contrast (DIC) optics, as previously described (Gumienny et al. 1999).

Brood size and oocyte counts

Brood size counts were performed as previously described (Hofmann et al. 2002). Oocyte counts were performed according to Hajnal and Berset (2002).

Northern analysis

Total RNA was isolated using TRIZOL reagent (GIBCO-BRL) from cultures of synchronized wild-type worms at different developmental stages as well as from *gla-3(op212)*, *glp-4(bn2*ts*)*, *fem-2(e2105*ts*)*, and *fem-3(q20*sd*)* adults. Poly(A)$^+$ selection of mRNAs from staged adults was performed using the Micro-PolyA kit (Ambion). RNA samples were subjected to formaldehyde agarose gel electrophoresis, transferred to Hybond N+ nylon membrane, and probed with a full-length *gla-3* cDNA amplified from plasmid yk6h11 and labeled with ^{32}P using the random hexamer primer method.

Generation of GLA-3 antibodies

Rabbit polyclonal antibody T02E1.3a (1301) was raised against the T02E1.3a peptide KTQEISVVIDPRDA, whereas antibody T02E1.3b (1297) was raised against the T02E1.3b peptide LLNSDMDPVRNLES. Peptides were synthesized (Sigma-Genosys) and injected into two rabbits according to Sigma protocols.

Western blot analysis

Adult worms were washed off the plates with water. Worm pellets were frozen in liquid nitrogen and kept at –80°C. To

extract proteins, an equal volume of acid-washed glass beads (Sigma) was added to the frozen worm pellet, and the tubes were put in a bead beater (FastPrep FP120) for 35 sec at speed 6.5. Following addition of 100–300 µL of RIPA buffer (50 mM Tris at pH 8.0, 150 mM NaCl, 1% NP-40, 1% deoxycholate, 1% SDS, 1 tablet/10 mL Complete Mini protease inhibitor [Roche]) or immunoprecipitation buffer (25 mM HEPES-NaOH at pH 7.4, 150 mM NaCl, 0.2 mM DTT, 10% glycerol, 1% Triton X-100, 1 tablet/10 mL Complete Mini protease inhibitor [(Roche]), tubes were vortexed and incubated on ice for 10 min. Extracts were centrifuged for 15 min at 13,000 rpm at 4°C. Supernatants were collected and kept at –80°C. Protein quantification was done using the Bio-Rad protein assay as recommended, with bovine serum albumin (BSA) as standard. The antibody dilutions used were 1:1000 for GLA-3 antibodies and 1:10,000 for α-tubulin (Upstate). Secondary HRP-labeled anti-rabbit and anti-mouse antibodies (Sigma) were used at 1:100,000 and 1:40,000, respectively, and detected using ECL (Sigma).

Transgenic worms

The $P_{gla\text{-}3a}$::*2xNLS*::*GFP unc-119(+)* construct (pEK1) was bombarded into *unc-119(ed3)* worms as previously described (Praitis et al. 2001; Hofmann et al. 2002). Integration of each construct was determined by loss of visible Unc-119 offspring. At least three integrated lines were generated; all showed the same expression pattern.

Reverse two-hybrid selection

The system we used is a variation of the original reverse two-hybrid protocol developed by Vidal (Vidal et al. 1996a,b). Briefly, the *mpk-1* wild-type ORF was mutagenized by PCR using 30 amplification cycles and Platinum *Taq* DNA polymerase (Invitrogen). To build the *mpk-1* mutant library, the gel-purified PCR product was cloned into the pDONR-Express vector using the Gateway in vitro cloning system (Invitrogen). In this vector, the ORF is cloned under control of an IPTG-inducible promoter in frame with the Kan^R gene. Clones containing PCR-induced STOP mutations are removed by plating TOP-10 (Invitrogen) bacteria transformants on IPTG (1 mM) and Kan (80 µg/mL) selective medium. About 500,000 independent transformants were obtained. The ORFs were LR cloned into the pPC-97 Gal-4 DNA-binding domain yeast two-hybrid vector and retransformed into electrocompetent TOP-10 cells. This library was transformed into MaV203 yeast cells containing GLA-3 fused to the Gal-4 activation domain. Cotransformed cells were selected for their ability to grow on –Leu, –Trp, +5-FOA (5-fluoro-orotic acid) medium, and the *mpk-1* ORF was amplified by PCR and sequenced so that the causative mutation could be identified. These *mpk-1* mutants were retested by gap repair in fresh MaV203 containing the AD GLA-3 fusion, to confirm that the interaction had been disrupted because of the mutation (Walhout and Vidal 2001).

Visualization of amino acid changes on MPK-1

Mutations identified in *mpk-1* using the yeast reverse two-hybrid system were mapped to the structure model of MPK-1 (SWISS-PROT P39745), which was derived from the rat ERK2 (SWISS-PROT P63086) crystal structure (Zhang et al. 1993, 1994). The location of the changed amino acids was visualized on the 3D structure using Swiss-PdbViewer (Guex and Peitsch 1997).

GST pull-downs

mpk-1a or *mpk-1b* ORFs were cloned into pDEST-27, which contains GST coding sequence upstream of the Gateway recombination site (Invitrogen). *gla-3a* and *gla-3b* ORFs were cloned into pDEST-CMV-myc, which contains the myc tag upstream of the Gateway recombination site (Invitrogen). Both vectors use the CMV promoter to drive expression of the fusion protein. Plasmids were transfected into 293T cells using Lipofectamin 2000 reagent according to the manufacturer's instructions (Invitrogen). Cells were cultured for 2 d in DMEM medium, and lysed in 0.1% NP-40 buffer (50 mM Tris-HCl at pH 7.5, 150 mM NaCl, 1 mM EDTA, and complete protease inhibitors [Amersham]). Lysates were centrifuged at 14,000*g*, before purification of protein complexes using glutathione Sepharose beads. Purified complexes and control lysate samples were run on NuPAGE acrylamide gels (Invitrogen), and Myc- and GST-tagged proteins were detected using standard immunoblotting techniques. Mouse monoclonal anti-Myc (clone 9E10) and rabbit polyclonal anti-GST were purchased from Sigma.

Immunofluorescence and imaging

Immunostaining was performed essentially as described (Page et al. 2001). Briefly, dissected gonads were fixed in 1% paraformaldehyde in PBS and permeabilized in TBS supplemented with 0.1% Triton X-100. The samples were subsequently incubated with the following antibodies: rabbit anti-GLA-3A 1301, 1:1000 or rabbit anti-GLA-3B 1297, 1:1000 in 5% BSA in TBS, at 4°C overnight. Anti-rabbit AlexaFluor 594 or anti-mouse AlexaFluor 594 IgG antibodies were used as secondary antibodies (Molecular Probes). DAPI was added to a final concentration of 200 ng/mL, and samples were mounted for microscopy. All images were analyzed by light microscopy with a Zeiss Axioskop equipped with epifluorescence and differential interference contrast (DIC) optics. Digital images were acquired and processed using a CCD camera and Openlab software. Histochemical staining of β-galactosidase with 5-bromo-4-chloro-3-indolyl-β-D-galactopyranoside (X-Gal) was performed as described (Zdinak et al. 1997).

Acknowledgments

We thank the *C. elegans* Gene Knockout Consortium and the *Caenorhabditis* Genetics Center for providing strains; M. Costa for the *gla-3(ep312)* allele; L. Broday for the developmental Northern blot; Y. Kohara for plasmid yk6h11; and A. Hajnal, M. Boxem, D. Hill, and T. Berset for discussions and comments. This work was supported by grants from the Swiss National Science Foundation, the Josef Steiner Foundation, the European Union (FP5 project Apoclear), and the Ernst Hadorn Foundation. P.-O.V. was supported by an integrated interactome mapping grant (NCI/NIH 1 R33 CA105405-01), and S.M. was supported by generation of a *C. elegans* protein interaction database grant (NHGRI/NIH 5 R01 HG01715-07) and training grant (NCI/NIH 5 T32 CA09361-25).

References

Ahmed, S., Alpi, A., Hengartner, M.O., and Gartner, A. 2001. *C. elegans* RAD-5/CLK-2 defines a new DNA damage checkpoint protein. *Curr. Biol.* **11:** 1934–1944.

Alessi, D.R., Cohen, P., Ashworth, A., Cowley, S., Leevers, S.J., and Marshall, C.J. 1995. Assay and expression of mitogen-activated protein kinase, MAP kinase kinase, and Raf. *Methods Enzymol.* **255:** 279–290.

Bai, C. and Tolias, P.P. 1996. Cleavage of RNA hairpins mediated by a developmentally regulated CCCH zinc finger protein. *Mol. Cell. Biol.* **16:** 6661–6667.

Barabino, S.M., Hubner, W., Jenny, A., Minvielle-Sebastia, L., and Keller, W. 1997. The 30-kD subunit of mammalian cleavage and polyadenylation specificity factor and its yeast homolog are RNA-binding zinc finger proteins. *Genes & Dev.* **11:** 1703–1716.

Barton, M.K., Schedl, T.B., and Kimble, J. 1987. Gain-of-function mutations of *fem-3*, a sex-determination gene in *Caenorhabditis elegans*. *Genetics* **115:** 107–119.

Beanan, M.J. and Strome, S. 1992. Characterization of a germline proliferation mutation in *C. elegans*. *Development* **116:** 755–766.

Bender, C.F., Sikes, M.L., Sullivan, R., Huye, L.E., Le Beau, M.M., Roth, D.B., Mirzoeva, O.K., Oltz, E.M., and Petrini, J.H. 2002. Cancer predisposition and hematopoietic failure in Rad50(S/S) mice. *Genes & Dev.* **16:** 2237–2251.

Berset, T., Hoier, E.F., Battu, G., Canevascini, S., and Hajnal, A. 2001. Notch inhibition of RAS signaling through MAP kinase phosphatase LIP-1 during *C. elegans* vulval development. *Science* **291:** 1055–1058.

Boag, P.R., Nakamura, A., and Blackwell, T.K. 2005. A conserved RNA–protein complex component involved in physiological germline apoptosis regulation in *C. elegans*. *Development* **132:** 4975–4986.

Bolanowski, M.A., Russell, R.L., and Jacobson, L.A. 1981. Quantitative measures of aging in the nematode *Caenorhabditis elegans*. I. Population and longitudinal studies of two behavioral parameters. *Mech. Ageing Dev.* **15:** 279–295.

Brenner, S. 1974. The genetics of *Caenorhabditis elegans*. *Genetics* **77:** 71–94.

Cao, H., Dzineku, F., and Blackshear, P.J. 2003. Expression and purification of recombinant tristetraprolin that can bind to tumor necrosis factor-α mRNA and serve as a substrate for mitogen-activated protein kinases. *Arch. Biochem. Biophys.* **412:** 106–120.

Carballo, E., Lai, W.S., and Blackshear, P.J. 2000. Evidence that tristetraprolin is a physiological regulator of granulocyte-macrophage colony-stimulating factor messenger RNA deadenylation and stability. *Blood* **95:** 1891–1899.

Chen, F., Hersh, B.M., Conradt, B., Zhou, Z., Riemer, D., Gruenbaum, Y., and Horvitz, H.R. 2000. Translocation of *C. elegans* CED-4 to nuclear membranes during programmed cell death. *Science* **287:** 1485–1489.

Chrestensen, C.A., Schroeder, M.J., Shabanowitz, J., Hunt, D.F., Pelo, J.W., Worthington, M.T., and Sturgill, T.W. 2004. MAPKAP kinase 2 phosphorylates tristetraprolin on in vivo sites including Ser178, a site required for 14–3–3 binding. *J. Biol. Chem.* **279:** 10176–10184.

Church, D.L., Guan, K.L., and Lambie, E.J. 1995. Three genes of the MAP kinase cascade, *mek-2*, *mpk-1/sur-1* and *let-60 ras*, are required for meiotic cell cycle progression in *Caenorhabditis elegans*. *Development* **121:** 2525–2535.

Derry, W.B., Putzke, A.P., and Rothman, J.H. 2001. *Caenorhabditis elegans* p53: Role in apoptosis, meiosis, and stress resistance. *Science* **294:** 591–595.

Detwiler, M.R., Reuben, M., Li, X., Rogers, E., and Lin, R. 2001. Two zinc finger proteins, OMA-1 and OMA-2, are redundantly required for oocyte maturation in *C. elegans*. *Dev. Cell* **1:** 187–199.

DuBois, R.N., McLane, M.W., Ryder, K., Lau, L.F., and Nathans, D. 1990. A growth factor-inducible nuclear protein with a novel cysteine/histidine repetitive sequence. *J. Biol. Chem.* **265:** 19185–19191.

Gartner, A., Milstein, S., Ahmed, S., Hodgkin, J., and Hengartner, M.O. 2000. A conserved checkpoint pathway mediates DNA damage-induced apoptosis and cell cycle arrest in *C. elegans*. *Mol. Cell* **5:** 435–443.

Guedes, S. and Priess, J.R. 1997. The *C. elegans* MEX-1 protein is present in germline blastomeres and is a P granule component. *Development* **124:** 731–739.

Guex, N. and Peitsch, M.C. 1997. SWISS-MODEL and the Swiss-PdbViewer: An environment for comparative protein modeling. *Electrophoresis* **18:** 2714–2723.

Gumienny, T.L., Lambie, E., Hartwieg, E., Horvitz, H.R., and Hengartner, M.O. 1999. Genetic control of programmed cell death in the *Caenorhabditis elegans* hermaphrodite germline. *Development* **126:** 1011–1022.

Hajnal, A. and Berset, T. 2002. The *C. elegans* MAPK phosphatase LIP-1 is required for the G_2/M meiotic arrest of developing oocytes. *EMBO J.* **21:** 4317–4326.

Hengartner, M.O. 1997. Apoptosis and the shape of death. *Dev. Genet.* **21:** 245–248.

Hofmann, E.R., Milstein, S., Boulton, S.J., Ye, M., Hofmann, J.J., Stergiou, L., Gartner, A., Vidal, M., and Hengartner, M.O. 2002. *Caenorhabditis elegans* HUS-1 is a DNA damage checkpoint protein required for genome stability and EGL-1-mediated apoptosis. *Curr. Biol.* **12:** 1908–1918.

Hubbard, E.J. and Greenstein, D. 2000. The *Caenorhabditis elegans* gonad: A test tube for cell and developmental biology. *Dev. Dyn.* **218:** 2–22.

Kamath, R.S., Fraser, A.G., Dong, Y., Poulin, G., Durbin, R., Gotta, M., Kanapin, A., Le Bot, N., Moreno, S., Sohrmann, M., et al. 2003. Systematic functional analysis of the *Caenorhabditis elegans* genome using RNAi. *Nature* **421:** 231–237.

Karashima, T., Sugimoto, A., and Yamamoto, M. 2000. *Caenorhabditis elegans* homologue of the human azoospermia factor DAZ is required for oogenesis but not for spermatogenesis. *Development* **127:** 1069–1079.

Kim, M.R. and Tilly, J.L. 2004. Current concepts in Bcl-2 family member regulation of female germ cell development and survival. *Biochim. Biophys. Acta* **1644:** 205–210.

Kinchen, J.M., Cabello, J., Klingele, D., Wong, K., Feichtinger, R., Schnabel, H., Schnabel, R., and Hengartner, M.O. 2005. Two pathways converge at CED-10 to mediate actin rearrangement and corpse removal in *C. elegans*. *Nature* **434:** 93–99.

Lackner, M.R. and Kim, S.K. 1998. Genetic analysis of the *Caenorhabditis elegans* MAP kinase gene *mpk-1*. *Genetics* **150:** 103–117.

Lai, W.S., Carballo, E., Strum, J.R., Kennington, E.A., Phillips, R.S., and Blackshear, P.J. 1999. Evidence that tristetraprolin binds to AU-rich elements and promotes the deadenylation and destabilization of tumor necrosis factor α mRNA. *Mol. Cell. Biol.* **19:** 4311–4323.

Lai, W.S., Carballo, E., Thorn, J.M., Kennington, E.A., and Blackshear, P.J. 2000. Interactions of CCCH zinc finger proteins with mRNA. Binding of tristetraprolin-related zinc finger proteins to Au-rich elements and destabilization of mRNA. *J. Biol. Chem.* **275:** 17827–17837.

Lettre, G. and Hengartner, M.O. 2006. Developmental apoptosis in *C. elegans*: A complex CEDnario. *Nat. Rev. Mol. Cell Biol.* **7:** 97–108.

Lettre, G., Kritikou, E.A., Jaeggi, M., Calixto, A., Fraser, A.G., Kamath, R.S., Ahringer, J., and Hengartner, M.O. 2004. Genome-wide RNAi identifies p53-dependent and -independent regulators of germ cell apoptosis in *C. elegans*. *Cell Death Differ.* **11:** 1198–1203.

Li, S., Armstrong, C.M., Bertin, N., Ge, H., Milstein, S., Boxem, M., Vidalain, P.O., Han, J.D., Chesneau, A., Hao, T., et al. 2004. A map of the interactome network of the metazoan *C. elegans*. *Science* **303:** 540–543.

Lim, D.S. and Hasty, P. 1996. A mutation in mouse rad51 re-

sults in an early embryonic lethal that is suppressed by a mutation in p53. *Mol. Cell. Biol.* **16:** 7133–7143.

Mahtani, K.R., Brook, M., Dean, J.L., Sully, G., Saklatvala, J., and Clark, A.R. 2001. Mitogen-activated protein kinase p38 controls the expression and posttranslational modification of tristetraprolin, a regulator of tumor necrosis factor α mRNA stability. *Mol. Cell. Biol.* **21:** 6461–6469.

Mello, C.C., Schubert, C., Draper, B., Zhang, W., Lobel, R., and Priess, J.R. 1996. The PIE-1 protein and germline specification in *C. elegans* embryos. *Nature* **382:** 710–712.

Miller, M.A., Nguyen, V.Q., Lee, M.H., Kosinski, M., Schedl, T., Caprioli, R.M., and Greenstein, D. 2001. A sperm cytoskeletal protein that signals oocyte meiotic maturation and ovulation. *Science* **291:** 2144–2147.

Moghal, N. and Sternberg, P.W. 2003. The epidermal growth factor system in *Caenorhabditis elegans*. *Exp. Cell Res.* **284:** 150–159.

Navarro, R.E., Shim, E.Y., Kohara, Y., Singson, A., and Blackwell, T.K. 2001. *cgh-1*, a conserved predicted RNA helicase required for gametogenesis and protection from physiological germline apoptosis in *C. elegans*. *Development* **128:** 3221–3232.

Page, B.D., Guedes, S., Waring, D., and Priess, J.R. 2001. The *C. elegans* E2F- and DP-related proteins are required for embryonic asymmetry and negatively regulate Ras/MAPK signaling. *Mol. Cell* **7:** 451–460.

Praitis, V., Casey, E., Collar, D., and Austin, J. 2001. Creation of low-copy integrated transgenic lines in *Caenorhabditis elegans*. *Genetics* **157:** 1217–1226.

Rual, J.F., Ceron, J., Koreth, J., Hao, T., Nicot, A.S., Hirozane-Kishikawa, T., Vandenhaute, J., Orkin, S.H., Hill, D.E., van den Heuvel, S., et al. 2004. Toward improving *Caenorhabditis elegans* phenome mapping with an ORFeome-based RNAi library. *Genome Res.* **14:** 2162–2168.

Schneider, S.Q. and Bowerman, B. 2003. Cell polarity and the cytoskeleton in the *Caenorhabditis elegans* zygote. *Annu. Rev. Genet.* **37:** 221–249.

Schubert, C.M., Lin, R., de Vries, C.J., Plasterk, R.H., and Priess, J.R. 2000. MEX-5 and MEX-6 function to establish soma/germline asymmetry in early *C. elegans* embryos. *Mol. Cell* **5:** 671–682.

Schumacher, B., Hofmann, K., Boulton, S., and Gartner, A. 2001. The *C. elegans* homolog of the p53 tumor suppressor is required for DNA damage-induced apoptosis. *Curr. Biol.* **11:** 1722–1727.

Seydoux, G. and Schedl, T. 2001. The germline in *C. elegans*: Origins, proliferation, and silencing. *Int. Rev. Cytol.* **203:** 139–185.

Shimada, M., Kawahara, H., and Doi, H. 2002. Novel family of CCCH-type zinc-finger proteins, MOE-1, -2 and -3, participates in *C. elegans* oocyte maturation. *Genes Cells* **7:** 933–947.

Sugiura, R., Kita, A., Shimizu, Y., Shuntoh, H., Sio, S.O., and Kuno, T. 2003. Feedback regulation of MAPK signalling by an RNA-binding protein. *Nature* **424:** 961–965.

Szewczyk, N.J., Hartman, J.J., Barmada, S.J., and Jacobson, L.A. 2000. Genetic defects in acetylcholine signalling promote protein degradation in muscle cells of *Caenorhabditis elegans*. *J. Cell Sci.* **113:** 2003–2010.

Szewczyk, N.J., Peterson, B.K., and Jacobson, L.A. 2002. Activation of Ras and the mitogen-activated protein kinase pathway promotes protein degradation in muscle cells of *Caenorhabditis elegans*. *Mol. Cell. Biol.* **22:** 4181–4188.

Tabara, H., Hill, R.J., Mello, C.C., Priess, J.R., and Kohara, Y. 1999. *pos-1* encodes a cytoplasmic zinc-finger protein essential for germline specification in *C. elegans*. *Development* **126:** 1–11.

Tanoue, T. and Nishida, E. 2002. Docking interactions in the mitogen-activated protein kinase cascades. *Pharmacol. Ther.* **93:** 193–202.

Taylor, G.A., Thompson, M.J., Lai, W.S., and Blackshear, P.J. 1995. Phosphorylation of tristetraprolin, a potential zinc finger transcription factor, by mitogen stimulation in intact cells and by mitogen-activated protein kinase in vitro. *J. Biol. Chem.* **270:** 13341–13347.

———. 1996. Mitogens stimulate the rapid nuclear to cytosolic translocation of tristetraprolin, a potential zinc-finger transcription factor. *Mol. Endocrinol.* **10:** 140–146.

Tilly, J.L. 2001. Commuting the death sentence: How oocytes strive to survive. *Nat. Rev. Mol. Cell Biol.* **2:** 838–848.

Varnum, B.C., Lim, R.W., Sukhatme, V.P., and Herschman, H.R. 1989. Nucleotide sequence of a cDNA encoding TIS11, a message induced in Swiss 3T3 cells by the tumor promoter tetradecanoyl phorbol acetate. *Oncogene* **4:** 119–120.

Vidal, M., Brachmann, R.K., Fattaey, A., Harlow, E., and Boeke, J.D. 1996a. Reverse two-hybrid and one-hybrid systems to detect dissociation of protein-protein and DNA-protein interactions. *Proc. Natl. Acad. Sci.* **93:** 10315–10320.

Vidal, M., Braun, P., Chen, E., Boeke, J.D., and Harlow, E. 1996b. Genetic characterization of a mammalian protein–protein interaction domain by using a yeast reverse two-hybrid system. *Proc. Natl. Acad. Sci.* **93:** 10321–10326.

Walhout, A.J. and Vidal, M. 2001. High-throughput yeast two-hybrid assays for large-scale protein interaction mapping. *Methods* **24:** 297–306.

Weischenfeldt, J., Lykke-Andersen, J., and Porse, B. 2005. Messenger RNA surveillance: Neutralizing natural nonsense. *Curr. Biol.* **15:** R559–R562.

Worthington, M.T., Pelo, J.W., Sachedina, M.A., Applegate, J.L., Arseneau, K.O., and Pizarro, T.T. 2002. RNA binding properties of the AU-rich element-binding recombinant Nup475/TIS11/tristetraprolin protein. *J. Biol. Chem.* **277:** 48558–48564.

Yan, N., Gu, L., Kokel, D., Chai, J., Li, W., Han, A., Chen, L., Xue, D., and Shi, Y. 2004. Structural, biochemical, and functional analyses of CED-9 recognition by the proapoptotic proteins EGL-1 and CED-4. *Mol. Cell* **15:** 999–1006.

Yan, N., Chai, J., Lee, E.S., Gu, L., Liu, Q., He, J., Wu, J.W., Kokel, D., Li, H., Hao, Q., et al. 2005. Structure of the CED-4-CED-9 complex provides insights into programmed cell death in *Caenorhabditis elegans*. *Nature* **437:** 831–837.

Zdinak, L.A., Greenberg, I.B., Szewczyk, N.J., Barmada, S.J., Cardamone-Rayner, M., Hartman, J.J., and Jacobson, L.A. 1997. Transgene-coded chimeric proteins as reporters of intracellular proteolysis: Starvation-induced catabolism of a lacZ fusion protein in muscle cells of *Caenorhabditis elegans*. *J. Cell. Biochem.* **67:** 143–153.

Zhang, F., Robbins, D.J., Cobb, M.H., and Goldsmith, E.J. 1993. Crystallization and preliminary X-ray studies of extracellular signal-regulated kinase-2/MAP kinase with an incorporated His-tag. *J. Mol. Biol.* **233:** 550–552.

Zhang, F., Strand, A., Robbins, D., Cobb, M.H., and Goldsmith, E.J. 1994. Atomic structure of the MAP kinase ERK2 at 2.3 Å resolution. *Nature* **367:** 704–711.

Zhang, J., Zhou, B., Zheng, C.F., and Zhang, Z.Y. 2003. A bipartite mechanism for ERK2 recognition by its cognate regulators and substrates. *J. Biol. Chem.* **278:** 29901–29912.

Supplementary figure legends

Supplementary Figure 1. Loss of *gla-3* function does not interfere with engulfment of apoptotic cells.

(A) Synchronized wild-type and *gla-3(op216)* mutant worms carrying the *opIs110[P_{lim-7}::ypf::act-5]* transgene were scored by DIC for germ-cell death and by fluorescence for engulfment, starting at the L4/adult molt. Corpses in the process of being engulfed were visualized with the *opIs110* transgene, which expresses a YFP-tagged actin in the somatic sheath cells (Kinchen et al. 2005). Most of the cell corpses observed in the *gla-3* mutants were surrounded by YFP::ACT-5 actin halos, indicating that they were in the process of being engulfed. Error bars represent S.D. of two experiments; 12 gonads were scored in each experiment. (B) Cell corpses in engulfment-defective animals are not surrounded by actin haloes. *ced-1(RNAi)*-treated *opIs110* animals show a greatly increased number of germ cell corpses, but very few of these are YFP::ACT-5-positive. *bir-1(RNAi)*, which does not affect germ-cell apoptosis or engulfment, was used as a negative control. Error bars represent S.D. of three experiments; 15 gonads were scored in each experiment.

A

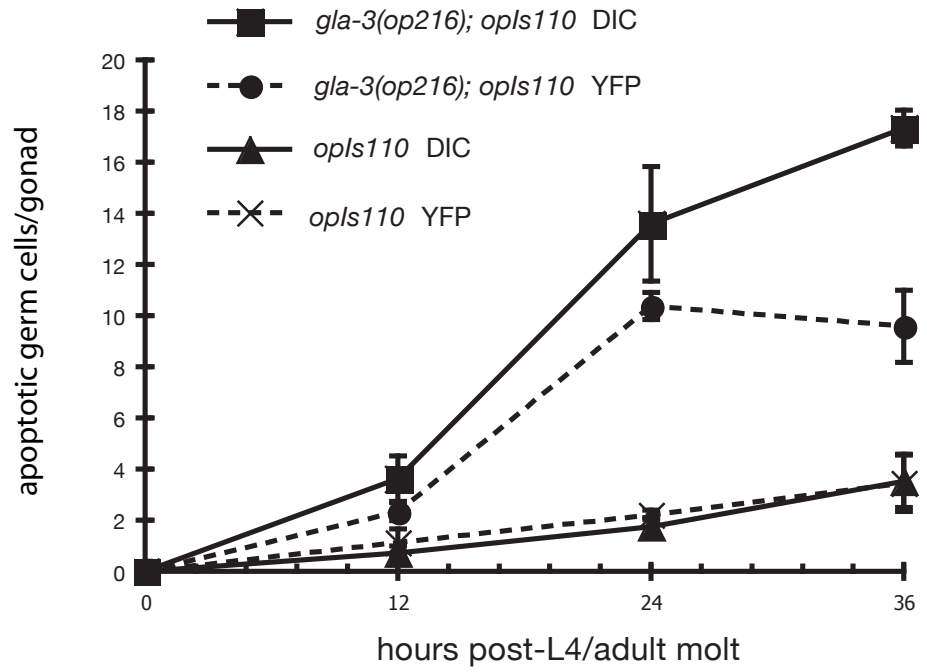
gla-3(op216); opIs110 DIC
gla-3(op216); opIs110 YFP
opIs110 DIC
opIs110 YFP
apoptotic germ cells/gonad
0
2
4
6
8
10
12
14
16
18
20
0
12
24
36
hours post-L4/adult molt

B

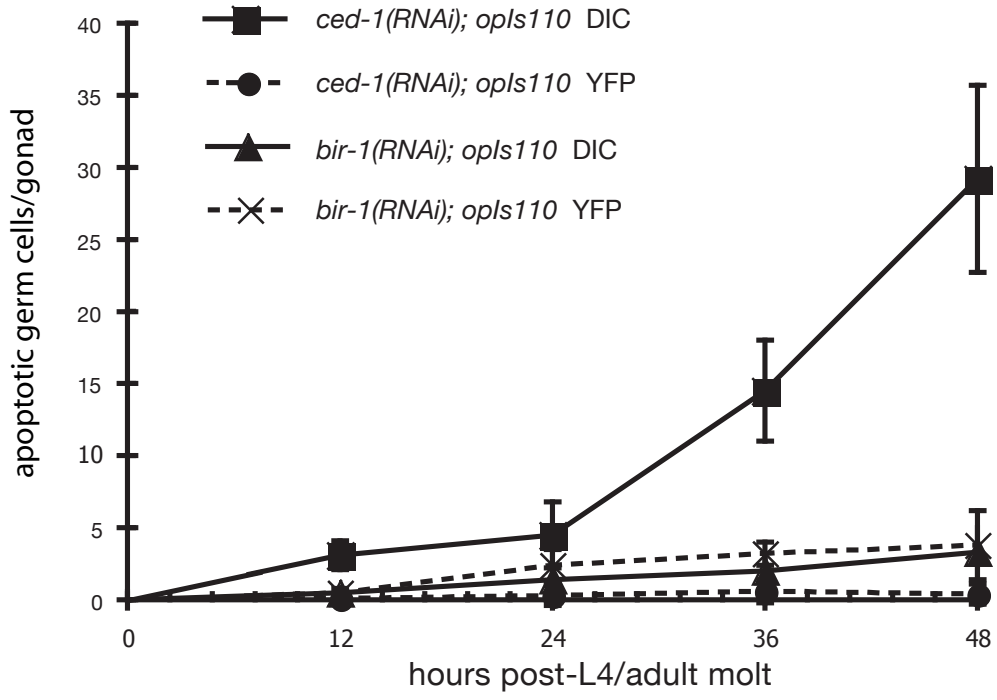
ced-1(RNAi); opIs110 DIC
ced-1(RNAi); opIs110 YFP
bir-1(RNAi); opIs110 DIC
bir-1(RNAi); opIs110 YFP
apoptotic germ cells/gonad
0
5
10
15
20
25
30
35
40
0
12
24
36
48
hours post-L4/adult molt

Supplementary Figure 2. DNA damage-induced germ cell-cycle arrest is normal in *gla-3* mutants.

Synchronized wild-type, *gla-3(op212)* and *hus-1(op244)* worms were exposed to 60 Gy of ionizing radiation at the L4/adult molt, and the number of cells in the proliferative region of the germ line (50μm from the distal end of the gonad) was scored 12 hours later by DIC (Hofmann et al. 2002). Error bars represent S.D. from three independent experiments; 5 gonads were scored in each experiment.

Supplementary Figure 2 Kritikou et al.

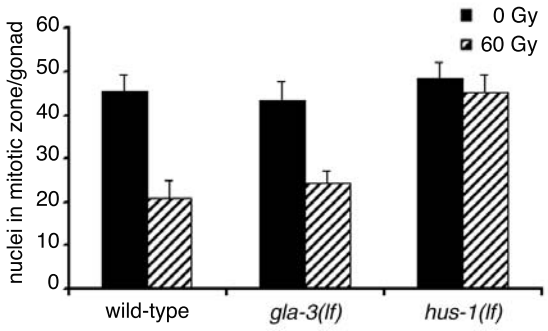

Supplementary Figure 3. *lip-1(lf)*-induced germline apoptosis is *ced-3*-dependent but *cep-1*-independent.

ced-3 and *cep-1* knockdown in wild-type and *lip-1(zh15)* worms was induced by RNAi feeding. Wild-type worms irradiated with 60 Gy were used as a positive control for CEP-1-dependent apoptosis. Error bars represent S.D. from two independent experiments; 20 gonads were scored in each experiment.

Supplementary Figure 3 Kritikou et al.

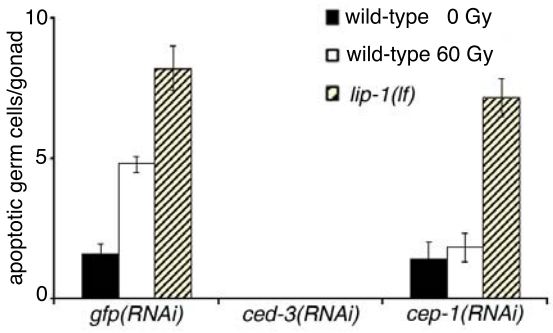

Supplementary Figure 4. Activated DP-MPK-1 staining in *gla-3(lf)* gonads.

(A) Activated MPK-1 (red) and DAPI staining (blue) in wild-type and *gla-3(lf)* gonads. The gonads of hermaphrodites 24 hours post L4/adult molt were dissected and stained with an antibody specific for the activated, di-phosphorylated form of MPK-1. Scale bar, 8 μm. (B) Relative MAPK activity was measured *in vitro* as previously described (Berset et al. 2001). *lip-1(zh15), let-60(n1046gf)* and *gaIs36[HS-mpk-1(+) EF1a-D-mek(+) unc-30(+)]* animals were used as positive controls. Data is representative of five independent experiments.

Supplementary Figure 4 Kritikou et al.

A

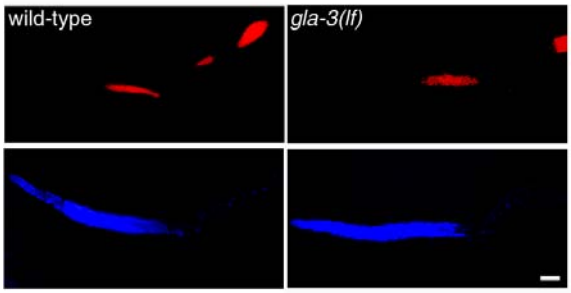

B

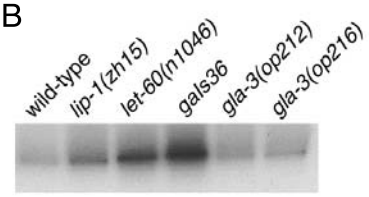

Supplementary Figure 5. GLA-3 expression in mutants of the MAPK pathway.

Western blot analysis of adult wild-type, *mpk-1(oz140), let-60(n1046), let-60(ga89) and lip-1(zh15)* worms using isoform-specific anti-GLA-3 antibodies. Total protein was extracted as described in Materials and Methods. 20 μg of total protein was loaded per lane; α-tubulin was used as a loading control.

Supplementary Figure 5 Kritikou et al.

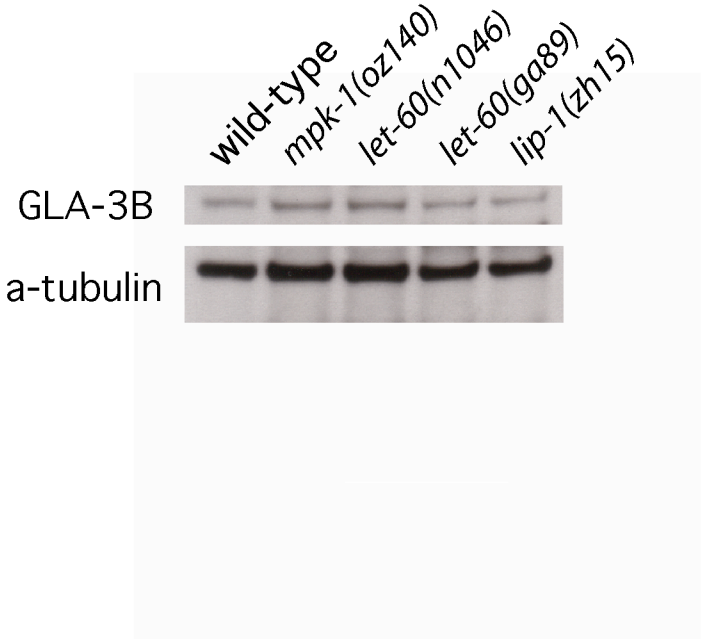

Supplementary Table I

Kritikou et al.

Supplementary Table I. *gla-3(lf)* males are fertile[a]

Cross: male x hermaphrodite	No. of embryos	No. of cross progeny
wild type x *unc-32(e189)*	431±75	417±60
gla-3(op212) x *unc-32(e189)*	405±95	389±81
gla-3(op216) x *unc-32(e189)*	365±74	370±63

[a] For each genotype, 12 crosses were set up with three males and one L4/adult molt stage hermaphrodite. Data shown are average ± SD.

Supplementary Table II

Kritikou et al.

Supplementary Table II. Oocyte development is impaired in *gla-3(lf)* mutants

Genotype	No. of diakinesis stage oocytes in proximal arm[a] *(n=60)*	% of sterile animals[b] *(n=50)*
wild type	7.5 ± 1.2	0
unc-32(e189) mpk-1(ga117)	0	100
gla-3(op212);unc32(e189)	1.5 ± 0.7	0
gla-3(op212);unc-32(e189) mpk-1(ga117)	0	100
let-60(ga89)	12.3 ± 2.3	0
lip-1(zh15)	10.1 ± 1.7	0
gla-3(op216)	7.1 ± 1.6	0
gla-3(op212)	2.0 ± 0.8	0
gla-3(op216);let-60(ga89)	7.5 ± 2.5	0
gla-3(op212);let-60(ga89)	1.6 ± 0.8	0
gla-3(op216);lip-1(zh15)	5.3 ± 1.4	0
gla-3(op212);lip-1(zh15)	1.2 ± 1.0	0

[a] Diakinetic stage oocytes present in the proximal gonad arm were scored by DAPI staining in synchronized hermaphrodites 24 hours post L4/adult molt, as described in Materials and Methods. Data shown are average ± S.D.

Supplementary Table III

Kritikou et al.

Supplementary Table III. Loss of *mpk-1* suppresses *ced-9(lf)*- and *gla-3(RNAi)*-mediated germ cell death

Genotype	No of apoptotic germ cell corpses at 25°C	
	12 hours post L4/adult molt	*36 hours post L4/adult molt*
gfp(RNAi); mpk-1(oz140) ced-9(n2812)	1.0 ± 0.4	0.9 ± 0.3
gla-3(RNAi); mpk-1(oz140) ced-9(n2812)	1.1 ± 0.2	1.2 ± 0.6
gfp(RNAi)	2.1 ± 0.6	4.3 ± 0.8
gla-3(RNAi)	8.2 ± 1.8	12.4 ± 1.3

Data shown are average ± S.D. of two independent experiments; 20 gonads were scored in each experiment.

CHAPTER 5

THE NUCLEOTIDE EXCISION REPAIR PATHWAY IS REQUIRED FOR UV-C-INDUCED APOPTOSIS IN *CAENORHABDITIS ELEGANS*

CHAPTER 5

THE NUCLEOTIDE EXCISION REPAIR PATHWAY IS REQUIRED FOR UV-C-INDUCED APOPTOSIS IN *CAENORHABDITIS ELEGANS*

5.1 PREFACE

Here I describe a collaborative project, which led to the first report of a genetic pathway mediating UV-C-induced apoptosis in the *C. elegans* germ line. This project was initiated by Dr. Lilli Stergiou during the last 2 years of her PhD studies in the Hengartner lab and was later continued and expanded upon her graduation for an additional year. Lilli's initial ambition was to use the worm's powerful genetics in order to characterize the role of ATM-1 and ATL-1, the *C. elegans* homologs of ataxia telengiectasia mutated-1 and ataxia telengiectasia and Rad3-related, respectively, two proteins located in the heart of DNA damage signaling in mammals. The project took an exciting turn when we realized that loss of function mutations in components of the nucleotide excision repair machinery exhibited a defect in apoptosis upon UV-C but not upon ionizing radiation. This prompted us to investigate further the genetic requirements for UV-C-induced cell death as well as the complex interplay between DNA repair factors and pro-apoptotic molecules.

All the experiments were designed and performed by Dr. Lilli Stergiou. My contribution to this study can be resumed as follows: I blindly scored germ cell apoptosis for the experiments depicted on Figure 2c, Figure 3d and Figure 5 to independently confirm the results we had obtained. Additionally, I performed all the cloning for the *xpc-1(RNAi)* bacterial clone and made the graphic figure of the different gene models in Figure S1.

Cell Death and Differentiation (2007), 1–10

www.nature.com/cdd

The nucleotide excision repair pathway is required for UV-C-induced apoptosis in *Caenorhabditis elegans*

L Stergiou[1], K Doukoumetzidis[1,2], A Sendoel[1,3,4] and MO Hengartner*,[1]

Ultraviolet (UV) radiation is a mutagen of major clinical importance in humans. UV-induced damage activates multiple signaling pathways, which initiate DNA repair, cell cycle arrest and apoptosis. To better understand these pathways, we studied the responses to UV-C light (254 nm) of germ cells in *Caenorhabditis elegans*. We found that UV activates the same cellular responses in worms as in mammalian cells. Both UV-induced apoptosis and cell cycle arrest were completely dependent on the p53 homolog CEP-1, the checkpoint proteins HUS-1 and CLK-2, and the checkpoint kinases CHK-2 and ATL-1 (the *C. elegans* homolog of ataxia telangiectasia and Rad3-related); ATM-1 (ataxia telangiectasia mutated-1) was also required, but only at low irradiation doses. Importantly, mutation of genes encoding nucleotide excision repair pathway components severely disrupted both apoptosis and cell cycle arrest, suggesting that these genes not only participate in repair, but also signal the presence of damage to downstream components of the UV response pathway that we delineate here. Our study suggests that whereas DNA damage response pathways are conserved in metazoans in their general outline, there is significant evolution in the relative importance of individual checkpoint genes in the response to specific types of DNA damage.
Cell Death and Differentiation advance online publication, 9 March 2007; doi:10.1038/sj.cdd.4402115

Maintenance of genome integrity is critically important for organisms to survive. In the presence of DNA damage, cells respond by activation of surveillance mechanisms that lead to cell cycle arrest and DNA repair. Highly damaged cells are often eliminated by apoptosis as a protective mechanism against the fixation of new mutations. The importance of these pathways is underscored by the observation that disruption of the DNA damage response pathway leads to an increased probability of cancer in humans.

In order to elucidate the complex molecular events that mediate the cellular responses to DNA damage, significant effort is being made in simple model organisms. The power of *Caenorhabditis elegans* as a system to genetically identify proteins that regulate apoptosis has been well established.[1,2] Recent analyses in *C. elegans* have identified a conserved checkpoint pathway that transduces the DNA damage signal caused by ionizing radiation (IR) to the cell cycle and the apoptotic machinery.[3,4] This pathway comprises the 9-1-1 complex (HUS-1/MRT-2/HPR-9) and a novel checkpoint protein, CLK-2, acting in parallel.[5,6] The CEP-1/p53 tumor suppressor protein is required for IR-induced apoptosis (but not cell cycle arrest). Activation of CEP-1/p53 leads to transcriptional upregulation of the BH3-only target genes, *egl-1* and *ced-13*,[5,7–9] which in turn activate the *C. elegans* apoptotic machinery.[1,10]

Ultraviolet (UV) light in the UV-B (<280 nm) and UV-C (280–315 nm) range damages DNA through the formation of cyclobutane pyrimidine dimers (CPDs) and 6-4 photoproducts (6-4 PPs).[11,12] UV radiation is a potent mutagen and both epidemiological and molecular evidence have established it as the major cause of human skin cancers. The removal of UV-induced DNA lesions is undertaken by the nucleotide excision repair (NER) machinery, which also removes adducts produced by chemotherapeutic agents, such as cisplatin.[13] Two branches of NER, global genome repair (GGR) and transcription-coupled repair (TCR), have been identified. Both require multiple proteins that act in a multistep process: DNA damage recognition, DNA unwinding and incision, and finally repair synthesis and ligation.[14,15] The presence of UV-induced DNA lesions also activates members of the PI3 kinase family, ATR (ataxia telangiectasia and Rad3-related) and ATM (ataxia telangiectasia mutated).[16,17] ATR mediates the response to both UV- and IR-induced lesions as well as to stalled replication forks, whereas ATM is primarily responsible for the response to double-strand breaks (DSBs).

In this study, we describe our genetic analysis of the responses to UV-C light in the adult germ line of the nematode *C. elegans*. We delineate a signaling pathway that leads to cell cycle arrest and apoptosis. This pathway comprises several previously described components of the IR response pathway, including CEP-1/p53, HUS-1, CLK-2 and the *C. elegans* ATR homolog ATL-1. We also provide for the first time evidence that the checkpoint kinase CHK-2 and participates in DNA damage response in *C. elegans*. Importantly, we show

[1]Institute of Molecular Biology, University of Zurich, Winterthurerstrasse, Zurich, Switzerland; [2]Ph.D. Program in Molecular Life Sciences, University of Zurich, Winterthurerstrasse, Zurich, Switzerland; [3]M.D./Ph.D. program, University of Zurich, Winterthurerstrasse, Zurich, Switzerland and [4]Ph.D. Program in Cancer Biology, University of Zurich, Winterthurerstrasse, Zurich, Switzerland
*Corresponding author: M Hengartner, Institute of Molecular Biology, University of Zurich, Room 55 L 24, Winterthurerstrasse 190, CH-8057 Zurich, Switzerland. Tel: +41 1 635 3140; Fax: +41 1 635 6861; E-mail: michael.hengartner@molbio.unizh.ch
Keywords: apoptosis; *C. elegans*; cell cycle arrest; NER; UV-C
Abbreviations: UV, ultraviolet light; IR, ionizing radiation; ATM, ataxia telangiectasia mutated; ATR, ataxia telangiectasia and Rad3-related; CHK1/2, checkpoint kinase 1/2; CPDs, cyclobutane pyrimidine dimers; 6-4 PPs, 6-4 photoproducts; NER, nucleotide excision repair; GGR, global genome repair; TCR, transcription-coupled repair; DSBs, double-strand breaks; XPA, xeroderma pigmentosum complementation group A; XPC, xeroderma pigmentosum complementation group C
Received 24.11.06; revised 17.1.07; accepted 24.1.07; Edited by E Baehrecke

that components of the NER machinery are required for UV-induced cell cycle arrest and apoptosis, and are necessary for the recruitment and activation of the 9-1-1 complex. Our results suggest that DNA damage response pathways evolved significantly during metazoan radiation, and confirm the usefulness of *C. elegans* as a model to dissect the responses to UV radiation in a multicellular organism.

Results

UV-C induces apoptosis in the *C. elegans* germ line. We previously showed that exposure of the adult *C. elegans* germ line to IR results in cell cycle arrest in the mitotic stem cell compartment and apoptotic death of pachytene cells.[18] To determine the effects of UV light on germline physiology, which causes a pattern of DNA damage distinct from the one observed following IR,[11] we exposed young adult hermaphrodites to increasing doses of UV-C radiation (254 nm) and measured the extent of germ cell apoptosis (Figure 1) and cell cycle arrest (see below) over time. We found that UV-C induces germ cell death in a dose-dependent manner, reaching a plateau at 100 J/m^2 (Figure 1a). The kinetics of UV-C induced cell death were similar to those observed with IR, with increased apoptosis visible as early as 3 h post-treatment and persisting for at least 36 h (Figure 1b). These results indicate the presence in *C. elegans* of a signaling pathway that senses UV-C-induced damage, and conveys this information to the apoptotic machinery.

UV-C-induced upregulation of *egl-1* and *ced-13* requires CEP-1/p53 and conserved checkpoint genes. To identify the genetic pathway that mediates UV-C-induced apoptosis, we concentrated our attention first on genes previously shown to mediate IR-induced apoptosis. An important step in IR-induced apoptosis in *C. elegans* is the CEP-1/p53-dependent transcriptional upregulation of *egl-1* and *ced-13*, which encode proapoptotic BH3 domain proteins.[5,9] Using real-time Q-RT-PCR, we found that transcript levels of both *egl-1* and *ced-13* were also increased following UV treatment, albeit to a lesser extent than following IR (Figure 1c). Furthermore, loss of *egl-1* and *ced-13* function abrogated or reduced, respectively, UV-C-induced apoptosis (Figure 1d and e). Taken together, these observations suggest that UV-C induces apoptosis by stimulating increased expression of the BH3 domain proteins EGL-1 and CED-13.

IR-induced cell death in the *C. elegans* germ line requires the p53 homolog, *cep-1*,[7,8] and the checkpoint genes *hus-1*, *mrt-2* and *rad*-5/*clk-2*.[4–6,18] HUS-1 and MRT-2 are components of the 9-1-1 complex in *C. elegans*, whereas CLK-2 is the *C. elegans* homolog of *Saccharomyces cerevisiae* Tel2p. To investigate whether these well-conserved components also participate in the response to UV-C light, we quantified germline apoptosis following UV radiation in the respective mutant backgrounds. Loss of *cep-1* and *clk-2* completely abrogated UV-induced cell death (Figure 2a), whereas apoptosis was strongly reduced but not abolished in *hus*-1 or *mrt-2* mutants (Figure 2b).

In mammals, the CHK2 kinase is known to activate p53 through phosphorylation on Ser20[19] to induce apoptosis

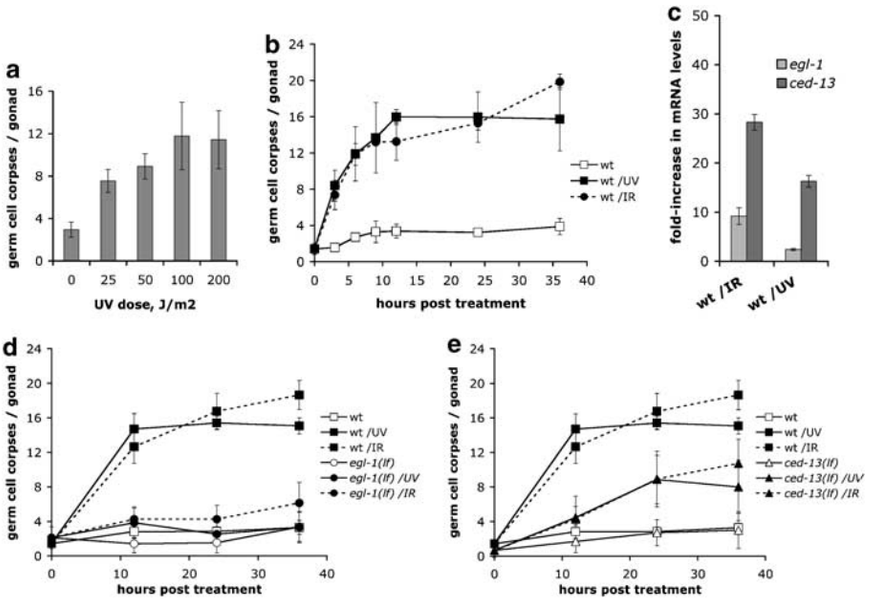

Figure 1 UV-C radiation induces apoptosis in the *C. elegans* germ line via transcriptional activation of *egl-1* and *ced-13*. (**a**) Dose–response. Apoptotic germ cell corpses were scored in young adult animals 12 h after treatment with different doses of UV-C radiation. (**b**) Time course. Apoptotic germ cell corpses were scored at the indicated times following exposure to 100 J/m^2 of UV-C radiation or 120 Gy of X-rays. (**c**) Transcriptional induction of *egl-1* and *ced-13* upon UV-C radiation. Relative mRNA levels of *egl-1* and *ced-13* were determined by real-time Q-RT-PCR in wild-type animals (wt), 12 h following treatment with either 120 Gy X-rays or 100 J/m^2 UV-C. Data shown represent the average fold-change of three independent experiments ± S.D. (**d**, **e**) Germ cell apoptosis following exposure to 100 J/m^2 UV-C or 120 Gy X-rays was scored in *egl-1*(*n1084n3082*) (**d**) or *ced-13*(*gk260*) (**e**) mutants. Data shown represent the average of three independent experiments ± S.D. ($n > 20$ animals for each experiment)

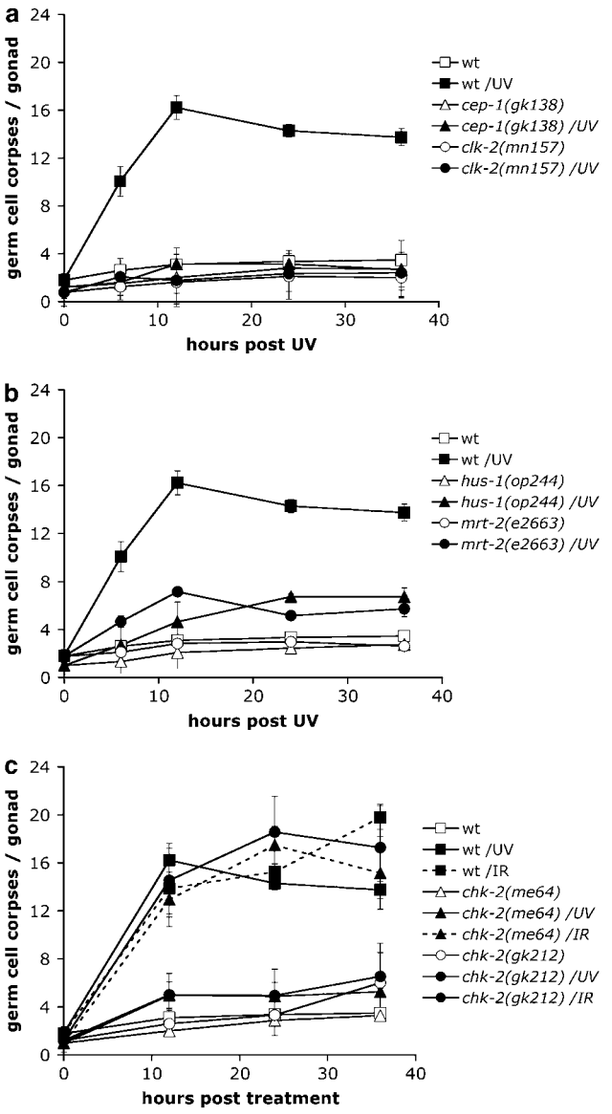

Figure 2 Genetic requirements for UV-C-induced apoptosis. Germ cell apoptosis following exposure to 100 J/m^2 UV-C or 120 Gy X-rays was scored in (**a**) *cep-1*(*gk138*), *clk-2*(*mn159*), (**b**) hus-*1*(*op244*), *mrt-2*(*e2663*) and (**c**) *chk-2*(*me64*), *chk-2*(*gk212*) mutants. Data shown represent the average of three independent experiments $\pm$ S.D. ($n > 20$ animals for each experiment)

following exposure to IR and UV.[20,21] Surprisingly, *C. elegans chk-2* mutants show a normal apoptotic response following IR.[22] To determine whether CHK-2 might play a role in UV response, we analyzed *chk-2* mutants for UV-induced germ cell apoptosis. Remarkably, both alleles of *chk-2* that we tested, *me64* (premature stop codon) and *gk212* (large deletion; see Supplementary Figure 1c), failed to exhibit increased cell death upon UV-C treatment (Figure 2c). In contrast, IR caused an increase indistinguishable from wild type (Figure 2c), confirming the results of MacQueen and Villeneuve.[22] Our findings are consistent with the hypothesis that UV-C induced phosphorylation of CEP-1 by CHK-2 leads to transcriptional activation of *egl-1* and *ced-13* and subsequent cell death.

The checkpoint kinase CHK1 has been implicated in UV-induced checkpoint activation in mammals.[23] To determine the function of the *C. elegans* CHK1 ortholog CHK-1 in DNA damage response, we scored *chk-1*(*RNAi*) animals for apoptosis (*chk-1* null mutants could not be tested, as they die during embryogenesis). Surprisingly, we found that *chk-1*(*RNAi*) animals were still proficient for both IR- and UV-C-induced germ cell apoptosis (Supplementary Figure 2). With the caveat that our analysis is based on RNAi, these results suggest that CHK-1 either plays a redundant role (perhaps together with CHK-2), or does not function at all in DNA damage-induced apoptosis.

ATL-1 is necessary to activate UV-induced germ cell apoptosis. In mammals, activation of CHK2 following DNA damage is mediated by the PI3K-like family members ATR and ATM.[24,25] Previous RNAi and genetic experiments have suggested that ATM-1 and ATL-1, the *C. elegans* orthologs of ATM and ATR, respectively, are required for apoptosis following IR.[26,27] To determine the role of these two kinases in the UV response pathway, we first analyzed germ cell apoptosis in animals carrying the null allele *atl-1*(*tm853*). We found that *atl-1*(*tm853*) mutants failed to induce germ cell apoptosis following treatment with either UV-C or IR (Figures 3a, b and 4a–d). Surprisingly, animals heterozygous for the *tm853* deletion allele also showed a reduced response to both treatments, suggesting either that the *tm853* deletion allele behaves as a dominant-negative mutation, or that the *atl-1* locus is partially haploinsufficient for DNA damage-induced apoptosis. To distinguish between these two possibilities, we determined the response to UV-C of animals heterozygous for *sDf29* or *mDf1*, two large genetic deficiencies that completely remove the *atl-1* locus. Both *sDf29*/+ and *mDf1*/+ animals showed a reduced apoptotic response following UV (Figure 3c), supporting the latter hypothesis. In contrast to our observations, previous experiments with *atl-1*(*tm853*) showed that animals heterozygous for this allele have a wild-type response to IR-induced apoptosis.[26] We do not know the cause for this discrepancy at the time being.

A dose-dependent requirement for ATM-1 in DNA damage-induced apoptosis. Whereas mammalian ATR responds primarily to UV or stalled replication forks, ATM reacts mainly to DSBs.[17] To determine the function of *C. elegans atm-1* in the DNA damage response, we characterized the behavior of *atm-1*(*gk186*) mutant animals. The *gk186* mutation results in a 550 bp deletion in the 4.9 kb *atm-1* ORF, which deletes parts of intron 1 and exon 2 (Supplementary Figure 1a). RT-PCR analysis revealed the presence of several truncated mRNA species in *gk186* mutants (Supplementary Figure 1a); sequencing of the major mRNA product revealed that the splicing machinery used a cryptic splice acceptor site within exon 2, resulting in a frame shift and the premature termination of translation. As all conserved domains are either within or downstream of the *gk186* deletion, we suspect that the mutant is a functional null.

The *atm-1*(*gk186*) mutants showed a strong induction of germ cell apoptosis following 120 Gy of X-rays (Figure 3d).

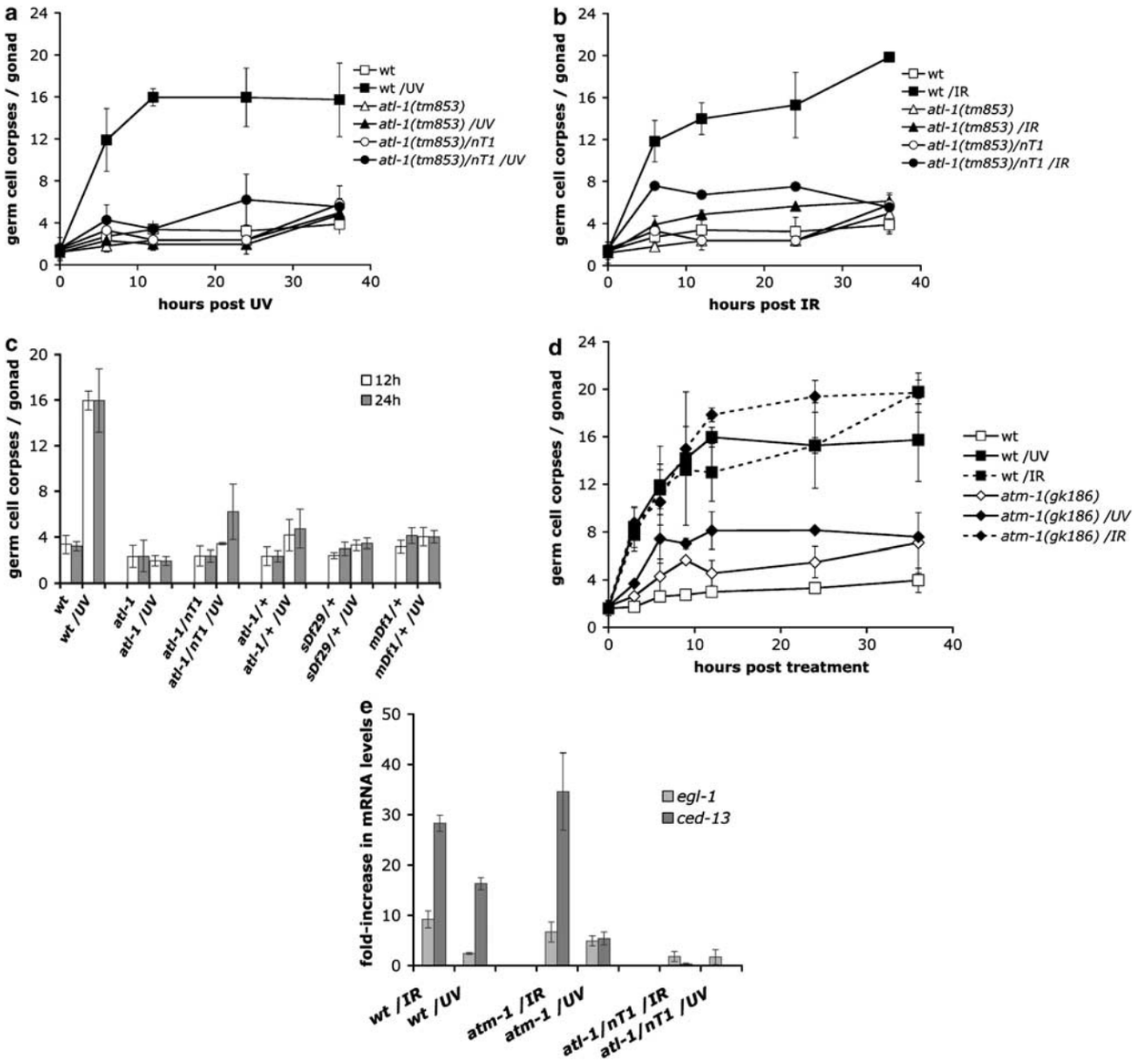

Figure 3 ATL-1 and ATM-1 are necessary for UV-C-induced *egl-1* and *ced-13* upregulation and germ cell apoptosis. (**a**, **b**) Time course of germ cell apoptosis in animals homozygous or heterozygous for the ATR deletion allele *atl-1*(*tm853*) following exposure to 100 J/m^2 of UV-C radiation (**a**) or 120 Gy of X-rays (**b**). Data shown represent the average of three independent experiments $\pm$ S.D. (**c**) Apoptotic germ cell corpses were scored 12 and 24 h post-exposure to 100 J/m^2 of UV-C in young adult animals of the following genotypes: wild type (wt), *atl-1*(*tm853*), *atl-1*(*tm853*)/*nT1*, *atl-1*(*tm853*)/+, *sDf29*/+ and *mDf1*/+, the last two being large deficiencies that remove, among other, the *atl-1* locus. Data shown represent the average of three independent experiments $\pm$ S.D. ($n > 15$ animals for each experiment). (**d**) DNA damage-induced germ cell apoptosis is compromised in *atm-1*(*gk186*) mutants after UV treatment, whereas it occurs normally upon X-ray irradiation. Young adult *atm-1*(*gk186*) animals were exposed to 100 J/m^2 of UV-C radiation or 120 Gy of X-rays and germ cell corpses scored as described. (**e**) Transcriptional induction of *egl-1* and *ced-13* upon UV-C radiation is dependent on *atl-1* and *atm-1*. Relative mRNA levels of *egl-1* and *ced-13* were determined by real-time Q-RT-PCR, 12 h following treatment with either 120 Gy of X-rays or 100 J/m^2 of UV-C, in the indicated genetic backgrounds. Data shown represent the average fold-change of three independent experiments $\pm$ S.D.

However, the response to lower doses of IR (15 or 30 Gy) was seriously compromised (Figure 4f). In contrast, the apoptotic response of *atm-1*(*gk186*) mutants to UV-C was significantly reduced at both high and low doses: death induction was reduced by more than 50% at 100 J/m^2 (Figure 3d), and appeared completely absent at 15 J/m^2 (Figure 4e). Dose–response studies confirmed these distinct response patterns (Figure 4g and h).

Our results suggest that, under low damage conditions, ATM-1 function is crucial for the induction of apoptosis following UV-C or IR. The reduced requirement for ATM-1 at higher doses of IR could be due to activation or recruitment of additional proteins or pathways that act redundantly with, or bypass ATM-1.

Where in the signaling pathway do ATL-1 and ATM-1 act? To determine whether *atl-1* or *atm-1* function is required for

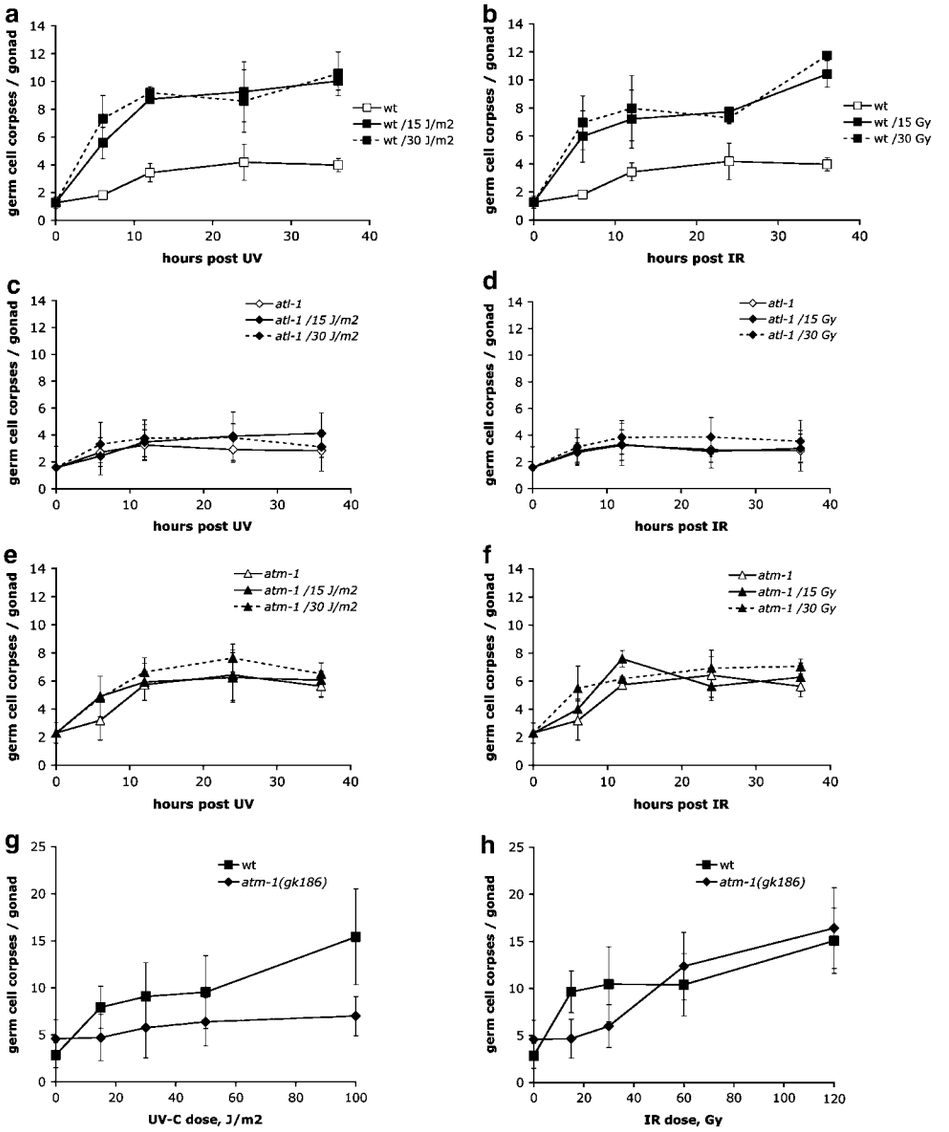

Figure 4 Apoptosis in response to low doses of DNA damage requires both *atl-1* and *atm-1*. Apoptotic germ cell corpses were scored in the meiotic region of wild-type (wt) animals (**a**, **b**), *atl-1*(*tm853*) (**c**, **d**) and *atm-1*(*gk186*) (**e**, **f**) mutants after exposure to either 15 or 30 J/m^2 of UV-C radiation (**a**, **c**, **e**) or 15 and 30 Gy of X-rays (**b**, **d**, **f**). Data shown represent the average of three independent experiments $\pm$ S.D. ($n > 20$ animals for each experiment). (**g**, **h**) Dose–response. Apoptotic germ cell corpses were scored in young adult wild-type (wt) or *atm-1*(*gk186*) animals 12 h after treatment with different doses of UV-C radiation (**g**) or X-rays (**h**). Data shown represent the average of three independent experiments $\pm$ S.D. ($n > 20$ animals for each experiment)

UV-induced transcriptional upregulation of *egl-1* and *ced-13*, we measured mRNA levels of these proapoptotic genes following DNA damage in *atl-1*(*tm853*) and *atm-1*(*gk186*) mutants (Figure 3e). Consistent with the apoptosis defect, we described above, upregulation of both genes was strongly impaired in *atl-1* mutants. The response pattern of *atm-1*(*gk186*) mutants was more complex: *ced-13* induction was significantly reduced following UV-C, whereas *egl-1* levels remain largely unaffected. These results indicate that ATL-1 and ATM-1 function upstream of *egl-1* and *ced-13* and suggest that ATM-1 might be preferentially required for upregulation of *ced-13* in response to UV-C.

The NER machinery is required for triggering UV-C-induced apoptosis. UV-induced DNA damage is normally recognized and repaired via the NER pathway in eukaryotes. We posited that recognition of UV lesions by the NER machinery might be required not only for DNA repair, but also to activate the downstream signaling pathways that lead to apoptosis. To test this hypothesis, we analyzed the effect on UV-C-induced apoptosis of two previously uncharacterized mutations in the NER genes *xpc-1*(Y76B12C.2) and *xpa-1*,[28] which encode the *C. elegans* homologs of xeroderma pigmentosum complementation group C (XPC) and xeroderma pigmentosum complementation group A (XPA), respectively.

Animals homozygous for the *xpc-1*(*ok734*) mutation showed reduced apoptosis following UV-C treatment, whereas their response to IR was normal (Figure 5a). Surprisingly, we found that the *ok734* mutation removes 1.7 kb of intron 3, but does not affect any exonic sequences (Supplementary Figure 1d). Indeed, a normal-size transcript could still be detected in *ok734* mutants, likely explaining the mild defect that we observed. Consistent with this hypothesis, animals treated with *xpc-1*(*RNAi*) resulted in a much more severe defect (Figure 5b), suggesting that XPC function is necessary for UV-induced apoptosis.

The *xpa-1*(*ok698*) deletes half of the ORF, and leads to a degradation of the deletion transcript (Supplementary Figure 1e). Thus, this mutation is likely to be a null. Koo and co-workers previously reported that *xpa-1*(*RNAi*) animals exhibit reduced embryonic survival and survival to adulthood rate upon UV-C.[29] We found that UV-induced apoptosis is completely abolished in the absence of *xpa-1* (Figure 5c), consistent with the hypothesis that lack of proper damage recognition can disturb signaling to the apoptotic machinery. In contrast to UV, IR-induced apoptosis still occurs in the absence of *xpa-1*, although with somewhat reduced levels compared with the wild type (Figure 5c). The slight defect that we observed implies that a fraction of the DNA damage generated by X-rays likely is recognized and repaired via the NER pathway.

Notably, non-UV-treated *xpc-1*(*RNAi*) and *xpa-1*(*ok698*) animals had more germ cell apoptosis than wild-type worms (Figure 5b and c). We postulate that the accumulation of unrepaired endogenous damage in these animals eventually

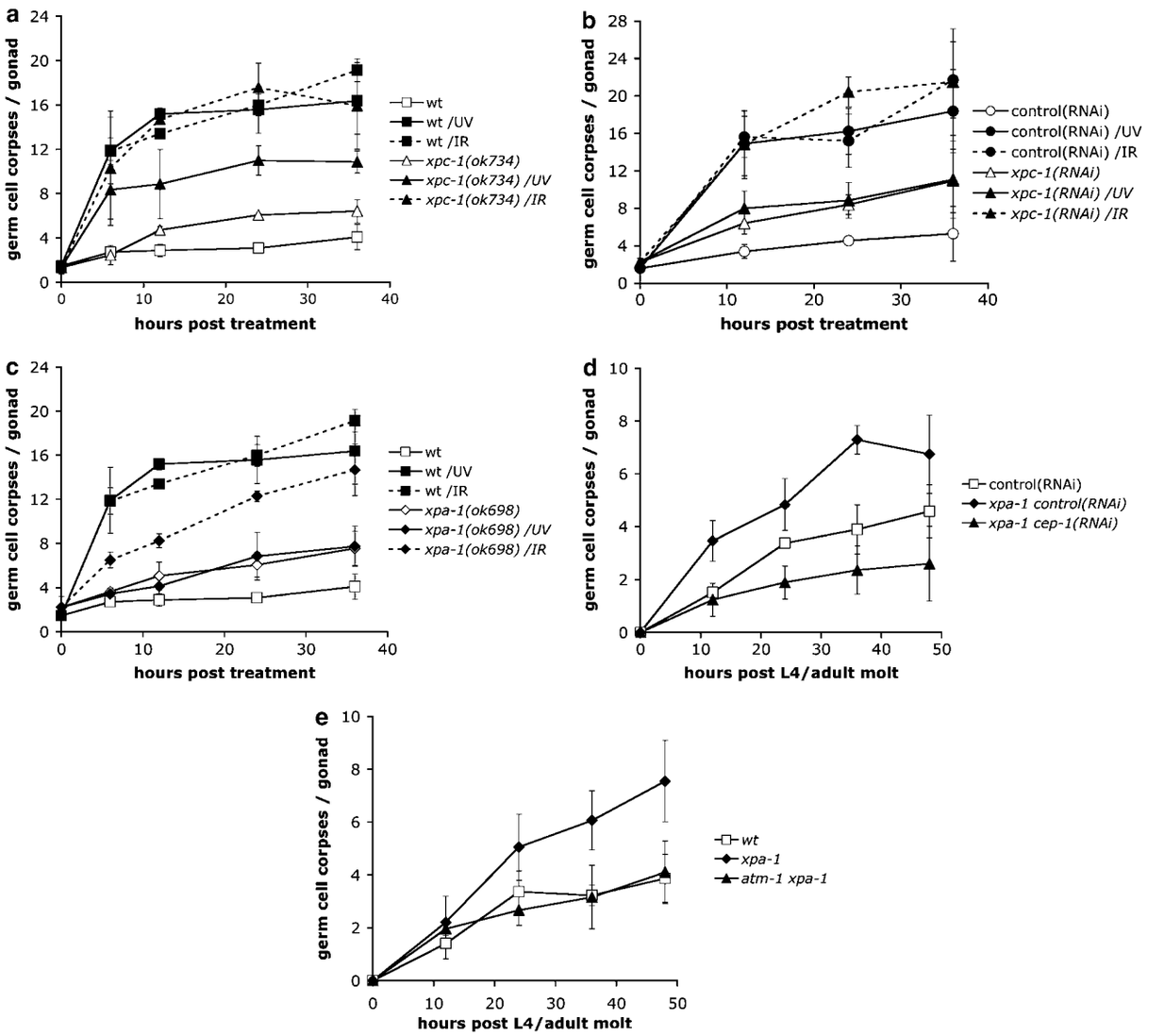

Figure 5 The NER machinery is required for triggering UV-C-induced germ cell apoptosis. Staged *xpc-1*(*ok734*) (**a**), *xpc-1*(*RNAi*) (**b**) and *xpa-1*(*ok698*) (**c**) young adults were treated with either 100 J/m^2 UV-C or 120 Gy X-rays and apoptotic germ cell corpses were scored at the indicated time points. (**d**, **e**) Germ cell apoptosis was scored every 12 h until 48 h post L4/adult molt in staged: *xpa-1*(*ok698*) and *xpa-1*(*ok698*) *cep-1*(*RNAi*) (**d**) or *atm-1*(*gk186*) *xpa-1*(*ok698*) (**e**) animals. Data shown represent the average of three independent experiments $\pm$ S.D. ($n > 20$ animals for each experiment)

leads to apoptosis through activation of (an)other DNA damage signaling pathway(s). Indeed, the increased basal germ cell apoptosis was abrogated in *xpa-1*(*ok698*); *cep-1* (*RNAi*) and *atm-1*(*gk186*) *xpa-1*(*ok698*) animals (Figure 5d and e), suggesting that this increase was due to activation of an *atm-1*- and *cep-1*-dependent pathway.

The HUS-1 complex acts downstream of NER to promote UV-C-induced apoptosis. The results we presented above suggest that recognition and/or processing of DNA damage by the NER machinery is an essential, and likely early step in UV-C-induced apoptosis. To more precisely position the NER components within this signaling cascade, we determined the subcellular distribution of the 9-1-1 complex subunit HUS-1 in some of the mutants we described above.

We previously showed that HUS-1::GFP, which is normally diffusely distributed in the nuclei of germ cells, accumulates into distinct foci upon IR.[5] We found that HUS-1::GFP also formed foci following exposure to UV-C light (Figure 6a and b), consistent with our observation that HUS-1 participates in UV-C-induced apoptosis (Figure 2b). Elimination of *xpa*-1 (which is required for apoptosis in response to UV-C but not IR) dramatically reduced the foci accumulation following UV treatment (Figure 6a and b). By contrast, foci formation following IR was still robust (Figure 6b). These results suggest that the NER proteins act upstream of 9-1-1 complex recruitment.

We also analyzed HUS-1::GFP recruitment in *atm-1* and *cep-1* mutants. We found that the basal levels of HUS-1::GFP foci was elevated in the absence of *atm-1*, suggesting elevated levels of endogenous DNA damage and/or decreased repair activity in the mutants (Figure 6b). Both IR and UV treatment further increased the number of HUS-1::GFP foci, indicating that ATM-1 is not required for the recruitment of the 9-1-1 complex. Similarly, knockdown of *cep-1* did not significantly alter HUS-1::GFP foci formation following DNA damage (Figure 6b). Thus, ATM-1 and CEP-1 likely act either downstream of, or in parallel to 9-1-1 complex recruitment.

Together, our findings suggest that recruitment of the HUS-1-containing 9-1-1 complex is likely a critical step in the UV-C response pathway, which occurs downstream of the action of the NER machinery, and which in turn is required for ATM-1- and CEP-1-dependent apoptosis and cell cycle arrest.

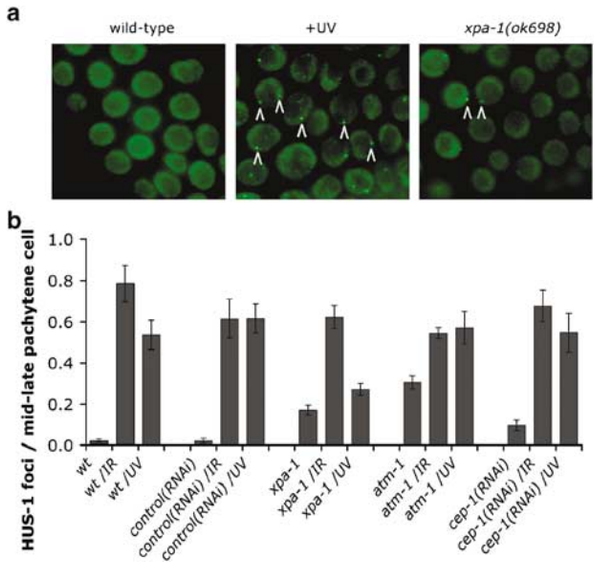

Figure 6 UV-C-induced germ cell apoptosis requires recruitment of HUS-1 downstream of NER. (**a**) Fluorescent microscopy of mid-late pachytene germ cells expressing HUS-1::GFP (*opls34*). Germ cell nuclei from staged young adult wild-type (wt) or *xpa-1*(*ok698*) hermaphrodites expressing HUS-1::GFP were scored for the presence of GFP, 4 h after exposure to 120 Gy of X-rays or 100 J/m^2 of UV-C. Relocalized HUS-1 is seen as bright foci marked by arrowheads, whereas it is diffusely distributed before treatment. (**b**) UV-C-induced HUS-1 foci require XPA-1. Quantification of the GFP-positive signals shown in (**a**) following treatment with IR or UV-C in wild-type, *xpa-1*(*ok698*), *atm-1*(*gk186*) and *cep-1*(RNAi)-treated animals

Cell cycle arrest upon UV-C requires a distinct set of genes that partially overlaps with that activated upon IR. We previously showed that IR treatment of *C. elegans* germ cells induced not only apoptosis but also cell cycle arrest of the mitotic stem cells present at the distal end of the germ line.[18] To determine whether UV treatment also interferes with germ cell proliferation, we measured the number of nuclei present at the distal end of the gonad. We found that UV-C induces a transient proliferation arrest in mitotic germ cells. Wild-type animals showed a detectable decrease in cell numbers already 4 h post-treatment that lasted for at least 12 h, but which recovered by 24 h post-treatment (Figure 7a). To confirm that the reduced number of mitotic germ cells was caused by a proliferation arrest, we quantified the number of germ cells in mitosis following DNA damage. We found that arrested mitotic germ cell compartments showed a reduced mitotic index, based both on DAPI staining and probing of fixed germ lines with an antibody that specifically recognizes phospho-Ser10 H3, which is a marker of mitosis (Supplementary Figure 3).

To determine the genetic requirements for UV-C-induced cell cycle arrest, we analyzed the cell cycle phenotype of the mutants we described above. We found that all genes required for UV-C-induced apoptosis also participate in UV-C-induced cell cycle arrest (Figure 7b). The relative strengths of the apoptosis and cell cycle arrest defects observed in the various mutants correlated well, with the exception of *atl-1* (*tm853*), which showed a strong loss of apoptosis but only a partial defect in cell cycle arrest. Interestingly, the pathway that induces cell cycle arrest in response to UV-C overlaps only partially with the IR response pathway that we and others described previously.[4,27] Whereas *hus-1*, *clk-2* and *atl-1* are clearly required in both situations, *cep-1*, *chk-2*, *atm-1* and the NER gene *xpa-1* are required only for UV response (Figure 7b).

NER and checkpoint proteins are required for efficient repair of UV-C-induced DNA damage. To assess the capacity of our various mutants to repair UV-C-induced lesions, we measured the survival of embryos generated from UV-treated germline nuclei. *xpa-1*(*ok698*) mutant animals showed the most severe reduction in survival following UV-C treatment, consistent with the predicted essential role of *xpa-1* in NER (Supplementary Figure 4). Additionally, their somatic tissues showed a strong sensitivity by arresting their development, when younger animals were

subjected to UV radiation (see Materials and methods). *atm-1*(*gk186*) mutants displayed slightly decreased embryonic survival already under normal growth conditions, as did the checkpoint mutants *hus-1*(*op244*) and *clk-2*(*mn159*) (Supplementary Figure 4). This, together with the increased incidence of HUS-1::GFP foci in *atm-1* mutants (Figure 6), supports the notion that ATM-1 plays an important role in promoting the repair of endogenous DNA damage. Following treatment with UV-C, we observed a further reduction in survival in all three mutants, suggesting that repair of UV-C lesions is slightly defective or slowed down in all three cases. Interestingly, both *atm-1 hus-1* and *atm-1; clk-2* double mutants showed a strong synthetic lethal phenotype, reaching levels of survival as low as 20 and 50%, respectively (Supplementary Figure 4). A similar synthetic phenotype was described previously in *hus-1; clk-2* double mutants.[6] These observations imply the existence of significant redundancy in the pathway(s) that mediate repair of endogenous DNA damage in the *C. elegans* germ line.

Interestingly, although *cep-1* animals are strongly defective in UV-induced apoptosis and cell cycle arrest, these mutants showed survival levels similar to the wild type (Supplementary Figure 4). This observation leads to two conclusions. First, CEP-1 is not required for DNA repair in response to UV-C. Second, and rather surprisingly, lack of apoptosis or cell cycle arrest does not appear to increase the proportion of cells that generate inviable embryos, at least under our experimental conditions. More precise assays will be required to determine the exact contribution of DNA damage-induced cell cycle arrest and apoptosis to the maintenance of genome stability.

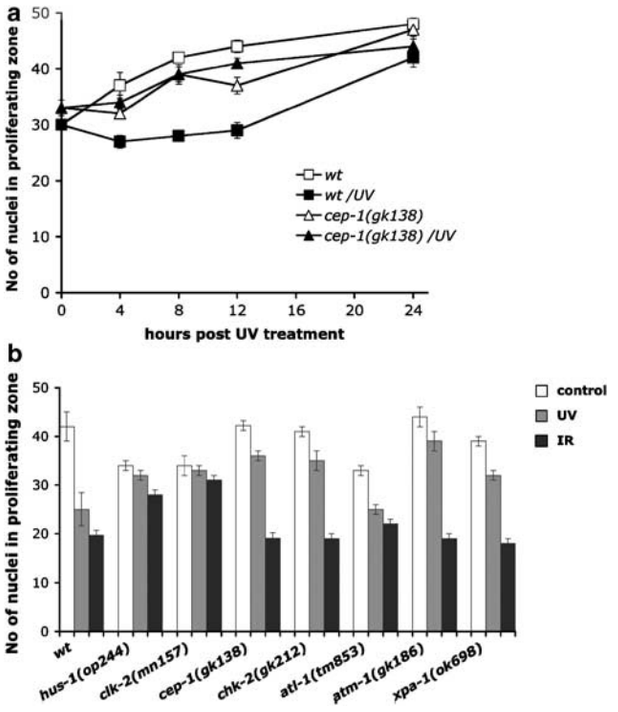

Figure 7 UV-C irradiation causes cell cycle arrest in the mitotic zone of the germ line. (**a**) Staged L4 wild-type animals or *cep-1*(*gk138*) mutants were irradiated with 100 J/m^2 UV-C. The number of germ cell nuclei present within the distal most 75 μm of the germ line was determined in a time course. (**b**) Staged L4 animals of the following genotypes were irradiated with 100 J/m^2 UV-C or 120 Gy X-rays: wild-type (wt), *hus-1*(*op244*), *clk-2*(*mn159*), *cep-1*(*gk138*), *chk-2*(*gk212*), *atl-1*(*tm853*), *atm-1*(*gk186*) and *xpa-1*(*ok698*). The number of germ cell nuclei was determined as above 8 h after treatment. White bars represent the non-treated and light/dark gray bars the UV-C/IR-treated condition. Data shown represent the average from 40 gonads $\pm$ S.E.M.

Discussion

In this paper, we describe our genetic analysis of the cellular responses to UV-C light in the adult *C. elegans* germ line. We showed, for the first time, that UV-C induces both apoptotic cell death of meiotic cells and cell cycle arrest of the proliferating mitotic stem cells. We identified over half a dozen genes required for both responses. These genes act in a signaling pathway that overlaps with, but is distinct from the pathway that is activated in response to IR[4] (Figure 8).

Importantly, we found that the NER pathway, which is implicated in the recognition and repair of UV-C-induced lesions (pyrimidine dimers and 6-4 PPs), also plays an essential role in activating cell cycle arrest and apoptosis. It is possible that assembly of the NER recognition complex at a site of damage is by itself sufficient to activate the signaling cascade. Alternatively, signaling could be activated upon recruitment of the repair machinery, or by the repair process itself (e.g., through the generation of regions of ssDNA). Further analysis of mutants defective in later steps in NER might allow us to distinguish between these various models. Interestingly, Cimprich and co-workers recently showed that XPA, but not other components of the NER pathway, is required for ATR activation in mammalian cell culture following UV damage.[30] Unfortunately, the authors did not comment on whether the effect on ATR activation correlated

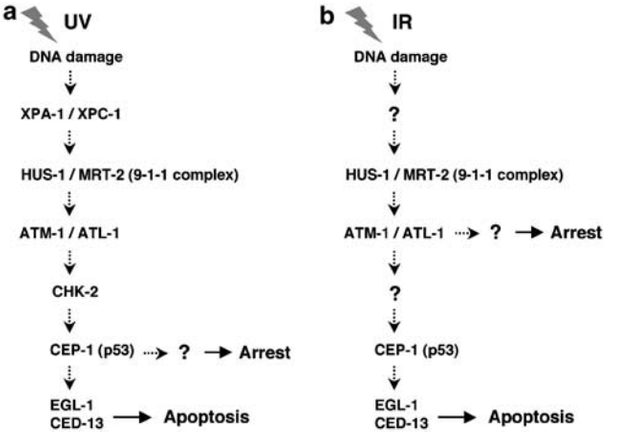

Figure 8 A genetic pathway for UV-C-induced apoptosis and cell cycle arrest. (**a**) Based on our genetic studies, our experiments with the *hus-1*::*gfp* reporter, and data from other species we propose that UV-C-induced damages are recognized by NER pathway components, which subsequently activate, directly or indirectly, the 9-1-1 complex. The 9-1-1 complex in turn promotes activation of the checkpoint kinase cascade, leading to p53-dependent apoptosis and cell cycle arrest. The requirement for some of the UV-C pathway components is different in response to IR-induced damages (**b** and see text)

with any change in apoptosis or cell cycle arrest in their experimental system.

Indeed, whereas mammalian cells defective in various NER components (e.g., the various XP complementation groups) often do show altered responses to UV light, the patterns of changes tend to be more complicated than the ones we observed in *C. elegans*: depending on the specific mutation and the gene affected, defective cells can either show increased or decreased levels of UV-induced apoptosis and/or cell cycle arrest.[31–34] It is likely that the complex response pattern observed in mammals in response to UV simply reflects the presence of multiple apoptosis-inducing pathways in these species. For example, unrepaired UV-induced lesions in ERCC1 or ERCC3-deficient (murine XP genes) cells do not activate the apoptotic machinery directly, but rather are converted into other types of damage (e.g., dsDNA strand breaks) during subsequent S phases, which in turn lead to apoptosis.[33] The presence of these additional pathways might have precluded identification of the role of the NER pathway in promoting apoptosis in mammals.

The greater simplicity of the *C. elegans* DNA damage response network is also underscored through our analysis of the 9-1-1 complex subunit HUS-1. Whereas *C. elegans hus-1* mutants are completely defective in both UV and IR-induced apoptosis and cell cycle arrest[5,18] (Figure 2b), implicating the 9-1-1 complex as an essential component in both pathways, mouse *hus-1*$^{-/-}$ cells in fact show increased apoptosis in response to IR.[35,36]

What is the exact function of the 9-1-1 complex in UV-C-induced apoptosis? We found that UV-C irradiation led to a significant increase in HUS-1::GFP foci (Figure 6); these foci are thought to represent either sites of persistent damage or of active repair.[5] Interestingly, the 9-1-1 complex is thought to be recruited in response to dsDNA breaks. HUS-1::GFP foci were not increased in *xpa-1* mutants, indicating that activation of NER is required, directly or indirectly, for 9-1-1 complex recruitment. One possibility is that NER generates as a by-product a significant number of dsDNA breaks, perhaps when damaged sites on opposite strands are repaired simultaneously.

In contrast to the situation in *xpa-1* mutants, HUS-1::GFP foci still formed upon UV treatment in *atm-1* and *cep-1* mutants. Thus, these genes act either in parallel to or downstream of the 9-1-1 complex (Figure 8). Further biochemical studies will be required to dissect in more detail the exact order of molecular events in this signaling cascade. The strong synthetic lethality that we observed in *atm-1 hus-1* double mutants suggests that these two proteins do have some non-overlapping activities, at least with respect to promotion of DNA repair.

In mammals, the checkpoint kinase CHK2 plays an important role in promoting apoptosis and cell cycle arrest in response to a variety of DNA damaging agents, including IR, UV and various mutagens and chemotherapeutic agents.[37] Surprisingly, *chk-2* mutants in *C. elegans* show a normal response to IR,[22] which raised the issue of whether *chk-2* might have a different function in invertebrates. We now showed that *chk-2* mutants are strongly defective in both apoptosis and cell cycle arrest following UV treatment (Figures 2c and 7b). Thus, the molecular function of CHK-2 is likely conserved also in *C. elegans*, although the signals to which it responds appear likely to be distinct in worms and mammals.

We also made a similar observation with ATM-1 and ATL-1, the orthologs of ATM and ATR, respectively. In mammals, ATM mainly mediates response to dsDNA breaks, whereas ATR is activated by UV and stalled replication forks.[16,17] In *C. elegans*, we found that ATL-1 was the more important player in both UV- and IR-response pathways, with loss of ATM-1 only showing a strong defect at low doses[27] (Figures 3a, d and 4c–f). Finally, we found a differential requirement for CEP-1/p53 in UV- and IR-induced cell cycle arrest: whereas mitotic germ cells in *cep-1* mutants showed a normal response following IR treatment, they failed to arrest in response to UV light (Figures 7a). We surmise that p53 either is not activated in response to IR or that it acts redundantly with another signaling protein under these conditions.

Taken together, our observations suggest that there is a certain flexibility for organisms to change, over evolutionary time, the types of damage a given checkpoint protein responds to. This flexibility might be important in allowing organisms to adapt to new challenges as they change their life history (e.g., longer lifespans) or ecological niches.

Materials and Methods

Genetics. All strains were grown at 20°C on NGM agar seeded with *Escherichia coli* OP50.[38] The Bristol N2 strain was used as the wild-type strain. The following mutations were used: LGI: *atm-1*(*gk186*), *hus-1*(*op244*), *xpa-1*(*ok698*), *cep-1*(*gk138*); LGIII: *clk-2*(*mn159*), *mrt-2*(*e2663*); LGIV: *xpc-1*(*ok734*); LGV: *atl-1*(*tm853*), *sDf29*, *mDf1*, *egl-1*(*n1084n3082*), *chk-2*(*me64*), *chk-2*(*gk212*); LGX: *ced-13*(*gk260*). Essential mutations were maintained as balanced strains: *atl-1*(*tm853*)*/nT1[qIs51](IV;V)*, *dpy-18*(*e364*)*/eT1 III*; *unc-46*(*e177*) *sDf29/eT1 V*, *dpy-18*(*e364*)*/eT1 III*; *mDf1/eT1 V* and *chk-2*(*me64*) *rol-9*(*sc148*)*/unc-51*(*e369*) *rol-9*(*sc148*).

Germline apoptosis. Staged young adult worms (12 h post the L4/adult molt) were exposed to different doses of UV-C light (254 nm) (J/m^2) or X-rays (Gy). A Stratalinker UV crosslinker, model 1800 (Stratagene) and an Isovolt 160/225/320/450 HS X-ray machine (Rich. Seifert & Co.) were used to deliver the appropriate doses. Corpses were scored in the meiotic region of one gonad arm at indicated time points using Nomarski optics, as described by Gumienny *et al*.[39] For the RNAi experiments, staged L1 larvae were transferred onto plates seeded with bacteria expressing the respective RNAi clone[40] and scored as young adults for germline apoptosis.

Relative quantification of transcripts. Staged young adults were treated with UV-C light or X-rays as described above. Animals were selected for processing 12 h post-treatment. Total RNA extraction, cDNA synthesis and quantitative real-time RT-PCR were performed as described previously.[5] Transcript levels of *egl-1* and *ced-13* were normalized to 18S rRNA, *tbp-1* and *pgk-1* mRNAs, which served as internal controls. The forward and reverse primer sequences for *tbp-1* and *pgk-1* were: 5′-TTGGATTTGAAGAAGATTGCATTG-3′, 5′-AATGACTGCTGCGAAACGTTT-3′ and 5′-GCGATATTTATGTCAATGATGCTTTC-3′, 5′-TGAGTGCTCGACTCCAACCA-3′, respectively. Primer sequences for the other genes were described in Hofmann *et al*.[5]

Cell cycle arrest studies. Staged L4 larvae were treated with either 100 J/m^2 of UV-C light or 120 Gy of X-rays. The cell cycle arrest phenotype was assessed at indicated time points by counting the number of mitotic nuclei present in one focal plane within 75 μm of the distal tip cell. Alternatively, dissected gonads were stained with an antibody against a phosphorylated form of histone H3 (anti-phospho-H3 (Ser10)) and DAPI, 7 h after treatment. DIC images were captured in both cases using an ORCA-ER digital CCD camera and analyzed using Openlab software.

Immunocytochemistry. For antibody staining of gonads, L4 hermaphrodites were dissected and fixed in 3% para-formaldehyde/0.1 M K_2HPO_4 (pH 7.2) for 50 min at room temperature, followed by a 10 min-incubation in 100% methanol on ice. Gonads were blocked in 5% BSA/PBS-Tween-20 0.1% for 1 h, followed by incubation with 1 : 100 anti-phospho-histone H3 polyclonal antibody (Ser10) (Upstate) overnight at 4°C. Alexa fluor 594 goat anti-rabbit IgG (Molecular Probes) was used as secondary antibody (1 : 500). The tissues were co-stained with DAPI before mounting. Fluorescent images were captured with a Leica DMRA2 microscope equipped with an ORCA-ER digital CCD camera and were processed with Openlab software.

Embryonic survival assay. Staged L4 larvae were subjected to 100 J/m^2 UV-C. After 24 h recovery period, animals were singly transferred to new seeded plates ($n \approx 50$) and were left to lay eggs for 4–6 h ($n \geqslant 30$ embryos/plate). As an exception, due to the strong sensitivity of the somatic tissues to the effects of UV-C, *xpa-1*(*ok698*) and *xpc-1*(*ok734*) mutants were treated 12 h post the L4 stage. Adults were then removed and the number of eggs laid was determined. Unhatched eggs were scored 24 h later to calculate the % embryonic survival. Moreover, owing to the fully penetrant maternal-effect lethal phenotype of *atl-1*(*tm853*) mutants, we did not include them in our assay.

Acknowledgements. We thank A Gartner, J Phelan, E Bogan and members of the Hengartner lab for discussions and critical comments on this paper. Some *C. elegans* strains were obtained from the *Caenorhabditis* Genetics Center, which is funded by the National Institute of Health (NIH) National Center for Research Resources (NCRR), and from the Shohei Mitani mutant collection of the National Bioresource Project in Japan. This work was supported by the Kanton of Zurich, the Swiss National Science Foundation, the Ernst Hadorn Foundation and the Josef Steiner Cancer Research Foundation. AS was supported by a MD-PhD fellowship from the Swiss National Science Foundation and Oncosuisse.

1. Metzstein MM, Stanfield GM, Horvitz HR. Genetics of programmed cell death in *C. elegans*: past, present and future. *Trends Genet* 1998; **14**: 410–416.
2. Kinchen JM, Hengartner MO. Tales of cannibalism, suicide, and murder: programmed cell death in *C. elegans*. *Curr Top Dev Biol* 2005; **65**: 1–45.
3. Hofmann ER, Milstein S, Hengartner MO. DNA-damage-induced checkpoint pathways in the nematode *Caenorhabditis elegans*. *Cold Spring Harb Symp Quant Biol* 2000; **65**: 467–473.
4. Stergiou L, Hengartner MO. Death and more: DNA damage response pathways in the nematode *C. elegans*. *Cell Death Differ* 2004; **11**: 21–28.
5. Hofmann ER, Milstein S, Boulton SJ, Ye M, Hofmann JJ, Stergiou L *et al*. *Caenorhabditis elegans* HUS-1 is a DNA damage checkpoint protein required for genome stability and EGL-1-mediated apoptosis. *Curr Biol* 2002; **12**: 1908–1918.
6. Ahmed S, Alpi A, Hengartner MO, Gartner A. *C. elegans* RAD-5/CLK-2 defines a new DNA damage checkpoint protein. *Curr Biol* 2001; **11**: 1934–1944.
7. Derry WB, Putzke AP, Rothman JH. *Caenorhabditis elegans* p53: role in apoptosis, meiosis, and stress resistance. *Science* 2001; **294**: 591–595.
8. Schumacher B, Hofmann K, Boulton S, Gartner A. The *C. elegans* homolog of the p53 tumor suppressor is required for DNA damage-induced apoptosis. *Curr Biol* 2001; **11**: 1722–1727.
9. Yan N, Gu L, Kokel D, Chai J, Li W, Han A *et al*. Structural, biochemical, and functional analyses of CED-9 recognition by the proapoptotic proteins EGL-1 and CED-4. *Mol Cell* 2004; **15**: 999–1006.
10. Sancar A, Lindsey-Boltz LA, Unsal-Kacmaz K, Linn S. Molecular mechanisms of mammalian DNA repair and the DNA damage checkpoints. *Annu Rev Biochem* 2004; **73**: 39–85.
11. Assefa Z, Van Laethem A, Garmyn M, Agostinis P. Ultraviolet radiation-induced apoptosis in keratinocytes: on the role of cytosolic factors. *Biochim Biophys Acta* 2005; **1755**: 90–106.
12. Balajee AS, Bohr VA. Genomic heterogeneity of nucleotide excision repair. *Gene* 2000; **250**: 15–30.
13. Prakash S, Prakash L. Nucleotide excision repair in yeast. *Mutat Res* 2000; **451**: 13–24.
14. Costa RMA, Chigançcas V, Galhardo R, Carvalho H, Menck CFM. The eukaryotic nucleotide excision repair pathway. *Biochimie* 2003; **85**: 1083–1099.
15. Yang J, Yu Y, Hamrick HE, Duerksen-Hughes PJ. ATM, ATR, and DNA-PK: initiators of the cellular genotoxic stress responses. *Carcinogenesis* 2003; **24**: 1571–1580.
16. Shiloh Y. ATM and ATR: networking cellular responses to DNA damage. *Curr Opin Genet Dev* 2001; **11**: 71–77.
17. Gartner A, Milstein S, Ahmed S, Hodgkin J, Hengartner MO. A conserved checkpoint pathway mediates DNA damage–induced apoptosis and cell cycle arrest in *C. elegans*. *Mol Cell* 2000; **5**: 435–443.
18. Schumacher B, Schertel C, Wittenburg N, Tuck S, Mitani S, Gartner A *et al*. *C. elegans ced-13* can promote apoptosis and is induced in response to DNA damage. *Cell Death Differ* 2005; **12**: 153–161.
19. Chehab NH, Malikzay A, Stavridi ES, Halazonetis TD. Phosphorylation of Ser-20 mediates stabilization of human p53 in response to DNA damage. *Proc Natl Acad Sci USA* 1999; **96**: 13777–13782.
20. Matsuoka S, Huang M, Elledge SJ. Linkage of ATM to cell cycle regulation by the Chk2 protein kinase. *Science* 1998; **282**: 1893–1897.
21. Hirao A, Cheung A, Duncan G, Girard PM, Elia AJ, Wakeham A *et al*. Chk2 is a tumor suppressor that regulates apoptosis in both an ataxia telangiectasia mutated (ATM)-dependent and an ATM-independent manner. *Mol Cell Biol* 2002; **22**: 6521–6532.
22. MacQueen AJ, Villeneuve AM. Nuclear reorganization and homologous chromosome pairing during meiotic prophase require *C. elegans chk-2*. *Genes Dev* 2001; **15**: 1674–1687.
23. Liu Q, Guntuku S, Cui XS, Matsuoka S, Cortez D, Tamai K *et al*. Chk1 is an essential kinase that is regulated by Atr and required for the G(2)/M DNA damage checkpoint. *Genes Dev* 2000; **14**: 1448–1459.
24. Matsuoka S, Rotman G, Ogawa A, Shiloh Y, Tamai K, Elledge SJ. Ataxia telangiectasia-mutated phosphorylates Chk2 *in vivo* and *in vitro*. *Proc Natl Acad Sci USA* 2000; **97**: 10389–10394.
25. Bartek J, Falck J, Lukas J. CHK2 kinase – a busy messenger. *Nat Rev Mol Cell Biol* 2001; **2**: 877–886.
26. Boulton SJ, Gartner A, Reboul J, Vaglio P, Dyson N, Hill DE *et al*. Combined functional genomic maps of the *C. elegans* DNA damage response. *Science* 2002; **295**: 127–131.
27. Garcia-Muse T, Boulton SJ. Distinct modes of ATR activation after replication stress and DNA double-strand breaks in *Caenorhabditis elegans*. *EMBO J* 2005; **24**: 4345–4355.
28. Thoma BS, Vasquez KM. Critical DNA damage recognition functions of XPC-hHR23B and XPA-RPA in nucleotide excision repair. *Mol Carcinog* 2003; **38**: 1–13.
29. Park HK, Yook JS, Koo HS, Choi IS, Ahn B. The *Caenorhabditis elegans* XPA homolog of human XPA. *Mol Cells* 2002; **14**: 50–55.
30. Bomgarden RD, Lupardus PJ, Soni DV, Yee MC, Ford JM, Cimprich KA. Opposing effects of the UV lesion repair protein XPA and UV bypass polymerase eta on ATR checkpoint signaling. *EMBO J* 2006; **25**: 2605–2614.
31. de Boer J, Hoeijmakers JHJ. Nucleotide excision repair and human syndromes. *Carcinogenesis* 2000; **21**: 453–460.
32. McKay BC, Becerril C, Spronck JC, Ljungman M. Ultraviolet light-induced apoptosis is associated with S-phase in primary human fibroblasts. *DNA Repair (Amsterdam)* 2002; **1**: 811–820.
33. Dunkern TR, Kaina B. Cell proliferation and DNA breaks are involved in ultraviolet light-induced apoptosis in nucleotide excision repair-deficient Chinese hamster cells. *Mol Biol Cell* 2002; **13**: 348–361.
34. Stout GJ, Oosten M, Acherrat FZ, Wit J, Vermeij WP, Mullenders LH *et al*. Selective DNA damage responses in murine Xpa(−/−), Xpc(−/−) and Csb(−/−) keratinocyte cultures. *DNA Repair (Amsterdam)* 2005; **4**: 1337–1344.
35. Heyer BS, MacAuley A, Behrendtsen O, Werb Z. Hypersensitivity to DNA damage leads to increased apoptosis during early mouse development. *Genes Dev* 2000; **14**: 2072–2084.
36. Weiss RS, Enoch T, Leder P. Inactivation of mouse Hus1 results in genomic instability and impaired responses to genotoxic stress. *Genes Dev* 2000; **14**: 1886–1898.
37. Ahn J, Urist M, Prives C. The Chk2 protein kinase. *DNA Repair (Amsterdam)* 2004; **3**: 1039–1047.
38. Brenner S. The genetics of *Caenorhabditis elegans*. *Genetics* 1974; **77**: 71–94.
39. Gumienny TL, Lambie E, Hartwieg E, Horvitz HR, Hengartner MO. Genetic control of programmed cell death in the Caenorhabditis elegans hermaphrodite germline. *Development* 1999; **126**: 1011–1022.
40. Kamath RS, Fraser AG, Dong Y, Poulin G, Durbin R, Gotta M *et al*. Systematic functional analysis of the *Caenorhabditis elegans* genome using RNAi. *Nature* 2003; **421**: 231–237.

Supplementary Information accompanies the paper on Cell Death and Differentiation website (http://www.nature.com/cdd)

Supplementary Figure 1 RT-PCR analysis to determine the presence of transcripts in the mutants used in this study.

Primers were designed to flank the deletions in the genetic loci or the coding regions of the following mutants: **(a)** *atm-1(gk186)*, **(b)** *atl-1(tm853)*, **(c)** *chk-2(gk212)*, **(d)** *xpc-1(ok734)* and **(e)** *xpa-1(ok698)*. Genomic DNA or total mRNA from wild-type (wt) animals and the corresponding mutants was used in a PCR or RT-PCR reaction. In each case, a picture of the genomic PCR amplification around the locus (left panel) and a picture of the transcript PCR detection (right panel) are shown. 18SrRNA was used as an internal control for the presence of transcripts. Below, the gene structures are illustrated and the location where the mutations map are depicted by bars and the corresponding allele name. The existence of a known SL1 splicing site is denoted by a star, while genes in an operon are indicated by a sharpened bar.

Stergiou et al., Supplementary Figure 1

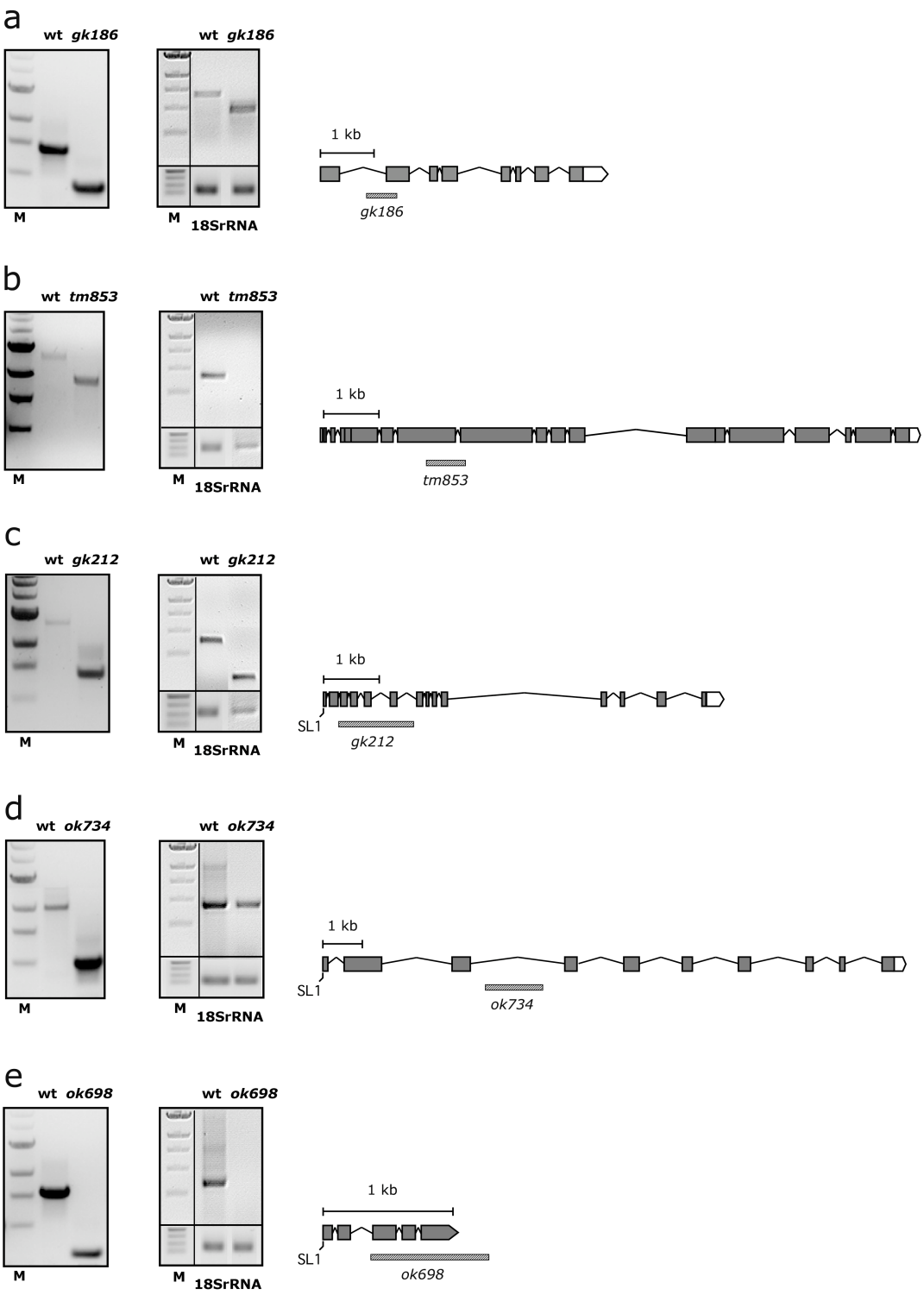

Supplementary Figure 2 *chk-1(RNAi)* animals are proficient for IR- and UV-C-induced germ cell apoptosis.

Staged *chk-1(RNAi)* young adults were treated with either 120 Gy X-rays or 100 J/m^2 UV-C and apoptotic germ cell corpses were scored 12 h and 24 h later. Data shown represent the average of two independent experiments ± SD (n>20 animals for each experiment).

Stergiou et al., Supplementary Figure 2

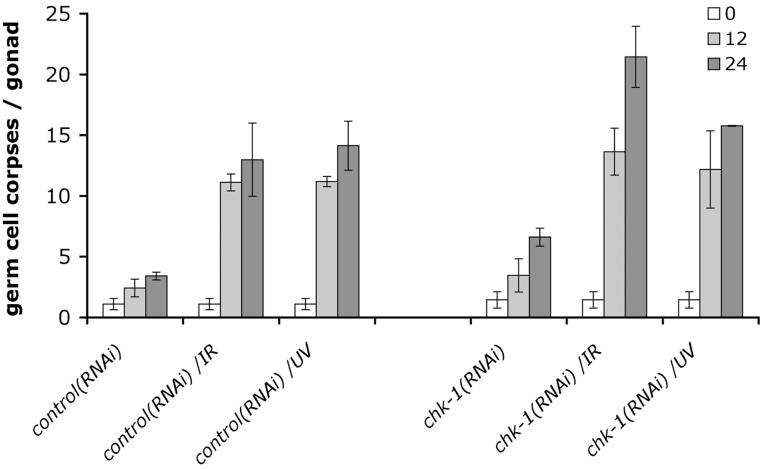

Supplementary Figure 3 Mitotic cell cycle arrest is induced following exposure to UV-C light. **(a)** Wild-type hermaphrodites were stained with Hoechst 33342 dye on slides, 7 h after treatment with 100 J/m^2 of UV-C or 120 Gy of X-rays, and germ lines were observed by fluorescent or DIC microscopy. **(b)** Dissected gonads of wild-type animals were stained with an antibody against a phosphorylated form of histone H3 (anti-PH3 (Ser10)) (red) and DAPI (blue), 7 h after treatment with 100 J/m^2 of UV-C or 120 Gy of X-rays. **(c)** Quantification of the a-PH3 positive cells and mitotic figures shown in (b) following treatment with UV-C or IR in wild-type animals. At least 14 cells were scored in each gonad, both in the control and the radiation-treated animals.

Stergiou et al., Supplementary Figure 3

a

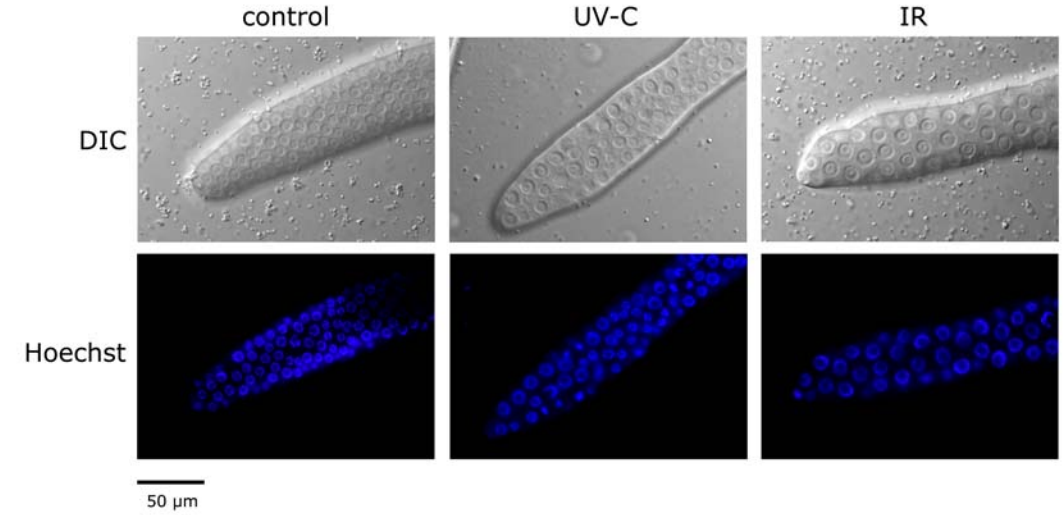

b

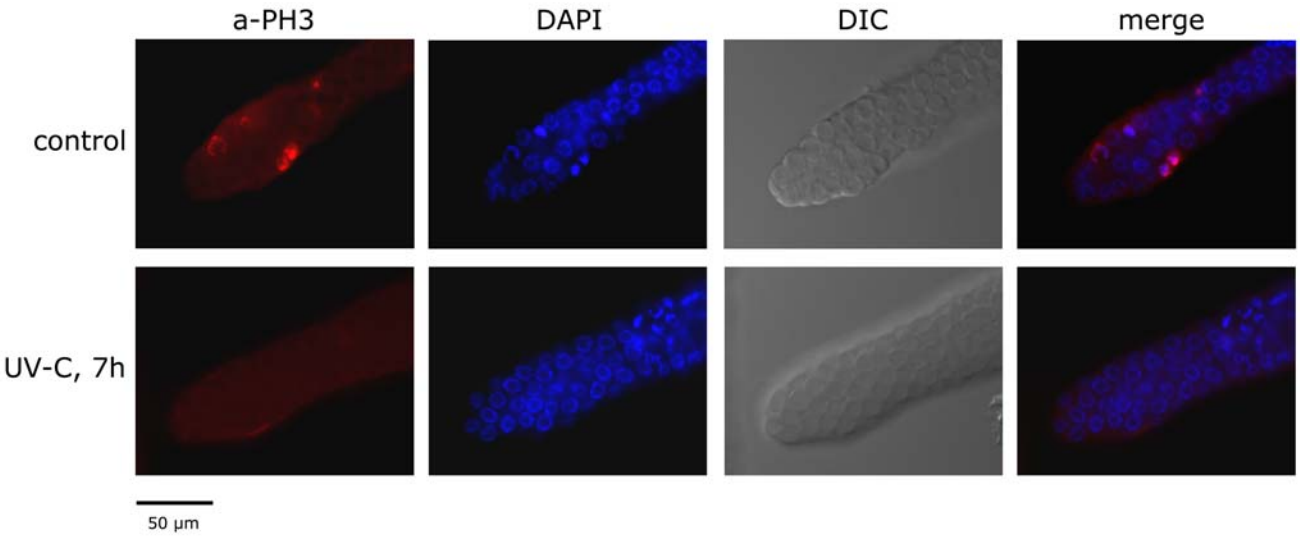

c

	% a-PH3 positive cells	% mitotic figures	n (gonads)
wt	7.8 ± 1.0	5.1 ± 0.9	22
wt /100 J/m2	2.0 ± 0.6	1.9 ± 0.6	27
wt /120 Gy	0.0 ± 0.0	0.0 ± 0.0	13

Supplementary Figure 4 NER and checkpoint proteins are required for efficient repair of UV-C-induced DNA damage. The percentage of hatched embryos following UV-C radiation was determined in the indicated single and double mutants. The animals had left lay eggs 24 h post treatment with 100 J/m^2 of UV-C. White bars represent the non-treated and grey bars the UV-treated condition. Data shown is the average percent survival of 50 animals ± SEM.

Stergiou et al., Supplementary Figure 4

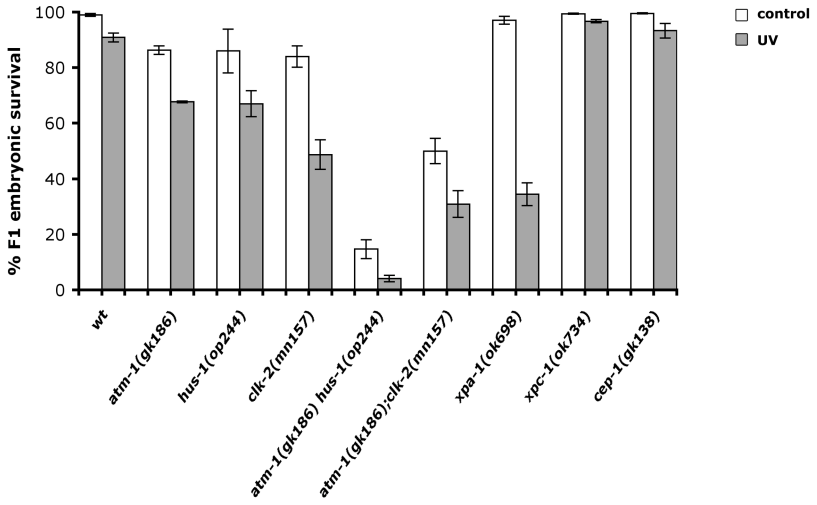

CHAPTER 6

COMBINED ACTION OF THE HR AND NER PATHWAYS

PROMOTES UV-C-INDUCED APOPTOSIS IN *C. ELEGANS*

CHAPTER 6

COMBINED ACTION OF THE HR AND NER PATHWAYS PROMOTES UV-C-INDUCED APOPTOSIS IN *C. ELEGANS*

6.1 PREFACE

The work presented in this chapter is the continuation of our previous studies on UV-C induced-apoptosis. Its aim was to understand in greater detail the mechanisms of the cellular responses to UV-C in the adult *C. elegans* hermaphrodite germ line and notably how NER signals to activate apoptosis. Similar to Chapter 5, this project was initiated by Dr. Lilli Stergiou during her 2 year post-doctoral stay in the Hengartner lab. Here, by means of genetics and protein localization experiments we demonstrate that, in addition to the NER machinery, components of the homologous recombination pathway, which are typically involved in the repair of DNA double-strand breaks, participate in the induction of germ cell apoptosis following UV-C. Our results reveal the existence of a crosstalk between two well-known repair pathways and suggest that repair factors can also have additional signaling properties.

Most of the experiments were designed and performed by Dr. Lilli Stergiou. Lilli also wrote the first draft manuscript (attached here), which we then edited together. My contribution to this study can be summarized as follows: I constructed the double mutant strains *hus-1(op244) xpa-1(ok698)*, *xpa-1(ok698); atl-1(tm853)/nT1, hus-1(op244) rad-54(ok615) and rad-54(ok516); chk-2(gk212)* and I determined the levels of germline apoptosis (shown on Figure 1a). Additionally, I blindly scored germ cell apoptosis for the experiments depicted on Figures 2 to independently confirm the results we had obtained. I also took the germline fluorescence pictures shown on Figure 3a and designed the gene model schemes shown in Supplementary Figure S1.

Combined Action of the HR and NER Pathways Promotes UV-C-induced Apoptosis in *C. elegans*

Running Head : HR is required for UV-C induced apoptosis in *C. elegans*

Lilli Stergiou [1], Kimon Doukoumetzidis [1,2], Ralf Eberhard [1,2,3] and Michael Hengartner [1,4]

1. Institute of Molecular Biology

2. Ph.D. Program in Molecular Life Sciences

3. M.D./Ph.D. program

University of Zurich

Winterthurerstrasse 190

CH-8057 Zurich, Switzerland

tel.: +41 1 635 3140

fax.: +41 1 635 6861

email: michael.hengartner@molbio.unizh.ch

4. corresponding author

October, 2007

Abstract

Ultraviolet radiation (UV) -induced DNA damage evokes multiple signaling pathways (or complex signaling network responses), which culminate in DNA repair, cell cycle arrest and apoptosis. We previously reported that components involved in early stages of the nucleotide excision repair pathway (NER) play an essential role in activating the apoptotic response in *C. elegans*. Here we provide an in-depth characterization of the molecular aspects of UV-C-induced apoptosis. We have found that components of the homologous recombination (HR) repair pathway act downstream of NER to promote apoptosis following UV-C. Importantly, apoptosis is initiated via two partially overlapping routes: common initial steps require the XPA-1 and XPB/XPD homologs, whereas the XPG-1 and MRE-11 endonucleases define two different branches. For the MRE-11 branch, recruitment of the RAD-54 homolog and, later, of the 9-1-1 complex are critical events in the induction of apoptosis. Our study uncovers new roles for the NER and HR repair factors and suggests that, upon exposure to UV-C, they can act at the junction of DNA repair and signaling to the apoptotic machinery to efficiently eliminate potentially hazardous cells.

Keywords: Apoptosis / *C. elegans* / NER / HR / UV-C

Abbreviations used

UV-C: Ultraviolet light C (254 nm)

IR: Ionizing Radiation

CPDs: cyclobutane pyrimidine dimers

6-4 PPs: 6-4 photoproducts

NER: nucleotide excision repair

DSBs: double-strand breaks

XPA, XPB, XPD, XPF, XPG : Xeroderma pigmentosum complementation group A, B, D, F, G

RPA-1: replication protein A homolog in *C. elegans*, large subunit

Introduction

DNA damage presents a major threat to genome integrity and cell viability. Activation of surveillance mechanisms involves a multitude of factors that, by sensing the damage and transducing the signals, initiate cell cycle arrest and DNA repair processes. Induction of apoptosis also acts in a protective manner against the introduction of new mutations in multicellular organisms. In fact, a major cause of malignant transformation emanates from disruption of pathways that regulate apoptosis (Hanahan and Weinberg, 2000).

To date, genetic and biochemical studies have provided us with a thorough mechanistic understanding of the distinct repair processes that are initiated upon different types of DNA lesions. Two well-documented examples involve, upon UV-C treatment, the activation of the Nucleotide Excision Repair (NER) pathway for the fixation of cyclobutane pyrimidine dimers (CPDs) and 6-4 photoproducts (6-4 PPs), and, following exposure to ionizing radiation, the Homologous Recombination (HR) machinery for the repair of double strand breaks (dsbreaks) (Sancar et al., 2004).

Simple model organisms have been proven very useful to decipher the complex molecular events that govern DNA damage responses. In *C. elegans*, the effects of ionizing radiation have been extensively studied (Stergiou and Hengartner, 2004) and we recently reported the existence of a UV-C responsive pathway that induces both apoptotic cell death of meiotic cells and cell cycle arrest of the proliferating mitotic stem cells (Stergiou et al., 2007). In that study, we identified several new genes required for

these two responses and genetically ordered them in a signaling pathway that overlaps with, but is distinct from the pathway(s) that are activated in response to ionizing radiation.

In the present study we further investigate the mechanism by which UV-C-induced damage triggers apoptosis in the *C. elegans* adult hermaphrodite germ line. We perform both genetic analyses and protein localization experiments to show that two major repair pathways, NER and HR, interact and co-operate to ensure apoptotic cell death of UV-C damaged germ cells. A critical step in the induction of apoptosis is the recruitment of the 9-1-1 complex, downstream of the action of the MRE-11/RAD-54 homologous recombination components. A 9-1-1-independent branch is also implicated in the route towards apoptosis, downstream of the action of the XPG nucleotide excision repair component. Our results suggest that UV-C-induced apoptosis in *C. elegans* is subject to extensive and elaborate regulation. Further, they validate the worm as a promising system to improve our understanding of the highly complex network that regulates apoptosis in mammals.

Results

The Homologous Recombination (HR) repair pathway is required for UV-C-induced apoptosis

Previous work from our lab has led to the identification of a genetic pathway that is required for cellular responses to UV-C radiation in the adult *C. elegans* germ line: apoptotic cell death of meiotic cells and cell cycle arrest of the proliferating mitotic

stem cells. Amongst the genes identified, we found that components of the NER pathway, namely the XPA-1 and XPC-1 DNA damage recognition factors, are implicated in the activation of these responses. Interestingly, animals with mutations in either of these two genes exhibit increased levels of apoptosis in the germ line without any UV-C treatment (Stergiou et al., 2007). Simultaneous loss of *hus-1* and *atl-1* function in *xpa-1(ok698); atl-1(tm853)* and *hus-1(op244) xpa-1(ok698)* mutants reduced the increased number of apoptotic corpses in *xpa-1* mutants (Figure 1a), similar to the effect of *atm-1* and *cep-1* loss of function (Stergiou et al., 2007). Thus, activation of pathways that are dependent on ATL-1/ATM-1 and HUS-1 must occur to secure elimination of cells with accumulated DNA damage.

Our observation that NER mutants have increased levels of apoptosis in the absence of exogenous DNA damage led us to investigate the interplay between the NER pathway and other DNA damage response pathways that might participate in UV response in *C. elegans*. Previous work had shown that the NER pathway can process interstrand crosslinks into double-strand DNA breaks, which are then repaired by the HR pathway (McHugh et al., 2001). To determine whether the NER pathway also processes a fraction of UV-C induced damage into other types of DNA damage in *C. elegans*, we determined the subcellular distribution of the ssDNA-binding protein RAD-51, normally involved in the Homologous Recombination (HR) repair pathway (Baumann & West, 1998, Alpi et al., 2003). Exposure to UV light led to the formation of distinct RAD-51 foci within the nucleus of mid- and late-stage pachytene germ cells (Figure 1b, c), suggesting that one or several additional to NER repair pathways are activated following UV-C treatment. RAD-51 foci number was elevated in non-irradiated *xpa-1* mutants, in agreement with our hypothesis that in the absence of NER other DNA damage repair pathways must be activated. Interestingly, RAD-51 foci

accumulation could still occur in *xpa-1* mutants upon UV-C treatment (Figure 1c), suggesting that at least one of these pathways or components of these pathways can act independently of the NER machinery.

To determine whether the Homologous Recombination (HR) pathway might contribute to UV-C-induced apoptosis, we characterized the phenotype of *C. elegans* mutants lacking RAD-54, which is known to functionally interact with Rad51 during recombinational repair in yeasts and mammals. Both human and yeast RAD54 proteins possess DNA-dependent ATPase activity that stimulate strand exchange by modifying the topology of breaks (Petukhova et al., 1998, Sigurdsson et al., 2002). We analyzed two different, previously uncharacterized *rad-54* mutants: *tm1268* deletes 811 bp in the middle of the gene, resulting in an out-of-frame fusion of exon 5 to exon 8, whereas *ok615* is a combined insertion/deletion that removes about 1 kb of *rad-54*, including the start codon, resulting in no mRNA transcript (Supplementary Figure 1a). Thus, both mutations likely are null. Homozygous *rad-54* progeny from heterozygous mothers are viable, but show a fully penetrant maternal-effect lethality. We thus could only analyze first-generation mutants for germ line apoptosis. We found that both *rad-54(ok615)* and *rad-54(tm1268)* mutants exhibit a strong increase in germ line apoptosis, an effect that could be phenocopied by RNAi (Figure 2a). This increase was dependent on both CEP-1 and on the endonuclease SPO-11, which generates the DSBs that initiate meiotic recombination (Figure 2b, c) (Roeder, 1997), suggesting that the increased germ cell death in *rad-54* mutants is due to accumulation of unresolved recombination intermediates. *rad-54(RNAi)*-induced apoptosis was abrogated in *atl-1(tm853)* mutants and reduced in *atm-1(gk186)* mutants (Figure 2d). This inhibition

pattern is consistent with the hypothesis that *rad-54(lf)* mutants accumulate DSBs, which, in turn, activate apoptosis in an ATL-1/ATM-1- and CEP-1-dependent manner.

Interestingly, exogenous damage, inflicted by X-rays or UV, failed to further increase the levels of germ cell apoptosis in *rad-54(ok615)* mutants (Figure 2e). Two hypotheses could explain this observation. First, the DNA damage response pathway (or the apoptotic machinery that it signals to) could already be "saturated" by the strong signal generated by the unresolved meiotic intermediates that accumulate in *rad-54* mutants. Alternatively, the HR pathway might be required for IR and UV-induced apoptosis. To distinguish between these two possibilities, we blocked the initiation of meiotic recombination through inactivation of the SPO-11 endonuclease. We found that *rad-54(RNAi);spo-11(ok79)* animals showed a greatly reduced response to IR and, surprisingly, to UV (Figure 2f). Importantly, *spo-11(ok79)* mutants respond normally to both IR and UV, demonstrating that the DNA damage response pathways are functional in this mutant background (Figure 2f). These results suggest that the HR pathway plays an important role in promoting apoptosis in response to UV-C.

We also tested for the requirement of other genes involved in HR. *C. elegans* mutants lacking the endonuclease responsible for the initial processing of dsDNA breaks during meiosis, MRE-11, were previously shown to have a defect in meiotic crossover formation and DNA repair upon ionizing radiation (Chin & Villeneuve, 2001). We found that *mre-11(ok179)* mutants showed a compromised apoptotic response to UV-C, suggesting a requirement for MRE-11 endonuclease in the initiation of UV-C-induced apoptosis (Figure 2g). However, they were still able to respond to IR, although not as proficiently as wild-type worms (Figure 2g), in

agreement with previous reports (Chin & Villeneuve, 2001). In contrast to *mre-11* animals, when we tested *rad-51(lf)* animals, we failed to detect any defect in the induction of apoptosis upon UV (Figure 2h). These results suggest that RAD-51 is not involved in UV-induced apoptosis. Indeed, RAD-51 foci formation and induction of apoptosis appear to be completely distinct events, as we could observe RAD-51 foci without apoptosis (in UV-treated *rad-54* or *xpa-1* mutants; Figure 1c, 1d), as well as UV-induced apoptosis without foci (in *rad-51(lf)* animals; data not shown).

In summary, our results support the idea that the proteins involved in early stages of HR also act to promote apoptosis in response to UV-C damage.

The HR pathway acts downstream of the NER pathway to promote UV-C-induced apoptosis

The results we have presented so far (Stergiou et al., 2007 and this study) lead to the conclusion that UV-C-induced apoptosis requires the action of two repair pathways, namely the NER and HR. Two mechanisms could explain our observations. First, it could be that both pathways act in parallel and are simultaneously required for the induction of apoptosis. Alternatively, the two pathways might act in succession, with NER recognizing and processing the initial UV-C lesions and HR continuing to relay the signal to the apoptotic machinery. To distinguish between these two possibilities, we determined the subcellular localization of selected components from one pathway in mutant animals of the other pathway.

We started our analysis by examining the distribution of a RAD-54::YFP fusion protein. When expressed in *rad-54(ok615)* mutants, this protein is able to fully rescue the increased levels of apoptosis observed in these animals (Supplementary Figure 1b)

and completely rescue the embryonic lethality associated with the lack of the endogenous protein (data not shown), suggesting that the fusion protein is fully functional. We found that RAD-54::YFP formed foci following exposure to both IR or UV-C, consistent with our observation that the HR pathway participates in UV-C-induced responses (Figure 3a). Elimination of *xpa*-1 (which is required for apoptosis in response to UV-C but not to IR) dramatically reduced the accumulation of foci following UV treatment, whereas left the foci formation following IR unaffected (Figure 3b). These results suggest that the NER component, XPA-1, acts mainly upstream of the RAD-54 recruitment in the UV-C responsive pathway. However, the basal levels of RAD-54::YFP foci were elevated in the absence of *xpa-1*, suggesting once more that elevated levels of endogenous DNA damage, can be compensated by the activity of other pathways in these mutants (Figure 3b).

We also analyzed the recruitment of RAD-54::YFP in *atm-1* and *hus-1* mutants. We found that both IR and UV treatment further increased the number of foci in *atm-1* mutants, indicating that ATM-1 is either not required for, or acts at subsequent steps of RAD-54 recruitment to sites of damage. Knockdown of *hus-1* increased the RAD-54::YFP foci formation following UV-C, but not significantly stronger compared to the wild-type response (Figure 3b). Based on this result, we speculate that HUS-1 and the 9-1-1 complex might be assisting in "loading" RAD-54 onto DNA lesions.

Finally we examined the localization of RAD-54::YFP following UV-C treatment in an *mre-11* mutant background. As expected, in non-treated animals foci were very scarce in the early meiotic germ cells, in accordance with the fact that the MRE-11 protein acts upstream of RAD-54 to execute meiotic recombination. Animals treated

with UV-C failed to show any focal accumulation of RAD-54::YFP in the mid-late pachytene cells (Figure 3b), yet foci were present in the mitotic zone (data not shown). In contrast to that, IR-treated animals exhibited the wild-type pattern, with foci appearing throughout the whole gonad (Figure 3b). These results phenocopy the apoptotic behavior of *mre-11* mutants (Figure 2g) and suggest that MRE-11 is required for UV-C-induced apoptosis, presumably by recruiting the RAD-54 protein onto sites of DNA damage.

We continued our analysis by examining the distribution of a RPA-1::YFP fusion protein. Replication protein A (RPA) is a heterotrimeric single-stranded DNA-binding protein that is highly conserved in eukaryotes. It plays an important role in many aspects of nucleic acid metabolism, including DNA replication and DNA repair (Zou et al., 2006). RPA and XPA have been reported to interact in forming a DNA damage recognition complex facilitating the processing of DNA lesions by the NER process (Patrick & Turchi, 2002). We chose to clone the largest subunit of RPA, ortholog of the human p70. We found that RPA-1::YFP formed foci following exposure to UV-C, as early as 30 min after treatment, and reached a plateau 3.5 h later (Figure 3c, d, Supplementary Figure 2a). We hypothesized that RPA-1 acts as a binding partner for XPA-1 in *C. elegans* as well, so we determined its distribution in a *xpa-1*-deficient background. Loss of XPA-1 completely blocked the increase of RPA-1 foci observed upon UV, confirming our hypothesis. Treatment of wild-type animals with IR also resulted in an increase in RPA-1::YFP foci number (Figure 3c, d, Supplementary Figure 2b), suggesting that this factor is also engaged in responses following IR. Indeed, during homologous recombinational repair of double-strand breaks RPA has been shown to interact with the Rad51 and Rad52 members of the RAD52 family to

modulate their activities (Park et al., 1996, Van Komen et al., 2002, Stauffer and Chazin, 2004). The lack of *xpa-1*, however, did not affect the number of foci generated upon IR, suggesting that the accumulation of RPA-1 on sites of double-strand breaks generated by the effects of IR is independent of the NER machinery (Figure 3d).

Because the RPA-1 protein shares its role in both the NER and the HR repair pathways, we also determined its re-localization and foci formation ability upon UV-C treatment in a *rad-54*-deficient background. We found that RPA-1::YFP formed an increased number of foci in *rad-54(ok615)* mutants under normal conditions (Figure 3e), apparently marking the sites of unresolved meiotic recombination intermediates. This result suggested to us that RAD-54 is dispensable for the loading of RPA-1 in *C. elegans*. Our observation is in accord with studies in other systems where Rpa stimulates the presynaptic phase of homologous recombination, whereas Rad54 acts at the subsequent synaptic step, to stimulate the function of Rad51-mediated DNA strand exchange (Solinger et al., 2001, Solinger and Heyer, 2001). Following both UV-C and IR treatment the number of foci tended to increase, likely representing the sites of the directly or indirectly, newly generated DNA breaks (Figure 3e). However, we believe that at this point the system is already "saturated" by the high steady state RPA-1::YFP levels in *rad-54* mutants, so we decided to perform the same experiment in a *spo-11*-deficient background. RNAi against *spo-11* prevented the accumulation of unresolved recombination intermediates in *rad-54(ok615)* mutants and the excess in apoptosis (Figure 2f). At the same time it also eliminated the high levels of RPA-1::YFP foci (Figure 3e). As expected, exposure to UV-C led to an increase in foci number, suggesting that the XPA-1/RPA-1 complex acts upstream of, or in parallel to, RAD-54 in the UV responses. Alternatively, the additional recruitment of RPA-1 protein upon

UV-C might represent RPA-1 molecules involved in the HR pathway. To clarify this, we scored RPA-1::YFP foci in an *mre-11*-deficient background. Spatiotemporal studies in yeast have shown that Mre11 is the first protein detected at the break site and that recruitment and foci formation of the RPA-1 yeast homolog is a subsequent event (Lisby et al., 2004). We observed that the number of RPA-1 foci following UV-C was increased in *mre-11(ok179)* mutants (Figure 3d). We, therefore, conclude that most if not all RPA-1::YFP molecules accumulated in nuclear foci do not require MRE-11 and presumably derive from the action of the NER machinery.

In summary, our results so far show that the HR repair pathway acts downstream of the NER DNA damage recognition step to trigger UV-C-induced apoptosis. This action presumably requires initial recruitment of the RPA-1 protein onto UV lesions, followed by recruitment of the RAD-54 protein onto damaged sites and subsequent signaling to the apoptotic machinery.

The NER components XPB, XPD and XPG, are required to promote UV-C-induced apoptosis partially via recruitment of the HR protein RAD-54

During the NER process local unwinding of the DNA produces the transition from a double-stranded to a single-stranded state, thus enabling the subsequent step of incision of the damaged part to occur (de Laat et al., 1999). Two DNA helicases with opposite polarities, XPB and XPD, are responsible for the unwinding step. The incision step is carried out by the two structure-specific endonucleases, XPF and XPG (Prakash & Prakash, 2000, Dip et al., 2004).

We next wanted to determine whether steps subsequent to the DNA lesion recognition step, carried out by XPA-1 and XPC-1, also play a role in the UV response pathway leading to apoptosis. For this, we analyzed germ cell apoptosis in animals where the function of the *C. elegans* XPB, XPD, XPF and XPG homologs was compromised or abolished. We found that RNAi treatment against the two helicases, XPB and XPD, gave rise to increased levels of apoptosis (Figure 4a, b). These findings are consistent with our notion that the accumulation of unrepaired endogenous damage in these animals can activate (an)other DNA damage signaling pathway(s) that will eventually lead to apoptosis. Additionally, RNAi against either of these two genes resulted in 100% embryonic lethality, suggesting a vital role for these proteins during early development. Following UV-C treatment, the germ line apoptotic response of *xpb-1(RNAi)* and *xpd-1(RNAi)*-treated animals was compromised, whereas they responded normally to IR treatment (Figure 4a, b). This result suggests a restricted role for the two helicases in promoting UV-C-induced apoptosis.

We also analyzed the effect on apoptosis of two mutations in the *xpg-1*(F576B10.6) gene, *tm1670* and *tm1682*. The first deletion removes the second and part of the third exon, whereas *tm1682* removes the first two exons and part of the sequences upstream of the start codon. A shorter or no mRNA transcript was detected in each case, respectively (Supplementary Figure 1c). Further, a region important for the endonuclease activity is missing from the *tm1670* mutant, suggesting that both mutants are null. We found that UV-C-induced apoptosis was severely reduced in *xpg-1* mutants (Figure 4c), suggesting that endonucleases of the NER pathway are also implicated in the UV apoptotic response. IR-induced apoptosis still occurs in the absence of XPG-1, although with reduced levels compared to the wild-type (Figure

4d). The defect that we observed implies that a fraction of the DNA damage generated by X-rays is likely repaired via the NER pathway, or that endonucleases of the NER might participate in the repair of double-strand breaks. Indeed, there have been suggested separate mechanisms of involvement for human XPG in the two distinct NER and BER (base excision repair) pathways (Klungland et al., 1999). XPG was shown to serve as a cofactor for the efficient function of hNth1 DNA glycosylase-AP lyase during oxidative DNA damage repair, a type of damage also caused by IR.

All together, our results suggest that, in addition to improper sensing, improper processing of UV lesions can disturb signaling to the apoptotic machinery.

We next wondered whether the localization of the HR protein RAD-54 is similarly affected when DNA damage processing is compromised. Knocking down XPB-1 and XPD-1 by RNAi resulted in reduced levels of RAD-54::YFP foci formation following UV-C, by two-fold or more (Figure 4e). In contrast to that, loss of XPG-1 function did not have any strong effect on the accumulation of RAD-54::YFP foci (Figure 4e). Notably, the levels of foci in untreated animals were elevated in all three cases, reflecting accumulation of unrepaired lesions in a NER-deficient background.

Taken together, our findings suggest that recruitment of the RAD-54 protein onto sites of UV-C damage does not require the whole complement of the NER machinery: the DNA binding protein XPA-1, and the XPB-1 and XPD-1 helicases are sufficient for this step. In addition, RAD-54 recruitment is likely a critical step for the processing of UV-C lesions into structures that signal to the apoptotic machinery.

The HUS-1 complex functions after the HR machinery to promote UV-C-induced apoptosis

We previously showed that recruitment of the HUS-1-containing 9-1-1 complex is an important step in the UV-C response pathway, which occurs downstream of the action of XPA-1 (Stergiou et al., 2007). We also showed that ATM-1 and CEP-1 likely act either downstream of, or in parallel to 9-1-1 complex recruitment, to promote UV-C-induced germ cell apoptosis. To precisely position the action of HR components within this signaling cascade, we also determined the subcellular distribution of the 9-1-1 complex subunit HUS-1 in *rad-54* mutants. Elimination of *rad-54* did not increase the foci accumulation of HUS-1 following UV treatment (Figure 5). By contrast, foci formation following IR was still robust (Figure 5). These results suggest that the proteins involved in early stages of HR act upstream of 9-1-1 complex recruitment.

Based on this result and our result with the RAD-54::YFP foci formation in the *hus-1* mutants (Figure 3b), we speculate that recruitment of the 9-1-1 complex might occur at two distinct steps in the UV-C signaling cascade: once to "load" RAD-54 onto DNA lesions and once, after this step, to signal to the ATM-1/CEP-1 axis (see also Stergiou et al., 2007). Alternatively, the proteins might act in a complex to perform their function.

To better assess the timing of the 9-1-1 complex activity in the NER-HR network, we investigated the requirement of the XPG-1 endonuclease for its recruitment. We showed above that XPG-1 is required to promote UV-C-induced apoptosis, but is dispensable for the recruitment of RAD-54. We therefore wondered whether the NER pathway branches at the level of XPB-1/XPD-1 helicases to promote *hus-1*-dependent apoptosis via either XPG-1 or MRE-11/RAD-54. Interestingly, lack of *xpg-1* did not

affect the formation of HUS-1::GFP foci following UV-C treatment (Figure 5). Similarly, IR treatment resulted in a normal accumulation of foci in the germ line, suggesting that *xpg-1* does not significantly affect recruitment of the 9-1-1 complex following DNA damage.

In conclusion, we posit that UV-C-induced apoptosis occurs via two distinct, equally essential routes: one that requires the XPA-1, XPB-1/XPD-1 and XPG-1 components of the NER pathway, and another that, downstream of XPB-1/XPD-1, recruits the MRE-11 and RAD-54 components of the HR machinery, as well as the 9-1-1 complex.

The HR repair factors are involved in a signaling process to the apoptotic machinery following UV-C

Our finding that components of the HR repair machinery are involved in the initiation of apoptosis upon UV-C let us speculate on their exact role: do these proteins only participate in active repair of UV lesions or, are they additionally or merely involved in actual signaling to the apoptotic apparatus?

To address this question we decided to assess the DNA repair activity when the activity of either the NER or the HR pathway is compromised. We started our analysis with an *in vivo* immunofluorescence assay to measure the presence of cyclobutane pyridine dimers (CPD) - one of the two types of lesions caused after UV exposure - at defined time intervals in wild-type animals. Already 5-10 min post UV-C treatment a total of 60% mid-late pachytene cells was found to be above a detectable threshold for CPDs (Figure 6a, b). Within 1 h, half of the initial number of stained cells was found

to be positive for CPDs, whereas 8 h no CPD-signal was present in the germ line tissue. This result shows that CPD lesions following UV-C must be disappearing with fast kinetics in the germ line. Interestingly, these lesions seem to be cleared with the same rate in *rad-54(ok615)* mutants as in wild-type (Figure 6c), suggesting that RAD-54 is not involved in repair of UV-C lesions per se. We were unable to look for the presence of CPDs in the *xpa-1(ok698)* mutants, since our antibody recognizes such structures in a single-stranded DNA state (data not shown). In *xpg-1(tm1670)* mutants, compared to the wild-type, a lower percentage of cells was detected to be positive for CPDs until the first 3 h (Figure 6c). It is likely that the DNA structure around UV lesions in animals lacking the XPG-1 activity is hindering the access of the antibody. However, we observed persistent signal at later time points. This pattern might also reflect the repair capacity of *xpg-1* mutants, which is lower or delayed with respect to the wild-type.

In total, our observations suggest that UV-C lesions themselves might not account for the apoptosis observed several hours post UV-C treatment. It is likely that initial lesions are converted into different types or intermediates, which then lead to enhanced levels of apoptosis in the germ line. Moreover, lack of apoptosis in mutants of the HR pathway is likely due to perturbed signaling to the apoptotic machinery rather than lack of repair of UV-C lesions in these mutants.

In our effort to determine or speculate on the nature of the cytotoxic lesions, we decided to quantify the sites where our RAD-54::YFP marker accumulates over time. We noticed that foci became visible 1 h following UV-C treatment whereas the peak of their appearance occurred only after 2 h (Supplementary Figure 3, Figure 6d).

Compared to the speed of the CPD lesions' appearance, we noticed that there is a certain delay suggesting that, the lesions or DNA structures that are marked positively for RAD-54 are indeed generated later. We surmise that this formation is probably the result of certain steps during the UV-C lesions repair process (Figure 6d). Furthermore, we observed that RAD-54::YFP foci persist longer in the germ line with only a 40% decrease from the highest levels, as late as 16 h following exposure to UV-C. At that or even earlier time-points no CPDs were detectable any more (Figure 6b, d). We presume that the RAD-54::YFP-positive sites are lesions either difficult to be repaired and/or the ones that signal strongly to the apoptotic machinery.

Discussion

In this paper, we extend our analysis of the cellular responses to UV-C light in the adult *C. elegans* germ line. We provide evidence, for the first time, that following UV-C exposure a well-characterized repair pathway responsible for the restoration of DNA double-strand breaks, the Homologous Recombination (HR) pathway, is actively involved in the induction of apoptotic cell death of meiotic germ cells. To do so, components at the early stages of this pathway act in conjunction with the Nucleotide Excision Repair (NER) machinery, the DNA damage recognition components of which, we previously showed to be required for UV-C-induced apoptosis (Figure 7 and Stergiou et al., 2007).

The crosstalk between the two repair pathways that we report here is another example of co-operation between different repair factors in order to efficiently accomplish DNA repair under certain conditions of DNA damage. Indeed, for

example, interstrand crosslinks (ICLs) processing is likely to be initiated during replication when the fork progression is stalled, and elimination of these lesions occurs via the combined actions of excision repair and recombination systems (McHugh et al., 2001, de Silva et al., 2000). In this study we show that *rad-54* meiotic recombination mutants in *C. elegans* exhibit high levels of germ cell apoptosis under normal conditions, due to accumulation of unresolved recombination intermediates (Figure 2). We believe that the lack of the ability to proceed with damage fixation results in high susceptibility towards apoptosis. The lack of further increase upon exogenous damage caused by UV-C, in a population of cells that are post-mitotic and therefore do not convert UV lesions into dsbreaks via replication, strongly suggests that the activation of the HR repair system is a prerequisite for the initiation of apoptosis following UV-C. Underscoring these results, disruption of HR genes like the Rad54 and Rad51 homologs in other systems leads to a dramatic decrease in the frequency of spontaneous and psoralen- or mitomycin C-induced recombination events (Saffran et al., 2004, Sasaki et al., 2004). Moreover, significant levels of lethality were observed in cells mutated for the XRCC2 and XRCC3 recombinational repair components upon treatment with the nitrogen mustard cross-linking agent (de Silva et al., 2000, Saffran et al., 2004).

The activation of the HR pathway in *C. elegans* upon exposure to UV-C is reinforced by the focal appearance of RAD-51 and RAD-54 on damaged chromosomal sites in the mid-late pachytene germ cells. However, disruption of the NER activity in the *xpa-1* mutants does not alter the RAD-51 foci pattern formation, suggesting that *xpa-1* is not responsible for RAD-51 recruitment (Figure 1). Moreover, although apoptosis initiated upon UV-C damage requires the MRE-11 and RAD-54 meiotic

recombination components, it does not require the RAD-51 protein; therefore, it seems that the apoptotic response deviates above the level of the latter. What loads the RAD-51 onto sites of damage or what its role is following infliction of damage remains to be defined. We speculate that it might compete with an initiator apoptotic factor for the same binding sites, leading presumably to repair. Our results support the idea that such a factor might lie in the 9-1-1 complex, since the appearance of HUS-1 foci is abrogated upon disruption of selected NER or HR pathway components (Figure 5).

Importantly, our analyses with the fluorescently tagged RAD-54 and RPA-1 proteins, as markers for both pathways, revealed that the NER machinery must be recruited first at the sites of UV damage (pyrimidine dimers and 6-4 photoproducts) (Figure 3, 4). The assembly of both the DNA damage recognition factors (XPA-1, XPC-1) and the DNA helicases (XPB-1, XPD-1) is likely to be sufficient for the activation of a signaling cascade that will eventually lead to apoptosis. We believe that these factors perform the initial processing of the UV-C lesions into DNA structures that will then serve to recruit additional components. Along the same line, human primary fibroblasts deficient in XPB and XPD DNA helicases were found to be deficient in UV-induced apoptosis, with the two proteins shown to be part of a p53-mediated apoptotic pathway (Wang et al, 1996).

Moreover, both our genetic data and localization experiments with the *rad-54::yfp*, *rpa-1::yfp* and *hus-1::gfp* fluorescent reporters suggested that the pathway leading to UV-C-induced apoptosis is branching at the level of the NER helicases (Figure 3, 4, 5 and 7). The action of structure-specific nucleases then defines two distinct routes towards cell demise: on one side, the nuclease activity of MRE-11 leads to the

accumulation of RAD-54 in a focal pattern on damaged DNA. At the moment we do not know the exact mechanism of MRE-11 action, but we suspect that functions other than its well-documented exonuclease activity might be involved in UV-C-induced signaling. Indeed, DNA-processing activities associated with the Mre11 complex, such as a single-stranded endonuclease and a hairpin loop cleavage activity, have been reported in mammalian cells (Trujillo et al., 1998, Paull & Gellert, 1998 and Trujillo & Sung, 2001). Following the MRE-11/RAD-54 engagement step, recruitment of the 9-1-1 complex is the decisive factor towards apoptosis. On the other side, the XPG single-stranded DNA endonuclease seems to act in a 9-1-1-independent manner to promote apoptosis. This could suggest that either the repair machinery or the repair process itself through the generation of certain DNA intermediates is the trigger for induction of apoptosis. The role of the XPG in UV-induced apoptosis has also been addressed in fibroblasts of XPG patients, where the severity of the phenotype as well as the dose of the applied radiation seemed to modify the cellular response, from low levels of death to high sensitivity (Clément et al., 2006). We made a similar observation when we used RNAi against the *xpg-1* gene: a hypersensitivity in the induction of apoptosis upon UV-C treatment (data not shown). *xpf-1(RNAi)* animals were also previously reported to exhibit reduced embryonic survival and increased germ cell apoptosis upon UV-C compared to the wild-type (Park et al., 2004). One possibility for the observed phenotype might be that residual mRNA product is sufficient to give a proper apoptotic response. Alternatively, an acute response to genotoxic stress might be different when protein function is temporarily knocked down or genetically eliminated.

In our attempt to identify the form of DNA lesions that likely lead to apoptosis

upon UV and to further elucidate the role of repair components in the death decision process, we monitored the course of UV-C-induced cyclobutane pyrimidine dimers (CPDs). Concomitant to their fast generation, those lesions are also rapidly resolved from the germ line: approximately 70% of the initial lesions that were detected were found to be resolved within 4 h after UV-C treatment (Figure 6). This finding is in close agreement with reports in mammalian cells where an immediate cellular response removes 50% of the CPDs and all of the 6-4PPs in the first 4 h following infliction of damage (Costa et al., 2003). Our observations imply that UV-C lesions themselves might not be the cause of the sustained apoptosis observed in UV-C-treated animals. Interestingly, in animals that lack the HR component, RAD-54, lesions seem to be resolved with the same rate as in wild-type animals, or to be converted into other types, non-detectable by the use of the anti-CPD antibody. This finding strongly implies that lack of apoptosis in HR mutants is likely due to lack of signaling to the apoptotic machinery rather than deficient repair of UV-C lesions, a cumulative amount of which would consequently cause cell death.

However, lesions or DNA structures that are positive for the presence of RAD-54 persist longer in the germ line (Figure 6). We suspect that these might be sites that are either difficult to be repaired or that present strong signals to the apoptotic machinery and mark cells for destruction. An important question remaining to be answered is whether RAD-54 itself plays any role in transforming UV lesions into this cytotoxic form of lesions. Overall, though, the findings of this study that an intact function of repair factors is required to trigger UV-C-induced apoptosis, point towards an active role of repair components as signaling factors.

Taken together, our genetic and protein localization studies with *C. elegans* suggest

the existence of a cross-talk between two major repair pathways, NER and HR, that leads to the induction of apoptosis following UV exposure. This is, to our knowledge, the first *in vivo* demonstration of a new role for NER and HR repair components as factors that possess signaling properties. As is the case with the involvement of the TFIIH component of NER in various cellular processes (basal transcription, DNA repair, cell cycle), it is possible for the cellular repair machinery and the apoptotic apparatus to utilize common proteins to achieve their purpose in a cost-effective, time-efficient way. This flexibility is likely conserved throughout evolutionary times and therefore allows us to use a simple system like *C. elegans* in order to dissect the complex biological pathways of DNA damage responses, as well as defects that are often associated with them.

Materials and methods

Genetics. All strains were grown at 20°C on NGM agar seeded with *E. coli* OP50 (Brenner 1974). The Bristol N2 strain was used as the wild-type strain. The following mutations were used: LGI: *atm-1(gk186)*, *hus-1(op244)*, *xpg-1(tm1670)*, *xpg-1(tm1682)*, *xpa-1(ok698)*, *rad-54(ok615)*, *rad-54(tm1268)*; LGIV: *spo-11(ok79)*; LGV: *atl-1(tm853)*, *mre-11(ok179)*, *chk-2(gk212)*. Essential mutations were maintained as balanced strains: *rad-54(ok615)/hT2[qIs51](IV;V)*, *rad-54(tm1268)/hT2[qIs51](IV;V)*, *spo-11(ok79)/nT1[n754 let](IV;V)*, *atl-1(tm853)/nT1[qIs51](IV;V)* and *mre-11(ok179)/nT1[n754 let](IV;V)*.

Germ line apoptosis. Staged young adult worms (12 h post the L4/adult molt) were exposed to different doses of UV-C light (254 nm) (J/m^2) or X-rays (Gy). A

Stratalinker UV crosslinker, model 1800 (Stratagene) and an Isovolt 160/225/320/450 HS X-ray machine, (Rich. Seifert & Co.) were used to deliver the appropriate doses. Corpses were scored in the meiotic region of one gonad arm at indicated time points using Nomarski optics, as described in Gumienny *et al*. For the RNAi experiments, staged L1 larvae were transferred onto plates seeded with bacteria expressing the respective RNAi clone and scored as young adults for germ line apoptosis.

Cell cycle arrest studies. Staged L4 larvae were treated with either 100 J/m^2 of UV-C light or 120 Gy of X-rays. The cell cycle arrest phenotype was assessed at indicated time points by counting the number of mitotic nuclei present in one focal plane within 75 μm of the distal tip cell. DIC images were captured in both cases using an ORCA-ER digital CCD camera and analyzed using Openlab software.

Immunocytochemistry. For antibody staining of gonads, L4 hermaphrodites were dissected and fixed in 3% para-formaldehyde/0.1 M K_2HPO_4 (pH 7.2) for 50 min at room temperature, followed by a 10 min-incubation in 100% methanol on ice. Gonads were blocked in 5% BSA/PBS-Tween-20 0.1% for 1 h, followed by incubation with 1:50 anti-RAD-51 polyclonal (Alpi et al., 2003) or 1:250 anti-CPD monoclonal antibody overnight at 4ºC. Alexa fluor 594 goat anti-rabbit or anti-mouse IgG (Molecular Probes) was used as secondary antibody (1:250). The tissues were co-stained with DAPI before mounting. Fluorescent images were captured with a Leica DMRA2 microscope equipped with an ORCA-ER digital CCD camera and were processed with Openlab software.

RNAi constructs. Fragments corresponding to exonic sequences of *xpb-1* (Y66D12A.15) and *xpd-1* (Y50D7A.2) were amplified by PCR from a wild-type cDNA library using primers listed in Supplementary table S1, and cloned into the L4440 RNAi vector (Kamath et al., 2003). The constructs were used to transform HT115(DH3) bacteria, which were subsequently used to feed worms in the RNAi experiments.

Transgenic worms. Genomic fragments corresponding to *rpa-1* and *rad-54* promoter and ORF, as well as the 3'UTR region were amplified by PCR from N2 genomic DNA using primers (Supplementary table S1) that added the appropriate restriction sites. The amplified fragments were cloned into pLN022 upstream of *yfp* to generate pLS69 (RPA-1::YFP) or pLS57 (RAD-54::YFP). Low copy transgenic worms were then generated by biolistic transformation as previously described (Praitis et al., 2001).

Acknowledgements

This work was supported by the Kanton of Zurich, the Ernst Hadorn Foundation and the Josef Steiner Cancer Research Foundation. RE was supported by a MD-PhD fellowship from the Swiss National Science Foundation. We thank the *Caenorhabditis* Genetics Center, which is funded by the National Institute of Health (NIH) National Center for Research Resources (NCRR), and Shohei Mitani of the National Bioresource Project in Japan for providing us with mutant strains.

References

Hanahan D, Weinberg RA (2000) The hallmarks of cancer. Cell 100(1): 57-70.

Sancar A, Lindsey-Boltz LA, Unsal-Kacmaz K, Linn S (2004) Molecular mechanisms of mammalian DNA repair and the DNA damage checkpoints. Annu Rev Biochem 73: 39-85.

Stergiou L, Hengartner MO (2004) Death and more: DNA damage response pathways in the nematode *C. elegans*. Cell Death Differ 11: 21–28.

Stergiou L, Doukoumetzidis K, Sendoel A, Hengartner MO (2007) The nucleotide excision repair pathway is required for UV-C-induced apoptosis in *Caenorhabditis elegans*. Cell Death Differ 14(6): 1129–1138.

McHugh PJ, Spanswick VJ, Hartley JA (2001) Repair of DNA interstrand crosslinks: molecular mechanisms and clinical relevance. Lancet Oncol 2(8): 483–490.

Baumann P, West SC (1998) Role of the human RAD51 protein in homologous recombination and double-stranded-break repair. Trends Biochem Sci 23(7): 247-251.

Alpi A, Pasierbeck P, Gartner A, Loidl J (2003) Genetic and cytological characterization of the recombination protein RAD-51 in *Caenorhabditis elegans*. Chromosoma 112(1): 6-16.

Petukhova G, Stratton S, Sung P (1998) Catalysis of homologous DNA pairing by yeast Rad51 and Rad54 proteins. Nature 393(6680): 91-94.

Sigurdsson S, Van Komen S, Petukhova G, Sung P (2002) Homologous DNA pairing by human recombination factors Rad51 and Rad54. J Biol Chem 277(45): 42790-4.

Roeder GS (1997) Meiotic chromosomes: it takes two to tango. Genes Dev 11(20): 2600-2621.

Chin GM, Villeneuve AM (2001) *C. elegans mre-11* is required for meiotic recombination and DNA repair but is dispensable for the meiotic G(2) DNA damage checkpoint. Genes Dev 15(5): 522-34.

Zou Y, Liu Y, Wu X, Shell SM (2006) Functions of human replication protein A (RPA): from DNA replication to DNA damage and stress responses. J Cell Physiol 208(2):267-273.

Patrick SM, Turchi JJ (2002) Xeroderma pigmentosum complementation group A protein (XPA) modulates RPA-DNA interactions via enhanced complex stability and inhibition of strand separation activity. J Biol Chem 277(18): 16096-16101.

Park MS, Ludwig DL, Stigger E, Lee SH (1996) Physical interaction between human RAD52 and RPA is required for homologous recombination in mammalian cells. J Biol Chem 271(31): 18996-19000.

Van Komen S, Petukhova G, Sigurdsson S, Sung P (2002) Functional cross-talk among Rad51, Rad54, and replication protein A in heteroduplex DNA joint formation. J Biol Chem 277(46): 43578-87.

Stauffer ME, Chazin WJ (2004) Physical interaction between replication protein A and Rad51 promotes exchange on single-stranded DNA. J Biol Chem 279(24): 25638-45.

Solinger JA, Lutz G, Sugiyama T, Kowalczykowski SC, Heyer WD (2001) Rad54 protein stimulates heteroduplex DNA formation in the synaptic phase of DNA strand exchange via specific interactions with the presynaptic Rad51 nucleoprotein filament. J Mol Biol 307(5): 1207-1221.

Solinger JA, Heyer WD (2001) Rad54 protein stimulates the postsynaptic phase of Rad51 protein-mediated DNA strand exchange. Proc Natl Acad Sci USA. 98(15): 8447-8453.

Lisby M, Barlow JH, Burgess RC, Rothstein R (2004) Choreography of the DNA damage response: spatiotemporal relationships among checkpoint and repair proteins. Cell 118(6): 699-713.

de Laat WL, Jaspers NG, Hoeijmakers JH (1999) Molecular mechanism of nucleotide excision repair. Genes Dev 13(7): 768-785.

Prakash S, Prakash L (2000) Nucleotide excision repair in yeast. Mutat Res 451(1-2): 13-24

Dip R, Camenisch U, Naegeli H (2004) Mechanisms of DNA damage recognition and strand discrimination in human nucleotide excision repair. DNA Repair (Amst) 3(11): 1409-1423.

Klungland A, Hoss M, Gunz D, Constantinou A, Clarkson SG, et al. (1999) Base excision repair of oxidative DNA damage activated by XPG protein. Mol Cell 3(1): 33-42.

de Silva IU, McHugh PJ, Clingen PH, Hartley JA (2000) Defining the roles of nucleotide excision repair and recombination in the repair of DNA interstrand cross-links in mammalian cells. Mol Cell Biol 20: 7980–7990.

Saffran WA, Ahmed S, Bellevue S, Pereira G, Patrick T, et al. (2004) DNA repair defects channel interstrand DNA cross-links into alternate recombinational and error-prone repair pathways. J Biol Chem 279(35): 36462-36469.

Sasaki, MS, Takata M, Sonoda E, Tachibana A, Takeda S (2004) Recombination repair pathway in the maintenance of chromosomal integrity against DNA interstrand crosslinks. Cytogenet Genome Res 104(1-4): 28-34.

Wang XW, Vermeulen W, Coursen JD, Gibson M, Lupold SE, et al. (1996) The XPB and XPD DNA helicases are components of the p53-mediated apoptosis pathway. Genes Dev 10(10): 1219-1232.

Trujillo KM, Yuan SS, Lee E, Sung P (1998) Nuclease activities in a complex of human recombination and DNA repair factors Rad50, Mre11, and p95. J Biol Chem 273(34): 21447–21450.

Paull TT, Gellert M (1998) The 3' to 5' exonuclease activity of Mre 11 facilitates repair of DNA double-strand breaks. Mol Cell 1(7): 969-979.

Trujillo KM, Sung P (2001) DNA structure-specific nuclease activities in the *Saccharomyces cerevisiae* Rad50-Mre11 complex. J Biol Chem 276(38): 35458-35464.

Clément V, Dunand-Sauthier I, Clarkson SG (2006) Suppression of UV-induced apoptosis by the human DNA repair protein XPG. Cell Death Differ 13(3): 478-488.

Park HK, Suh D, Hyun M, Koo HS, Ahn B (2004) A DNA repair gene of *Caenorhabditis elegans*: a homolog of human XPF. DNA Repair (Amst) 3(10): 1375-1383.

Costa RM, Chigançcas V, Galhardo R, Carvalho H, Menck CF (2003) The eukaryotic nucleotide excision repair pathway. Biochimie 85: 1083–1099.

Brenner S (1974) The genetics of *Caenorhabditis elegans*. Genetics 77(1): 71-94.

Gumienny TL, Lambie E, Hartwieg E, Horvitz HR, Hengartner MO (1999) Genetic control of programmed cell death in the Caenorhabditis elegans hermaphrodite germline. Development 126(5): 1011-22.

Kamath RS, Fraser AG, Dong Y, Poulin G, Durbin R, et al. (2003) Systematic functional analysis of the *Caenorhabditis elegans* genome using RNAi. Nature 421(6920): 231-237.

Praitis V, Casey E, Collar D, Austin J (2001) Creation of low-copy integrated transgenic lines in *Caenorhabditis elegans*. Genetics 157(3): 1217-1226.

Figure 1 The loss of XPA-1 function results in apoptosis via activation of other signaling pathways.

(a) Increased levels of apoptosis in *xpa-1* mutants are suppressed by *hus-1* and *atl-1*. Germ cell apoptosis was scored 12, 24 and 36 h post L4/adult molt in staged: wild-type(wt), *xpa-1(ok698)*, *hus-1(op244)*, *atl-1(tm853)*, *hus-1(op244) xpa-1(ok698)* and *xpa-1(ok698); atl-1(tm853)* animals. **(b, c, d)** UV-C induces formation of RAD-51 foci, independently of XPA-1 and RAD-54. **(b)** Fluorescent microscopy of mid-late pachytene germ cell nuclei from staged wild-type (wt) young adult hermaphrodites stained with an anti-RAD-51 antibody, 3 h after exposure to 100 J/m^2 of UV-C. **(c)** Quantification of the RAD-51 foci shown in (b) in mid-late pachytene germ cell nuclei from wild-type, *xpa-1(ok698)* and *atm-1(gk186)* **(c)**, or *rad-54(ok615)* **(d)** young adult animals, 3 h following treatment with 120 Gy of X-rays or 100 J/m^2 of UV-C.

Stergiou et al., Figure 1

a

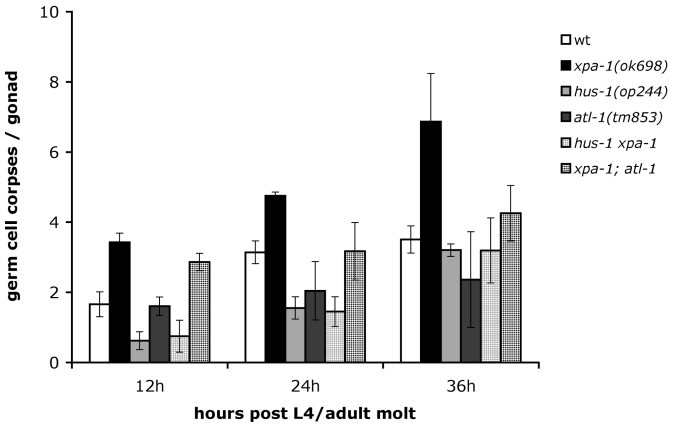

b

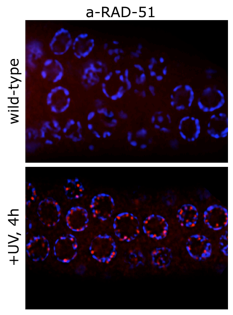

c

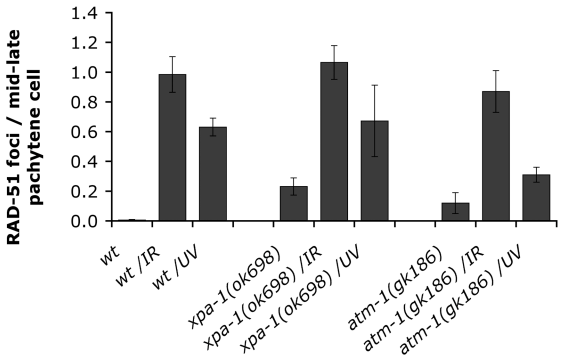

d

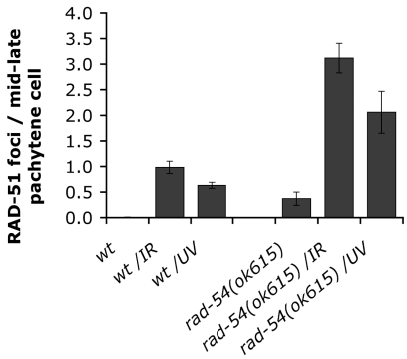

Figure 2 The Homologous Recombination Repair (HR) machinery is required for triggering UV-C-induced germ cell apoptosis.

(a) *rad-54(lf)* results in increased levels of germ cell apoptosis. Germ cell corpses were scored every 12 h until 36 h post L4/adult molt in staged: *rad-54(ok615)* or *rad-54(tm1268)* mutants, or *rad-54(RNAi)*-treated animals. **(b)** *rad-54(lf)*-dependent germ cell apoptosis is suppressed by *cep-1(lf)*. Staged *rad-54(ok615)* L1 larvae were raised on bacteria expressing *cep-1* or gfp dsRNA, and germ cell corpses scored in the adult germ line. **(c)** *rad-54(lf)*-dependent germ cell apoptosis is suppressed by *spo-11(lf)*. Staged wild-type (wt) or *spo-11(ok79)* L1 larvae were raised on bacteria expressing *rad-54* or gfp dsRNA, and germ cell corpses scored in the adult germline. **(d)** *rad-54(lf)*-dependent germ cell apoptosis is suppressed by *atm-1(lf)* and *atl-1(lf)*. Staged wild-type (wt), *atm-1(gk186)* or *atl-1(tm853)* L1 larvae were raised on bacteria expressing *rad-54* or gfp dsRNA, and germ cell corpses scored in the adult germ line. **(e-g)** *rad-54* and *mre-11* mutants fail to induce apoptosis in response to UV-C and IR. Staged young adult *rad-54(ok615)* **(e)** and *mre-11(ok179)* **(g)** animals were treated with either 100 J/m^2 UV-C or 120 Gy X-rays and germ cell corpses were scored at the indicated time points. **(f)** Staged *spo-11(ok79)* L1 larvae were raised on bacteria expressing *rad-54* or gfp dsRNA, and were treated with either 100 J/m^2 UV-C or 120 Gy X-rays as young adults. Germ cell corpses were scored at the indicated time points. **(h)** *rad-51(lf)* animals normally induce apoptosis in response to UV. Staged wild-type L1 larvae were raised on bacteria expressing *rad-51* or control dsRNA, and were treated with either 100 J/m^2 UV-C or 120 Gy X-rays as young adults. Germ cell corpses were scored at the indicated time points. Data shown in all cases represent the average of two-three independent experiments ± SD (n>20 animals for each experiment).

Stergiou et al., Figure 2

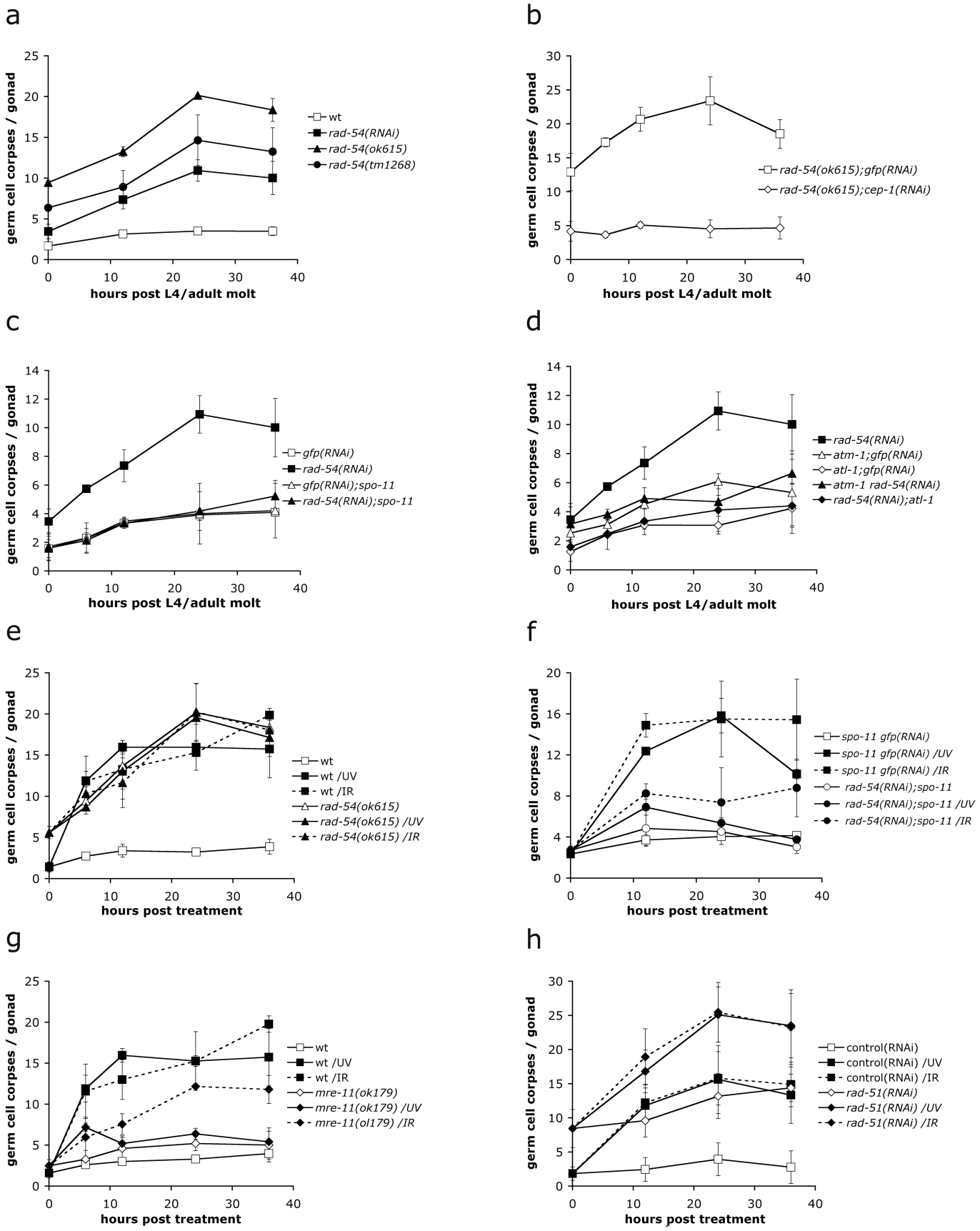

Figure 3 The HR pathway acts downstream of the NER pathway to induce UV-C-induced germ cell apoptosis.

(a, c) Fluorescent microscopy of mid-late pachytene germ cells expressing RAD-54::YFP (*opIs257*) or RPA-1::YFP (*opIs263*). Germ cell nuclei from staged young adult animals were scored for the presence of YFP, 3 h after exposure to 100 J/m^2 of UV-C or 120 Gy of X-rays. Relocalized RAD-54 or RPA-1 is seen as bright foci marked by arrowheads, whereas it is diffusely distributed before treatment. **(b)** UV-C-induced RAD-54 foci require XPA-1 and MRE-11. Quantification of the YFP positive signals shown in (a) following treatment with UV-C or IR in wild-type, *xpa-1(ok698)*, *hus-1(op244)*, *atm-1(gk186)* and *mre-11(ok179)* animals. **(d, e)** UV-C-induced RPA-1 foci require XPA-1 but not RAD-54. Quantification of the YFP positive signals shown in (c) following treatment with UV-C or IR in wild-type, *xpa-1(ok698)* **(d)**, or *rad-54(ok615)*, *spo-11(RNAi)* and *rad-54(ok615)*;*spo-11(RNAi)* animals.

Stergiou et al., Figure 3

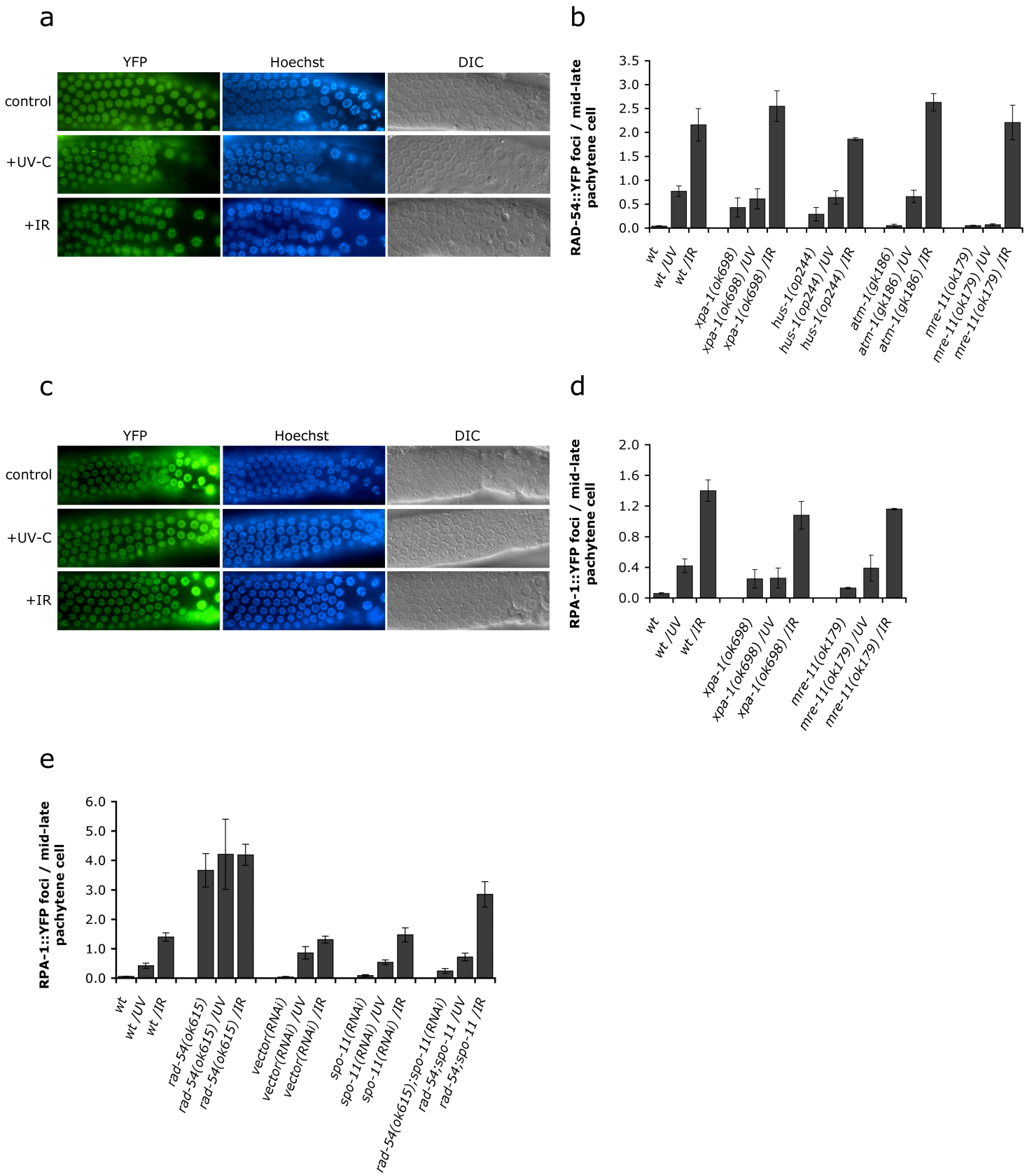

Figure 4 *C. elegans* NER components XPB, XPD and XPG, are required for UV-C-induced germ cell apoptosis, partially via recruitment of RAD-54.

Staged wild-type L1 larvae were raised on bacteria expressing *xpb* **(a)**, *xpd* **(b)** or control dsRNA, and were treated with either 100 J/m^2 UV-C or 120 Gy X-rays as young adults. Germ cell corpses were scored at the indicated time points. **(c, d)** Apoptosis was scored in *xpg-1(tm1670)* or *xpg-1(tm1682)* mutant animals after treatment with 100 J/m^2 UV-C **(c)** or 120 Gy X-rays **(d)**. Data shown in all cases represent the average of three independent experiments ± SD (n>15 animals for each experiment). **(e)** UV-C-induced RAD-54 foci require XPB and XPD. Quantification of the RAD-54 foci following treatment with 100 J/m^2 UV-C in *xpb* and *xpd* RNAi-treated or in *xpg-1(tm1670)* mutant animals.

Stergiou et al., Figure 4

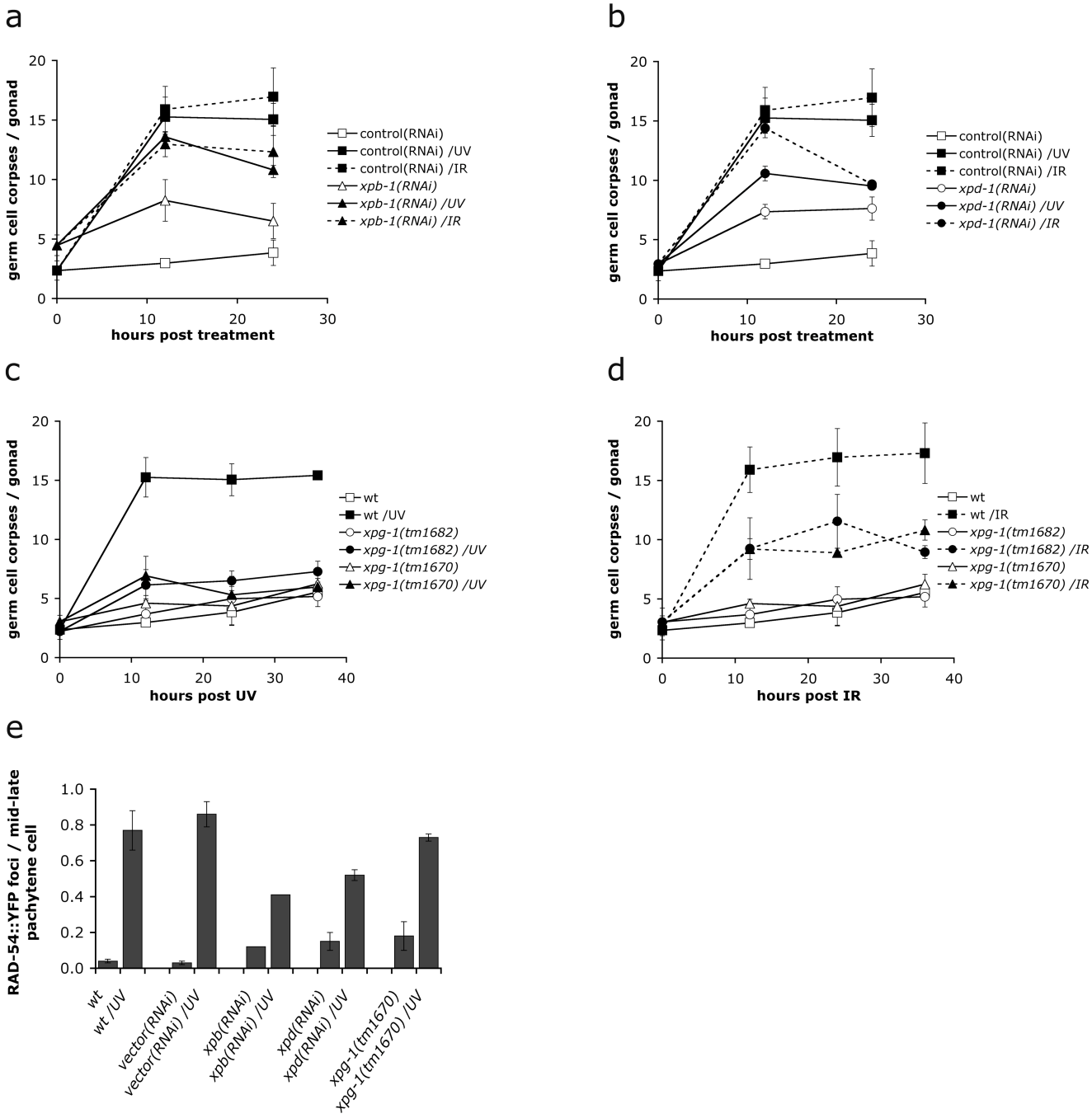

Figure 5 UV-C-induced germ cell apoptosis requires recruitment of HUS-1, ATM-1 and ATL-1 downstream of RAD-54 action.

(a) UV-C-induced HUS-1 foci require RAD-54. Mid-late pachytene germ cell nuclei from staged young adult wild-type (wt), *rad-54(ok616)* and *xpg-1(tm1670)* animals expressing HUS-1::GFP (*opIs34*) were scored for the presence of GFP, 3 h after exposure to 120 Gy of X-rays or 100 J/m^2 of UV-C. Relocalized HUS-1 is seen as bright foci, whereas it is diffusely distributed before treatment (Stergiou et al., 2007). **(b)** *rad-54(lf)*-dependent germ cell apoptosis is suppressed by *atm-1(lf)* and *atl-1(lf)*. Staged wild-type (wt), *atm-1(gk186)* or *atl-1(tm853)* L1 larvae were raised on bacteria expressing *rad-54* or gfp dsRNA, and germ cell corpses were scored in the adult germ line every 12 h until 36 h post L4/adult molt. Data shown represent the average of three independent experiments ± SD (n>15 animals for each experiment).

Stergiou et al., Figure 5

a

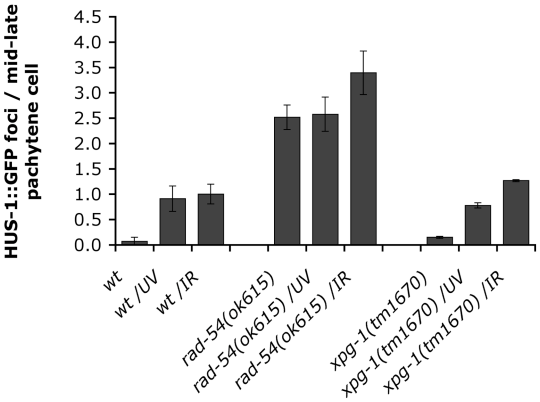

b

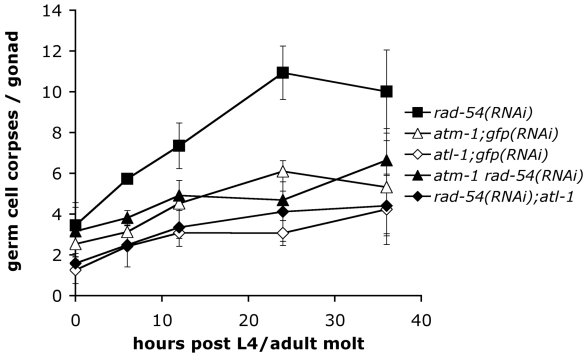

Figure 6 The lack of UV-C-induced apoptosis in *rad-54* mutants is due to lack of signaling to the apoptotic machinery.

(a) Fluorescent microscopy of germ cell nuclei from staged wild-type (wt) young adult hermaphrodites stained with an anti-CPD antibody, 20 min after exposure to 100 J/m^2 of UV-C. **(b)** Quantification of the CPD positive cells shown in (a) in mid-late pachytene germ cell nuclei from wild-type at 5 min, 10 min, 20 min, 1 h, 2 h, 4 h, 8 h and 16 h post 100 J/m^2 of UV-C treatment. **(c)** Quantification of the CPD positive cells in mid-late pachytene germ cell nuclei from wild-type, *xpg-1(tm1670)* and *rad-54(ok615)* animals at 20 min, 1 h and 6 h post UV-C. **(d)** Mid-late pachytene germ cell nuclei from staged young adult wild-type animals were scored for the presence of RAD-54::YFP positive cells at 5 min, 10 min, 20 min, 1 h, 2 h, 4 h, 8 h and 16 h post 100 J/m^2 of UV-C treatment. The generated curve was superimposed on the one shown in (b).

Stergiou et al., Figure 6

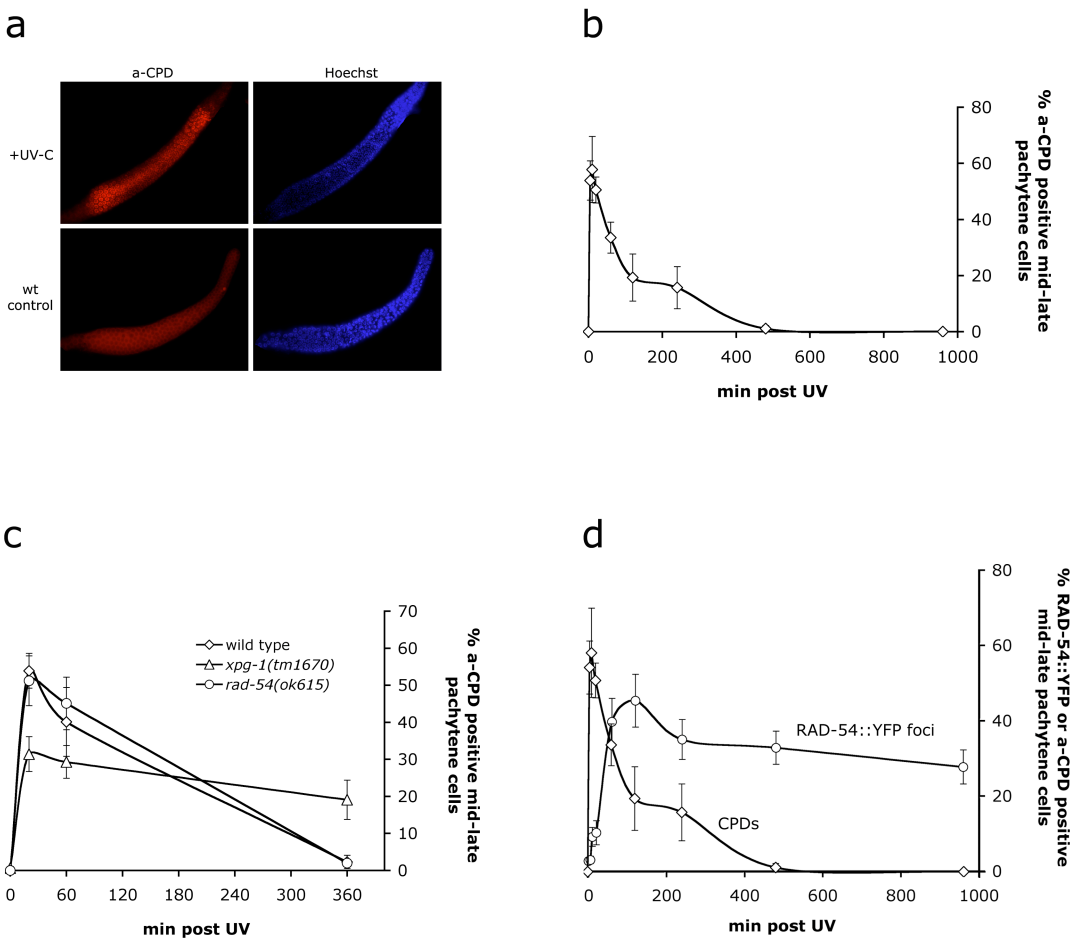

Figure 7 UV-C-induced apoptosis requires the action of both the NER and HR pathways.

Based on our genetic studies and our analyses with the *rad-54::yfp*, *rpa-1::yfp* and *hus-1::gfp* reporters we propose that UV-C-induced apoptosis occurs via two partially overlapping routes. The first one requires the XPA-1, XPB/XPD and XPG-1 components of the NER pathway. The second one is initiated downstream of XPB/XPD by recruiting the MRE-11 and RAD-54 components of the HR machinery as well as the 9-1-1 complex, upstream of the apoptotic machinery.

OR

Based on our genetic studies and our analyses with the *rad-54::yfp*, *rpa-1::yfp* and *hus-1::gfp* reporters we propose that UV-C-induced apoptosis is initiated via two partially overlapping routes. The common steps require the XPA and XPB/XPD homologs, whereas the XPG-1 and MRE-11 endonucleases define two different branches. The latter one requires recruitment of the RAD54 homolog and the 9-1-1 complex, upstream of the apoptotic machinery.

Stergiou et al., Figure 7

a

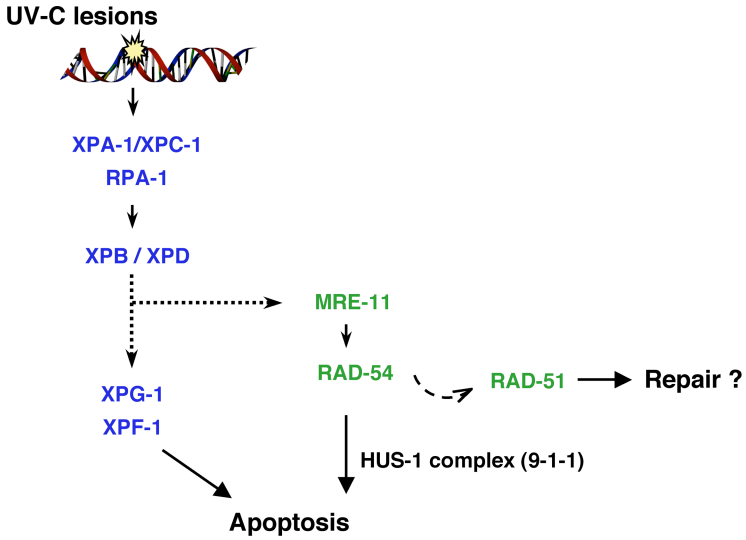

Supplementary Figure 1 RT-PCR analysis to determine the presence of transcripts in the mutants used in this study.

Primers were designed to flank the deletions in the genetic loci or the coding regions of *rad-54(ok615)* **(a)**, *xpg-1(tm1670)* and *xpg-1(tm1682)* **(c)** mutants. Genomic DNA or total mRNA from wild-type (wt) animals and the corresponding mutants was used in a PCR or RT-PCR reaction. In each case, a picture of the genomic PCR amplification around the locus (left panel) and a picture of the transcript PCR detection (right panel) are shown. 18SrRNA was used as an internal control for the presence of transcripts. Below, the gene structures are illustrated and the location where the mutations map are depicted by bars and the corresponding allele name. The existence of a known SL1 splicing site is denoted by a star, while genes in an operon are indicated by a sharpened bar. **(b)** Rescue of the increased germ cell apoptosis in *rad-54(ok615)* mutants in transgenic animals carrying a *Prad-54::rad-54::yfp::3'UTR* construct (*opIs257*). Germ cell corpses were scored 24 h post the L4/adult molt.

Stergiou et al., Supplem. Figure 1

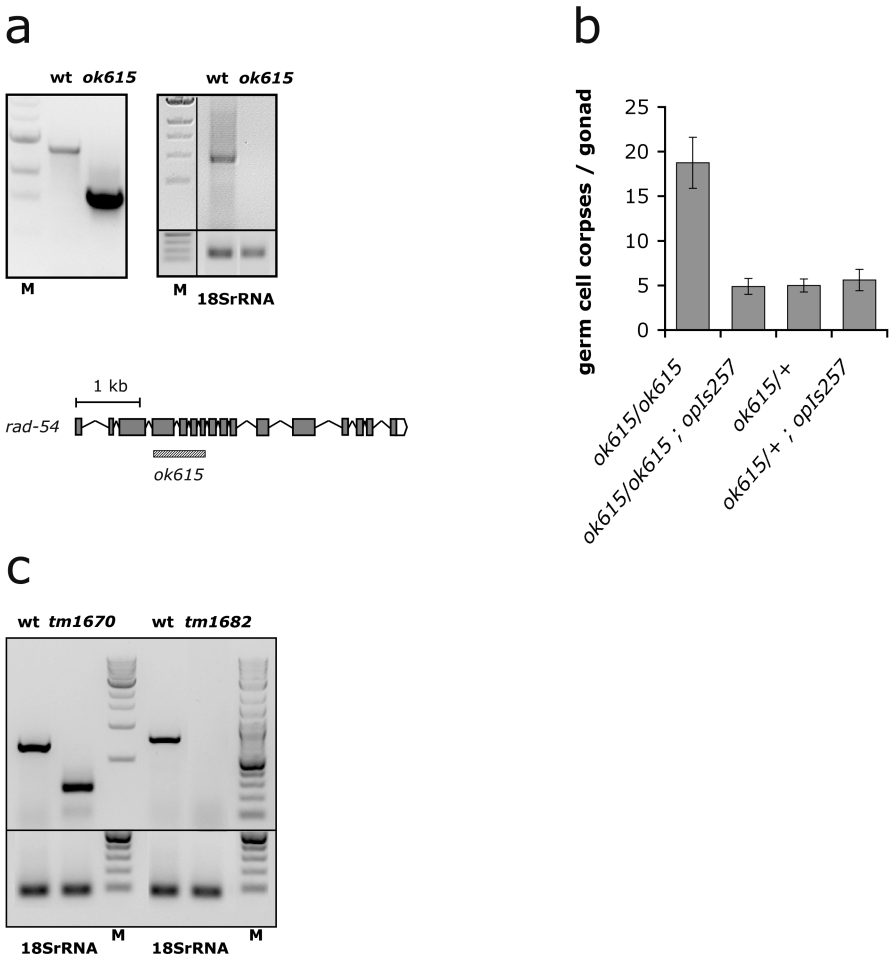

Supplementary Figure 2 RPA-1::YFP foci are formed shortly after treatment with UV-C or X-rays.

Staged wild-type young adults were treated with either 100 J/m^2 UV-C (a) or 120 Gy X-rays (b) and the mid-late pachytene germ cell nuclei were scored for the presence of foci 0.5 h, 1.5 h and 3.5 h later. Data shown represent the average of 15-20 gonads ± SEM.

Stergiou et al., Supplem. Figure 2

a

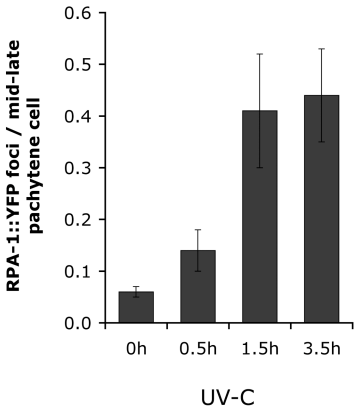

b

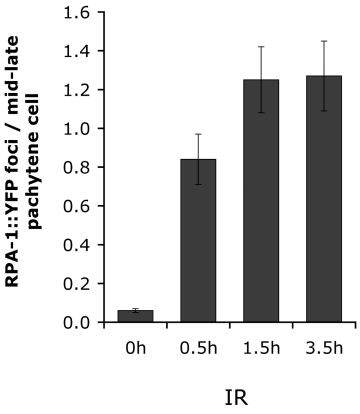

Supplementary Figure 3 RAD-54::YFP foci are formed after UV-C treatment and remain long in the germ line.

Mid-late pachytene germ cell nuclei from staged young adult wild-type animals were scored for the presence of RAD-54::YFP foci at 5 min, 10 min, 20 min, 1 h, 2 h, 4 h, 8 h and 16 h post 100 J/m^2 of UV-C treatment. Data shown represent the average of 15-25 gonads ± SEM.

Stergiou et al., Supplem. Figure 3

a

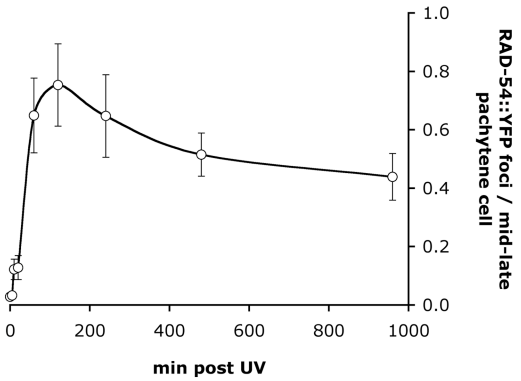

Supplementary Table S1: Primers corrsponding to exonic sequences for the generation of the RNAi constructs

(a) Primers for the RNAi constructs of *xpb-1* (Y66D12A.15) and *xpd-1* (Y50D7A.2) genes

Fw_(xpb-1)RNAi	TGGAGCCGGAAAGACGCTTGTC
Rv_(xpb-1)RNAi	GATCTTGTCGTTACGACGTTCGTG
Fw_(xpd-1)RNAi	TGAACCACAGGATGGTAGTCAACTG
Rv_(xpd-1)RNAi	TCTGAGTACTCGGCTCTCGGTGTA

(b) Primers for the generation of pLS69 and pLS57 translational reporters for *rpa-1* and *rad-54*

SbfI-Fw-rpa-1	GATCCCTGCAGGATGATATCATCAACGACAGGGTTGAGAC
FseI-Rv-rpa-1	GTACGGCCGGCCGTAGTCACTCATTTGTTGCATCTGCTC
PacI-Fw-3'UTRrpa-1	GTACTTAATTAAATGTTCTGTTTTTTATTACATCGTGCCGATC
ApaI-Rv-3'UTRrpa-1	GTACGGGCCCGACTGTCACTGATCTGAAAATGCTATTTTAC
SbfI-Fw-rad-54	GATCCCTGCAGGCTGAGTTCATTTTGATGTCCGTATAGTTG
FseI-Rv-rad-54	GTACGGCCGGCCATCGTCGTTTTCTTCGGCTTCAGAAG
SpeI-Fw-3'UTRrad-54	GTACACTAGTTTAAATGTTTCCAAGTTGAAACAAATCTAG
ApaI-Rv-3'UTRrad-54	GTACGGGCCCTAGTCTGAATTTCCAAAAAGTAA

CHAPTER 7

A ROLE FOR THE *C. ELEGANS* DNaseII HOMOLOG NUC-1 IN REGULATING LIFESPAN AND DNA DAMAGE-INDUCED APOPTOSIS

CHAPTER 7

A ROLE FOR THE *C. ELEGANS* DNaseII HOMOLOG NUC–1 IN REGULATING LIFESPAN AND DNA DAMAGE-INDUCED APOPTOSIS

7.1 ABSTRACT

This chapter deals with the preliminary characterization and the molecular cloning of the *op428* mutation, which turned out to be a novel allele of *nuc-1*, the *C. elegans* DNase II homolog. *op428* was originally believed to regulate programmed cell death in the *C. elegans* germline because of the increased levels of germ cell corpses these mutants exhibited. While this phenotype turned out to be due to a defect in cell corpse clearance rather than to increased apoptosis, the project took a very interesting turn when I discovered that loss of NUC-1 function would also compromise the apoptotic response of the worm upon DNA damage and lead to an increased life span. The data presented in this chapter fail to provide a clear mechanism of how NUC-1 is regulating these two processes but they will be extremely useful to the person who will continue with this puzzling project, if any. This project also inspired me to investigate the potential relationship between the mechanisms mediating increased stress resistance at the level of the organism with the mechanisms regulating DNA damage responses in the *C. elegans* germ line, presented in the last chapter of my thesis.

7.2 INTRODUCTION

As already mentioned in Chapters 1 and 4 an important fraction of germ cells undergoes apoptosis in the *C. elegans* adult hermaphrodite germ line in the absence of any external stimulus or damage. This type of death is referred to as “physiological” germ cell death. While developmental apoptosis occurring in somatic tissues and DNA damage-induced germ cell death have been studied and understood in great details (Lettre and Hengartner, 2006; Lettre et al., 2004; Stergiou and Hengartner,

2004), the mechanisms behind physiological germ cell apoptosis remain completely unknown.

During the course of the first year of my Ph.D. studies, the Hengartner lab received two novel mutants, named *op427* and *op428,* which seemed to exhibit increased levels of germ cell corpses. They had been originally isolated in a forward genetic screen for mutants with meiotic defects, which would result in high levels of germ cell death via activation of apoptosis through the pachytene checkpoint. The screen was performed in the laboratories of Dr. Anton Gatrner (University of Dundee) and Dr. Josef Loidl (University of Vienna) as follows: wild type worms were mutagenized with ethyl-methane-sulfonate (EMS) and the F_2 population was screened using Acridine Orange to visualize apoptotic germ cells. Forty thousand haploid genomes were approximately screened and several mutants were isolated. For most of the isolated mutants the increased levels of germ cell death were accompanied by meiotic defects; these were placed into 2 major complementation groups and are currently being studied by the aforementioned laboratories. A few of the isolated mutants, however, displayed increased levels of germ cell apoptosis but no meiotic defects. *op427* and *op428* belong to this category of mutants and, as such, they were originally believed to be good candidates to investigate the mechanisms that regulate physiological programmed cell death in the *C. elegans* germ line.

The experiments reported in this chapter were performed during the first two years of my Ph.D. until I was entirely absorbed by my work on *dyn-1*. Most of them are presented in a chronological order, something that rarely happens in scientific manuscripts, since I found that this allows for a better understanding of the turnovers of this chapter.

7.3 RESULTS

7.3.1 op427 and op428 exhibit increased levels of germ cell corpses and define a novel complementation group

op427 and op428 mutants exhibit a significant increase in the number of apoptotic germ cell corpses compared to the wild type strain, this being quantitated by timecourse analysis using Differential Interference Contrast microscopy (DIC) (Figure 7.1). Interestingly, neither of these mutations seems to have an effect on

developmental apoptosis in somatic tissues (Table 7.1), where the levels of cell death were comparable to wild type. A classical dominance/recessivity test revealed that both *op427* and *op428* were recessive mutations. After backcrossing each of the mutants four times back to the wild type strain N2 Bristol, I performed complementation tests with *gla-1* and *gla-3,* the two other major Gla (**G**erm **l**ine **a**poptosis) mutants the Hengartner lab was working on, as well as with each other. I found that *op427* and *op428* are not allelic to the previously known Gla mutations but they are allelic to each other, thus defining a novel complementation group (Figure 7.2). The observation that *op427* and *op428* act in a different pathway than *gla-1* and *gla-3* is further supported by the fact that they display neither a meiotic phenotype nor a reduced brood size (241 ± 23 for *op428*, *n=10* vs 248 ± 16, *n=10* for wild type), both of which are hallmarks of the "typical" *gla* mutants (Kritikou et al., 2006). For most of the experiments described in this chapter I decided to use *op428* since it seemed to be the strongest of the two alleles.

7.3.2 The increased germ cell death in op428 mutants is cep-1-, egl-1(lf)- and ced–9(gf)-independent

in order to understand how *op428* might modulate programmed germ cell death with respect to other known cell death regulators, I performed epistasis analyses. This has been done in parallel with the mapping, believing that it would facilitate the identification of the mutated locus. To investigate whether the increased levels of germ cell corpses observed in *op428* mutants are dependent on the core apoptotic machinery, I generated double mutants between *op428* and strong loss-of-function alleles of *ced-3* and *ced-4,* which completely suppress both physiogical and DNA-damage induced apoptosis. Loss of *ced-3* and *ced-4* function completely suppressed the increased levels of corpses in *op428* mutants thereby confirming their apoptotic nature (Figure 7.3). I also used a *ced-9* gain-of-function allele that has been shown to reduce the binding of CED-9 to EGL-1 and which strongly suppresses DNA-damage induced apoptosis without affecting physiological germ cell death. This *ced-9(n1950)* allele had no effect on germ cell apoptosis in *op428* mutants implying that the regulation of germ cell apoptosis by *op428* is independent of the DNA-damage induced apoptotic pathway (Figure 7.4A).

To corroborate this observation I constructed double mutants between *op428* and loss-of-function mutations in *egl-1,* a BH3-only protein, *cep-1*, the *C. elegans* p53 homolog, as well as in *hus-1* and *clk-2/rad-5*, which code for two conserved checkpoint proteins. All these components are necessary for activation of germ cell apoptosis in response to DNA damage. Interestingly, loss of *cep-1* function, does not suppress the increased levels of germ cell death, suggesting that *op428* acts downstream or in parallel to p53 (Figure 7.4B). Moreover, *op428* is epistatic to *egl-1(n1084n3082)* as the double mutant *egl-1(n1083n3082);op428* exhibits germ cell death levels similar to *op428* alone (Figure 7.4A). Similar results were obtained using strong loss-of-function mutations in the checkpoint genes *hus-1* and *clk-2* (Figure 7.5). Together, all these results strongly indicate that the increased levels of germ cell corpses in *op428* mutants cannot be attributed to the presence of DNA damage in the germ line and that they do not involve transcriptional upregulation of *egl-1* via CEP-1 (see also section *7.3.4*).

7.3.3 op428 mutants are defective in the apoptotic response upon DNA damage

To further test the above hypothesis I performed irradiation experiments. For this, synchronised populations of *op428* worms were irradiated with various doses of X-rays or UV-C radiation and the effect of these treatments on germ cell death was assessed by DIC microscopy at different timepoints. If the death observed in *op428* worms was physiological, then I would expect to see a dose- and time-dependent increase in the number of germ cell corpses upon irradiation, due to the parallel activation of the DNA damage-induced apoptotic response. Surprisingly, the initial cell death levels in *op428* mutants are not dramatically altered after treatment with either source of irradiation (Figure 7.6 and 7.7), suggesting that *op428* might also play a role in sensing and/or transducing signals of the DNA damage pathway. This observation is rather surprising as the other two major physiological cell death mutants the Hengartner lab is working on, *gla-1* and *gla-3*, do exhibit a significant increase in the number of apoptotic corpses upon treatment with X-rays (Kritikou et al., 2006). The above results suggest that *op428* might play an additional role in regulating DNA damage-induced apoptosis in the *C. elegans* germ line.

To further investigate the potential involvement of *op428* in the DNA damage response pathway I examined whether the affected genes could have a checkpoint function. Checkpoint proteins promote cell-cycle arrest in the mitotic region of the worm's germ line in response to DNA damage. Additionally, checkpoint mutants produce inviable embryos after treatment with ionizing radiation or UV-C because they are unable to repair damaged DNA. To test whether *op428* could have a role in checkpoint signaling I examined the cell cycle arrest response by scoring the number of mitotic germ cell nuclei in a defined area 6h and 12h after irradiation of L4 stage worms with either X-rays or UV-C. I also performed radiation sensitivity experiments by measuring the survival of embryos generated from irradiated, proliferating germ line nuclei. I found that germ cell cycle arrest was not altered in either *op427* or *op428* (Figure 7.8). Moreover, the survival of progeny from irradiated or UV-C-treated *op428* mutant animals was similar to wild type worms (Figure 7.9). Taken together these results indicate that the product of *op428* does not act as a checkpoint protein but likely acts downstream of the DNA damage checkpoint to regulate apoptosis.

7.3.4 Transcriptional induction of egl-1 is not compromised in op428 mutants upon DNA damage

Since all the currently known mediators of the DNA damage response trigger activation of the apoptotic machinery through transcriptional activation of *egl-1*, I then asked whether *egl-1* was properly induced in *op428* mutants, upon genotoxic stress. If *op428* had an involvement in DNA damage response signaling, at least via the known pathway, then I would expect the transcriptional induction of *egl-1* to be compromised in these mutants. Quantitative Real Time-PCR experiments revealed, however, that this was not the case, as induction of *egl-1* transcripts upon DNA damage occurred at levels similar to those in wild type worms (Figure 7.10). While the above result is relatively puzzling, it might also suggest that mutations in *op428* do not affect DNA damage signaling *per se*, but rather act at a later step to control activation of the programmed cell death machinery. *op428* would then act at a step downstream of *egl-1* mRNA induction.

7.3.5 Additional phenotypes of op428

Even though *op428* mutants look superficially wild type, a detailed inspection revealed two additional phenotypes. The most obvious one is a localized loss of the lipofuscin pigments, which seem to affect only the posterior part of the intestine, close to the worm's anus (Figure 7.11A). This confers to the worms a characteristic "clear tail" appearance when viewed under low magnification miscroscopy. While the precise origin of this phenotype remains unclear it probably reflects some kind of defect in lysosomal biogenesis; the intestinal lipofuscin granules have been shown to represent secondary lysosomes, which remain active recipients of endocytosed material (Clokey and Jacobson, 1986) The second, and less obvious, phenotype of *op428* mutants is a dramatic increase in the worm's lifespan. The mean lifespan of a *C. elegans* wild type strain is approximately 15 days with a maximum lifespan of approximately 30 days at 20°C. In *op428* mutants the average lifespan was found to be significantly longer than wild type by almost 70% (Figure 7.11B). Interestingly, *op428* mutants grow at the same rates as wild type worms but appear to be much fitter after 15 days (assessed by the ability of worms to move on the plate and by the rate of pharyngeal pumping), suggesting that *op428* is specifically involved in regulating *C. elegans* lifespan. This phenotype was a critical determinant in confirming the nature of the gene during *op428* mapping.

7.3.6 op428 is allelic to nuc-1

I used standard two-factor together with automated Fragment Length Polymorphism (FLP) mapping (Zipperlen et al., 2005) to map *op428* close to the center of LGX (Figure 7.12). The FLP analysis also gave me a physical interval within a region of approximately 2 Mb corresponding to roughly 400 predicted genes.

To genetically confirm the FLP mapping interval and to generate marker strains suitable for Single Nucleotide Polymorphism (SNP) mapping I performed three factor-mapping using the following three sets of markers: *unc-6* (-2.01 cM) *dpy-6* (0 cM), *dpy-6* (0 cM) *unc-9* (+10.25 cM) and *dpy-6* (0 cM) *unc-115* (+1.88 cM). The cross between *op428* and *unc-6 dpy-6* revealed that *op428* is on the right, or very close to the left of *dpy-6* because 17/17 Unc-non-Dpy were Gla while none of the 26 Dpy-non-Unc recombinants was Gla. In agreement with this result, two additional

crosses with *dpy-6 unc-9* and *dpy-6 unc-115* placed *op428* on the right arm of chromosome X between *dpy-6* and *unc-115*. From the cross between *op428* and *dpy-6 unc-9,* 22/27 Unc-non-Dpy and 4/23 Dpy-non-Unc recombinants were Gla, whereas from the cross between *op428* and *dpy-6 unc-115*, 11/30 Unc-non-Dpy recombinants were Gla and 13/20 Dpy-non-Unc recombinants were also Gla. Thus, the three-factor mapping placed *op428* within a genetic interval of 1,87 cM close to the center of chromosome X, flanked by the visible markers *dpy-6* and *unc-115*. This genetic interval is included in the initial physical interval obtained using FLP mapping.

To further narrow down the genetic interval where *op428* is located I used SNP mapping. Recombinants between *dpy-6 op428 unc-115* and the *C. elegans* polymorphic strain CB4856 placed *op428* between the molecular markers *snp_T20B5[1]* on the left and *pkP6159* on the right. This genetic interval corresponds to a physical region of roughly 300 kb, which contains 47 predicted genes. After several unsuccessful attempts to phenocopy the Gla phenotype of *op428* using RNAi against 37 out of 47 predicted genes located in the interval I decided to follow another strategy: I ordered all the available mutant strains included in the mapping interval and examined them for increased germ line apoptosis. For one of these mutants, *unc-5(e53);nuc-1(e1392)*, I observed elevated levels of AO positive germ cell corpses. Additionally *nuc-1(e1392)* failed to complement *op428* suggesting that the two mutations are allelic. Finally, sequencing of the *nuc-1* coding region in *op428* mutant worms revealed a single point mutation, a G to A transition that affects the acceptor site of the first intron. This mutation was found in various outcrossed *op428* strains as well as in the original unbackcrossed isolate, suggesting that it was tightly linked to the increased levels of AO positive corpses.

7.3.6 New roles for old friends

The *nuc-1* gene encodes a homolog of mammalian DNaseII (Wu et al., 2000). Both the worm NUC-1 and its mammalian counterpart are deoxyribonucleases involved in the degradation of the DNA of apoptotic cells. *nuc-1* was the first gene identified to affect cell death in *C. elegans*; it was discovered by John Sulston during his search for mutants defective in the cell lineages of the central nervous system

(Sulston, 1976). John Sulston also showed for the first time that this mutant is defective in the degradation of DNA in cells undergoing apoptosis (Horvitz, 2003).

Subsequent studies have established that DNA degradation during programmed cell death is a multistep and complex process, involving at least 9 different players (Parrish and Xue, 2003), *nuc-1* included. Loss of NUC-1 function has been associated with the accumulation of TUNEL-positive nuclei in mutant embryos, indicating that NUC-1 acts to resolve 3'OH DNA breaks (labelled by TUNEL) generated during apoptosis (Wu et al., 2000). Additionally, the same study reported that *nuc-1* mutants fail to digest the DNA of ingested bacteria in the intestine and exhibit an accumulation of Syto-11 positive pycnotic bodies, due to the inability of engulfing cells to degrade DNA derived from postembryonic cell deaths. How is the activity of NUC-1 regulated in each one of these tissues is not well understood.

At this point of the project it was unclear how the loss of a nuclease could account for any of the various phenotypes observed, raising the possibility that these were due to a background mutation. I thus tested whether I could dissociate *e1392,* the canonical *nuc-1* allele, from the increased levels of refractile corpses and the defect in the apoptotic response upon DNA damage. For this, I used an unbackcrossed *unc-5(e53);nuc-1(e1392)* strain and after outcrossing the *unc-5* gene I isolated worms exhibiting AO positive corpses. The worms were also examined for a defect in the apoptotic response upon DNA damage, which was found to be severely compromised. After repeating this procedure during several rounds of backcrossing, I concluded that these two phenotypes are tightly linked and are most likely due to a single mutation. Sequencing of the *nuc-1* locus, in several of these backcrossed strains, revealed that *e1392* tightly cosegregated with the two aforementioned phenotypes (Figure 7.13). The tight linkage between these phenotypes and *e1392* strongly suggests that these were due to a loss of NUC-1 function. Indeed, *nuc-1(e1392)* exhibited a similar behaviour to *op428* regarding the apoptotic response upon different doses of ionizing radiation or UV-C light (Figure 7.14).

Two additional pieces of evidence indicate that *op428* is a novel *nuc-1* allele. First, RNAi against *nuc-1* has been reported to significantly increase the worm's life span (Murphy et al., 2003) similar to the results obtained with *op428* mutants. Second in *op428* mutants undegraded bacterial DNA persists in the intestine, which is characteristic of mutations in the *nuc-1* locus (Wu et al., 2000, data not shown).

7.3.6 nuc-1(lf) mutants exhibit a germ line-specific defect in cell corpse clearance

How can loss of a nuclease involved in apoptotic DNA degradation result in increased apoptosis on one hand and in an apoptotic defect on the other? To address this issue I considered the possibility that the increased levels of corpses in *nuc-1* mutants were not due to an increase in apoptosis but rather to a slowed down clearance, similar to the accumulation of pycnotic bodies from defects in DNA degradation during somatic postembryonic cell deaths.

To test this I constructed double mutants between two different alleles of *nuc-1* and a loss-of-function mutation in the engulfment receptor *ced-1*. Additionally, I used the *opIs110* transgene, which expresses a YFP-tagged actin in the somatic sheath cells, to visualize corpses in the process of being engulfed (Kinchen et al., 2005). If the increased levels of corpses in *op428* were due to increased apoptosis, I would expect to see a further enhancement in the *ced-1* background, where a large fraction of the dying cells remain unengulfed and persist in the germ line. For the same reason, I would also expect the number of actin halos to be increased (similar to the results obtained with *gla-3* mutants, presented in Chapter 4). The results of these experiments clearly demonstrated that the germ cell corpses in *nuc-1(op428)* and *nuc-1(e1392)* mutants accumulate not because the rate of cell death is increased (i.e. there are more corpses dying in the course of time) but because the process of apoptotic cell corpse clearance is slowed down (Figure 7.15).

This finding was rather puzzling for two reasons: first *nuc-1* mutants don not have increased numbers of embryonic corpses. That would suggest that the kinetics of cell corpse clearance are dramatically different between the soma (at least during embryogenesis) and the germ line and/or a differential requirement for NUC-1 function between these two tissues. Second, germ cell corpses in *nuc-1(lf)* mutants are AO positive suggesting that NUC-1 is required after acidification of the phagosome (see chapter 3 for more details). This was the first identification of a mutant exhibiting a late "engulfment" defect characterized by the accumulation of AO positive corpses (this observation preceded by more than 1 year all the experiments reported in chapter 3 and the discovery of *rab-7*).

7.3.7 Expression pattern of nuc-1 and tissue-specific rescue experiments

To further investigate the novel roles of *nuc-1* I performed expression studies by constructing both transcriptional and translational reporters. Despite being the first cell death gene to be identified there were no available expression data about NUC-1.

I first constructed a transcriptional fusion using a 3.6kb genomic fragment upstream of the *nuc-1* ATG, corresponding to the endogenous *nuc-1* promoter *Pnuc-1,* driving expression of GFP. Several lines were obtained using biolistic transformation and many of these displayed a strong GFP signal during embryogenesis (Figure 7.16) and larval development but also later during adulthood, consistent with the known roles of *nuc-1* in apoptotic DNA degradation. During adulthood *Pnuc-1* was found to be particularly active in the vulva and in a subset of cells close to the anus of the worm, although *nuc-1* has not been reported to have a role in these tissues (Figure 7.17). Expression was also observed in the somatic sheath cells which encase the hermaphrodite germ line and engulf apoptotic germ cells. In contrast, GFP expression in the intestine was very weak, a rather unexpected finding knowing the prominent role of NUC-1 in this tissue. Intriguingly, some lines exhibited a GFP signal in neuronal structures in the vicinity of the worm's nerve ring, suggesting that NUC-1 might also play a role in neuronal cells (Figure 7.17). This observation is quite fascinating as it might be linked to the role of NUC-1 in regulating lifespan.

In order to pin down the mechanism of *nuc-1* action I performed tissue-specific rescue experiments using the following set of promoters: *Peft-3,* a strong, ubiquitous promoter, *Ppie-1,* a germ line- and early embryo-specific promoter and the endogenous promoter *Pnuc-1*, all of them driving the expression of a genomic fragment covering the entire coding region of *nuc-1* and fused upstream of GFP. Despite several attempts using biolistic transformation I never managed to obtain transgenic animals expressing NUC-1 at a detectable level, even for the constructs containing the *Peft-3* promoter. High levels of NUC-1 expression might be toxic to the worm, which would explain why only low expressing lines were selected; this toxicity might also be due to the position of the GFP tag. Alternative strategies such as N-terminal protein fusions or raising antibodies against NUC-1 might be more useful to study the expression of pattern of *nuc-1*, which I consider to be a paramount element in deciphering the mode of action of this gene.

7.4. DISCUSSION

Here I described the mapping and the genetic characterization of *op428,* a mutation originally believed to regulate germ line apoptosis. Using standard genetic approaches I demonstrated that *op428* is a novel allele of *nuc-1*, the *C. elegans* DNaseII homolog. I also reported that the increased levels of refractile germ cell corpses in *nuc-1* mutants are due to a defect in corpse degradation rather than to increased apoptosis. Finally, I presented evidence suggesting that NUC-1 has at least two novel functions, in modulating the apoptotic response upon DNA damage as well as in regulating the lifespan of the worm.

7.4.1 nuc-1, a novel player in DNA damage signaling?

The idea that a nuclease, such as NUC-1, might be part of the worm's arsenal against DNA damage seems reasonable and, as a result, it has already been investigated to a certain extent. Hartman and Herman in their original screen for radiation sensitive mutants (Hartman and Herman, 1982) tested *nuc-1* for a potential role in DNA repair. They performed embryonic survival assays upon irradiation with X-rays and UV where the survival of *nuc-1* mutants was no different from wild type. The experiments presented in this chapter point towards the same direction, as *nuc–1(op428)* exhibits no cell cycle arrest defect and no increased embryonic lethality upon ionizing radiation, both of which are common features of checkpoint genes or genes involved in repair.

The data presented here show, however, that *nuc-1* mutants fail to mount a robust apoptotic response upon ionizing radiation or UV-C. This suggests that the function of NUC-1 in the DNA damage response might be confined only to the apoptotic output. Interestingly, preliminary results have shown that transcriptional induction of *egl-1,* which is a hallmark of DNA damage-induced cell death, seems to occur normally in *nuc-1(lf)* mutants upon irradiation, implying that *nuc-1* acts downstream of or in parallel to *egl-1*. This observation also suggests that NUC-1 is able to modulate the apoptotic output without interfering with the transcriptional activity of CEP-1/p53, perhaps by interfering directly with the core apoptotic machinery. Interestingly, recent studies revealed the existence of such a CEP-1/p53-independent pathway regulating apoptotis upon genotoxic stress (Quevedo et al.,

2007). Whether NUC-1 belongs to or activates the same pathway remains to be determined.

A key question in understanding the mechanim of action of NUC-1, is whether it exerts its pro-apoptotic function in a cell-autonomous way or whether it is a non cell-autonomous process. In the absence of any experimental evidence pointing towards the one or the other possibility, I believe that both scenarios are equally possible. A cell-autonomous model could involve, for instance, a feedback mechanism where NUC-1 acts to amplify the originally few DNA lesions caused by exogenous DNA damage. This would lead to an overactivation of the DNA damage reponse pathway which would then result in the potent activation of the apoptotic machinery and cellular demise. While this is certainly an appealing model, it remains purely speculative as there is little evidence that such a feedback mechanism exists in the *C. elegans* germ line.

Loss of *nuc-1* could also interfere with the DNA damage apoptotic response as well as with the regulation of the worm's lifespan via non cell-autonomous mechanisms. The persistence of undegraded DNA inside the phagocytes and/or the accumulation of undegraded bacterial DNA in the intestine could activate stress signaling pathways, thereby influencing apoptosis and increasing lifespan by enhancing the worm's ability to cope with stress. In Drosophila analysis of several DNase deficiencies revealed that specifically the lack of DNase II activity resulted in the upregulation of the antibacterial peptides attacin A and diptericin (Mukae et al., 2002). The same study also showed that this effect was limited to antibacterial activities since expression of the antifungal gene drosomycin was not affected. Thus, DNase II deficiency can lead to increased antibacterial gene expression, presumably due to increased susceptibility to bacterial infection. Importantly, this also indicates that defects in DNase II function can have a significant impact upon systems other than DNA degradation. Whether *nuc-1(lf)* mutants also exhibit increased expression of antimicrobial effectors or increased detoxifying activities remains to be determined. This will be an important step towards understanding how NUC-1 acts in *C. elegans*.

7.4.2 nuc-1 as critical determinant of C. elegans lifespan

The data presented in this chapter are in agreement with previous studies reporting that reduction of NUC-1 activity using RNAi leads to an increased lifespan (Murphy et al., 2003). Why and how would a nuclease regulate the lifespan of *C. elegans*? One possible theory is that since NUC-1 is also involved in the degradation of dietary bacterial DNA, the inability to properly digest the ingested food would compromise the ability of the worm to feed properly and lead to caloric restriction. This theory would also explain the fact that *nuc-1* mRNA is downregulated in *daf-2(lf)* mutants (Murphy et al., 2003), since upon entry into dauer diapause the worms stop feeding.

Several observations suggest, however, that *nuc-1* mutants are not calorically restricted, at least not enough to comply with the typical description of a calorically restricted worm. To subject *C. elegans* to caloric restriction three approaches have been take so far: dilution of the bacterial source food (Hosono et al., 1989; Klass, 1977; Vanfleteren and Braeckman, 1999), use of behavioural mutants which cannot feed normally (Avery, 1993; Lakowski and Hekimi, 1998; McKay et al., 2004), and culture in an axenic liquid medium (Vanfleteren and Braeckman, 1999). In all these studies, under conditions leading to a noticeable lifespan extension, calorically restricted worms grew very slowly and developed into adults which were thinner, smaller and clearer than wild type worms with a dramatically reduced broodsize. Additionally, these worms also suffered from major germ line defects. In contrast, *nuc-1(lf)* mutants are indistinguishable from wild type in terms of growth rates, size, fertility and germ line morphology. Even if these mutants were slightly calorically restricted it is unlike that caloric restriction is the sole mechanism accounting for the dramatic increase in the lifespan observed.

So how does *nuc-1* regulate lifespan? While several possibilities might be envisaged, I consider that most of them are variations on the same central theme: loss of NUC-1 activates stress protection-specific pathways the activity of which leads to an increase in the lifespan of the worm. The nature of these pathways and the exact mode of *nuc-1* action remain to be determined and constitute an extremely interesting project.

7.4.3 Future perspectives

A first step in deciphering the role of this nuclease would be to examine whether the increased lifespan of *nuc-1* mutants can be suppressed by loss of function mutations in *daf-16* and whether it can be enhanced by *daf-2(lf)*. This is a very informative experiment because it could indicate whether *nuc-1* exerts its aging effects by activating the insulin signaling pathway, via a positive feedback loop (as a reminder *nuc-1* is DAF-16 transcriptional target and its expression is downregulated in *daf-2(lf)* mutants). The tissue-specific rescue experiments together the expression data will also be extremely useful in understanding how, and where, NUC-1 acts. Additionally, large-scale studies of *nuc-1* mutants using quantitative proteomics methods might provide us with valuable hints regarding any potential difference in the levels of detoxifying or bactericidal activities. Last but not least, inspection of mutants of other nucleases involved in apoptotic DNA degradation for DNA damage or lifespan-related phenotypes will certainly help elucidate how *nuc-1* is affecting these two fundamental processes.

In conclusion, even though the *nuc-1* project has not been completed I believe that my work so far has led to some important observations. First, this project helped us realize that we can identify genes involved in late steps of apoptotic cell corpse engulfment and this had been a valuable observation for all the work we performed on phagosone maturation (Chapter 3). *nuc-1* mutants were the first mutants exhibiting an engulfment defect but where the corpses stained with Acridine Orange. Second, the results obtained so far regarding the unexpected role of NUC-1 in DNA damage induced-apoptosis and aging raise the possibility that these two processes might be connected to a certain extent. If *nuc-1* turns out to act non cell-autonomously, this will indicate that the DNA damage responses we observe in the germ line also depend on signals emanating from somatic tissues, an idea that before encountering *nuc-1* sounded completely absurd.

Michael Hengartner once told me he thought *nuc-1* was the most boring *C. elegans* gene. For me this gene remains a mystery and I hope that the results presented here illustrate this. Even though I run out of time trying to decipher the "*nuc-1* mystery" I hope that some of the future graduate students will read this chapter, will become intrigued and will provide us with exciting answers about the multiple functions of this nuclease!

7.5 METHODS

7.5.1 General methods and strains

Methods for culturing *C. elegans* have been described by Brenner (Brenner, 1974). All mutant strains used in these study were grown at 20°C and were derived from the wild type variety Bristol N2. Mutations used were as follows: LGI: *dpy-5(e61), hus-1(op244)/nT1, gla-1(op234), gla-3(op216), ced-1(e1735),* LGIII: *ced-4(n1162), rad-5/clk-2(mn159ts),* LGIV: *unc-5(e53), ced-3(n717),* and LGIV: *opIs110[Plim-7::yfp::act-5],* LGX: *unc-6(e78), dpy-6(e14), nuc-1(e1392), nuc-1(op428), unc-115(mn481), unc-9(e101)*. Unless noted otherwise mutations were previously described (Bieri et al., 2007)

7.5.2 DIC microscopy and cell corpse counts

For the Nomarski analysis animals were placed on 4% agar slides in a drop of M9 salt solution containing either 30 mM NaN_3 (Hodgkin, 1980) or 3-5mM levamisole (Sigma) and mounted under a coverslip for observation. For most animals observed only one gonad arm was scored, as the other arm was usually concealed by the intestine. For each targeted gene associated with a suppression of the AO staining the average corpse number with the standard deviation (s.d) were determined using the Excel program (Microsoft).

7.5.3 Photography

Pictures were captured using a ORCA-ER digital CCD camera on a Leica DM-RA research microscope and processed using OpenLab software (Improvision) and Photoshop (Adobe).

7.5.4 Plasmid construction and cloning

To generate a transcriptional *Pnuc-1::gfp* fusion a 3.6 kb genomic fragment upstream of the *nuc-1* ATG was amplified from *C. elegans* genomic DNA using primers that added an SbfI site upstream and an FseI site downstream of the fragment (SbfI - FseI cassette). This SbfI-FseI cassette was cloned into the pCR2.1-TOPO

vector (Invitrogen) and sequenced to ensure fidelity (pKD2). The cassette was then excised using SbfI and FseI and cloned into SbfI/FseI sites of pLN020, immediately upstream of *gfp*, to generate (pKD12).

To generate translational reporters for tissue-specific rescue experiments a 2,4 kb genomic fragment corresponding to the coding sequence of the *nuc-1* locus was amplified by PCR from N2 genomic DNA using primers that added an AscI site upstream and an FseI site downstream of the coding sequence (AscI - FseI cassette). This AscI - FseI cassette were cloned in the pCR2.1-TOPO vector (Invitrogen) and sequenced to ensure fidelity (pKD3). AscI and FseI were used to excise the 2,4 kb *nuc-1* genomic fragment from pKD3 which was subsequently cloned into the AscI/FseI sites of pKD13, under the control of *Ppie-1* (to make pKD16), and of pLN21 under the control of *Plim-7* which is expressed in the somatic sheath cells (to make pKD10). Additionally, *nuc-1* was also placed under the control of *Peft-3* (to make pKD35). A 1kb region downstream of *nuc-1* stop codon (3'UTR) was PCR-amplified as a PacI or a SpeI cassette and was cloned into the aforementioned plasmids downstream of *gfp*.

To place *nuc-1* under the control of the endogenous promoter *Pnuc-1* a 3.6 kb genomic fragment upstream of the *nuc-1* ATG was amplified from *C. elegans* genomic DNA using primers that added an SbfI site upstream and an AscI site downstream of the fragment (SbfI - AscI cassette). This SbfI-AscI cassette was cloned into the pCR2.1-TOPO vector (Invitrogen) and sequenced to ensure fidelity (pKD1). The cassette was then excised using SbfI and AscI and cloned into SbfI/AscI sites of pKD13, immediately upstream of the *nuc-1* genomic fragment C-terminaly fused to *gfp*, to generate (pKD19).

7.5.5 Transgenic animals

Low copy transgenic worms were obtained by microparticle bombardment using a PDS-1000 (Bio-Rad) biolistic transformation apparatus previously described (Praitis et al., 2001). *unc-119* was used as a transformation marker.

7.5.6 Lifespan assays

Lifespan assays were carried out at 20°C using NGM plates seeded with OP50. Worms were picked as L4 and were monitored every day for survival. Animals were scored as dead if they didn't exhibit pharyngeal pumping and if they failed to respond to prodding with a pick.

7.5.7 Relative quantification of transcripts

Total RNA was extracted from wild type and *op428* mutants after treatment with 120 Gy of X-rays and/or from untreated worms. cDNA synthesis and quantitative real-time RT-PCR were performed as previously described (Hofmann et al., 2002). Transcripts of the pro-apoptotic genes *egl-1* and *ced-13* were measured after normalization with 18S rRNA, which was used as internal control. The average fold-change upon treatment was deduced based on two independent experiments.

7.6 REFERENCES

Avery, L. (1993). The genetics of feeding in Caenorhabditis elegans. Genetics *133*, 897-917.

Bieri, T., Blasiar, D., Ozersky, P., Antoshechkin, I., Bastiani, C., Canaran, P., Chan, J., Chen, N., Chen, W. J., Davis, P., *et al.* (2007). WormBase: new content and better access. Nucleic Acids Res *35*, D506-510.

Brenner, S. (1974). The genetics of Caenorhabditis elegans. Genetics *77*, 71-94.

Clokey, G. V., and Jacobson, L. A. (1986). The autofluorescent "lipofuscin granules" in the intestinal cells of Caenorhabditis elegans are secondary lysosomes. Mech Ageing Dev *35*, 79-94.

Hartman, P. S., and Herman, R. K. (1982). Radiation-sensitive mutants of Caenorhabditis elegans. Genetics *102*, 159-178.

Hofmann, E. R., Milstein, S., Boulton, S. J., Ye, M., Hofmann, J. J., Stergiou, L., Gartner, A., Vidal, M., and Hengartner, M. O. (2002). Caenorhabditis elegans HUS-1 is a DNA damage checkpoint protein required for genome stability and EGL-1-mediated apoptosis. Curr Biol *12*, 1908-1918.

Horvitz, H. R. (2003). Nobel lecture. Worms, life and death. Biosci Rep *23*, 239-303.

Hosono, R., Nishimoto, S., and Kuno, S. (1989). Alterations of life span in the nematode Caenorhabditis elegans under monoxenic culture conditions. Exp Gerontol *24*, 251-264.

Kinchen, J. M., Cabello, J., Klingele, D., Wong, K., Feichtinger, R., Schnabel, H., Schnabel, R., and Hengartner, M. O. (2005). Two pathways converge at CED-10 to mediate actin rearrangement and corpse removal in C. elegans. Nature *434*, 93-99.

Klass, M. R. (1977). Aging in the nematode Caenorhabditis elegans: major biological and environmental factors influencing life span. Mech Ageing Dev *6*, 413-429.

Kritikou, E. A., Milstein, S., Vidalain, P. O., Lettre, G., Bogan, E., Doukoumetzidis, K., Gray, P., Chappell, T. G., Vidal, M., and Hengartner, M. O. (2006). C. elegans GLA-3 is a novel component of the MAP kinase MPK-1 signaling pathway required for germ cell survival. Genes Dev *20*, 2279-2292.

Lakowski, B., and Hekimi, S. (1998). The genetics of caloric restriction in Caenorhabditis elegans. Proc Natl Acad Sci U S A *95*, 13091-13096.

Lettre, G., and Hengartner, M. O. (2006). Developmental apoptosis in C. elegans: a complex CEDnario. Nat Rev Mol Cell Biol *7*, 97-108.

Lettre, G., Kritikou, E. A., Jaeggi, M., Calixto, A., Fraser, A. G., Kamath, R. S., Ahringer, J., and Hengartner, M. O. (2004). Genome-wide RNAi identifies p53-dependent and -independent regulators of germ cell apoptosis in C. elegans. Cell Death Differ *11*, 1198-1203.

McKay, J. P., Raizen, D. M., Gottschalk, A., Schafer, W. R., and Avery, L. (2004). eat-2 and eat-18 are required for nicotinic neurotransmission in the Caenorhabditis elegans pharynx. Genetics *166*, 161-169.

Mukae, N., Yokoyama, H., Yokokura, T., Sakoyama, Y., and Nagata, S. (2002). Activation of the innate immunity in Drosophila by endogenous chromosomal DNA that escaped apoptotic degradation. Genes Dev *16*, 2662-2671.

Murphy, C. T., McCarroll, S. A., Bargmann, C. I., Fraser, A., Kamath, R. S., Ahringer, J., Li, H., and Kenyon, C. (2003). Genes that act downstream of DAF-16 to influence the lifespan of Caenorhabditis elegans. Nature *424*, 277-283.

Parrish, J. Z., and Xue, D. (2003). Functional genomic analysis of apoptotic DNA degradation in C. elegans. Mol Cell *11*, 987-996.

Praitis, V., Casey, E., Collar, D., and Austin, J. (2001). Creation of low-copy integrated transgenic lines in Caenorhabditis elegans. Genetics *157*, 1217-1226.

Quevedo, C., Kaplan, D. R., and Derry, W. B. (2007). AKT-1 regulates DNA-damage-induced germline apoptosis in C. elegans. Curr Biol *17*, 286-292.

Stergiou, L., and Hengartner, M. O. (2004). Death and more: DNA damage response pathways in the nematode C. elegans. Cell Death Differ *11*, 21-28.

Sulston, J. E. (1976). Post-embryonic development in the ventral cord of Caenorhabditis elegans. Philos Trans R Soc Lond B Biol Sci *275*, 287-297.

Vanfleteren, J. R., and Braeckman, B. P. (1999). Mechanisms of life span determination in Caenorhabditis elegans. Neurobiol Aging *20*, 487-502.

Wu, Y. C., Stanfield, G. M., and Horvitz, H. R. (2000). NUC-1, a caenorhabditis elegans DNase II homolog, functions in an intermediate step of DNA degradation during apoptosis. Genes Dev *14*, 536-548.

Zipperlen, P., Nairz, K., Rimann, I., Basler, K., Hafen, E., Hengartner, M., and Hajnal, A. (2005). A universal method for automated gene mapping. Genome Biol *6*, R19.

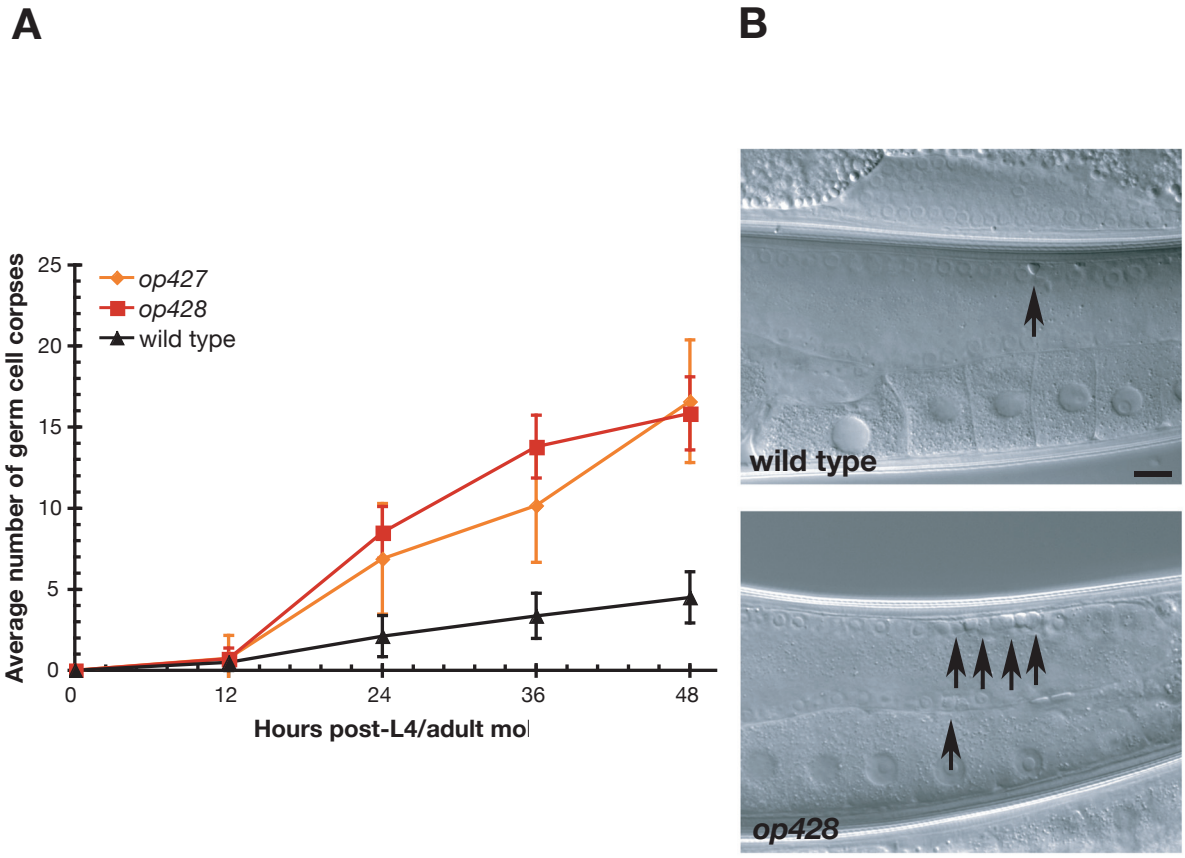

FIGURE 7.1 *op427* and *op428* exhibit increased levels of apoptotic corpses in the *C. elegans* germline

(A) Timecourse analysis was performed using N2, *op427* and *op428* mutant worms. Apoptotic germ cell corpses were scored in the meiotic region of one gonad arm using DIC optics at 12h, 24h, 36h and 48h after the L4/adult molt. Data shown represent the average of the mean of at least two independent experiments (n=10-15 worms per experiment). Error bars represent the SD. (B) DIC photomicrographs of wild type and *op428* mutant worms 24h post-L4/adult molt. Arrows indicate areas with apoptotic nuclei. Size bar 10µm.

Table 7.1 *op427* and *op428* do not affect programmed cell death during development

Genotype	Refractile Corpses (DIC)		
	comma	**2-fold**	**L1**
wild type	8.4 ± 1.8	14.7 ± 1.9	0
ced-1(e1735)	20.3 ± 3.6	38.8 ± 7.1	22.1 ± 3.2
op427	7.8 ± 1.6	15.6 ± 2.1	0
op428	8.2 ± 1.9	13.9 ± 2.4	0

The mean number of apoptotic corpses at three different developmental stages (comma, 2-fold and the first larval stage L1) was determined by DIC. At least 15 embryos or L1 larvae were scored for each genotype and for each stage. Error represents SD.

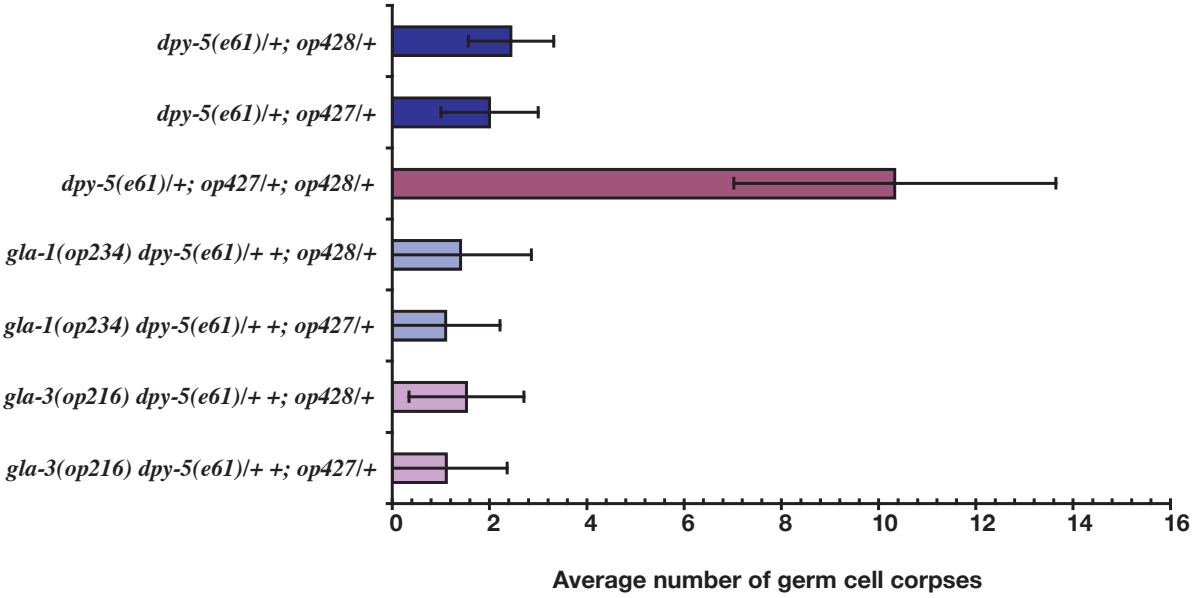

FIGURE 7.2 *op427* and *op428* are recessive mutations and define a novel complementation group

op427 and *op428* mutant males were crossed to either *dpy-5* single mutants or to *gla-1 dpy-5* and *gla-3 dpy5* double mutant hermaphrodites. From each cross the non-Dpy cross-progeny was examined for germ cell apoptosis 24h post-L4 using DIC. At least 15 worms were scored for each experiment. Error bars represent the SD.

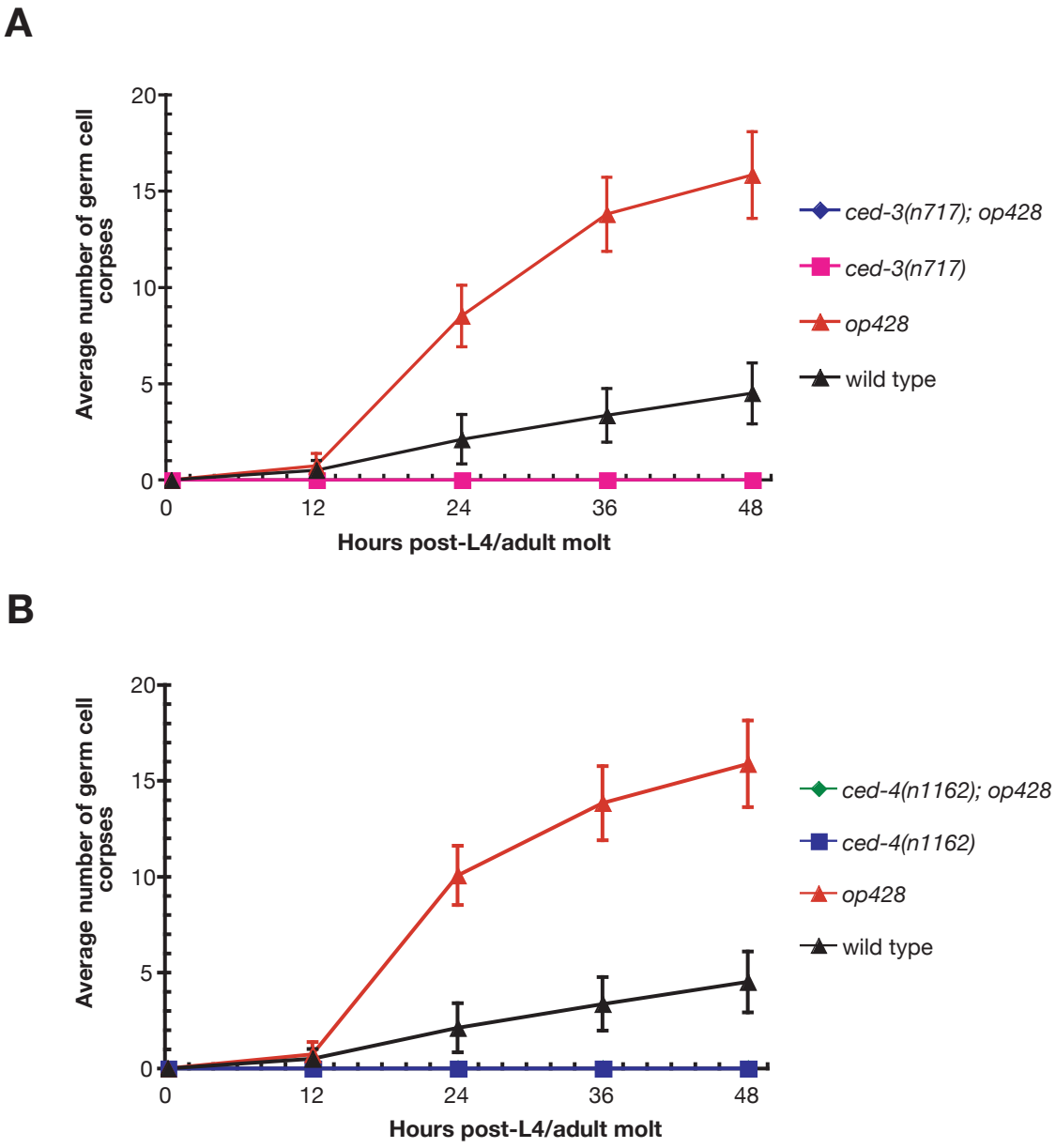

FIGURE 7.3 Epistasis analysis places *op428* upstream of the core apoptotic machinery

Timecourse analysis was performed using wild type, *op428*, *ced-3(n717)* and *ced-4(n1162)*single mutant worms, and *ced-3(n717);op428* (A) or *ced-4(n1162);op428* (B) double mutants. Apoptotic germ cell corpses were scored in the meiotic region of the germline using DIC optics at 12h, 24h, 36h and 48h after the L4/adult molt. Data shown represent the average of the mean of at least two independent experiments (n=10-15 worms per experiment). Error bars represent the SD.

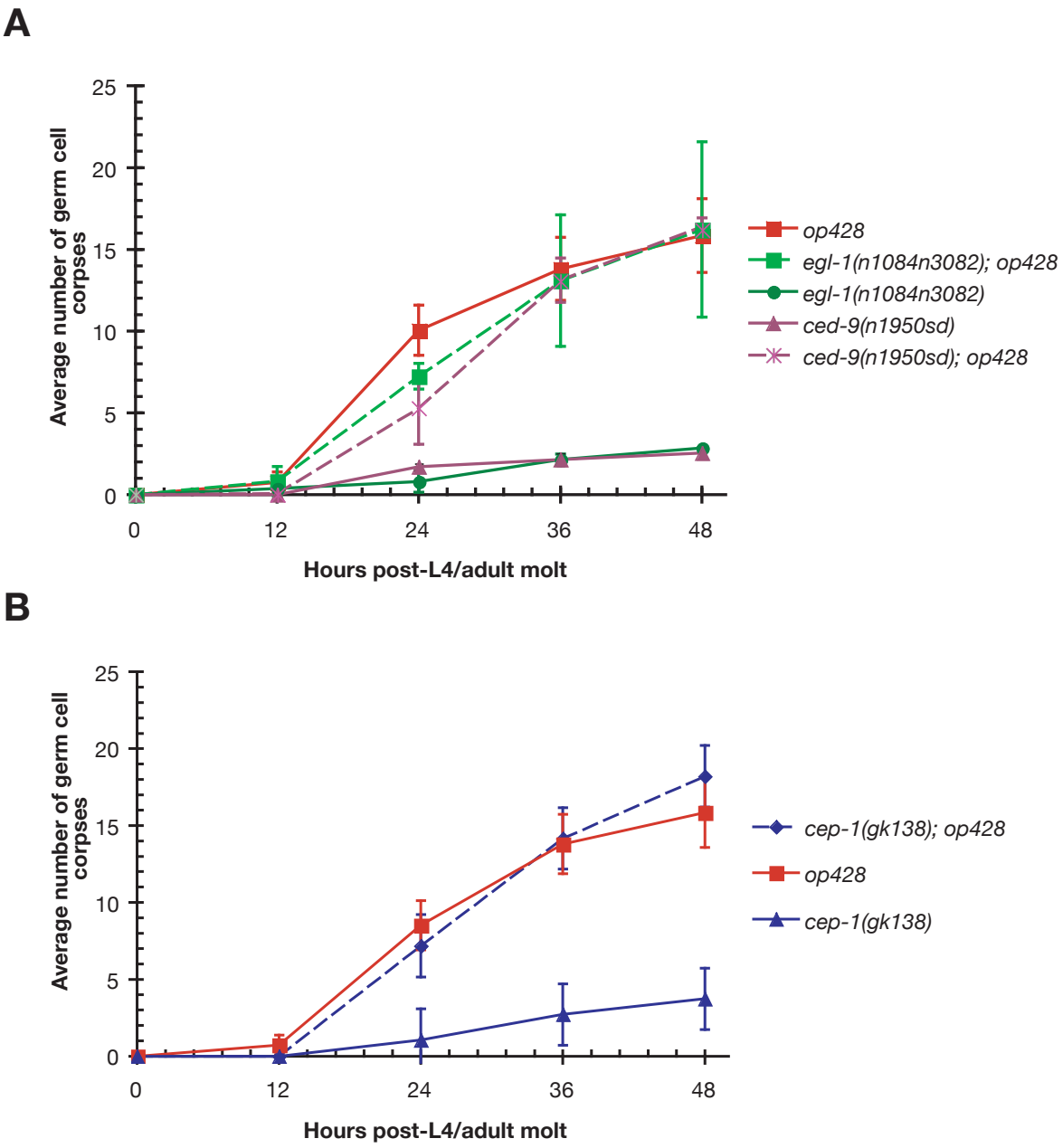

FIGURE 7.4 The increased levels of germ cell corpses in *op428* mutants are not dependent on the pro-apoptotic activity of *egl-1*

Timecourse analysis was performed using *op428, cep-1(gk138), egl-1(n084n3082)* and *ced-9(n1950sd)* single mutant worms, and *egl-1(n1084n3082);op428* and *ced-9(n950sd);op428* (A) or *cep-1(gk138);op428* (B) double mutants. Apoptotic germ cell corpses were scored in the meiotic region of the germline using DIC optics at 12h, 24h, 36h and 48h after the L4/adult molt. Data shown represent the average of the mean of at least two independent experiments (n=10-15 worms per experiment). Error bars represent the SD.

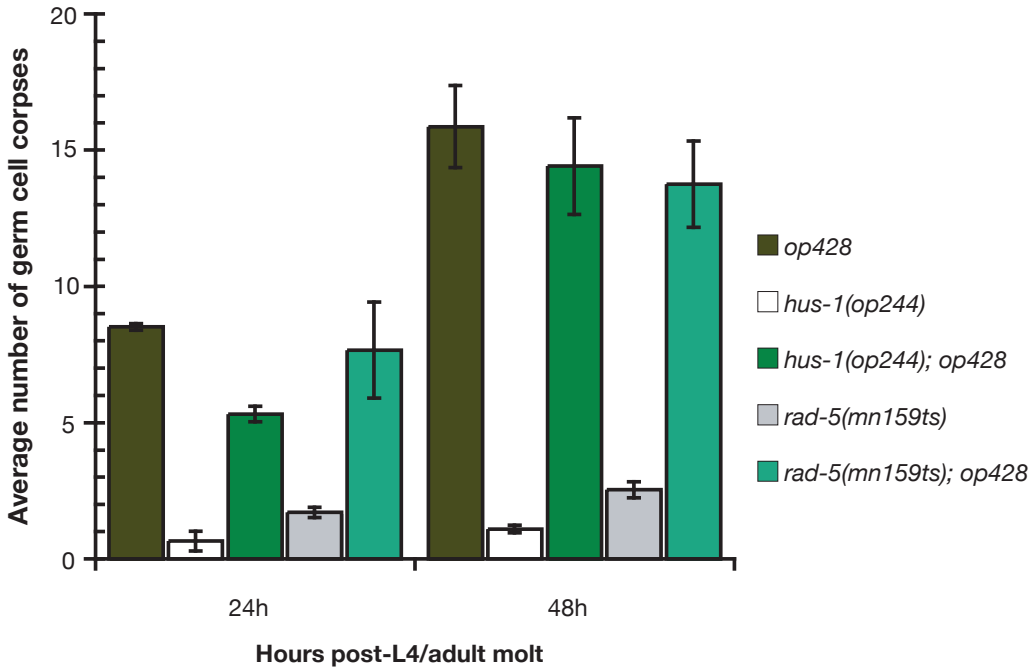

FIGURE 7.5 Mutations in the DNA damage checkpoint proteins HUS-1 and CLK-2 do not suppress the increased levels of germ cell corpses of *op428* mutants

Timecourse analysis was performed using *op428, hus-1(op244)* and *rad-5/clk-2(mn159ts)* single mutant worms as well as *hus-1(op244);op428* and *rad-5/clk-2(mn159ts);op428*. Apoptotic germ cell corpses were scored in the meiotic region of one gonad arm using DIC optics at 24h and 48h after the L4/adult molt. Data shown represent the average of the mean of at least two independent experiments (n=10-15 worms per experiment). Error bars represent the SD.

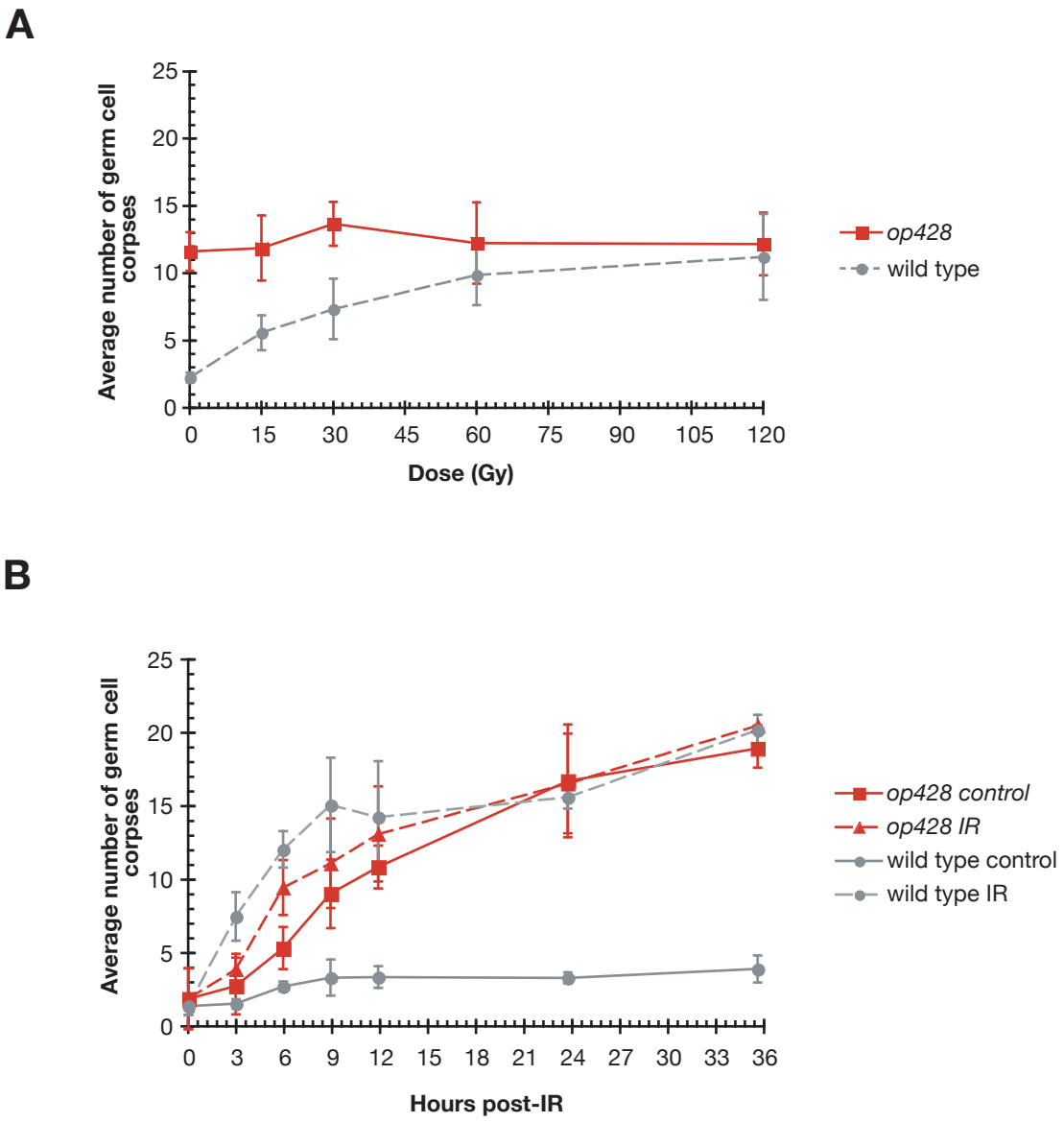

FIGURE 7.6 *op428* is defective in the apoptotic response upon ionizing radiation

(A) Wild type and *op428* mutant hermaphrodites were treated at the young adult stage with increasing doses of ionizing radiation (15, 30, 60 and 120Gy) and germ cell apoptosis was assessed 12h after treatment. (B) Wild type and *op428* mutant hermaphrodites were treated at the young adult stage with 120Gy of ionizing radiation (t=0). Germ cell apoptosis was assessed 3h, 6h, 9h, 12h, 24h and 36h after treatment. In both cases, data shown represent the average of the mean of at least two independent experiments (n=10-15 worms per experiment). Error bars represent the SD.

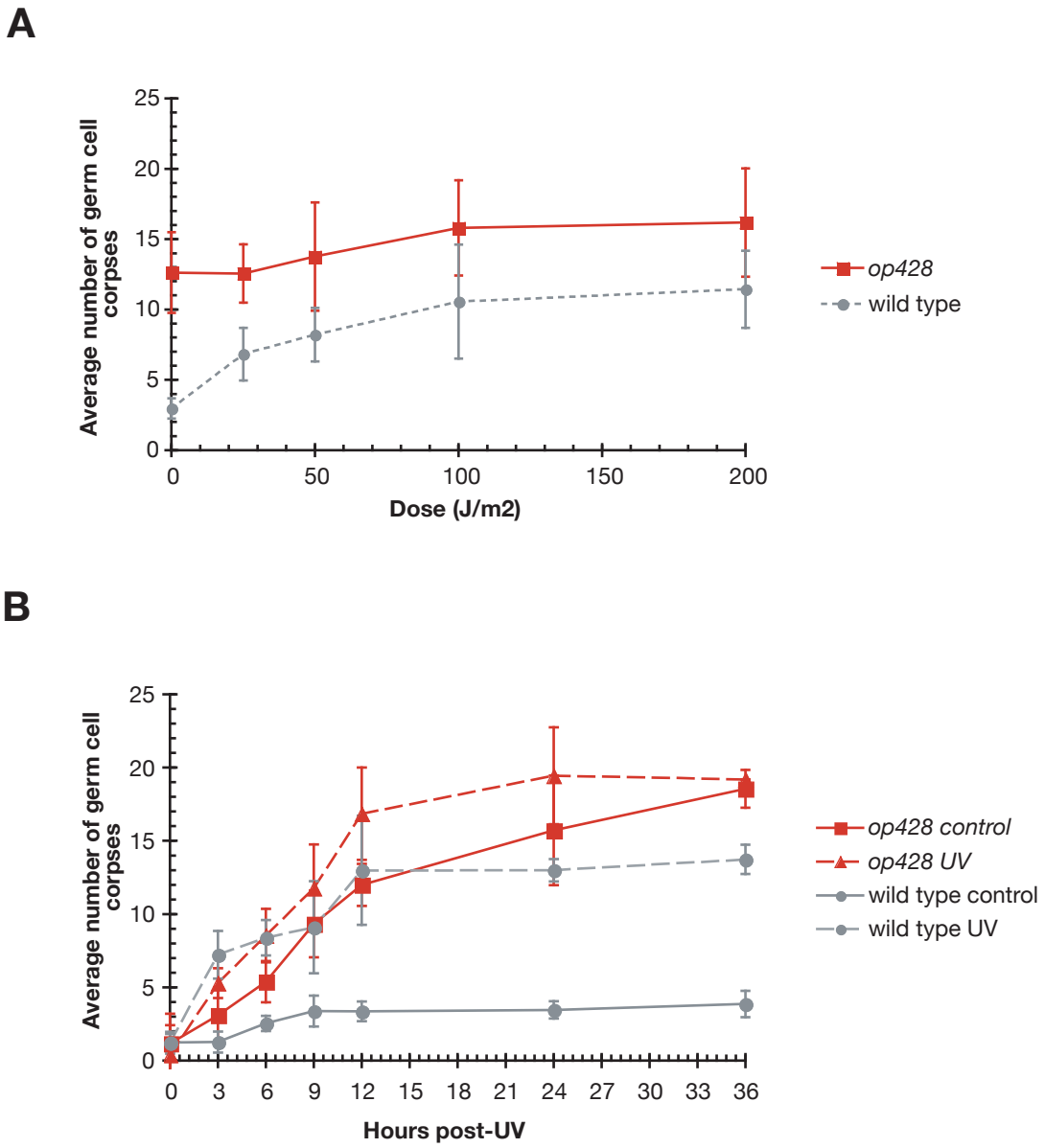

FIGURE 7.7 *op428* is defective in the apoptotic response upon ultraviolet light

(A) Wild type and *op428* mutant hermaphrodites were treated at the young adult stage with increasing doses of UV-C (25, 50, 100 and 200J/m^2) and germ cell apoptosis was assessed 12h after treatment. (B) Wild type and *op428* mutant hermaphrodites were treated at the young adult stage with 200J/m^2 of ionizing radiation (t=0). Germ cell apoptosis was assessed 3h, 6h, 9h, 12h, 24h and 36h after treatment. In both cases, data shown represent the average of the mean of at least two independent experiments (n=10-15 worms per experiment). Error bars represent the SD.

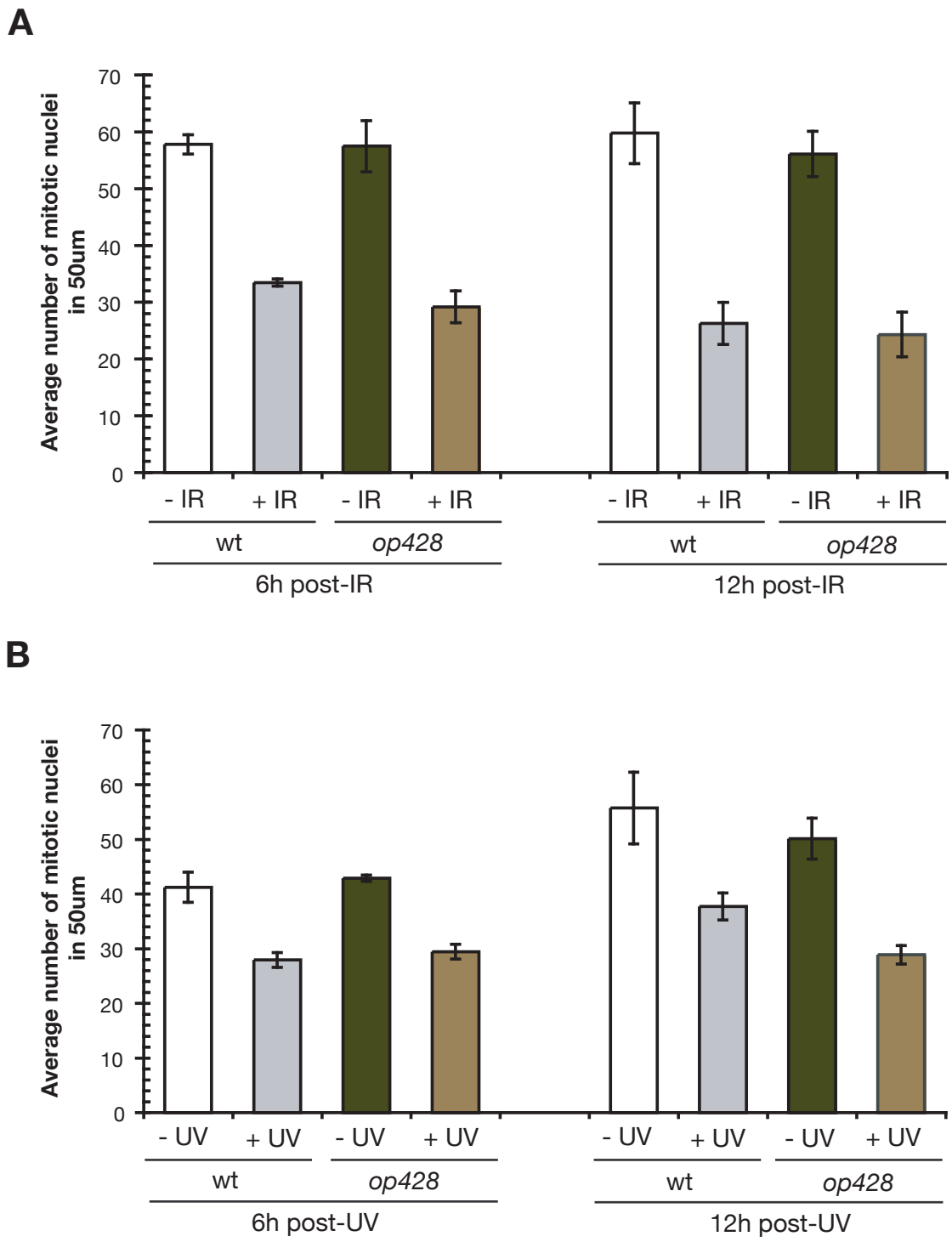

FIGURE 7.8 *op428* does not exhibit a cell cycle arrest defect upon either ionizing radiation or ultraviolet treatment

Wild type and *op428* mutant worms were treated with either 120Gy (A) or 200J/m^2 (B) at the L4 stage. In each case the number of nuclei within 50μm of the mitotic region of the germline was determined 6h and 12h post-treatment. At least 10 worms were examined per experiment and data is shown as the average of the mean of two independent experiments. Error bars represent the SD.

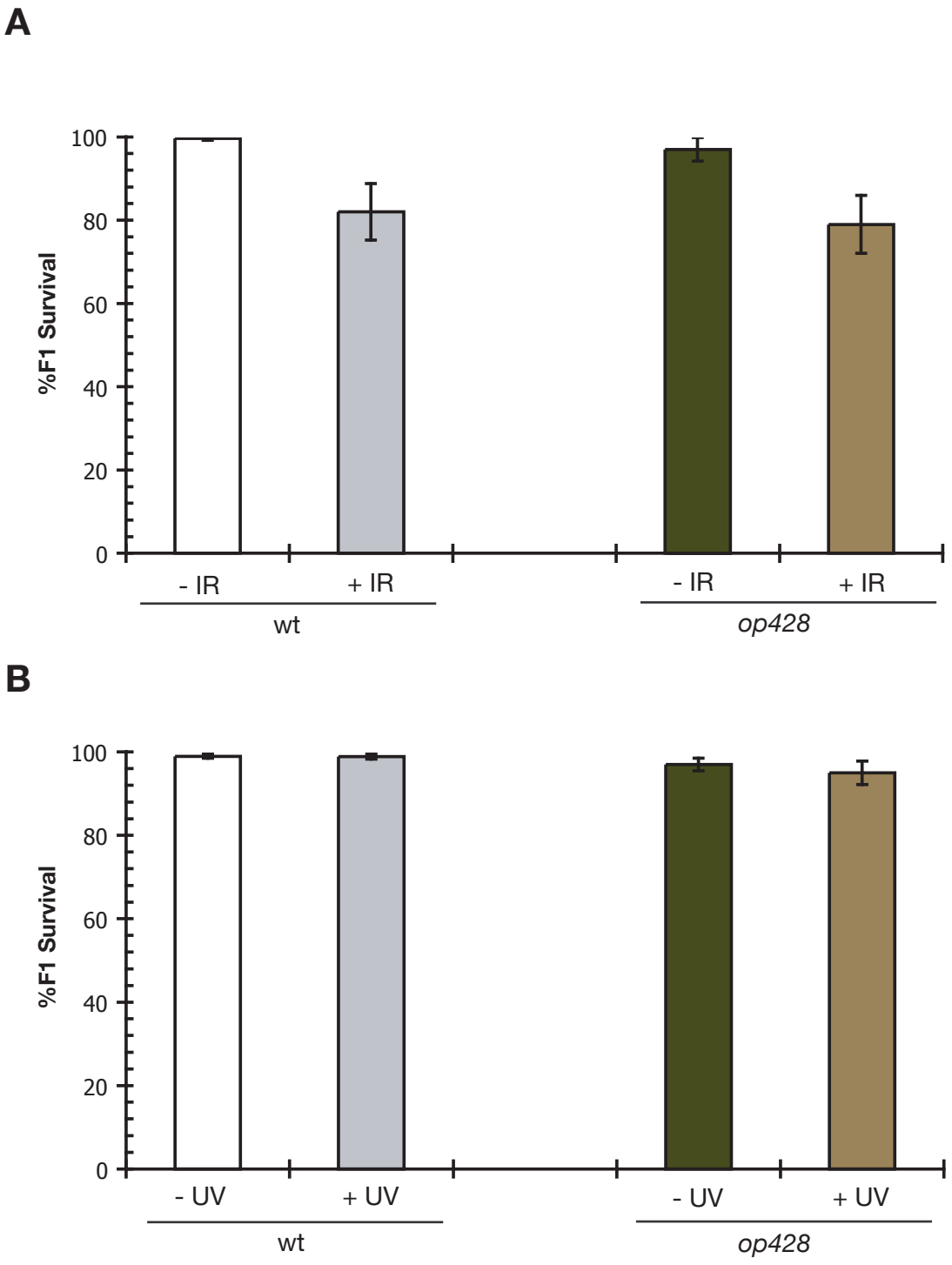

FIGURE 7.9 *op428* is not hypersensitive to either ionizing radiation or ultraviolet light treatment

Wild type and *op428* mutant worms were irradiated at the L4/adult molt with 120Gy (A) or 200J/m^2 (B) and the total number of eggs laid 10-12h after irradiation was determined in each case. Unhatched eggs and surving animals were counted 1 and 3 days later respectively in order to assess progeny survival. Data shown represent the percent of survival of embryos from at least six different worms per genotype. Error bars represent the SEM.

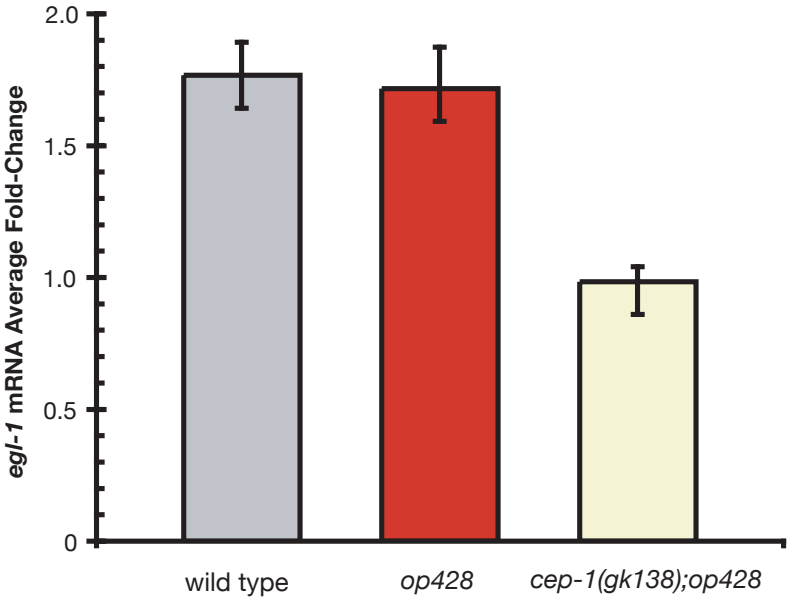

FIGURE 7.10 Transcriptional induction of *egl-1* upon ionizing radiation is not compromised in *op428* mutants

The change in the mRNA levels of *egl-1* was determined by real-time Q-RT-PCR 3h after treatment with 120Gy of X-rays. Data shown is the average fold-change of two independent experiments, each one performed in triplicates. Error bars represent the SD.

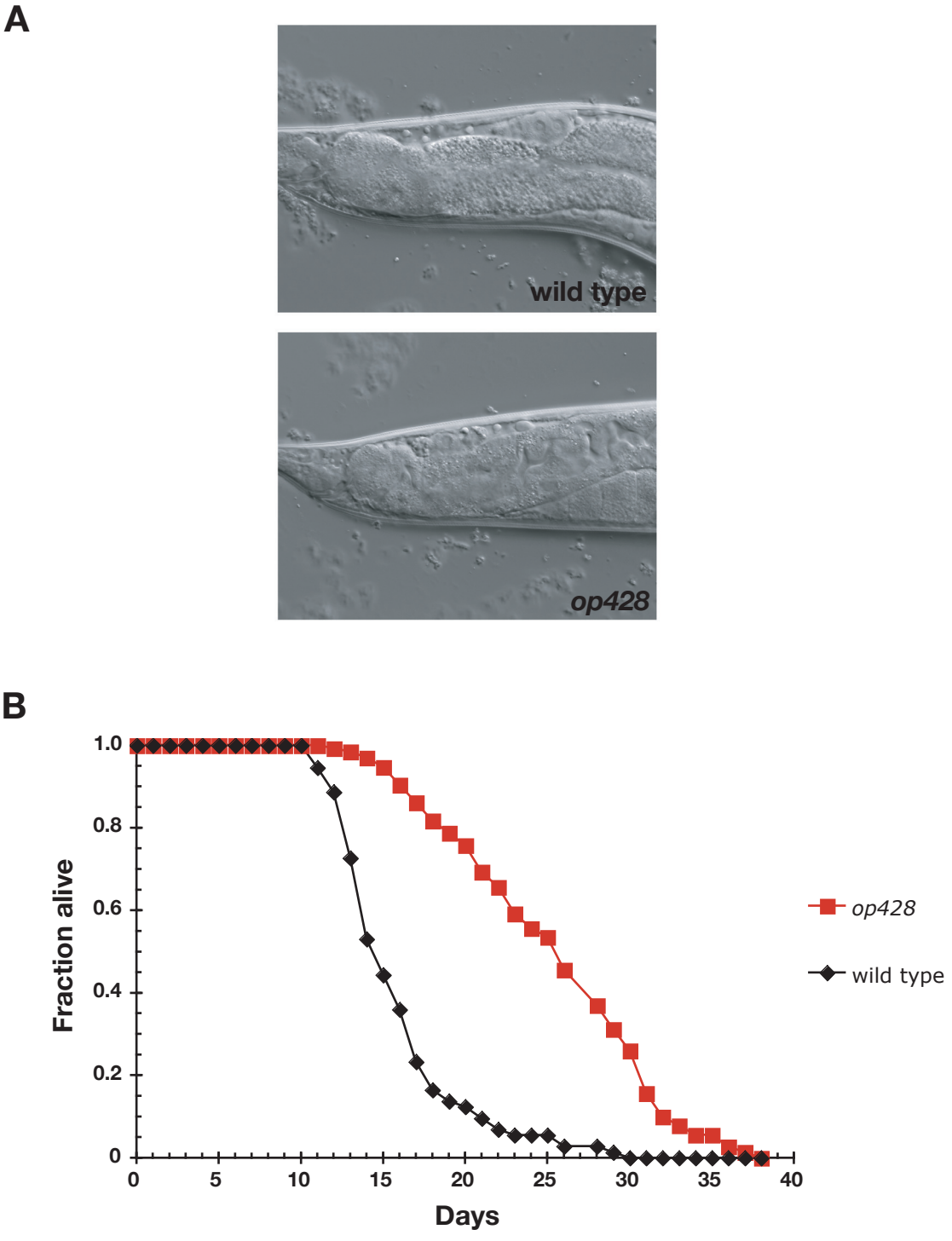

FIGURE 7.11 Additional phenotypes of *op428* mutant worms

(A) DIC photomicrographs of the posterior part of the intestine in wild type and *op428* mutant animals. Note the loss of intestinal pigmentation in *op428* mutants. (B) *op428* mutants exhibit an extended life span. Survival curves of wild type and *op428* mutant worms. Each curve represents the sum of all animals examined in two experiments. At least 50 worms were scored per genotype.

A

Chromosome	LGI	LGII	LGIII	LGIV	LGV	LGX
Marker	dpy-5	rol-6	lon-1	bli-6	dpy-11	lon-2
Genetic position (cM)	0	0.87	-1.63	3.19	0	-6.75
Number of op428 animals picked	53	33	33	29	29	29
Number of op428 animals segregating the marker	**39**	**20**	**16**	**22**	**20**	**8**
% of op428 animals segregating the marker	**74**	**61**	**48**	**76**	**69**	**28**

B

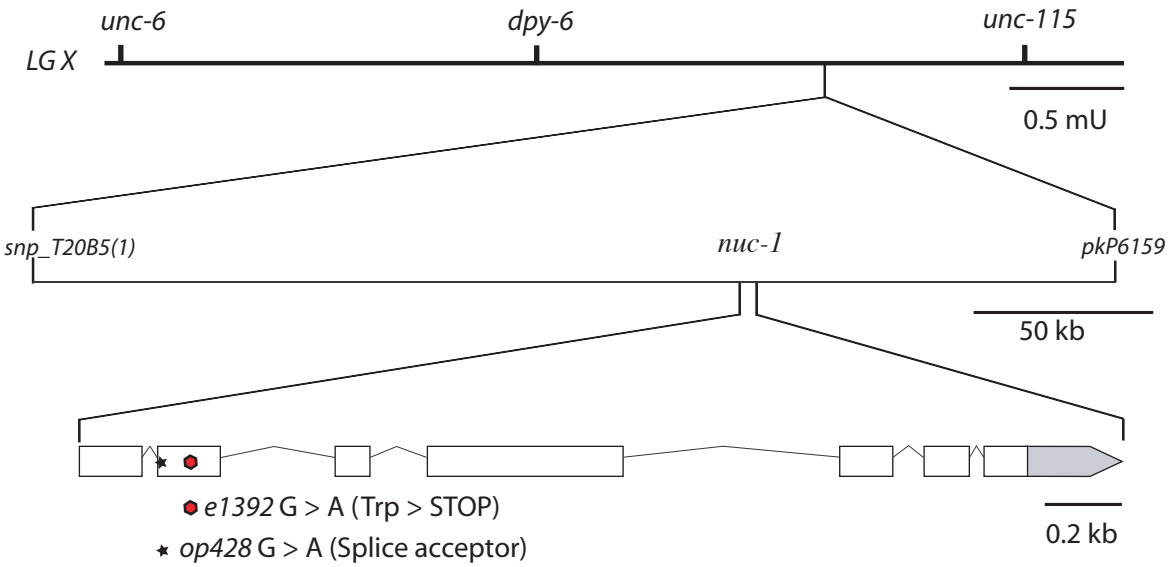

FIGURE 7.12 Mapping and molecular cloning of *op428*

(A) Two-factor mapping reveals a linkage of *op428* to chromosome X. (B) Genetic and physical map of the *nuc-1* region on the X chromosome. The position of genetic markers (*unc-6, dpy-6, unc-115*) and of SNPs (T20B51, pkP6159) used for three-factor and SNP mapping respectively is shown. Intron-exon structure of *nuc-1*. Solid boxes designate exons. The position and the nature of the the point mutations in *e1392* and *op428* are also indicated.

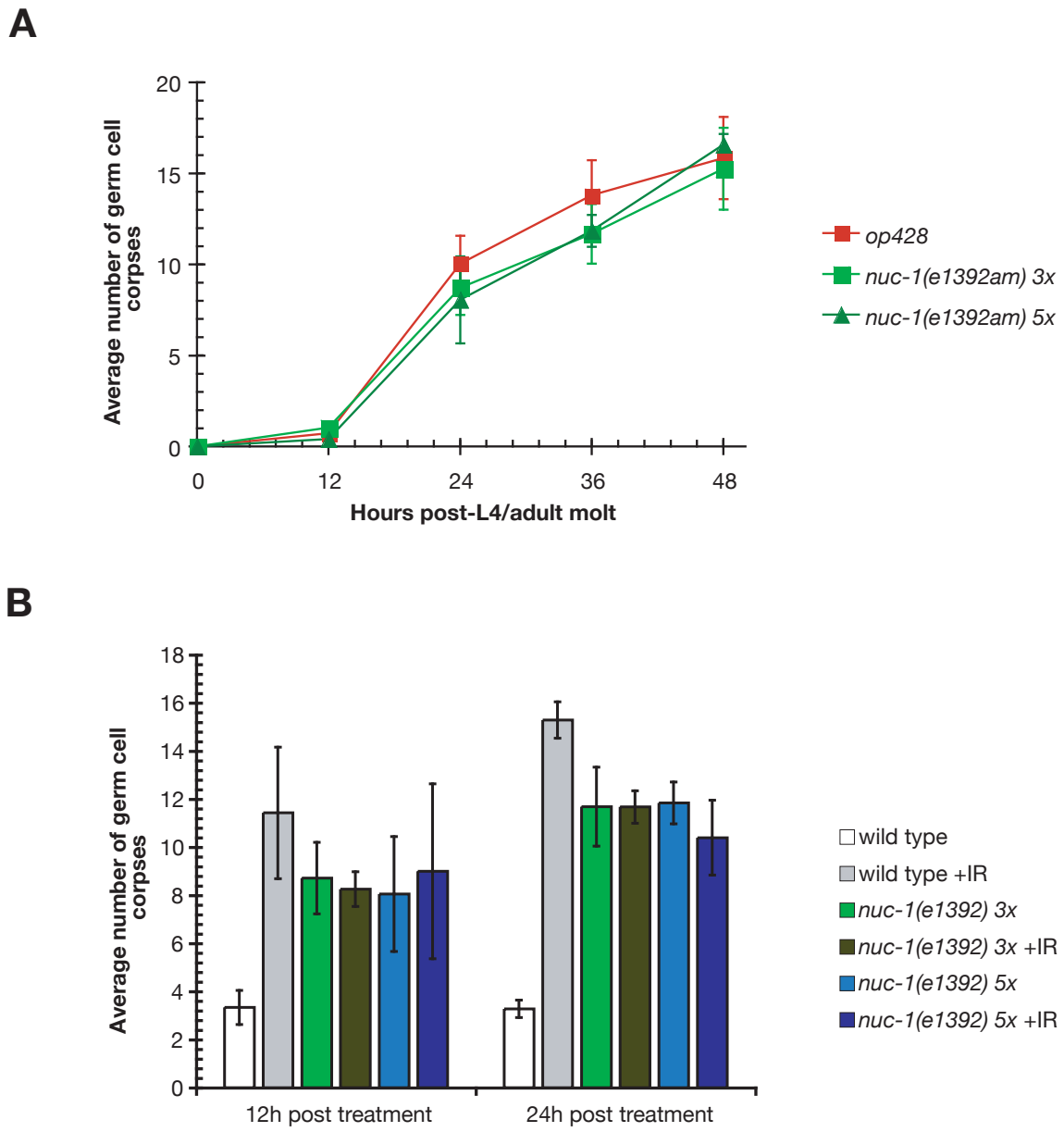

FIGURE 7.13 The increased levels of germ cell corpses and the apoptotic defect upon DNA damage cosegregate with *e1392* during backcrossing

A) Timecourse analysis was performed using *op428* and *nuc-1(e1392)* mutant worms (3x and 5x times backcrossed). Apoptotic germ cell corpses were scored in the meiotic region of one gonad arm using DIC optics at 12h, 24h, 36h and 48h after the L4/adult molt. Data shown represent the average of the mean of at least two independent experiments (n=10-15 worms per experiment). Error bars represent the SD. (B) Wild type and *nuc-1(e1392)* mutant worms (3x and 5x times outcrossed) were treated at the young adult stage with 120Gy of ionizing radiation and germ cell apoptosis was assessed 12h and 24h after treatment.Data shown represent the average of the mean of at least two independent experiments (n=10-15worms per experiment). Error bars represent the SD.

A

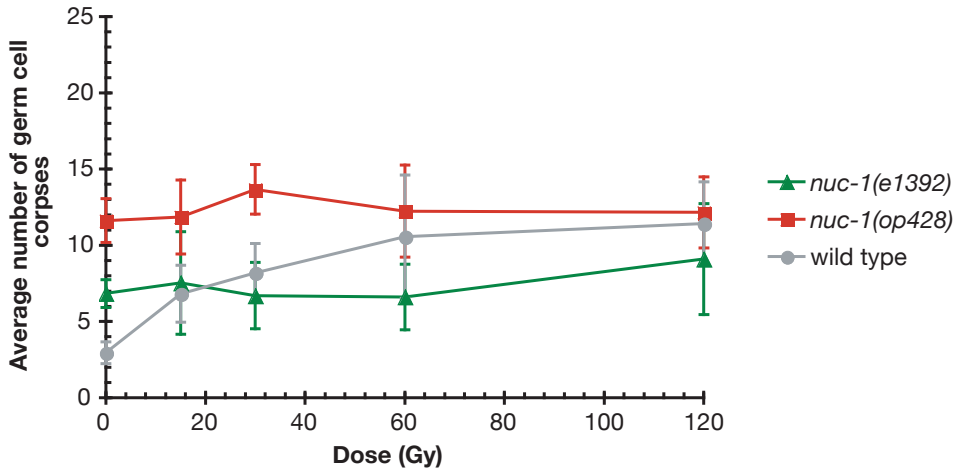

B

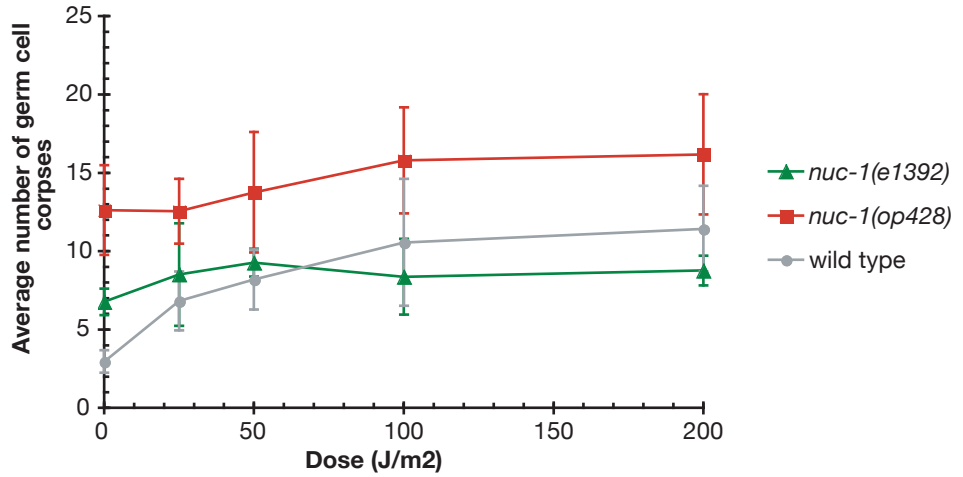

FIGURE 7.14 Similar to *op428*, loss of NUC-1 function compromises the apoptotic response upon DNA damage in the *C. elegans* germ line

Wild type, *op428* and *nuc-1(e1392)* mutant hermaphrodites were treated at the young adult stage with increasing doses of ionizing radiation (15, 30, 60 and 120Gy) (A) and of UV-C light (25, 50, 100 and 200J/m^2) (B), and germ cell apoptosis was assessed 12h after treatment. In both cases, data shown represent the average of the mean of at least two independent experiments (n=10-15 worms per experiment). Error bars represent the SD.

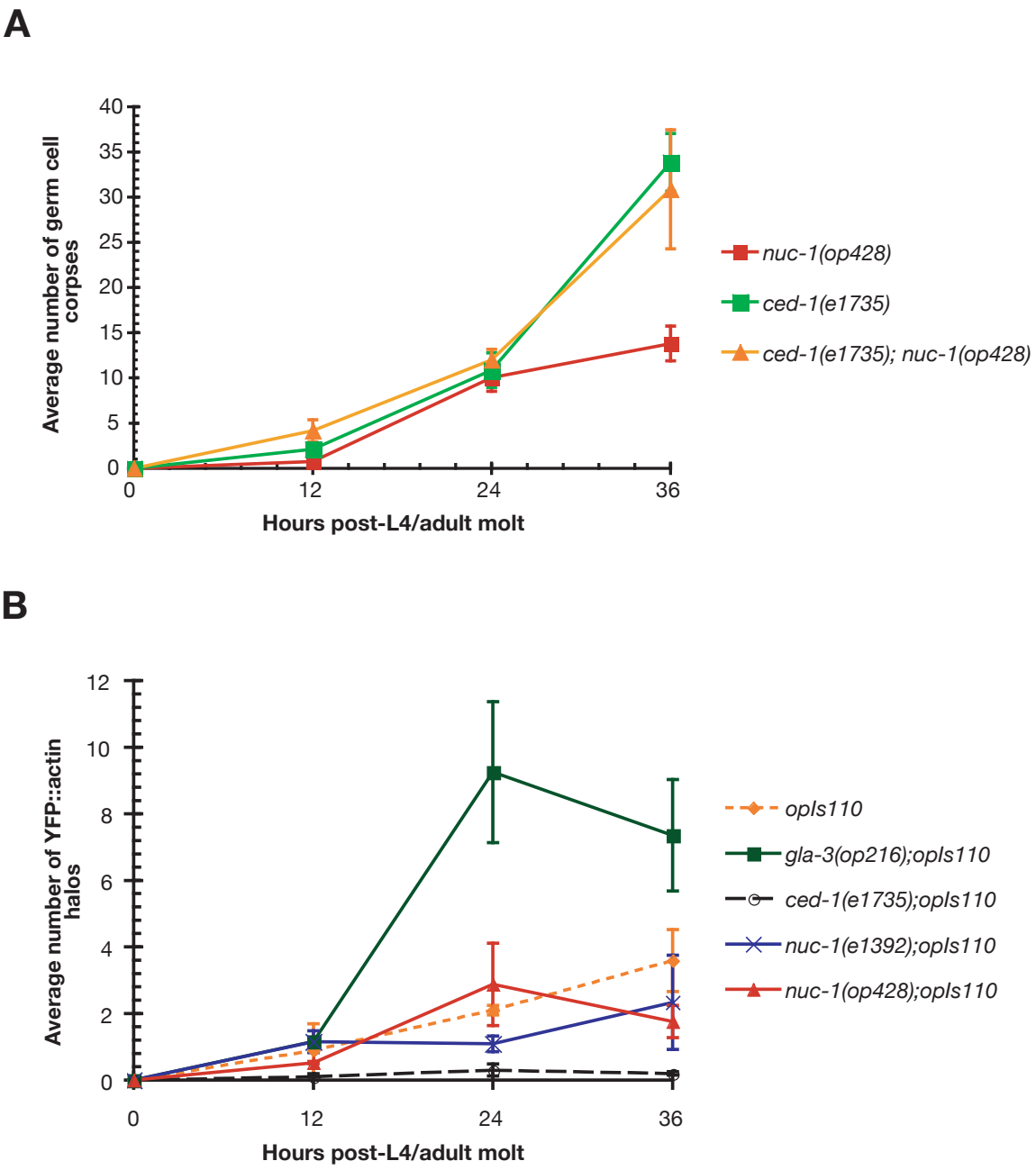

FIGURE 7.15 The increased levels of corpses in *nuc-1* mutants likely arise from defects in cell corpse degradation, rather than increased cell death

(A) Timecourse analysis was performed using *op428* and *ced-1(e1735)* single mutant worms and *ced-1(e1735); nuc1(op428)* double mutants. Apoptotic germ cell corpses were scored in the meiotic region of the germline using DIC optics at 12h, 24h and 36h after the L4/adult molt. Data shown represent the average of the mean of at least two independent experiments (n=10-15 worms per experiment). Error bars represent the SD. (B) Synchronized wild type, *nuc-1(op428), nuc1(e1392)* and *ced-1(e1735)* mutant worms all carrying the *opIs110[Plim 7::ypf::act-5]* were scored for fluorescent YFP::actin halos starting at the L4/adult molt. YFP::actin surrounds early corpses in the process of being engulfed. Data shown represent the average of the mean of at least two independent experiments (n=10-15 worms per experiment). Error bars represent the SD.

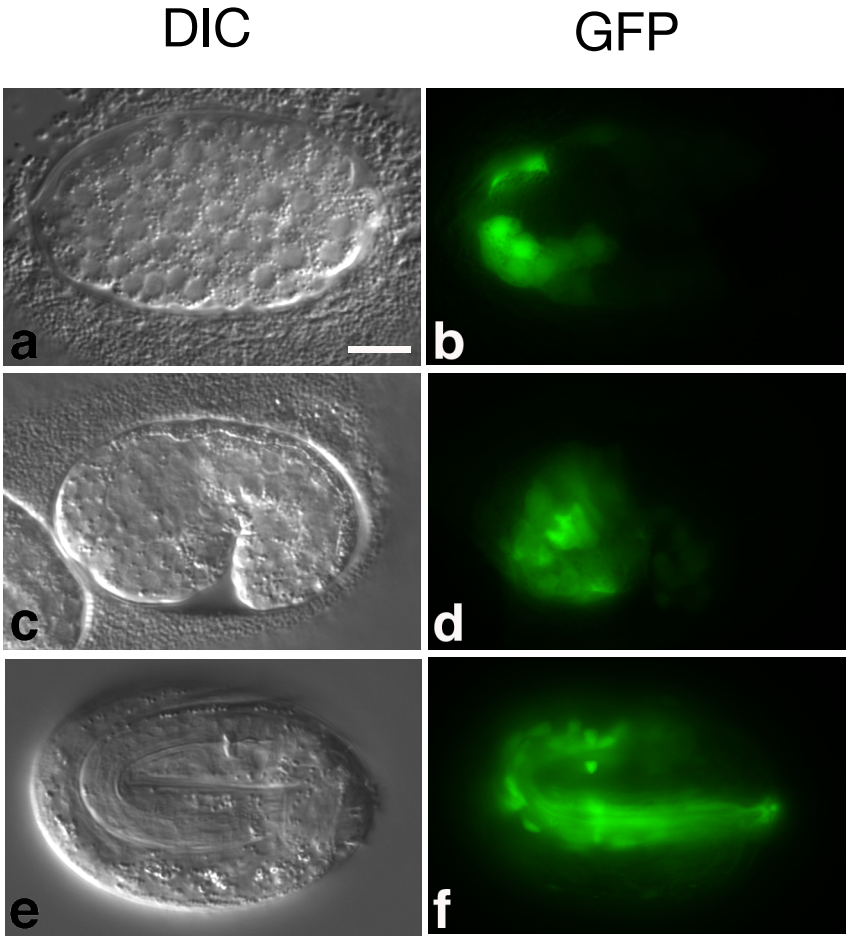

FIGURE 7.16 GFP expression from the transcriptional *Pnuc-1::GFP* reporter in embryos

Pictures are in pairs; the left panel shows the DIC image and the right panel shows the fluorescence image.Different stages of embryogenesis are shown: ball of cells (a,b), comma stage (c,d) exhibiting a strong GFP signal in the anterior region and late four-fold embryo shortly before hatching (e,f) where strong GFP expression is seen primarily in the head region. Scale bar is 10μm.

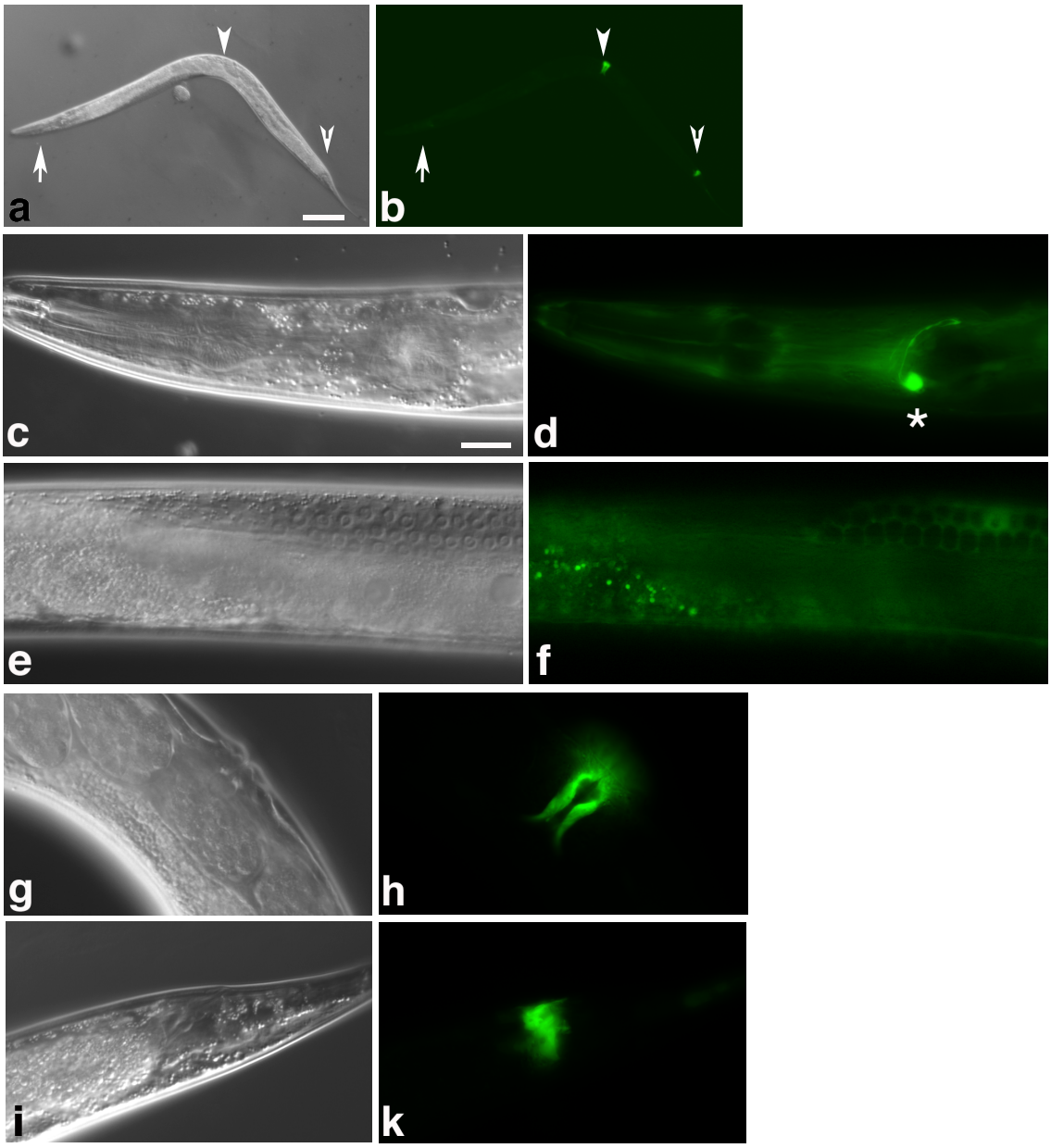

FIGURE 7.17 GFP expression from the transcriptional *Pnuc-1::GFP* reporter in adults

Pictures are in pairs; the left panel shows the DIC image and the right panel shows the fluorescence image. (a,b) Low magnification picture showing low GFP expression in the head (arrow) and strong GFP signal in the vulva (plain arrowhead) as well as in a group of cells close to the anus (open arrowhead). Scale bar is 100μm. High-magnification pictures of the regions of the head (c,d) where the asterisk shows GFP signal in the nerve ring, the gonad (e,f) where expression is seen in the somatic sheath cells, the vulva (g,h) and the anus (i,k) where GFP expression is restricted to a group of cells. Scale bar is 10μm.

CHAPTER 8

COMPONENTS OF THE DAF-2/INSULIN SIGNALING PATHWAY REGULATE DNA DAMAGE-INDUCED APOPTOSIS IN THE *C. ELEGANS* GERM LINE

CHAPTER 8

COMPONENTS OF THE DAF-2/INSULIN SIGNALING PATHWAY REGULATE DNA DAMAGE-INDUCED APOPTOSIS IN THE *C. ELEGANS* GERM LINE

8.1 ABSTRACT

The work presented in the last chapter of my thesis was largely inspired by my previous observations regarding the unexpected role of NUC-1 in DNA damage-induced cell death (Chapter 7). My motivation behind the experiments described here was two-fold. First, as I described previously, *nuc-1* mRNA has been reported to be down-regulated in *daf-2(lf)* mutants (Murphy et al., 2003) and loss of NUC-1 function results in extended lifespan, suggesting a potential connection between this gene and the DAF-2/insulin pathway. Second, *daf-2(lf)* mutants were known to be resistant to various types of stress including stimuli causing DNA damage. I reasoned that since these mutants exhibited cell-protecting activities (acting either at the level of the genetic material or at the level of any other cellular component) these might also be conserved in the worm's germline. I thus, investigated the potential role of components of the DAF-2/insulin pathway in protecting against genotoxic stress and found out that reduction of DAF-2 function severely compromises DNA damage-induced cell death. Intriguingly, this phenotype, which was shared among a few known members of the insulin pathway, was not dependent on the presence of the transcription factor DAF-16, unlike Dauer formation and regulation of lifespan, suggesting that a *daf-16*-independent branch of the pathway might exist. Last but not least, I have to point out that the results obtained in this chapter are exactly the opposite from the results recently published by the Kenyon group in the journal Science (Pinkston et al., 2006) regarding the roles of *daf-2* and *daf-16* in apoptosis. The reasons for this discrepancy are to date unknown but, hopefully, they will be discovered in the near future.

8.2 INTRODUCTION

8.2.1 Pathways regulating dauer larva formation

The DAF-2 /insulin signaling pathway was identified more than 20 years ago for its effects on dauer larvae formation (*Da*uer *f*ormation). The dauer larva is an alternative *C. elegans* larval stage which is highly stress resistant, non-aging, non-feeding and adapted for dispersal and long-term survival (Cassada and Russell, 1975). The choice to develop into dauer larvae is made early during development, at the L1 stage, and is controlled by a pheromone (Golden and Riddle, 1982), whose secretion is stimulated by unfavorable conditions such as nutritional deprivation, stress and/or overcrowding. When conditions improve, dauers may exit from diapause and molt to the fourth larval stage to become fertile adults.

The regulation of dauer formation is a very complex process. Entry into and exit from dauer diapause are tightly controlled by a very elaborate network of neuroendocrine signaling which integrates various chemosensory inputs, originally processed in the nervous system. Over the past years more than 30 genes involved in the regulation of dauer formation have been identified (Hu, 2007). Mutations in *daf* genes are grouped into two classes based on their ability either to promote entry into dauer diapause under non-dauer-inducing conditions (dauer-constitutive, Daf-c) or to prevent dauer formation under favourable conditions (dauer-defective, Daf-d). Epistasis analysis between daf-c and daf-d mutations has allowed the *daf* genes to be ordered into branched pathways, which comprise at least three different signaling cascades. The first two are a neuronal *daf-11* guanylyl cyclase pathway (Birnby et al., 2000; Vowels and Thomas, 1992; Vowels and Thomas, 1994) and a TGF-beta pathway which regulates dauer diapause via expression of the DAF-7/TGF-beta ligand (Ren et al., 1996). Both the *daf-11* and *daf-7* pathways act on a nuclear hormone receptor, encoded by *daf-12* (Antebi et al., 2000; Vowels and Thomas, 1992).

The third pathway regulating dauer arrest is an insulin-like signaling cascade, known as the DAF-2/insulin pathway. It quickly became the most “popular” from all the three pathways regulating dauer formation after the seminal observation by Kenyon and colleagues that *daf-2(lf)* mutants live longer than wild type worms (Kenyon et al., 1993), suggesting that this pathway can also regulate lifespan. This observation marked a milestone in the biology of aging and made the *daf-2* pathway

the subject of very intensive genetic, biochemical and functional genomic studies. In addition to dauer formation and lifespan, subsequent studies have uncovered even more novel roles notably in stress resistance during hypoxia (Scott et al., 2002), heat (McElwee et al., 2003), UV treatment (Murakami & Johnson, 1996), heavy metals (Barsyte et al., 2001), and infection by pathogens (Garsin et al., 2003). All these observations quickly made the DAF-2/Insulin signaling cascade one of the major stress response pathways in *C. elegans*.

To date, the DAF-2/Insulin signaling pathway consists of 8 main genes: *daf-2*, an insulin/IGF-I receptor-like protein, *age-1*, the *C. elegans* ortholog of the Phopshoinositide-3 Kinase (PI3K) p110 catalytic subunit, *aap-1*, the ortholog of a p50/p55 adaptor/regulatory subunit of PI3K, *daf-18* a lipid phosphatase homologous to the human PTEN tumor suppressor, as well as a collection of downstream protein kinases encoded by the genes *akt-1*, *akt-2*, *pdk-1* and *sgk-1* (Hertweck et al., 2004; Kimura et al., 1997; Morris et al., 1996; Ogg and Ruvkun, 1998; Paradis et al., 1999; Paradis and Ruvkun, 1998). All these genes converge at the level of the FOXO transcription factor, DAF-16, and act to regulate its function. The mammalian orthologs of DAF-16 are FOXO1, FOXO3a and FOXO4 (Lin et al., 1997; Ogg et al., 1997) and have been shown to regulate various processes including differentiation, metabolism, proliferation and survival (Accili and Arden, 2004). Genetic studies in the worm have shown that *daf-16(lf)* mutations are usually epistatic to *daf-2(lf)* mutations and in the majority of cases *daf-16* mutants have phenotypes that are opposite to those of *daf-2*. For example, the canonical *daf-16* mutant is Daf-d and has a shorter lifespan in standard conditions compared to wild type animals (Lin et al., 2001).

8.2.2 The DAF-2/insulin signaling pathway in C. elegans: mode of action

Upon binding of largely uknown insulin-like ligands to the DAF-2 receptor, AGE-1/PI3K generates 3-phosphoinositides such as PIP2 and PIP3 (phosphatidylinositol-3,4-bisphosphate and phosphatidylinositol-3,4,5-trisphosphate respectively). The adaptor subunit of PI3-kinase, AAP-1, functions to potentiate signaling by the DAF-2/AGE-1 module, although it is not strictly required for insulin signaling under most conditions (Wolkow et al., 2002). The activity of AGE-1 is

antagonized by DAF-18, a PTEN lipid phosphatase (Ogg and Ruvkun, 1998), which limits the activation of downstream kinases by decreasing PIP3 levels. AGE-1/PI3K-generated phospholipids activate PDK-1 which, in turn, activates a trimeric protein complex composed of the two Akt/PKB-like Serine/Threonine kinases, AKT-1 and AKT-2, and the serum- and glucocorticoid-inducible kinase SGK-1. AKT-2 is also able to bind to the phosphoinositides generated by AGE-1/PI3K and upon binding undergoes a conformational change which facilitates phosphorylation by PDK-1. All three kinases of the AKT-1, AKT-2 and SGK-1 complex are able to phosphorylate and control the activity DAF-16, but have slightly different outputs. SGK-1 acts in parallel to the AKT/PKB kinases and is the crucial factor for the regulation of post-embryonic development, stress response and life span, whereas AKT-1 and AKT-2 are mainly involved in the control of the dauer larval stage (Hertweck et al., 2004; Ogg et al., 1997; Paradis and Ruvkun, 1998). Phosphorylation of DAF-16 by the kinase complex blocks its nuclear entry and inhibits its function (Henderson and Johnson, 2001; Lee et al., 2001; Lin et al., 2001). This inhibition of DAF-16 is relieved when signaling through the DAF-2 pathway is turned off; then, DAF-16 translocates into the nucleus to promote the expression of target genes.

For a longtime it was assumed that the direct transcriptional targets of DAF-16 are responsible for the stress resistance and longevity phenotypes associated with *daf-2(lf)* mutants. Several groups have successfully used genome-wide approaches including transcriptional profiling by Serial Analysis of Gene Expression (SAGE) (Halaschek-Wiener et al., 2005) or cDNA and DNA microarrays (McElwee et al., 2003; Murphy et al., 2003), as well as a genome-wide search for binding sites using Chromatin Immunoprecipitation assays (ChIP) (Oh et al., 2006). These studies identified a plethora of genes regulated by DAF-16 typically involved in cellular stress responses, as well as antimicrobial and metabolic factors.

Despite this successful identification of many DAF-16 targets, it is not clear, to date, whether a specific set of genes is necessary for the long-lived phenotype of the *daf-2* mutants or whether a combinatorial effect of all the genes that are directly or indirectly controlled by DAF-16 accounts for it. This question is hard to address because, as genetic studies have demonstrated, *daf-2* can function cell non-autonomously and within multiple cell types to influence dauer formation and adult lifespan, by regulating the production of secondary signals that coordinate growth and

longevity in a systemic way, throughout the entire animal. Thus, insulin signaling is able to elicit different responses in different cell types and the combinatorial effect of these cellular responses will result in distinct physiological outputs. However, with the development of sensitive systems biology approaches and automated processes allowing the isolation of specific *C. elegans* cells in a high-throughput way these questions are likely to find an answer in the near future.

8.3 RESULTS

8.3.1 daf-2(e1370ts) mutants are defective in DNA damage-induced apoptosis

To test for the potential involvement of the DAF-2/insulin pathway in DNA damage signaling I performed irradiation experiments. For this, synchronised populations of *daf-2(e1370ts)* worms were irradiated with various doses of X-rays or UV-C radiation and the effect of these treatments on germ cell death was assessed by DIC microscopy 12 and 24h after treatment. Loss of *daf-2* function was found to severely compromise DNA damage-induced cell death independently of the source of genotoxic stress, suggesting a novel role for the DAF-2/insulin pathway in regulating apoptosis in *C. elegans* (Figure 8.1). Importantly, this role seems to be germ line-specific since neither loss of DAF-2 nor of DAF-16 has a dramatic effect on developmental apoptosis in somatic tissues (Table 8.1).

To further investigate the potential involvement of *daf-2* in the DNA damage response I tested whether it could have a checkpoint function. For this, I examined the cell cycle arrest response by observing the number of mitotic germ cell nuclei in a defined area after irradiation at the L4 stage with either X-rays or UV-C. Preliminary results have shown that loss of DAF-2 function has no significant influence on cell cycle arrest, suggesting that DAF-2 likely acts downstream of the checkpoint response to regulate apoptosis upon DNA damage (Data not shown). As a reminder, *nuc-1* loss of function mutants exhibit a similar phenotype (Chapter 7).

8.3.2 Not all members of the DAF-2/insulin pathway are defective in DNA damage-induced apoptosis

In order to better understand the role of the DAF-2/insulin signaling pathway in DNA damage-induced cell death we (Dr. Lilli Stergiou, a former graduate student and then a post-doc in the lab, Martina Mettler, a former diploma student, and myself) tested several mutants of this pathway for defects in apoptotic responses upon ionizing radiation (Figure 8.2). Intriguingly, among the different mutants examined only loss of AGE-1 activity was found to reproducibly result in a very strong apoptotic defect upon genotoxic stress. In contrast, loss of function mutations in *akt-2* and *sgk-1*, two of the kinases involved in the phosphorylation of the DAF-16 transcription factor, had no effect on IR-induced germ cell death. We also examined the response of two gain of function mutations in *akt*-1 and *pdk-1*, *akt-1(mg144)* and *pdk-1(mg142)* respectively, and found them to be only partially defective. These results suggest a possible redundancy between several pathways regulating DNA damage-induced apoptosis and are in agreement with the recently reported anti-apoptotic role of AKT-1 (Quevedo et al., 2007) and with the observation that *pdk-1(gf)* and *akt-1(gf)* mutants usually exhibit the same phenotypes (Paradis et al., 1999). Interestingly, *daf-16(lf)* mutants showed a slightly higher apoptotic response upon genotoxic stress compared to wild type, consistent with previous findings that *daf-16* mutants have the opposite phenotypes from *daf-2(lf)* worms.

8.3.3 daf-2(e1370) mutants influence DNA damage induced apoptosis in a daf-16-independent manner

As described in the introduction of this chapter, activation of insulin signaling in *C. elegans* culminates in the inhibition of the activity of the FOXO transcription factor DAF-16, the most downstream component of the pathway. Typically, *daf-16(lf)* mutations are epistatic to *daf-2(lf)* mutations and in most of the cases *daf-16* mutants have phenotypes that are opposite to those of *daf-2*. Since DAF-16 mediates the majority of the biological effects of the DAF-2/insulin pathway I next examined whether the defect of *daf-2(lf)* in DNA damage-induced cell death was also dependent on the presence of functional DAF-16. To test this, I performed irradiation experiments using a *daf-16(m26);daf-2(e1370ts)* double mutant strain and quantified germ cell apoptosis as previously described. Surprisingly, *daf-2* was epistatic to *daf-16* as the double mutant strain exhibited a defect in apoptosis upon ionizing radiation (Figure 8.3). This suggests that, first, *daf-16* is dispensable for DNA damage-induced

cell death and, second, that there must be additional, *daf-16*-independent, branches of the DAF-2 pathway. Also, this finding is in agreement with the results obtained for individual components of the pathway: loss of function mutations in the kinases immediately upstream of DAF-16, that typically result in its activation, have little effect on DNA damage-induced cell death. All the above hint that, in the context of DNA damage, the DAF-2 pathway might bifurcate at the level of *age-1*. The existence of such an alternative branch and the molecular factors downstream of AGE-1 conveying these signals remain to be discovered.

8.3.4 daf-2(e1370) mutants exhibit normal levels of physiological germ cell apoptosis

In the absence of any exogenous treatment *daf-2(lf)* mutants seem to have less germ cell corpses compared to wild type worms. To examine this I performed timecourses scoring apoptotic germ cell corpses using DIC optics. Because wild type worms already have very low levels of physiological germ cell apoptosis it was hard to accurately estimate if, and to which extent, loss of DAF-2 function influences this process. To bypass this problem, I constructed double mutants between *daf-2(e1370)* and a strong loss of function mutation in the engulfment receptor gene *ced-1;* in *ced-1(lf)* mutants apoptotic germ cell corpses persist because they are not properly engulfed by the somatic sheath cells that encase the gonad. This background is, therefore, useful for amplifying originally small differences in the levels of germ cell death. Timecourse analysis showed that in *ced-1(e1735); daf-2(e1370ts)* double mutants germ cells die with kinetics similar to *ced-1(e1735)* single mutants, which in terms of germ line apoptosis reflects the wild type situation (Figure 8.4). This clearly demonstrates that loss of DAF-2 function does not affect physiological germ cell apoptosis. Interestingly, this analysis also shows that, unlike previously published results from Pimkston and colleagues, *daf-2* mutants are far from having increased apoptosis in the germ line (Pinkston et al., 2006). The origin of this discrepancy is not well-understood but underscores, once more, the importance of establishing a consensus for scoring germ cell apoptosis using DIC microscopy. As an example the use of fluorescent dyes which stain apoptotic germ cells at very specific stages of programmed cell death, mostly after acidification of the phagosome (e.g. such as the Syto dyes used by Pinkston and colleagues) can be misleading.

8.3.5 Germ cells have the ability to die in daf-2(lf) mutants

daf-2(e1370ts) mutants exhibited wild type levels of germ cell corpses in the absence of any stimulus, suggesting that the DAF-2 pathway specifically regulates DNA damage-induced apoptosis. To further corroborate this finding I introduced a loss of function mutation in the germ line apoptosis gene *gla-3* and examined the resulting double mutant *gla-3(op216);daf-2(e12370ts)* for germ line apoptosis using DIC microscopy. Interestingly, *gla-3(op216)* was epistatic to *daf-2(lf)* suggesting that the death-suppressing activities of the DAF-2 do not protect against *gla-3*-mediated apoptosis (Figure 8.5A).

To better understand where *daf-2* acts with respect to the core apoptotic machinery I used a loss of function mutation in the anti-apoptotic gene *ced-9,* which results in increased levels of somatic and germ cell apoptosis. Analysis of the *daf-2(e1370ts) ced-9(n1653ts)* double mutant strain revealed increased levels of germ line apoptosis, similar to the *ced-9* single mutant (Figure 8.5B). This indicates that the apoptotic machinery is functional in *daf-2* mutants and that although germ cells have the potential to die they are protected via a *ced-9*-dependent mechanism. Thus, DAF-2 would be expected to act at a step upstream of CED-9.

8.3.6 daf-2(lf) mutants are able to partially respond to endogenous DNA damage

The genetic material of a cell can be damaged either by an external source of genotoxic stress, or during endogenous biological processes. For instance, double-strand breaks can occur normally during meiotic prophase as the initiating events in meiotic recombination. Previous studies in *C. elegans* have shown that such breaks can initiate germ cell apoptosis (Gartner et al., 2000). Loss of RAD-51 function, a member of the RecA family that catalyzes the invasion of DNA single-strand overhangs into a recipient double-strand DNA to initiate the formation of D loops and the later steps of meiotic recombination, results in unresolved DNA breaks and elevated levels of germ cell corpses. This type of death is typically suppressed in mutants for the IR responsive pathway, such as *hus-1(lf)*, *mrt-2(lf)* and *clk-2*/*rad-5(lf)* as well as for the p53 homolog *cep-1(lf)*.

To test whether *daf-2* mutants can respond to endogenous DNA damage we used RNAi to inactivate *rad-51* in *daf-2(e1370ts)* and performed a timecourse analysis of germ cell death by DIC microscopy (Figure 8.6). Interestingly, inhibition of RAD-51 activity resulted in elevated levels of germ cells corpses in *daf-2(lf)* mutants compared to control RNAi-treated worms. Artificially generated double strand breaks have, thus, a different effect from radiation-induced double strand breaks. This finding is particularly interesting as it suggests that these two different ways to generate the same type of DNA lesions, might require recruitment of different factors in order to be resolved. Moreover it raises the possibility that DAF-2/insulin signaling pathway acts upstream of the creation of double strand breaks to, for instance, upregulate cell protective activities (increased DNA repair, protection against ROS etc) involved in reducing the amount of DNA damage after IR. Further experiments should focus on examining this theory.

8.4. DISCUSSION

In this chapter I investigated the potential involvement of DAF-2/insulin signaling pathway components in regulating DNA damage-induced apoptosis in the *C. elegans* germline. Using genetic methods I demonstrated that loss of function mutations in *daf-2* and *age-1*, two of the most upstream components of the insulin signaling cascade abrogate programmed cell death upon ionizing radiation or UV-C treatment. *daf-2* mutants exhibited otherwise normal levels of developmental programmed cell death in the somatic tissues and of physiological cell death in the hermaphrodite germ line, suggesting that they specifically regulate DNA damage-induced apoptosis. Epistasis analysis was also used to show that germ cells in *daf-2(lf)* mutant animals are able to die but are protected via a CED-9-dependent mechanism, suggesting that insulin signaling acts upstream of the core apoptotic machinery. Interestingly, the apoptotic defect observed in *daf-2(lf)* mutants was found to be independent of the FOXO transcription factor DAF-16, which is the most downstream known point of convergence of insulin signaling in the worm. The mode of action by which this is accomplished remains to be elucidated.

Surprisingly, the observations presented in these chapter are in profound disagreement with a recent study from the Kenyon lab reporting that *daf-2* mutants

exhibit, not only a normal DNA damage-induced apoptotic response, but also increased levels of germ cell death (Pinkston et al., 2006). According to the same study *daf-16(lf)* mutants were found to exhibit lower levels of germ cell death than wild type worms and were unable to mount a potent apoptotic response upon ionizing radiation. These two findings were used as arguments to claim that mutations which are able to increase lifespan also exhibit a tumor suppressing effect since there are accompanied by increased apoptosis. Unfortunately, the authors were unable to accurately quantify the levels of dying germ cells using DIC microscopy. Instead, they used a Syto fluorescent dye that stains only specific subpopulations of germ cells (Kinchen et al., 2005) and which can lead to systematic errors. The findings of Pinkston and colleagues were recently questioned by an independent study (Quevedo et al., 2007) where DIC microscopy was used to quantify germ cell death. Quevedo et al. found that loss of DAF-16 activity resulted in increased levels of germ cell corpses (rather than lower levels according to the study of Pinkston et al.) and a normal/hypersensitive response upon genotoxic stress (rather than a defect reported in the study of Pinkston et al.); these observations are identical to mine. Future studies aiming at understanding how the DAF-2/insulin signaling pathway interferes with the apoptotic response upon DNA damage at the biochemical level will be paramount in providing us with a concrete explanation regarding these discrepancies.

Another rather puzzling question arises from that fact that while *daf-2(lf)* and *age-1(lf)* are defective in DNA damage-induced cell death, partial defects were also observed with the gain of function mutations *akt-1(mg144)* and *pdk-1(mg142)*. Additionally, another group reported an anti-apoptotic role for both AKT-1 and AKT-2 but the mechanism by which these kinases regulate cell death upon genotoxic stress has not been defined (Quevedo et al., 2007). These results suggest that the function of DAF-2 and AGE-1 in apoptosis might deviate from their known and relatively well-studied role in the insulin signaling cascade. This hypothesis is further strengthened by my finding that loss of DAF-16 function, the member of the DAF-2 pathway responsible for the transcriptional outcome finetuning the corresponding biological responses, does not suppress the apoptotic defect of *daf-2(lf)* mutant animals. The precise dissection of the mechanism these factors utilize to regulate cell death will require intensive analysis.

8.4.1 The DAF-2/insulin pathway and DNA damage-induced apoptosis

In mammals IGF-1R (Insulin-like Growth Factor-Receptor), the DAF-2 homolog, is important for fetal and post-natal development, but it also controls tissue homeostasis throughout life by regulating cell proliferation and apoptosis. Importantly, in humans it has also been implicated in the pathogenesis of a variety of neoplastic diseases primarily due to its well-documented mitogenic and anti-apoptotic properties (Pollak et al., 2004; Samani et al., 2007). Although IGF-1R is believed to predominantly convey pro-survival signals, an increasing number of studies suggest that it can also act to promote apoptosis, though how IGF-IR functions as a pro-apoptotic factor is still unclear (Kooijman, 2006). It is believed that this is largely achieved via cell type-specific effects involving the expression of growth factors, cytokines and of their cognate receptors. For example, stimulation of the production of pro-apoptotic molecules such as TNFα (Renier et al., 1996) or Fas (Kawakami et al., 1998) or down-regulation of IFNγ R2 receptors which compromises STAT-1 signaling can all lead to increased apoptosis (Bernabei et al., 2003). Remarkably, a series of experiments using fragments of IGF-1R have suggested that this receptor can also have intrinsic pro-apoptotic features. Two overlapping parts of the C-terminal region of the β-subunit of IGF-1R (residues 1223-1337 or 1282-1298) were shown to trigger apoptosis when expressed in MCF-7 breast tumor cells (Liu et al., 1998) and in a human prostate-derived cell line respectively (Reiss et al., 1999). The mechanism by which this is accomplished is currently unknown.

Very recently, a pro-apoptotic function in the context of DNA damage responses was assigned to IGF-IR, by regulating the activity of p53 (Xiong et al., 2007). The authors reported that inactivation of IGF-1R by a specific inhibitor results in a specific and cell type-dependent inhibition of p53 and mdm2 mRNA translation involving their 5' UTR regions. They concluded that IGF-1R signaling is able to regulate p53, on one hand, by enhancing its stability and, on the other hand, by decreasing its translation, which lead to impaired p53 induction in response to DNA damage. This work constitutes the first report of a role of IGF-1R in apoptosis after DNA damage and is a significant advancement towards understanding the pro-apoptotic properties of this receptor.

When I started studying the involvement of the DAF-2/insulin signaling in DNA damage-induced cell death, my first results were met with an excruciating lack of interest. I hope that in light of similar results obtained in mammalian systems, the importance of this chapter will be reconsidered. Today it is conceivable that, not only IGF-1R/DAF-2 can have both anti- and pro-apoptotic functions but also that they can act, at least partially, by similar mechanisms. In line with this, the model proposed by Quevedo and colleagues regarding the mechanism of AKT-1 action in DNA damage signaling relied on the decreased stability of CEP-1 in *akt-1(gf)*, and that proved to be sufficient to impair the apoptotic response upon genotoxic stress (Quevedo et al., 2007). Analysis of CEP-1/p53 levels by western blots or by fluorescent reporters in *daf-2(lf)* mutants should rapidly provide us with an answer with regards to this question.

8.4.2 Future directions

The work presented in this chapter is far from being complete, as it does not provide us with any mechanistic insights into how *daf-2* signaling regulates DNA damage-induced apoptosis. In the following paragraphs I outline what I consider to be key experiments towards elucidating the mode of action of this pathway. I hope this will be inspirational to the graduate student who will take over this project, if any.

Previous work from the Hengartner lab has demonstrated that an important feature of DNA damage responses in *C. elegans* is the transcriptional upregulation of *egl-1* and *ced-13*, two genes coding for BH3-only domain proteins, upon ionizing radiation or UV-C treatment. This process, which was found to be dependent on the presence of functional HUS-1 and CEP-1- factors, is essential for the induction of germ cell apoptosis following genotoxic stress (Hofmann et al., 2002; Stergiou et al., 2007). It would thus be interesting to assess, by means of Q-RT-PCR, whether the transcripts of *egl-1* and *ced-13* are properly induced in *daf-2* mutants upon treatment with ionizing radiation.

Genetic studies have shown that *daf-2* acts in a cell non-autonomous manner to influence lifespan and dauer formation. Tissue-specific rescue experiments will be extremely valuable in understanding whether this is also the case in the context of DNA damage-induced apoptosis or whether, in this case, *daf-2* acts directly in germ

cells via a cell-autonomous process. Interestingly, *in situ* expression data show a strong expression of *daf-2* mRNA in the germline but whether these mRNAs are actively translated into proteins remains to be determined. The presence of *daf-2* transcripts, which code for a receptor protein, in the *C. elegans* syncytial germline where germ cells are partially enclosed by membranes and have access to a common pool of cytosplasmic factors, is particularly intriguing. Expression studies by means of reporter constructs or immunocytochemistry in the worm's gonad will be helpful in assessing the presence of functional DAF-2 protein in this tissue.

Recently, a p53-independent pathway mediating germ cell apoptosis in response to various environmental stresses was characterized (Salinas et al., 2006). Salinas and co-workers subjected various mutants to oxidative, osmotic, heat-shock as well as starvation stress and defined the genetic requirements for stress-induced germ cell death. They found that, in these cases, germ cell apoptosis was triggered via a pathway different from the one mediating DNA damage-induced cell death, as it involved neither the presence of functional CEP-1 molecules nor the transcriptional upregulation of the pro-apoptotic gene *egl-1*. Since mutants in components of the insulin pathway are known to be resistant to these types of stress, as essayed by survival studies, it would be interesting to examine the apoptotic response of these animals under the conditions utilized by Salinas and colleagues.

Last but not least, the development of sensitive and high-throughput proteomic methods will undoubtedly lead to the in-depth characterization of the proteome of *daf-2(lf)* mutants and should allow for a better understanding of how this pathway influences lifespan and DNA damage responses. This approach should be complemented by old-school genetic approaches, which will certainly constitute an important step in identifying the factors relaying the signal downstream of the DAF-2 receptor. DIC screens aiming to identify suppressors of the *daf-2*-mediated apoptotic defect upon genotoxic stress could yield exciting results.

Despite the advances we have made in understanding DNA damage signaling the last 6 years, the work described in this chapter illustrates that there are plenty of questions remaining to be answered. It also reveals that even a simple model system, like *C. elegans,* is characterized by a surprising degree of complexity in its responses and interactions with the surrounding environment.

8.5 METHODS

8.5.1 General methods and strains

Methods for culturing *C. elegans* have been described by Brenner (Brenner, 1974). All mutant strains used in these study were grown at 20°C unless otherwise indicated and were derived from the wild type variety Bristol N2. Mutations used were as follows: LGI: *ced-1(e1735), gla-3(op216), daf-16(m26), LGII: age-1(hx546), LGIII daf-2(e1370ts), ced-9(n1653ts). LGV: akt-1(mg144), LGX: pdk-1(mg142), akt-2(ok393), sgk-1(ok538),* Unless noted otherwise mutations were previously described (Bieri et al., 2007).

8.5.2 DIC microscopy and cell corpse counts

For the Nomarski analysis animals were placed on 4% agar slides in a drop of M9 salt solution containing either 30 mM NaN_3 (Hodgkin, 1980) or 3-5mM levamisole (Sigma) and mounted under a coverslip for observation. For most animals observed only one gonad arm was scored, as the other arm was usually concealed by the intestine. For each targeted gene associated with a suppression of the AO staining the average corpse number with the standard deviation (s.d) were determined using the Excel program (Microsoft).

8.6 REFERENCES

Accili, D., and Arden, K. C. (2004). FoxOs at the crossroads of cellular metabolism, differentiation, and transformation. Cell *117*, 421-426.

Antebi, A., Yeh, W. H., Tait, D., Hedgecock, E. M., and Riddle, D. L. (2000). daf-12 encodes a nuclear receptor that regulates the dauer diapause and developmental age in C. elegans. Genes Dev *14*, 1512-1527.

Bernabei, P., Bosticardo, M., Losana, G., Regis, G., Di Paola, F., De Angelis, S., Giovarelli, M., and Novelli, F. (2003). IGF-1 down-regulates IFN-gamma R2 chain surface expression and desensitizes IFN-gamma/STAT-1 signaling in human T lymphocytes. Blood *102*, 2933-2939.

Bieri, T., Blasiar, D., Ozersky, P., Antoshechkin, I., Bastiani, C., Canaran, P., Chan, J., Chen, N., Chen, W. J., Davis, P., *et al.* (2007). WormBase: new content and better access. Nucleic Acids Res *35*, D506-510.

Birnby, D. A., Link, E. M., Vowels, J. J., Tian, H., Colacurcio, P. L., and Thomas, J. H. (2000). A transmembrane guanylyl cyclase (DAF-11) and Hsp90 (DAF-21) regulate a common set of chemosensory behaviors in caenorhabditis elegans. Genetics *155*, 85-104.

Brenner, S. (1974). The genetics of Caenorhabditis elegans. Genetics *77*, 71-94.

Cassada, R. C., and Russell, R. L. (1975). The dauerlarva, a post-embryonic developmental variant of the nematode Caenorhabditis elegans. Dev Biol *46*, 326-342.

Gartner, A., Milstein, S., Ahmed, S., Hodgkin, J., and Hengartner, M. O. (2000). A conserved checkpoint pathway mediates DNA damage--induced apoptosis and cell cycle arrest in C. elegans. Mol Cell *5*, 435-443.

Golden, J. W., and Riddle, D. L. (1982). A pheromone influences larval development in the nematode Caenorhabditis elegans. Science *218*, 578-580.

Halaschek-Wiener, J., Khattra, J. S., McKay, S., Pouzyrev, A., Stott, J. M., Yang, G. S., Holt, R. A., Jones, S. J., Marra, M. A., Brooks-Wilson, A. R., and Riddle, D. L. (2005). Analysis of long-lived C. elegans daf-2 mutants using serial analysis of gene expression. Genome Res *15*, 603-615.

Henderson, S. T., and Johnson, T. E. (2001). daf-16 integrates developmental and environmental inputs to mediate aging in the nematode Caenorhabditis elegans. Curr Biol *11*, 1975-1980.

Hertweck, M., Gobel, C., and Baumeister, R. (2004). C. elegans SGK-1 is the critical component in the Akt/PKB kinase complex to control stress response and life span. Dev Cell *6*, 577-588.

Hofmann, E. R., Milstein, S., Boulton, S. J., Ye, M., Hofmann, J. J., Stergiou, L., Gartner, A., Vidal, M., and Hengartner, M. O. (2002). Caenorhabditis elegans HUS-1 is a DNA damage checkpoint protein required for genome stability and EGL-1-mediated apoptosis. Curr Biol *12*, 1908-1918.

Hu, P. J. (2007). Dauer. In WormBook.

Kawakami, A., Nakashima, T., Tsuboi, M., Urayama, S., Matsuoka, N., Ida, H., Kawabe, Y., Sakai, H., Migita, K., Aoyagi, T., *et al*. (1998). Insulin-like growth factor I stimulates proliferation and Fas-mediated apoptosis of human osteoblasts. Biochem Biophys Res Commun *247*, 46-51.

Kenyon, C., Chang, J., Gensch, E., Rudner, A., and Tabtiang, R. (1993). A C. elegans mutant that lives twice as long as wild type. Nature *366*, 461-464.

Kimura, K. D., Tissenbaum, H. A., Liu, Y., and Ruvkun, G. (1997). daf-2, an insulin receptor-like gene that regulates longevity and diapause in Caenorhabditis elegans. Science *277*, 942-946.

Kinchen, J. M., Cabello, J., Klingele, D., Wong, K., Feichtinger, R., Schnabel, H., Schnabel, R., and Hengartner, M. O. (2005). Two pathways converge at CED-10 to mediate actin rearrangement and corpse removal in C. elegans. Nature *434*, 93-99.

Kooijman, R. (2006). Regulation of apoptosis by insulin-like growth factor (IGF)-I. Cytokine Growth Factor Rev *17*, 305-323.

Lee, R. Y., Hench, J., and Ruvkun, G. (2001). Regulation of C. elegans DAF-16 and its human ortholog FKHRL1 by the daf-2 insulin-like signaling pathway. Curr Biol *11*, 1950-1957.

Lin, K., Dorman, J. B., Rodan, A., and Kenyon, C. (1997). daf-16: An HNF-3/forkhead family member that can function to double the life-span of Caenorhabditis elegans. Science *278*, 1319-1322.

Lin, K., Hsin, H., Libina, N., and Kenyon, C. (2001). Regulation of the Caenorhabditis elegans longevity protein DAF-16 by insulin/IGF-1 and germline signaling. Nat Genet *28*, 139-145.

Liu, Y., Lehar, S., Corvi, C., Payne, G., and O'Connor, R. (1998). Expression of the insulin-like growth factor I receptor C terminus as a myristylated protein leads to induction of apoptosis in tumor cells. Cancer Res *58*, 570-576.

McElwee, J., Bubb, K., and Thomas, J. H. (2003). Transcriptional outputs of the Caenorhabditis elegans forkhead protein DAF-16. Aging Cell *2*, 111-121.

Morris, J. Z., Tissenbaum, H. A., and Ruvkun, G. (1996). A phosphatidylinositol-3-OH kinase family member regulating longevity and diapause in Caenorhabditis elegans. Nature *382*, 536-539.

Murphy, C. T., McCarroll, S. A., Bargmann, C. I., Fraser, A., Kamath, R. S., Ahringer, J., Li, H., and Kenyon, C. (2003). Genes that act downstream of DAF-16 to influence the lifespan of Caenorhabditis elegans. Nature *424*, 277-283.

Ogg, S., Paradis, S., Gottlieb, S., Patterson, G. I., Lee, L., Tissenbaum, H. A., and Ruvkun, G. (1997). The Fork head transcription factor DAF-16 transduces insulin-like metabolic and longevity signals in C. elegans. Nature *389*, 994-999.

Ogg, S., and Ruvkun, G. (1998). The C. elegans PTEN homolog, DAF-18, acts in the insulin receptor-like metabolic signaling pathway. Mol Cell *2*, 887-893.

Oh, S. W., Mukhopadhyay, A., Dixit, B. L., Raha, T., Green, M. R., and Tissenbaum, H. A. (2006). Identification of direct DAF-16 targets controlling longevity, metabolism and diapause by chromatin immunoprecipitation. Nat Genet *38*, 251-257.

Paradis, S., Ailion, M., Toker, A., Thomas, J. H., and Ruvkun, G. (1999). A PDK1 homolog is necessary and sufficient to transduce AGE-1 PI3 kinase signals that regulate diapause in Caenorhabditis elegans. Genes Dev *13*, 1438-1452.

Paradis, S., and Ruvkun, G. (1998). Caenorhabditis elegans Akt/PKB transduces insulin receptor-like signals from AGE-1 PI3 kinase to the DAF-16 transcription factor. Genes Dev *12*, 2488-2498.

Pinkston, J. M., Garigan, D., Hansen, M., and Kenyon, C. (2006). Mutations that increase the life span of C. elegans inhibit tumor growth. Science *313*, 971-975.

Pollak, M. N., Schernhammer, E. S., and Hankinson, S. E. (2004). Insulin-like growth factors and neoplasia. Nat Rev Cancer *4*, 505-518.

Quevedo, C., Kaplan, D. R., and Derry, W. B. (2007). AKT-1 regulates DNA-damage-induced germline apoptosis in C. elegans. Curr Biol *17*, 286-292.

Reiss, K., Yumet, G., Shan, S., Huang, Z., Alnemri, E., Srinivasula, S. M., Wang, J. Y., Morrione, A., and Baserga, R. (1999). Synthetic peptide sequence from the C-terminus of the insulin-like growth factor-I receptor that induces apoptosis and inhibition of tumor growth. J Cell Physiol *181*, 124-135.

Ren, P., Lim, C. S., Johnsen, R., Albert, P. S., Pilgrim, D., and Riddle, D. L. (1996). Control of C. elegans larval development by neuronal expression of a TGF-beta homolog. Science *274*, 1389-1391.

Renier, G., Clement, I., Desfaits, A. C., and Lambert, A. (1996). Direct stimulatory effect of insulin-like growth factor-I on monocyte and macrophage tumor necrosis factor-alpha production. Endocrinology *137*, 4611-4618.

Salinas, L. S., Maldonado, E., and Navarro, R. E. (2006). Stress-induced germ cell apoptosis by a p53 independent pathway in Caenorhabditis elegans. Cell Death Differ *13*, 2129-2139.

Samani, A. A., Yakar, S., LeRoith, D., and Brodt, P. (2007). The role of the IGF system in cancer growth and metastasis: overview and recent insights. Endocr Rev *28*, 20-47.

Stergiou, L., Doukoumetzidis, K., Sendoel, A., and Hengartner, M. O. (2007). The nucleotide excision repair pathway is required for UV-C-induced apoptosis in Caenorhabditis elegans. Cell Death Differ *14*, 1129-1138.

Vowels, J. J., and Thomas, J. H. (1992). Genetic analysis of chemosensory control of dauer formation in Caenorhabditis elegans. Genetics *130*, 105-123.

Vowels, J. J., and Thomas, J. H. (1994). Multiple chemosensory defects in daf-11 and daf-21 mutants of Caenorhabditis elegans. Genetics *138*, 303-316.

Wolkow, C. A., Munoz, M. J., Riddle, D. L., and Ruvkun, G. (2002). Insulin receptor substrate and p55 orthologous adaptor proteins function in the Caenorhabditis elegans daf-2/insulin-like signaling pathway. J Biol Chem *277*, 49591-49597.

Xiong, L., Kou, F., Yang, Y., and Wu, J. (2007). A novel role for IGF-1R in p53-mediated apoptosis through translational modulation of the p53-Mdm2 feedback loop. J Cell Biol *178*, 995-1007.

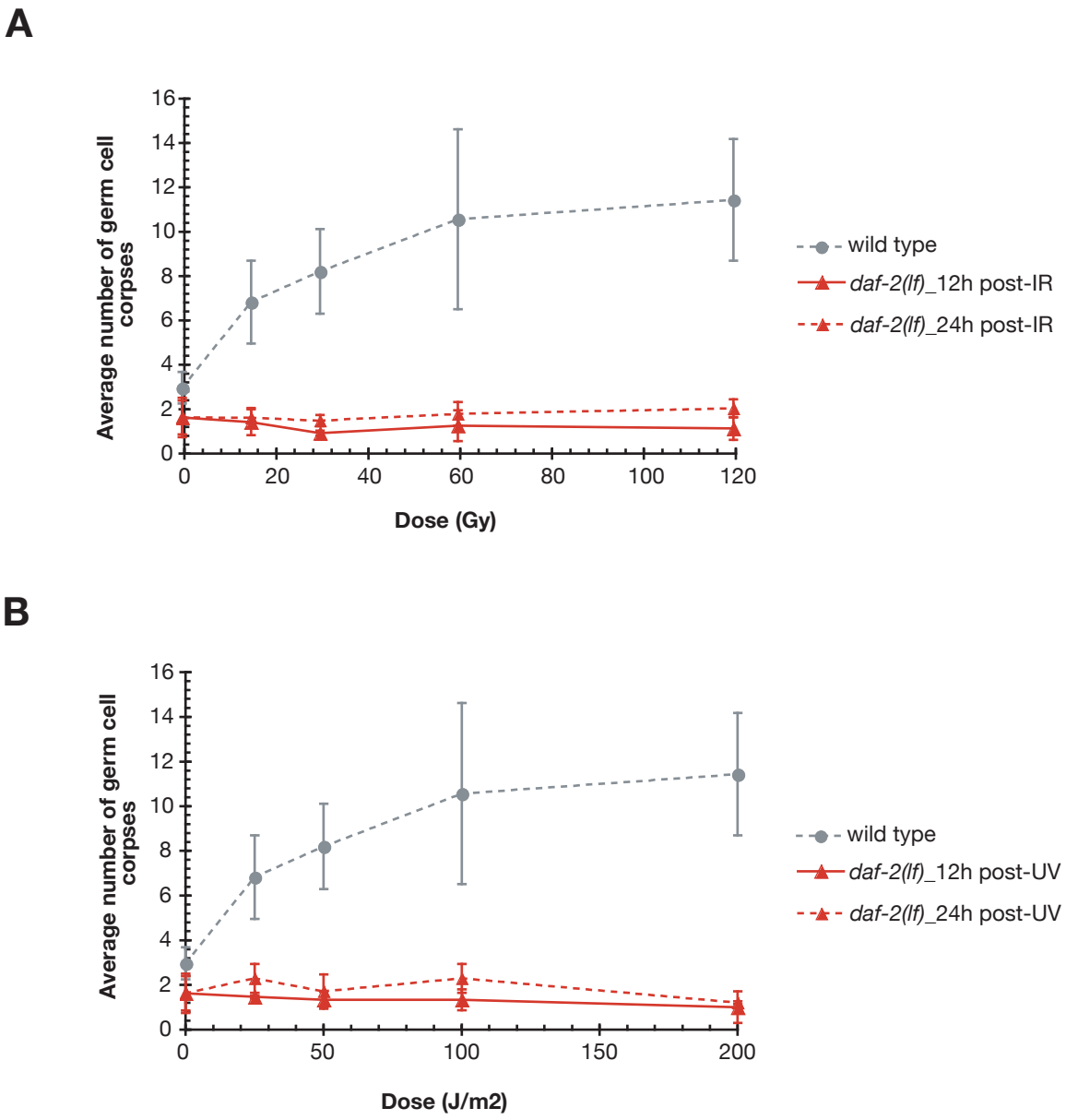

FIGURE 8.1 *daf-2(e1370ts)* mutants are defective in the apoptotic response upon ionizing radiation and ultraviolet light treatment

(A) Wild type and *daf-2(e1370)* mutant hermaphrodites were treated at the young adult stage with increasing doses of ionizing radiation (15, 30, 60 and 120Gy) and germ cell apoptosis was assessed 12h and 24h after treatment. (B) Wild type and *daf-2(e1370)* mutant hermaphrodites were treated at the young adult stage with increasing doses of UV-C (25, 50, 100 and 200Gy) and germ cell apoptosis was assessed 12h and 24h after treatment. In both cases, data shown represent the average of the mean of at least three independent experiments (n=10-15 worms per experiment) scored by two independent observers. Error bars represent the SD.

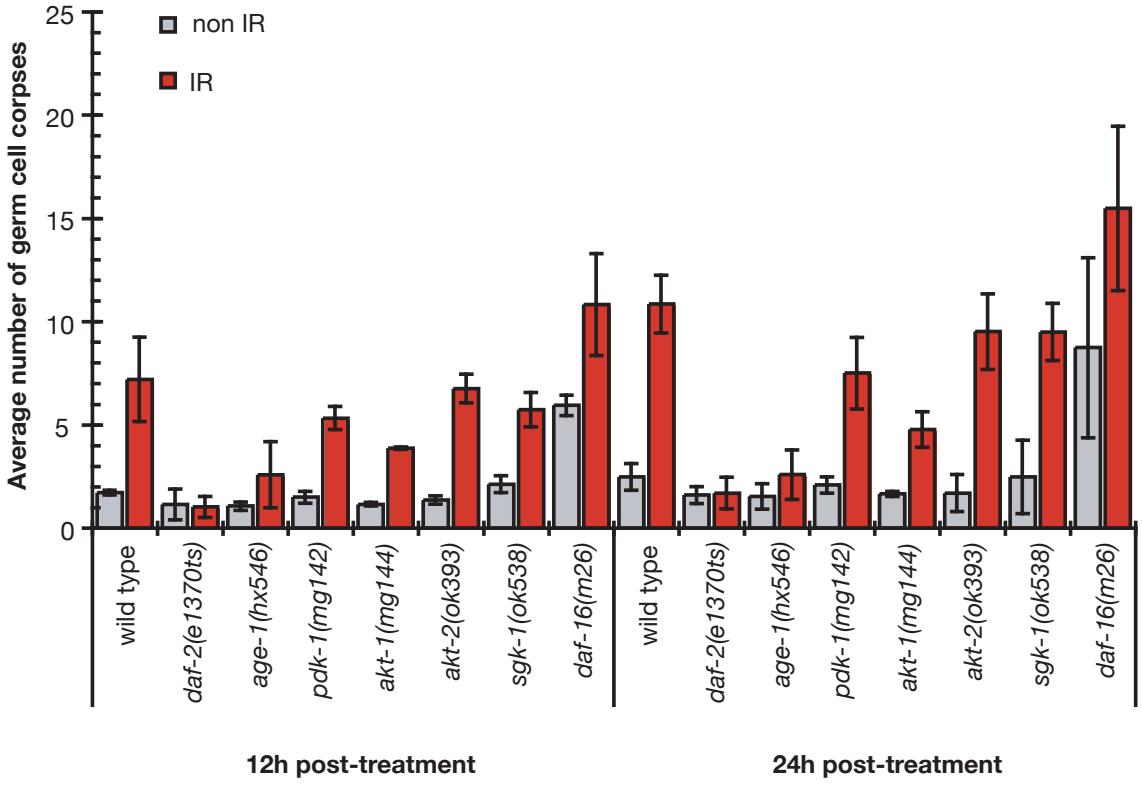

FIGURE 8.2 Not all members of the DAF-2/insulin pathway are defective in the apoptotic response upon DNA damage

Wild type, *daf-2(e1370ts)*, *daf-16(m26)*, *akt-1(mg144)*, *akt-2(ok393)*, *pdk-1(mg142)* and *sgk-1(ok538)* mutant hermaphrodites were treated at the young adult stage with 120Gy of ionizing radiation and germ cell apoptosis was assessed 12h and 24h after treatment. See text for details regarding the nature of the mutations. Data shown represent the average of the mean of at least three independent experiments (n=10-15 worms per experiment) scored by two independent observers. Error bars represent the SD.

Table 8.1 Loss of DAF-2 or DAF-16 function does not affect programmed cell death during development

Genotype	Refractile Corpses (DIC)		
	comma	2-fold	L1
wild type	8.4 ± 1.8	14.7 ± 1.9	0
ced-1(e1735)	20.3 ± 3.6	38.8 ± 7.1	22.1 ± 3.2
daf-2(e1307ts)	8.7 ± 2.0	14.1 ± 1.7	0
daf-16(m26)	7.9 ± 1.7	14.3 ± 1.8	0

The mean number of apoptotic corpses at three different developmental stages (comma, 2-fold and the first larval stage L1) was determined by DIC. At least 15 embryos or L1 larvae were scored for each genotype and for each stage. Error represents SD.

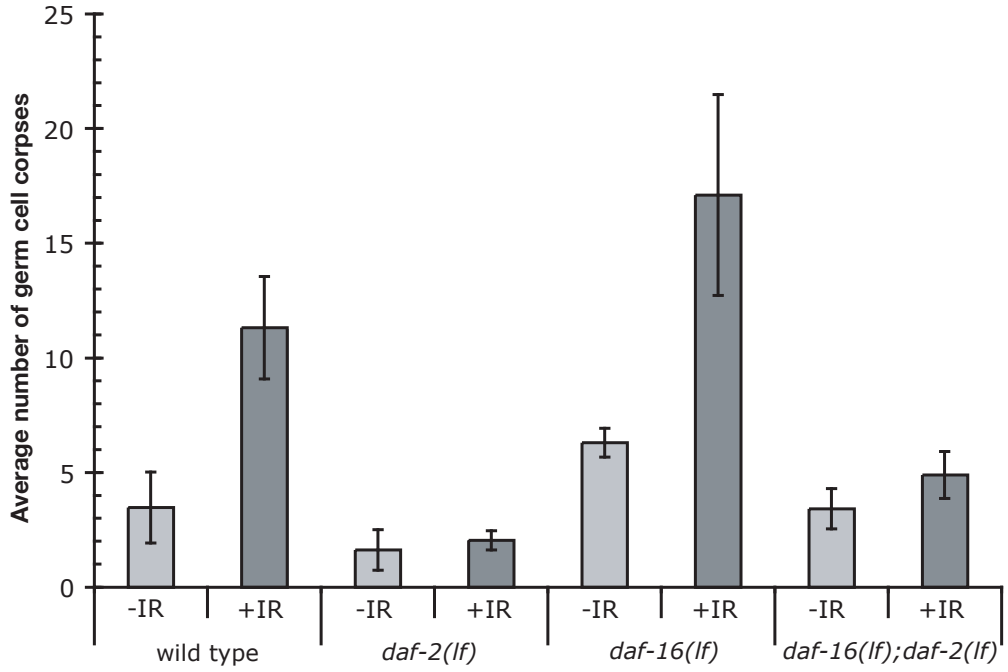

FIGURE 8.3 *daf-2* regulates DNA damage-induced apoptosis in a *daf-16*-independent manner

Wild type, *daf-2(e1370)*, *daf-16(m26)* single mutant hermaphrodites and *daf-16(m26);daf-2(e1370)* double mutants were treated at the young adult stage with 120Gy ionizing radiation and germ cell apoptosis was assessed 24h after treatment. Data shown represent the average of the mean of at least three independent experiments (n=10-15 worms per experiment) scored by two independent observers. Error bars represent the SD.

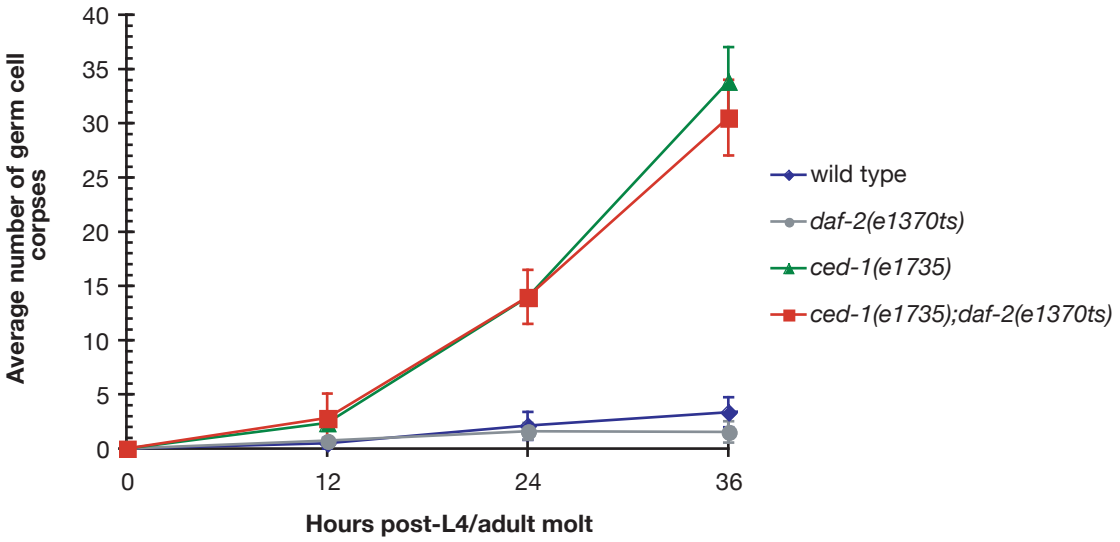

FIGURE 8.4 Loss of DAF-2 activity does not affect physiological germ cell apoptosis

Timecourse analysis was performed using wild type, *daf-2(e1370)*, and *ced-1(e1735)* single mutants and *ced-1(e1735); daf-2(e1370ts)* double mutant hermaphrodite worms. Apoptotic germ cell corpses were scored in the meiotic region of one gonad arm using DIC optics at 12h, 24h, and 36h after the L4/adult molt. Data shown represent the average of the mean of at least two independent experiments (n=10-15 worms per experiment). Error bars represent the SD.

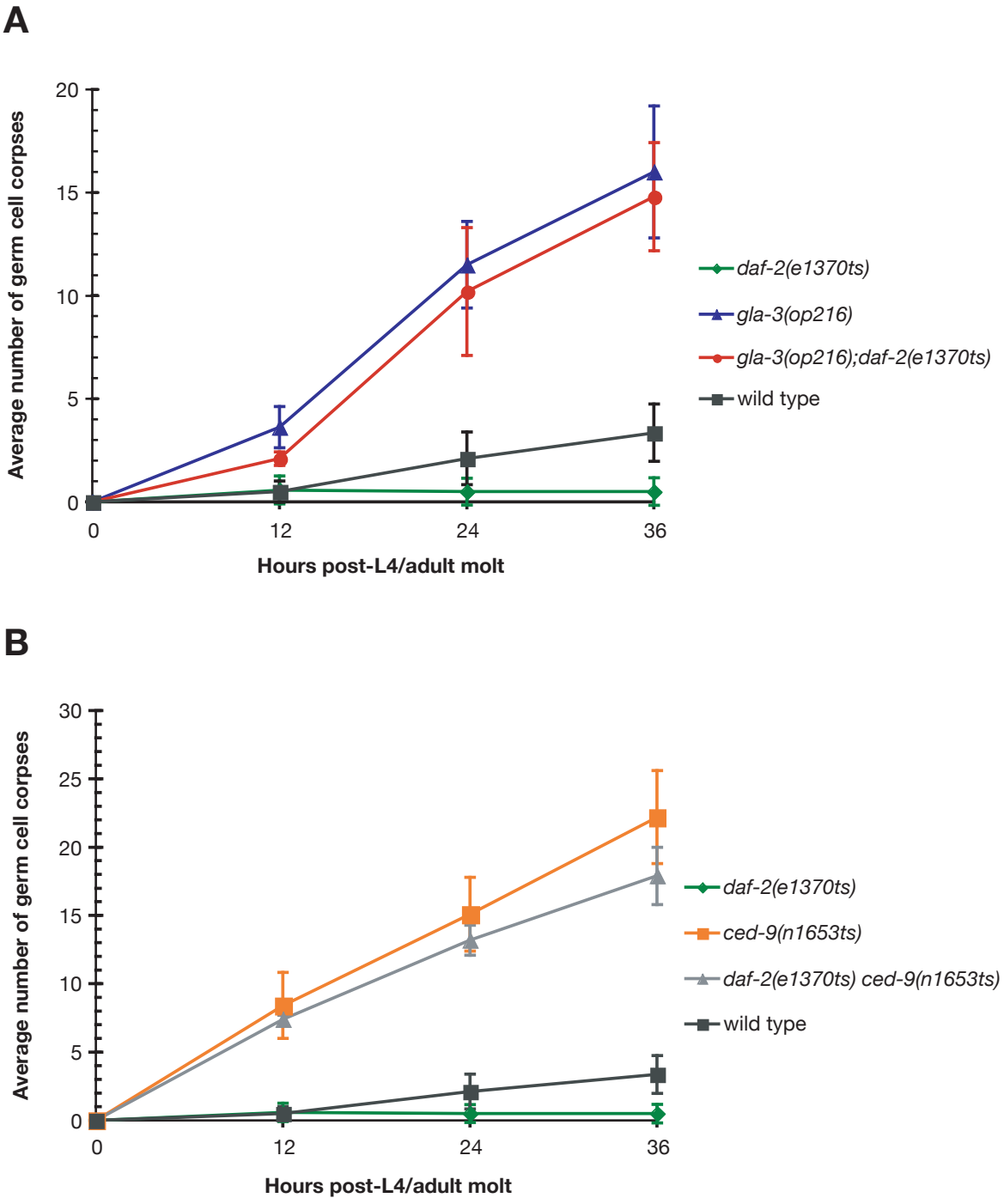

FIGURE 8.5 Germ cells have the ability to die in *daf-2(e1370ts)* mutants

Timecourse analysis was performed using wild type, *daf-2(e1370ts)*, *gla-3(op216)* and *ced-9(n1653ts)* single mutant worms, and *daf-2(e1370ts) ced-9(n1653ts)* (A) or *gla-3(op216);daf-2(e1370ts)* (B) double mutants. Apoptotic germ cell corpses were scored in the meiotic region of the germline using DIC optics at 12h, 24h, and 36h after the L4/adult molt. Data shown represent the average of the mean of at least two independent experiments (n=10-15 worms per experiment). Error bars represent the SD.

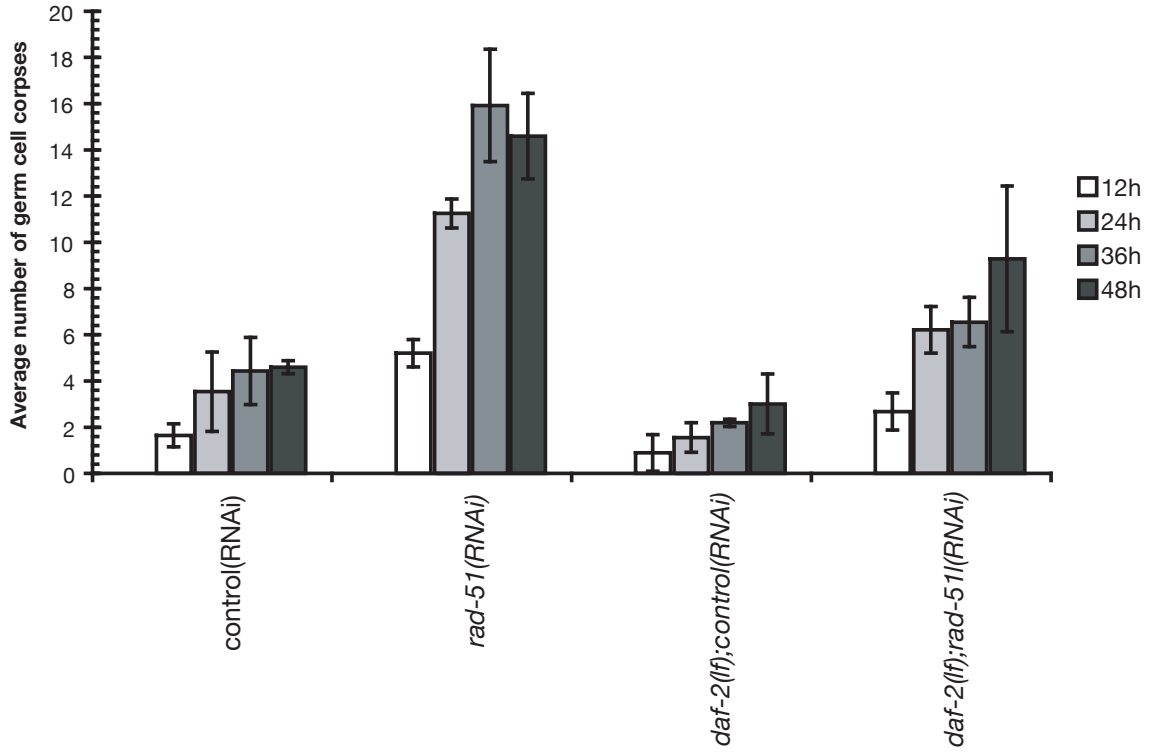

FIGURE 8.6 *daf-2(e1370ts)* mutants are able to partially respond to endogenous DNA damage

Synchronized wild type or *daf-2(e1370)* mutant hermaphrodites were fed with bacteria expressing dsRNA against *rad-51,* as described in materials and methods. Apoptotic corpses were scored using DIC optics at 12, 24, 36 and 48 after the L4/adult molt. Data shown represent the average of the mean of at least two independent experiments (n=10-15 per experiment). Errors bars represent the SD.

CHAPTER 9

OPEN QUESTIONS AND FUTURE PERSPECTIVES

CHAPTER 9

OPEN QUESTIONS AND FUTURE PERSPECTIVES

During one of the first meetings I attended as a graduate student a rather famous scientist told me: "a biological model can be two things: wrong or incomplete". After working with *C. elegans* for almost 4 years now I have the impression that the answers my work has given are fewer than the questions it generated. In the following few paragraphs I tried to summarize some of these key, in my opinion, cell death questions which to date remain unanswered.

9.1 APOPTOTIC CELL CORPSE ENGULFMENT – WHAT'S NEXT?

The reverse genetics screens described in Chapters 2 and 3 have provided us with a significant number of interesting candidates, and have opened several new doors in the *C. elegans* biology of apoptotic cell corpse engulfment. Cell biology and biochemical studies in both the worm and a cell culture system were used to establish a pathway for phagosome maturation and cell corpse processing, and which was found to be conserved across species. This work has also led to the development of important novel tools, notably reporter constructs, which can be now used to either analyze further the function of candidate genes or to screen for novel factors involved in specific stages of cell corpse clearance. The characterization of the pathway mediating phagosome maturation is an important step towards a more comprehensive view of apoptotic cell corpse engulfment in the worm but also in other systems. Further, it has also demonstrated that *C. elegans* is an attractive and powerful model system to study, not only corpse internalization, but also the subsequent fate of phagocytosed apoptotic cells.

It is unlike, however, that we discovered the full complement of the factors involved in corpse clearance. Additionally, even when we consider only the genes identified so far there are still plenty of gaps in our understanding of their mode of action. So two important questions arise: first "how are we going to analyze further the candidates we identified so far in order to understand their function" and second "how are we going too find *even more* new genes"? Regarding the first question I

believe that we posses most, if not all, of the necessary tools allowing us to study the function of newly identified genes involved in cell corpse clearance. We have established fluorescent markers for early, intermediate and late stages of cell corpse allowing us to perform extensive cell biology studies, which nicely complement the traditional double mutant/epistasis analysis. The work presented in Chapter 3 constitutes a good example of, what I consider to be, a complete study of apoptotic cell corpse engulfment (assuming that one study can be considered as complete). We also need to move towards more biochemical studies and structure-function analysis which in combination with genetics will prove extremely important in identifying the precise function of each phagocytic factor.

So how are we going to find even more new genes? The most efficient way to identify the remaining missing links would be to follow custom-tailored candidate-based approaches or focus more on either forward or reverse modifier screens. Two graduate students in the Hengartner lab, Johann Amendinger and Sérgio Pinto, have already started working in this direction under my guidance. They used bioinformatics approaches to selectively define a subset of potentially interesting genes based on their functional domain content and constructed a mini-RNAi library containing approximately 500 clones. The next step will be to specifically inactivate each one of these genes using RNAi by feeding in several different mutant backgrounds and screen for genes that either suppress or re-allow AO staining of germ cell corpses. This new approach has already started yielding very exciting results. Genetic together with cell biology studies will be used to characterize the role of these genes in apoptotic cell corpse engulfment as discussed previously.

9.2 DNA DAMAGE-INDUCED APOPTOSIS ET AL.

As described in Chapter 5, we also identified and characterized a UV-C-induced apoptotic pathway. This was found to be distinct from the previously described pathway mediating cell death upon ionizing radiation, although a number of factors were shared between these two signaling cascades. Importantly, our analysis of the cellular responses upon UV-C has also uncovered a novel role for a subgroup of factors, typically involved in DNA repair, as pro-apoptotic signaling molecules. We found that components of the Nucleotide Excision Repair (NER) pathway, which

is involved in the recognition and repair of UV-C induced lesions (pyrimidine dimmers and 6-4 PPs) also play a crucial role in activating cell cycle arrest and apoptosis. The molecular mechanism, however, by which this is accomplished is not well understood and requires further investigation.

In a separate study (Chapter 6) we focused on better characterizing the link between UV-C-induced apoptosis and the NER machinery. Using genetic and cell biology approaches we discovered that components of the Homologous recombination (HR) pathway, which is responsible for the restoration of DNA double strand breaks, are actively involved in the induction of cell death after UV-C treatment. Additional experiments confirmed further the existence of an extensive crosstalk between the NER and the HR pathway following UV exposure, demonstrating for the first time *in vivo* that NER and HR components can possess signaling properties different from their role in DNA repair. The extent to which these features are conserved in mammals remain to be determined.

All these findings have significantly improved our understanding of DNA damage response pathways and have unraveled a surprising degree of complexity. Further they have elegantly demonstrated that the worm is a powerful system to study biological responses to different types of genotoxic stress. Because of its simplicity compared to mammalian systems *C. elegans* will continue to be instrumental in elucidating the pathway activated upon DNA damage.

9.3 THE NUC-1 MYSTERY

In Chapter 7, I described the isolation and a preliminary genetic characterization of a novel allele of *nuc-1*, the *C. elegans* DNase II homolog. I also presented results suggesting that NUC-1 has at least two novel functions, one in modulating the apoptotic response upon DNA damage and a second one in regulating the lifespan of the worm. Previous studies of DNase II mutants in different model organisms have demonstrated that this enzyme plays a crucial role in engulfment-mediated DNA degradation (Samejima and Earnshaw, 2005). How does DNA degradation affect aging and DNA damage-induced apoptosis remains a very intriguing but largely unanswered question.

In Drosophila loss of DNase II function has been found to result in large amount of undegraded DNA, which leads to the activation of innate immunity responses. Interestingly, similar responses were observed in fetal liver macrophages in DNase II -/- mice bearing an inducible deletion, as demonstrated by the increased production of IFN-beta and TNF-alpha (Kawane et al., 2006). It would be interesting to test whether in *C. elegans* loss of NUC-1 activity also results in increased antimicrobial responses. If this turns out to be the case, then lifespan extension could be in part due to an increased antibacterial resistance towards the *E. coli* strain OP50, which in the laboratory is used as the standard *C. elegans* food. When grown on standard nematode media OP50 is considered non-pathogenic to the nematode but previous work has suggested that it can act as an opportunistic pathogen in old immunosenescent worms (Garigan et al., 2002; Gems and Riddle, 2000) limiting their lifespan by colonizing their intestines. Experiments aiming to test whether *nuc-1(lf)* mutants exhibit increased antimicrobial resistance should help address these questions.

How and why does NUC-1 regulate apoptosis upon DNA damage? Is this effect *nuc-1* specific or is it a common and more general feature of nucleases involved in the degradation of DNA during apoptosis? A careful examination of mutant worms for other nucleases for defects in DNA damage-induced cell death should give a quick answer as to whether the pathways utilized to destroy DNA have also other "hidden" functions. One of the major difficulties in addressing these issues will be to effectively distinguish between a biological response which is triggered by the presence of undegraded DNA in a given tissue and a signaling cascade specifically affected by a nuclease independently on its function in DNA degradation, if such a function exists. The powerful *C. elegans* genetics should allow researchers to chose between these two different scenarios. Regarding the mode of action of DNaseII, one interesting idea comes from a recent study reporting a link between apoptotic DNA degradation and the activation of a p53/Chk2 DNA damage checkpoint inside the phagocytes (Bergsmedh et al., 2006). The authors hypothesize that the phagocytic cells are able to sense the presence of undegraded DNA within the apoptotic cell and trigger a DNA damage response in order to prevent replication of "foreign" DNA. Whether the findings of this study are applicable to the worm remain to be determined. In any case, all these interesting, and to a certain extent unexpected,

observations will help reconsider the importance of apoptotic DNA degradation and put it in a broader biological context.

nuc-1(lf) mutants live longer than wild type and have a defect in the apoptotic response upon genotoxic stress. Could these two phenotypes be linked? To date it is unclear whether there is a connection between the mechanisms that lead to increased lifespan and the mechanisms that regulate DNA damage-induced apoptosis but there are emerging pieces of evidence that hint at a possible connection. In Chapter 8, I described a novel phenotype for some components of the DAF-2/insulin signaling pathway. Loss of function mutations in *daf-2* and *age-1* result in a strong defect in the apoptotic response upon genotoxic stress. The discovery of two additional mutants exhibiting both of these phenotypes raises questions about how aging and cell death are linked, in other words which elements are shared between these two processes and which are unique to each. Intriguingly, while the defect in the apoptotic response of *daf-2* mutants was found to be DAF-16-independent, DAF-16 remains the only most downstream known component of the DAF-2 pathway. Suppressor screens will be important in identifying novel components of this pathway.

The novel phenotypes of *nuc-1* and of the *daf-2* mutants described in this thesis nicely illustrate the biological complexity that one encounters even in a tiny nematode, such as *C. elegans*. It is becoming increasingly obvious that signaling pathways that look superficially unrelated might cooperate and might even share key components. Even in case of such cross-talks the worm is the first choice model organism because it remains comparatively simple compared to vertebrates and mammals. Future research will certainly address all the above questions.

9.4 THE FUTURE OF THE WORM

Ever since its introduction by Sydney Brenner as a model organism, *C. elegans* has been successfully used to study, and to subsequently answer, several fundamental questions in developmental biology. The contribution of the worm has been instrumental in elucidating the signaling pathways regulating programmed cell death, aging, as well as organ and nervous system development, to list only a few. *C. elegans* has also significantly contributed to the field of RNA interference which changed the landscape of modern biology and has pioneered research on microRNAs

which were later found to be widespread among different species and possibly involved in human pathologies. All these discoveries were crowned by two Nobel prizes in Physiology and Medicine awarded to *C. elegans* researchers in 2002 and in 2007.

During the course of my Ph.D. studies I had the pleasure to witness some of these breakthroughs, notably the establishment of genome-wide RNAi libraries and genome-wide screens together with several other "large-scale" projects that would deal with thousands of genes/factors/proteins rather than with just a couple of genetic alleles. I think that this is a very good example of a field that has continued to evolve and which adopts new technologies to complement the traditional genetic approaches. Following this tendency the Hengartner laboratory has invested time and money to annotate the complete proteome of the worm, which will open the way to novel exciting studies. The next step will likely be to quantitatively compare the proteomes of different mutant strains in order to understand the effect of single mutations at the level of the whole organism. The development of very sensitive proteomic approaches combined with large-scale expression and physical interaction projects can accelerate the identification of novel factors involved in a particular biological process. All these tools will complement the traditional forward and reverse genetic approaches. *C. elegans* will thus continue to be in the frontline of fundamental research and it seems that, because of its simplicity and its invariant cell lineage, it will be the first organism to be characterized as a system.

After so many glorious discoveries within such a short period of time it is very hard to imagine what else *C. elegans* has to teach us. My personal feeling is, however, that the tiny worm hasn't said its last word yet…

9.5 REFERENCES

Bergsmedh, A., Ehnfors, J., Kawane, K., Motoyama, N., Nagata, S., and Holmgren, L. (2006). DNase II and the Chk2 DNA damage pathway form a genetic barrier blocking replication of horizontally transferred DNA. Mol Cancer Res *4*, 187-195.

Garigan, D., Hsu, A. L., Fraser, A. G., Kamath, R. S., Ahringer, J., and Kenyon, C. (2002). Genetic analysis of tissue aging in Caenorhabditis elegans: a role for heat-shock factor and bacterial proliferation. Genetics *161*, 1101-1112.

Gems, D., and Riddle, D. L. (2000). Defining wild-type life span in Caenorhabditis elegans. J Gerontol A Biol Sci Med Sci *55*, B215-219.

Kawane, K., Ohtani, M., Miwa, K., Kizawa, T., Kanbara, Y., Yoshioka, Y., Yoshikawa, H., and Nagata, S. (2006). Chronic polyarthritis caused by mammalian DNA that escapes from degradation in macrophages. Nature *443*, 998-1002.

Samejima, K., and Earnshaw, W. C. (2005). Trashing the genome: the role of nucleases during apoptosis. Nat Rev Mol Cell Biol *6*, 677-688.